



**Universidad de Cantabria**

**Escuela Técnica Superior de Ingenieros Industriales y de  
Telecomunicación**

Departamento de Ingenierías Química y Biomolecular



**“Efecto de la temperatura en la recuperación de CO<sub>2</sub>  
mediante membranas y líquidos iónicos”**

**“Temperature effect on CO<sub>2</sub> recovery by  
membranes and ionic liquids”**

Memoria de Tesis Doctoral presentada para optar al título de  
Doctora por la Universidad de Cantabria

Programa Oficial de Doctorado en Ingeniería Química y de Procesos  
(BOE núm. 36, de 10 de febrero de 2010. RUCT: 5311209)  
con Mención hacia la Excelencia  
(BOE núm. 253, de 20 de Octubre de 2011. Referencia: MEE2011-0031)

**Lucía Gómez Coma**

Directores de Tesis:

Prof. Dr. Ángel Irabien Gulías  
Dra. Aurora Garea Vázquez

Santander, octubre 2016

---

---

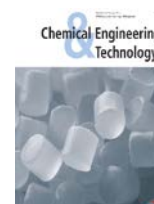
---

La presente Tesis Doctoral se presenta como un resumen de trabajos previamente publicados o enviados para su publicación en revistas científicas incluidas en el Journal of Citation Reports-Science Edition (JCR), cumpliendo con la normativa existente en la Universidad de Cantabria y en el Departamento de Ingenierías Química y Biomolecular referente a la elaboración de Tesis Doctorales por compendio de artículos. Durante la elaboración de la Tesis Doctoral se ha realizado una estancia predoctoral de tres meses de duración (febrero-abril 2014) en el Laboratorio de Ingeniería Química en la Universidad de Toulouse III-Paul Sabatier bajo la supervisión de Jean Christophe Remigy.

A continuación se listan las contribuciones científicas publicadas (1-4) y en proceso de revisión (5):

a) Artículos en revistas científicas:

1. Gomez-Coma L., Garea, A., Irabien A., Carbon dioxide capture by [emim][Ac] ionic liquid in a polysulfone hollow fiber membrane contactor, *Int. J. Greenh. Gas Control.* **2016**, 52, 1-9. Índice de impacto: 4.064. Cuartil: Q1; Ingeniería Medioambiental 10/50.
2. Gomez-Coma L., Garea A., Rouch J.C., Savart T., Lahitte J.F., Remigy J.C., Irabien A., Membrane modules for CO<sub>2</sub> capture based on PVDF hollow fibers with ionic liquids immobilized, *J. Membr. Sci.* **2016**, 498, 218-226. Índice de impacto: 5.557. Cuartil: Q1; Ingeniería Química 7/135.
3. Gomez-Coma L., Garea, A., Irabien A., Non-Dispersive absorption of CO<sub>2</sub> in [emim][EtSO<sub>4</sub>] and [emim][Ac]: Temperature influence, *Sep. Purif. Technol.* **2014**, 132, 120-125. Índice de impacto: 3.299. Cuartil: Q1; Ingeniería Química 21/135.
4. Gomez-Coma L., Garea, A., Irabien A., Hybrid solvent ([emim][Ac]+water) to improve the CO<sub>2</sub> capture efficiency in a PVDF hollow fiber contactor. *ACS Sustain. Chem. Eng.* **2016**, aceptado, octubre 2016. Índice de impacto: 5.267. Cuartil: Q1; Ingeniería Química 9/135.
5. Gomez-Coma L., Garea, A., Irabien A. PVDF Membrane contactor for CO<sub>2</sub> capture using the ionic liquid [emim][Ac]: mass transfer analysis. *Chem. Eng. Technol.* **2016**, en proceso de revisión. Índice de impacto: 2.385. Cuartil: Q2; Ingeniería Química 39/135.



- 
- b) Contribuciones a congresos publicadas en libros (*Proceedings*) con ISBN:
1. Gomez-Coma L., Casado-Coterillo C., Garea A., Irabien A. CO<sub>2</sub> absorption using PVDF self-made membrane contactors and [emim][Ac] ionic liquid. 10th European Congress of Chemical Engineering (ECCE10). 27 septiembre - 1 octubre 2015, Niza (Francia) ISBN: 978-2-910239-82-4. Comunicación poster.
  2. Gomez-Coma L., Garea A., Irabien A. Acoplamiento de la etapa de desorción a una planta de absorción no dispersiva. XXXV Reunión Bienal de la Real Sociedad Española de Química. 19-23 julio 2015, La Coruña (España). ISBN: 978-84-606-9786-2. Comunicación oral.
  3. Gomez-Coma L., Albo J., Garea A., Irabien A. CO<sub>2</sub> capture using polysulfone membrane contactor and [emim][Ac] ionic liquid. XXI International Conference on Chemical Reactors CHEMREACTOR-21. 22-25 septiembre 2014, Delf (Holanda). ISBN: 978-5-906376-06-0 Comunicación poster.
  4. Gomez-Coma L., Casado-Coterillo C., Garea A., Irabien A. Temperature effect in polypropylene and polysulfone hollow fibre membrane contactors using ionic liquids. 21st Int. Congress of Chemical and Process Engineering CHISA. 23-27 agosto 2014, Praga (República Checa). ISBN: 978-80-02-02555-9. Comunicación poster.
  5. Gomez-Coma L., Santos E., Garea A., Irabien A., Rouch J.C., Lahitte J.F., Remigy J.C. Manufacture of membrane contactors for CO<sub>2</sub> absorption. The ANQUE•ICCE•BIOTEC 2014 Congresses on Chemistry, Chemical Engineering and Biotechnology. 1-4 julio 2014, Madrid (España). ISBN: 978-84-697-0726-5. Comunicación Oral.
  6. Gomez-Coma L., Garea A., Irabien A., Rouch J.C., Lahitte J.F., Remigy J.C. Characterization of different type of fibers with PVDF for CO<sub>2</sub> absorption. IX Ibero-American Congress on Membrane Science and Technology. 25-28 mayo 2014, Santander (España). ISBN: 978-84-697-0397-7. Comunicación poster y flash.
  7. Gomez-Coma L., Garea A., Irabien A. CO<sub>2</sub> capture by non-dispersive absorption in membrane contactors: enhancement factor by chemical reaction with ionic liquids. 4th International Congress on Green Process Engineering (GPE). 7-10 abril 2014, Sevilla (España). ISBN: 978-84-15107-50-7. Comunicación póster.
  8. Gomez-Coma L., Garea, A., Irabien A. Captura de CO<sub>2</sub> mediante líquidos iónicos: Influencia de la temperatura. XXXIV Reunión Bienal de la Real Sociedad Española de Química. 15-18 septiembre 2013, Santander (España). ISBN: 978-84-695-8511-5 Comunicación poster.

---

Este trabajo ha sido financiado por el Ministerio de Economía y Competitividad de España a través de los proyectos CTQ2013-48280-C3-1-R "*Desarrollo e Integración de Procesos con Membranas para la Captura y Valorización de Dióxido de Carbono*" y ENE2010-14828 "*Desarrollo de un proceso de captura y reciclado de CO<sub>2</sub>*".

Durante la ejecución del presente trabajo, Lucía Gómez Coma, ha disfrutado de una beca ERASMUS para la realización de una estancia breve de investigación de tres meses de duración en la Universidad de Toulouse III-Paul Sabatier (Francia).

Por todo ello, expresamos nuestro más sincero agradecimiento hacia dichas instituciones y entidades.

---

---

## **AGRADECIMIENTOS**

Ha llegado el momento de agradecer a mucha gente toda la ayuda y el apoyo prestado durante estos años. Sé que es imposible acordarme de todo el mundo, así que, antes de seguir, quiero disculparme por todas las ausencias.

En primer lugar, quiero agradecerle al profesor Angel Irabien haber confiado en mí y haberme dado esta oportunidad, a quien espero poder demostrarle algún día lo infinitamente agradecida que le estoy. A la profesora Aurora Garea porque me encantaría parecerme a ella, tanto personal como profesionalmente. Mi gratitud a ellos dos es infinita.

También me gustaría dar las gracias a todo el profesorado del Departamento de Ingenierías Química y Biomolecular cuyos conocimientos y consejos siempre me han resultado muy útiles.

Tampoco me quiero olvidar del personal administrativo Pilar Alesón y Rosa Álvarez por su competente y profesional labor de gestión y su predisposición a ayudar siempre.

También quiero agradecer a Beatriz Arce, por conseguir que sea más fácil nuestro trabajo.

Al profesor Jean Christophe Remigy por haberme dado la oportunidad de trabajar con su grupo y enseñarme tanto de membranas. Merci beaucoup!

A Jonathan Albo, por iniciarme en la investigación y haber tenido tanta paciencia conmigo.

A Ana, Isabel, Andrés, Gema, Mariana, Clara, Iván, Gabriel, Leticia, Paula y Manuel por todo el tiempo compartido, su ayuda y su amistad que durará en el tiempo.

A Sara, Carolina, Germán, Jenifer, Ana H., Selene, Pablo, Esther y Azucena compañeros durante casi todo este tiempo compartiendo éxitos y fracasos, días buenos y días malos.

A María y a Antonio porque, cuando he necesitado algo de ellos, siempre han tenido tiempo para escucharme y ayudarme.

A todos mis amigos que, aunque no entienden mucho lo que hago, saben que me encanta lo que hago y con eso les vale.

A mis padres porque me han dado lo más valioso que tengo: la libertad. Jamás me han impuesto nada y siempre me han hecho ver que todo tiene dos caras y que, antes de tomar decisiones o posicionarse, es necesario conocer ambas.

A Ismail porque me encanta el viaje que estamos realizando juntos cada día, y que espero que no acabe nunca.

A mi hermana Ana, porque sabe, igual que sé yo, que siempre, pase lo que pase, nos tendremos la una a la otra. A Andrés, su mitad, porque son muy felices juntos y eso me alegra.

A Maripaz porque, con su cariño, demuestra que la familia no tiene por qué ser sólo de sangre.

Y a ti, por estar leyendo estas líneas que espero que te ayuden.

*Me gustan los amigos que tienen pensamientos independientes, porque suelen hacerte ver los  
problemas desde todos los ángulos*

*Nelson Mandela (1918-2013) Abogado, activista contra el apartheid y político sudafricano*

---

# Índice

---

---

*“Lo que con mucho trabajo se adquiere, más se ama”*

Aristóteles (384-322 A.C)

Filósofo de la Antigua Grecia



---

RESUMEN/ABSTRACT .....	1
CAPÍTULO 1: PLANTEAMIENTO .....	7
1.1. Problemática del CO <sub>2</sub> .....	9
1.2. Tecnologías convencionales de absorción de CO <sub>2</sub> .....	10
1.3. Intensificación del proceso de captura de dióxido de carbono .....	13
1.3.1. Tecnología de membranas: módulos de fibras huecas .....	14
1.3.2. Líquidos iónicos .....	19
1.4. Objetivos y estructura de la Tesis .....	23
1.5. Referencias del capítulo 1 .....	25
CAPÍTULO 2: DESARROLLO .....	31
2.1. Método experimental .....	33
2.1.1. Líquidos iónicos .....	33
2.1.2. Preparación de módulos de PVDF .....	33
2.1.2.1. Materiales y métodos utilizados .....	33
2.1.2.2. Caracterización de las fibras de PVDF .....	35
2.1.2.3. Propiedades mecánicas de las fibras .....	35
2.1.2.4. Ensayos de permeabilidad .....	36
2.1.2.5. Cálculo del punto burbuja .....	36
2.1.3. Captura de CO <sub>2</sub> .....	37
2.1.4. Calculo de las resistencias que afectan al proceso .....	40
2.1.5. Modelado de la absorción de dióxido de carbono .....	43
2.2. Resultados .....	45
2.2.1 Caracterización de los módulos de fibras huecas de PVDF fabricados .....	45
2.2.1.1. Caracterización SEM de las fibras huecas .....	45
2.2.1.2. Propiedades mecánicas de las fibras huecas .....	47
2.2.1.3. Permeabilidad de las fibras huecas .....	49
2.2.1.4. Punto burbuja de las fibras huecas .....	52
2.2.2. Captura de CO <sub>2</sub> en diferentes contactores de fibras huecas empleando líquidos iónicos. Estudio de variables de operación .....	53
2.2.2.1. Resultados experimentales de Eficacia de captura de CO <sub>2</sub> . Influencia de la temperatura .....	53
2.2.2.2. Aproximación al modelado del proceso: cálculo de resistencias en serie y coeficiente global de transferencia de materia .....	57
2.2.3. Simulación y modelado del proceso de captura de CO <sub>2</sub> en contactores de fibras huecas .....	62
2.2.3.1. Descripción del proceso mediante el modelo de difusión convección 2D .....	63
2.2.3.2. Análisis de sensibilidad .....	65
2.2.3.3. Factor de intensificación .....	69
2.3. Nomenclatura usada en el capítulo 2 .....	71
2.4. Referencias del capítulo 2 .....	72

---

CAPÍTULO 3: CONCLUSIONES/CONCLUSIONS.....	79
3.1. Conclusiones.....	81
3.2. Trabajo futuro.....	84
3.1. Conclusions.....	85
3.2. On going-research.....	88
CAPÍTULO 4: ARTÍCULOS CIENTÍFICOS/SCIENTIFIC ARTICLES .....	89
4.1. Gómez-Coma L., Garea A., Irabien A., Non-dispersive absorption of CO <sub>2</sub> in [emim][EtSO <sub>4</sub> ] and [emim][Ac]: Temperature influence. Sep. Purif. Technol. 2014, 132, 120-125. ....	91
4.2. Gómez-Coma L., Garea A., Rouch J.C., Savart T., Lahitte J.F., Remigy L.C., Irabien A., Membrane modules for CO <sub>2</sub> capture based on PVDF hollow fibers with ionic liquids immobilized. J. Membr. Sci. 2016, 498, 218-226. ....	99
4.3. Gómez-Coma L., Garea A., Irabien A., Carbon dioxide capture by [emim][Ac] ionic liquid in a polysulfone hollow fiber membrane contactor. Int. J. Greenh. Gas Control. 2016, 52, 1-9. ....	111
4.4. Gómez-Coma L., Garea A., Irabien A., Hybrid solvent ([emim][Ac]+water) to improve the CO <sub>2</sub> capture efficiency in a PVDF hollow fiber contactor. ACS Sustain. Chem. Eng. 2016. Accepted paper.....	123
4.5. Gómez-Coma L., Garea A., Irabien A., PVDF membrane contactor for CO <sub>2</sub> capture using the ionic liquid [emim][Ac]: mass transfer analysis. Chem. Eng. Technol. 2016. under review. ....	141
Anexo: Difusión de resultados en congresos.....	167

# Resumen

---

---

## Abstract

*“Ciencia es todo aquello sobre lo cual siempre cabe discusión”*

José Ortega y Gasset (1883-1955)

Filósofo y ensayista español



**Resumen/Abstract**

La disminución de las emisiones de dióxido de carbono es uno de los principales retos del siglo XXI para paliar el impacto de los gases de efecto invernadero producidos en la combustión de combustibles fósiles en procesos industriales y de generación de energía. Desde 1750 la concentración de CO<sub>2</sub> en la atmósfera ha aumentado en más de 100 ppm llegando a situarse en la actualidad en torno a los 400 ppm. La captura y almacenamiento o utilización de carbono es considerada, como una de las tecnologías más prometedoras para reducir las emisiones atmosféricas de carbono.

Entre todas las tecnologías existentes para la captura de CO<sub>2</sub>, este trabajo está centrado en la post-combustión. La captura de gases de post-combustión, por lo general, trabaja a presión ambiente y a una temperatura entre 318 y 352K, con una composición de CO<sub>2</sub> de la corriente de entrada en torno a un 15%. En este contexto, la presente Tesis Doctoral, sustituye (i) el absorbedor tradicional por contactores de membranas de fibras huecas y (ii) los absorbentes tradicionales por líquidos iónicos, para llevar a cabo una absorción no dispersiva con cero emisiones de disolvente.

Se ha llevado a cabo la preparación y caracterización de módulos de fibras huecas de PVDF con y sin líquidos iónicos inmovilizados; se ha realizado un estudio del proceso en función de distintas variables, claves en los procesos de captura tales como caudal de gas, temperatura y material de las fibras; una evaluación para determinar el coeficiente global de transferencia de materia así como de las distintas resistencias que afectan al proceso y finalmente, un modelado del proceso para determinar los parámetros del modelo y estimar el factor de intensificación que proporcione esta tecnología de membranas aplicada a la captura de CO<sub>2</sub> de gases de postcombustión.

A lo largo de la presente Tesis Doctoral, se han utilizado módulos de fibras huecas de escala laboratorio de polipropileno, de PVDF y polisulfona. Para la absorción no dispersiva de CO<sub>2</sub>, se han utilizado los líquidos iónicos 1-etil-3-metilimidazolio etilsulfato [emim][EtSO<sub>4</sub>], (por su baja viscosidad, bajo coste y baja toxicidad) y 1-etil-3-metilimidazolio acetato [emim][Ac] (por su alta solubilidad al CO<sub>2</sub>), así como este último con distintas cantidades de agua (que permiten reducir la viscosidad).

Se ha realizado un estudio que contribuye al progreso de la captura de dióxido de carbono, consiguiendo resultados novedosos competitivos en relación con el estado actual de la investigación en la aplicación de la tecnología de membranas para la absorción no-dispersiva de CO<sub>2</sub>, además de dar las claves para lograr un proceso también competitivo respecto a los procesos convencionales que emplean columnas de absorción con aminas.

El reto actual se traslada a la implantación industrial de la tecnología de membranas para llevar a cabo la absorción no-dispersiva de CO<sub>2</sub>, evitando de este modo los problemas asociados a (i) la pérdida de solvente (y contaminación asociada), y (ii) el elevado coste energético del proceso.

**Resumen/Abstract**

The mitigation of carbon dioxide emissions is one of the main challenges of the 21<sup>st</sup> century to alleviate the impact of greenhouse gases produced from combustion fossil fuels in industrial processes and power generation. Since 1750, CO<sub>2</sub> concentration in the atmosphere has increased by more than 100 ppm. Nowadays this value is around 400 ppm. Carbon capture and storage or valorization is considered, as one of the most promising technologies to reduce atmospheric carbon emissions.

Among all existing CO<sub>2</sub> capture technologies, this work is focused on the post-combustion. Post-combustion gas capture is usually performed at ambient pressure and temperature between 318 and 352K. The CO<sub>2</sub> composition in the gas stream is around 15%. In this context, this thesis, replaces (i) the conventional absorption tower by hollow fiber membrane contactors and (ii) the traditional absorbents by ionic liquids, to carry out a non-dispersive absorption with zero solvent emissions.

The preparation and characterization of PVDF hollow fiber modules with and without immobilized ionic liquids has been carried out. Moreover, a study of the influence of key variables in capture processes such as gas flow rate, temperature and fiber material has been conducted. An assessment to determine the overall mass transfer coefficient and the different resistances that affect the process has also been carried out. Finally, the process has been modelled with the aim of determining the module parameters and the intensification factor for CO<sub>2</sub> capture of post-combustion gases.

Throughout this thesis, different modules of different materials have been used in an experimental set-up at laboratory scale for CO<sub>2</sub> non-dispersive absorption: polypropylene, PVDF and polysulfone. As solvents two different ionic liquids have been used: 1-ethyl-3-methylimidazolium ethylsulfate [emim][EtSO<sub>4</sub>] (due to its low viscosity, low cost and low toxicity) and 1-ethyl-3-methylimidazolium acetate [emim][Ac] (because of its high CO<sub>2</sub> solubility). The effect of the addition of different amounts of water to [emim][Ac] (to reduce its viscosities) was also analyzed.

This work contributes to the progress of the carbon dioxide capture, achieving innovate values related to the state of the art of the non-dispersive absorption for CO<sub>2</sub> capture. Moreover, the thesis also gives the keys to accomplish a competitive process compared with the conventional processes operated in absorption towers with amines.

Based on the results obtained in this thesis the challenge is transferred to the industrial implementation of membrane technology in order to accomplish a non-dispersive CO<sub>2</sub>

absorption, avoiding the problems associated with (i) solvent losses (and associated pollution), and (ii) the high energy cost of the conventional process.

# Planteamiento

---

---

*“La ciencia siempre vale la pena porque sus descubrimientos, tarde o temprano, siempre se aplican”*

Severo Ochoa (1905-1993)

Médico español premio Nobel de medicina (1959)

---



## **CAPITULO 1: PLANTEAMIENTO**

### **1.1. Problemática del CO<sub>2</sub>**

El dióxido de carbono es un gas de efecto invernadero que contribuye al cambio climático global. La eliminación de este gas junto con los demás gases ácidos es uno de los grandes objetivos del siglo XXI (Khaisri et al., 2011). En este sentido, el quinto Panel Intergubernamental sobre el Cambio Climático (IPCC, por sus siglas en inglés) alertó acerca de la necesidad de recortar las emisiones de CO<sub>2</sub> en un rango entre 50-80% para el año 2050 con el fin de evitar un daño irreversible por el aumento de la concentración de CO<sub>2</sub> en la atmósfera (Fang et al., 2015). La mitigación del Cambio Climático es uno de los principales retos del siglo XXI recogido en la "Estrategia Española de Ciencia y Tecnología 2013-2020. Ejes Prioritarios" y en el Programa HORIZONTE 2020 de la Unión Europea.

La concentración de dióxido de carbono en la atmósfera ha aumentado de manera significativa en los últimos años pasando de 280 ppm en la era pre-industrial (1750), a los 367 ppm en 1999 y llegando a 384 ppm en 2007 lo que equivale a un aumento de más de 100 ppm (Luis et al., 2012; Zhao et al., 2016). Además, si no se llevasen a cabo medidas para la mitigación de las emisiones de dióxido de carbono, se estima que este valor podría llegar a estar entre los 540 y los 970 ppm para el año 2100 (Liu et al., 2016). Este aumento de CO<sub>2</sub> en la atmósfera proviene tanto de las emisiones antropogénicas como de las naturales, sin embargo hay evidencias de que este aumento atmosférico global se debe principalmente a las emisiones de CO<sub>2</sub> de la combustión de combustibles fósiles, la quema de gas y la producción de cemento. A nivel mundial, las centrales eléctricas alimentadas mediante combustibles fósiles son las mayores fuentes de emisiones de CO<sub>2</sub> (Mansourizadeh and Ismail, 2011; Luis et al., 2012; Mansourizadeh et al., 2014; Saeed and Deng, 2015).

La captura y almacenamiento de carbono (CCS por sus siglas en inglés) es considerada, en la actualidad, como una de las tecnologías más prometedoras para reducir las emisiones atmosféricas de carbono y se prevé que, gracias a ella, en el año 2050 se podrá reducir en un 14% las emisiones de gases de efecto invernadero provocados por el hombre (Roussanaly et al., 2016). El proceso CCS consta de tres etapas: la captura, en la que el dióxido de carbono es separado de los otros componentes, concentrado y comprimido a 100-150 bares; el transporte, que se puede realizar mediante tuberías, barco o tren y finalmente, el almacenamiento, donde el gas es aislado (Rao y Rubin, 2002; Rubin et al., 2012).

Si bien la captura de CO<sub>2</sub> mediante disolventes es la tecnología más madura y desarrollada, existen otras tecnologías emergentes para la captura, como las membranas, la separación criogénica, y la adsorción. Entre todas ellas la captura de CO<sub>2</sub> a base de membranas está considerada como una de las opciones más prometedoras (IEAGHG, 2014; Roussanaly et al., 2016).

Por otra parte, el CO<sub>2</sub>, como fuente de carbono, tiene el potencial para ser usado en la fabricación de combustibles, carbonatos, polímeros y productos químicos. La Captura y la Utilización de Carbono o la Utilización de Dioxido de Carbono (CCU y CDU por sus siglas en inglés) pueden representar una contribución a una nueva economía circular en la que el CO<sub>2</sub> se use como materia prima en sustitución de productos derivados del carbón, petróleo o gas natural (European Commission, 2016). Estas tecnologías tienen beneficios potenciales tales como la reducción de emisiones, la seguridad energética y la innovación industrial, por lo que está más que justificado el creciente interés de la investigación. Además, la opción CCU puede servir de apoyo para la implantación de la captura y almacenamiento de dióxido de carbono, mediante la creación de ingresos adicionales que pueden compensar parcialmente los costes de establecer una cadena de CCS (Hendriks et al., 2013).

## 1.2. Tecnologías convencionales de absorción de CO<sub>2</sub>

Tres son los sistemas básicos para la captura de dióxido de carbono derivados del uso de combustibles fósiles y/o biomasa: pre-combustión, oxy-combustión y post-combustión (Kunze and Spliethoff 2012). La Figura 1.1, muestra un esquema de estas tres rutas con sus principales características adaptado de los textos de Merkel et al. (2010), Singh et al., (2011) y Sanders et al., (2014).

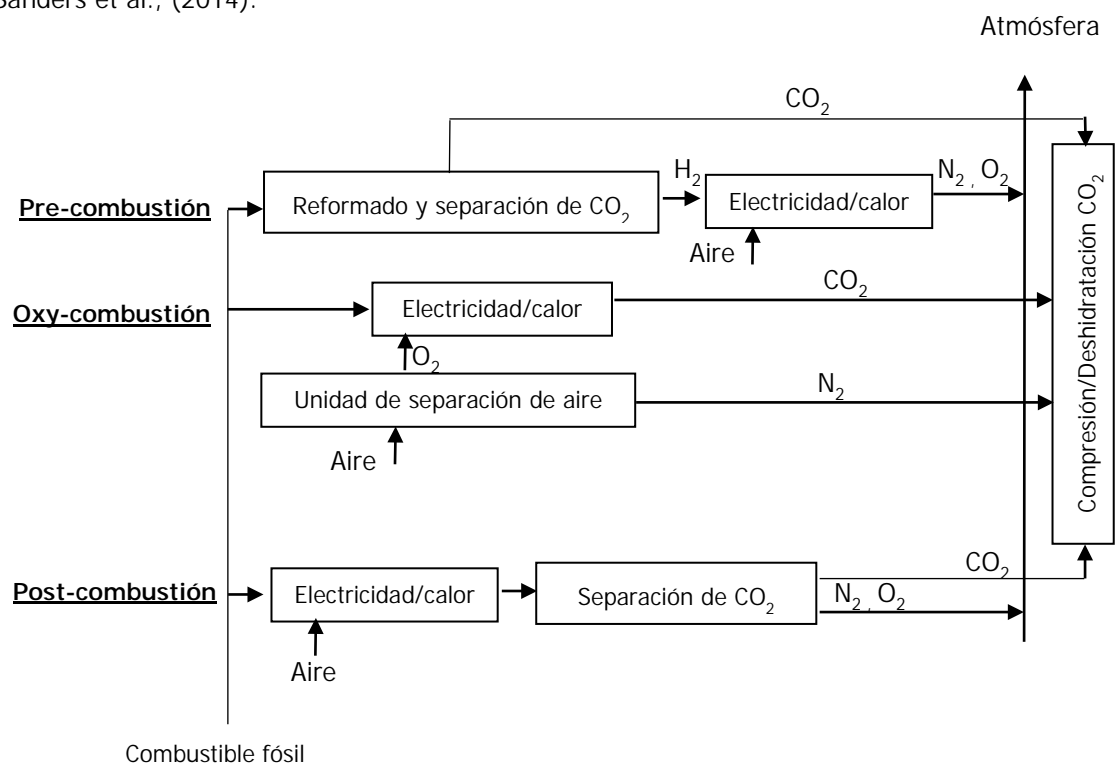


Figura 1.1: Esquema de las tres rutas de captura de CO<sub>2</sub> derivados del uso de combustibles fósiles.

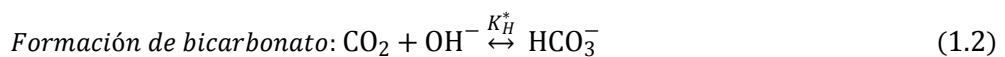
- Pre-combustión: En este tipo de separación el CO<sub>2</sub>, a presiones elevadas, es separado del gas de síntesis (principalmente H<sub>2</sub> y CO) antes de que éste vaya a la turbina de combustión. Se trata de una técnica utilizada mayoritariamente en plantas de gasificación.
- Oxy-combustion: En este caso el oxígeno es separado del aire antes de la combustión y se produce un efluente de salida de alta concentración de CO<sub>2</sub> listo para almacenar.
- Post-combustión: El CO<sub>2</sub>, a baja presión parcial, es separado de la corriente de gas (principalmente N<sub>2</sub>) después de que el combustible haya sido quemado completamente.

La Tabla 1.1, presenta a modo de resumen, las distintas características principales de los tres sistemas básicos para la captura de CO<sub>2</sub> (editado de Favre, 2011).

Tabla 1.1: Principales características de las tres rutas para la captura de CO<sub>2</sub>.

Captura de CO <sub>2</sub>	Mezcla Principal	Condiciones	Proceso separación 1ª generación	Tecnología emergente
Pre-combustión	CO <sub>2</sub> /H <sub>2</sub>	P ≤ 80 bar T = 573-973K	Absorción gas-líquido en solventes físicos	Reactor de membranas
Oxy-combustión	O <sub>2</sub> /N <sub>2</sub>	P = 1 bar T = ambiente	Criogénico	Transferencia iónica de membranas para separar O <sub>2</sub>
Post-combustión	CO <sub>2</sub> /N <sub>2</sub>	P = 1 bar T = 318-523K	Absorción gas-líquido en solventes químicos	Membrana de separación de gases

En el proceso tradicional de post-combustión, la corriente de gases generada en la combustión se compone principalmente de entre 10-16% de CO<sub>2</sub>, entre un 70-75% de N<sub>2</sub>, 5-7% de H<sub>2</sub>O y otros componentes en menores proporciones (O<sub>2</sub>, CO, NO<sub>x</sub>, SO<sub>x</sub>...) (Ramdin et al., 2012; Zhao et al., 2016). Como absorbentes, se utilizan alcanolaminas en solución acuosa, principalmente una primaria como la monoetilamina (MEA). Las reacciones con el CO<sub>2</sub> que se producen en las soluciones acuosas de alcanolaminas primarias se muestran a continuación (Liu et al., 2014):



El sistema por su parte, consta de dos columnas (Puxty et al., 2009 Luis et al., 2012); la primera en la que se produce la absorción y la segunda en la que se produce la desorción. En la primera de ellas el gas se introduce por la parte inferior de la columna y el MEA por la parte superior. Las dos corrientes se ponen en contacto a presión atmosférica y en modo contracorriente, generalmente a baja temperatura, entre 318 y 353K. Una vez que se ha producido la absorción, la solución de amina rica en CO<sub>2</sub> pasa a la segunda columna, la cual

opera a alta temperatura (393K aproximadamente). A esta temperatura, el dióxido de carbono absorbido se libera y sale a través de la parte superior de la columna. Además la solución de amina regenerada se recircula de nuevo a la columna de absorción. El diagrama de flujo simplificado del proceso empleado se muestra en la Figura 1.2 (editado de Ramdin et al., 2012 y Khalilpour et al., 2015).

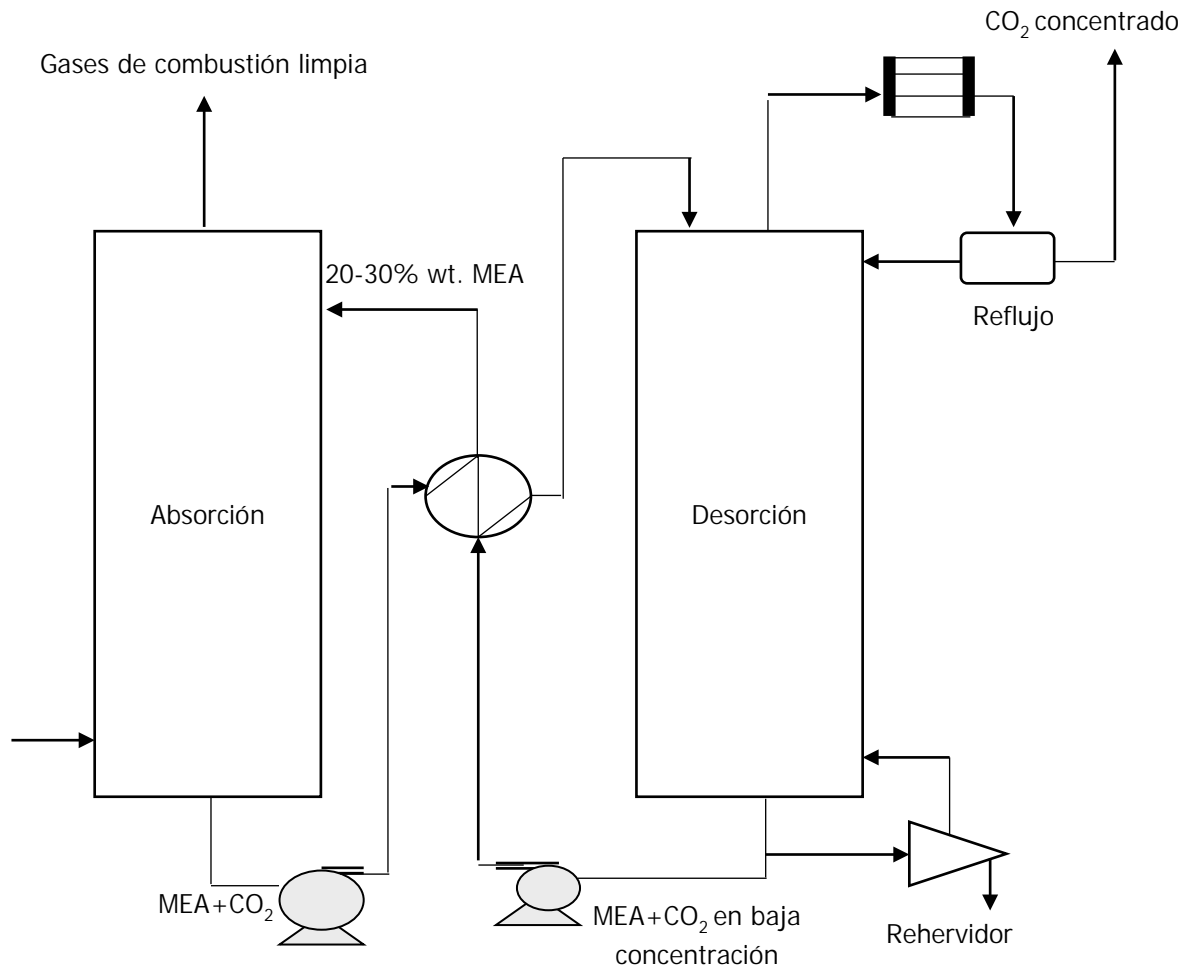


Figura 1.2: Diagrama del proceso tradicional de absorción-desorción de CO<sub>2</sub>.

Aunque este proceso tiene grandes ventajas, como una alta capacidad de absorción por parte de las aminas, altas eficacias (mayores al 90%) y una alta estabilidad térmica, tiene importantes desventajas tales como, gran tamaño de los equipos, pérdida, arrastre, vaporización y degradación química del disolvente y un alto consumo de energía. Esto último, el coste del consumo de energía, es la principal barrera para comercializar la captura de CO<sub>2</sub> y el proceso de almacenamiento a gran escala. La captura de CO<sub>2</sub> con aminas implica una reacción química con una gran entalpía de reacción y, en consecuencia, se requiere una gran cantidad de calor para liberar el CO<sub>2</sub> capturado en la etapa de regeneración.

El consumo de energía para la captura de CO<sub>2</sub> en un proceso convencional de absorción con aminas, en concreto, con MEA 30% acuosa, asumiendo un 90% de captura, se sitúa en el

intervalo de 2,5-3,6 GJ/ton CO<sub>2</sub>, y los costes asociados al proceso de captura están en el intervalo de \$50-150/ton CO<sub>2</sub> (Ramdin et al., 2012). En relación a los costes de captura de CO<sub>2</sub>, se han de tener en cuenta los valores que se plantean como objetivos a no superar en la implantación de las alternativas tecnológicas, como por ejemplo, el objetivo indicado por la DOE para el año 2025 de \$40/ton CO<sub>2</sub>.

### **1.3. Intensificación del proceso de captura de dióxido de carbono**

Actualmente, la absorción mediante torres de absorción a base de aminas es la tecnología líder para la captura de dióxido de carbono, ocupando más del 90% del mercado (Zhao et al., 2016). La eliminación de pérdidas en el disolvente manteniendo los valores de eficacia que ofrecen los sistemas tradicionales se propone en este estudio mediante dos estrategias de intensificación. Por un lado, mediante la sustitución de los equipos convencionales de contacto dispersivo, por módulos de membrana de fibras huecas que permitan un transporte selectivo y eficiente de componentes específicos mejorando el desarrollo de procesos reactivos y por otro lado, mediante la sustitución de los disolventes convencionales basados en aminas, por absorbentes de baja volatilidad como son los líquidos iónicos (ILs por sus siglas en inglés). La Figura 1.3 muestra el esquema propuesto de intensificación del proceso de absorción de CO<sub>2</sub>.

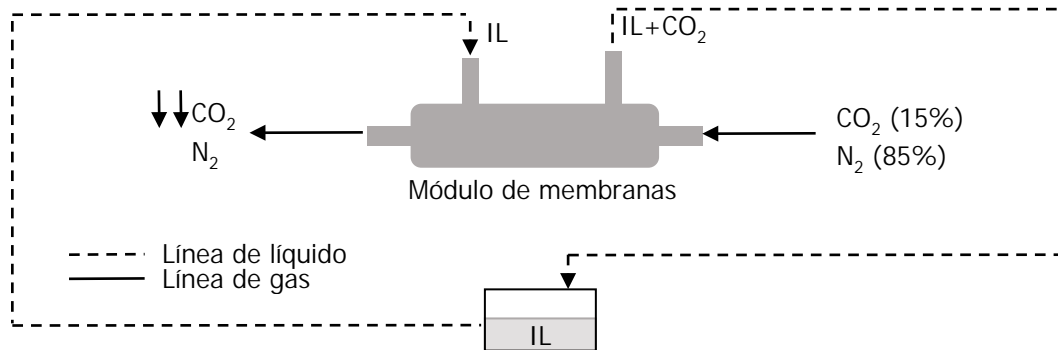


*Figura 1.3: Propuesta de intensificación del proceso de absorción de CO<sub>2</sub> mediante módulo de membranas y líquidos iónicos objeto de este estudio*

### **1.3.1. Tecnología de membranas: módulos de fibras huecas**

Los procesos de captura de dióxido de carbono tradicionales, requieren la aplicación de altas temperaturas para la regeneración del disolvente, así como para la concentración de CO<sub>2</sub>, lo que plantea como inconveniente principal el consumo de energía. Por ello, la búsqueda de nuevos métodos de absorción innovadores que mejoren las características de los sistemas tradicionales ha sido objeto de estudio durante los últimos años. Los contactores de membranas de fibras huecas han sido considerados tradicionalmente como una de las estrategias más prometedoras para lograr la captura de CO<sub>2</sub> mediante absorción de gas-líquido (Fearon et al., 1992).

Un contactor de membranas es un dispositivo que permite la transferencia de materia entre dos sistemas gas/líquido, líquido/líquido o gas/gas sin dispersión de una fase en otra. La Figura 1.4 muestra un esquema de un contactor de membranas de fibras huecas.

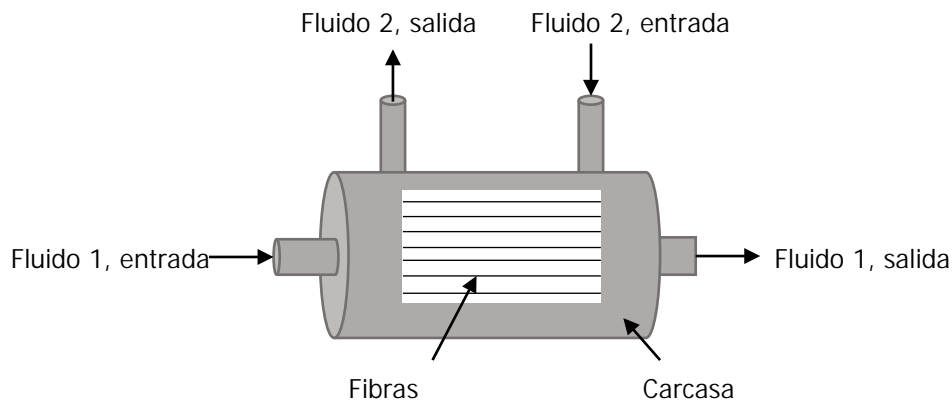


*Figura 1.4: Módulo de membranas de fibras huecas.*

Los módulos de fibras huecas se han utilizado para multitud de aplicaciones tales como extracción líquido/líquido, destilación, pertracción, ultrafiltración-nanofiltración-ósmosis inversa, pervaporación, electrodiálisis o absorción. Este tipo de sistemas ofrecen numerosas ventajas entre las que destacan (Mavroudi et al., 2006; Rongwong et al., 2009; Lin et al., 2009a; Lin et al., 2009b; Albo et al., 2010; Luis et al., 2012; Zhang y Wang, 2013):

- Flexibilidad operacional: Cada una de las fases fluye a través de un lado del módulo (fibras o carcasa) gracias a lo cual se tiene un control independiente de los flujos. Esto es especialmente ventajoso para evitar los problemas típicos, de los sistemas tradicionales como columnas de relleno y torres de absorción, inundaciones, formación de espuma, corrosión, canalización y arrastre.

- Economía: Debido a la naturaleza compacta de los contactores de membrana de fibras huecas, poseen una gran área de contacto por unidad de volumen por lo tanto son menos voluminosos y mucho más económicos que los sistemas tradicionales.
- Escalado lineal: La modularidad hace que los diseños de estos sistemas de absorción sea simple y fácil.
- Facilidad de predicción: El área interfacial es conocida y constante por lo que es más fácil predecir el rendimiento de un contactor de membrana.

Algunos trabajos ya han cuantificado los beneficios de utilizar módulos de membranas, entre los que se destacan: ahorro en los costes de funcionamiento: 38-42%; reducción en el peso en seco del equipo: 32-37%; reducción del peso del equipo de funcionamiento: 34-40%; ahorro total del peso en seco: 44-47%; ahorro total del peso en operación: 44-50%; y ahorro del coste total: 35-40% (Falk-Pedersen et al., 2005; Zhao et al., 2016).

Los módulos de fibras huecas están formados por una carcasa que contiene en su interior un conjunto de fibras unidas entre sí mediante un material de sellado (normalmente resina epoxi). Por lo general, el contactor de fibras huecas opera con los fluidos fluyendo en contracorriente en configuración paralela (Luis et al., 2012), sin embargo, en ocasiones se utilizan contactores de flujo cruzado (Albo et al., 2010). Una de las dos fases circula por el interior de las fibras (generalmente la menos viscosa) y la otra por el exterior, la carcasa (Levenspiel, 1993). El contacto entre ambas fases tendrá lugar por tanto en la boca de los poros de las fibras.

Entre los materiales que se utilizan para las membranas, los más comunes son el polipropileno (PP) (Bottino et al., 2008; Zhang et al., 2008; Lu et al., 2009; Ly et al., 2012; Albo e Irabien 2012; Wang et al., 2013; Zhang et al., 2015), fluoruro de polivinilideno (PVDF) (Lin et al., 2008; Zhang et al., 2008; Mansourizadeh et al., 2012; Fashandi et al., 2016) y polisulfona (Ps) (Mansourizadeh e Ismail, 2010; Korminouri et al., 2015). La Tabla 1.2 muestra ejemplos de mezcla de la corriente de gas, así como los distintos absorbentes referidos por otros investigadores que han utilizado contactores de membrana de fibras huecas.

Tabla 1.2: Captura de CO<sub>2</sub> mediante el contacto no dispersivo utilizando membranas microporosas: ejemplos de materiales de las fibras huecas y los absorbentes.

Material Fibras	Mezcla Principal	Absorbente*	Referencia
PP	15%CO <sub>2</sub> /85%N <sub>2</sub>	MEA	Bottino et al., 2008
PP	20%CO <sub>2</sub> /80%N <sub>2</sub>	Agua	Zhang et al., 2008
PP	20%CO <sub>2</sub> /80%N <sub>2</sub>	DEA	Zhang et al., 2008
PP	10%CO <sub>2</sub> /90%N <sub>2</sub>	Glycin salt	Lu et al., 2009
PP	20%CO <sub>2</sub> /80%N <sub>2</sub>	MEA	Lv et al., 2012
PP	8.8–41.4% CO <sub>2</sub> /N <sub>2</sub>	[emim][EtSO <sub>4</sub> ]	Albo e Irabien., 2012
PP	14%CO <sub>2</sub> /86%N <sub>2</sub>	MEA, DEA, MDEA, AMP, MDEA/Pz	Wang et al., 2013
PP	12%CO <sub>2</sub> /88%N <sub>2</sub>	MEA	Zhang et al., 2015
PVDF	8.8–41.4% CO <sub>2</sub> /N <sub>2</sub>	Pz-AMP	Lin et al., 2008
PVDF	20%CO <sub>2</sub> /80%N <sub>2</sub>	Agua	Zhang et al., 2008
PVDF	20%CO <sub>2</sub> /80%N <sub>2</sub>	DEA	Zhang et al., 2008
PVDF	CO <sub>2</sub> /N <sub>2</sub>	Agua	Mansourizadeh, 2012
PVDF	CO <sub>2</sub>	Agua	Fashandi et al., 2016
Ps	CO <sub>2</sub>	Agua	Mansourizadeh e Ismail, 2010
Ps	CO <sub>2</sub>	Agua	Korminouri et al., 2015
PEEK	13%CO <sub>2</sub> /87%N <sub>2</sub>	MDEA, DEA	Li et al., 2013
PDMS	CO <sub>2</sub> /CH <sub>2</sub>	Agua	Heile et al., 2014

\*Acrónimos: [emim][EtSO<sub>4</sub>]: 1-etil-3-metilimidazolio etilsulfato; MEA: Monoetanolamina; DEA: Dietanolamina; MDEA: metildietanolamina; AMP: 2-amino-2-metil-1-propanol; Pz: piperazina.

A altas temperaturas, las propiedades de los polímeros cambian drásticamente. Por ello es importante conocer la temperatura de transición vítrea, T<sub>g</sub> de los polímeros amorfos o el punto de fusión, T<sub>m</sub> de los polímeros cristalinos, ya que el material de la membrana puede sufrir degradación o descomposición. La T<sub>g</sub> de un polímero se determina a través de su estructura química, la flexibilidad e interacción de la cadena. Tanto el polipropileno como el fluoruro de polivinilideno tienen un valor de T<sub>g</sub> muy bajo, de 258K y 233K respectivamente, lo que puede contribuir a la inestabilidad y problemas de mojado en la membrana. La polisulfona, en cambio tiene un alto valor de T<sub>g</sub> muy alto, 463K, por lo que es mucho más estable y un polímero a tener en cuenta si se quiere recrear las condiciones reales de los procesos de post-combustión, especialmente la etapa de desorción ya que ésta a menudo se lleva a cabo a altas temperaturas (Li y Chen 2005).

Por su parte, la aplicación de contactores de membranas de fibras huecas ya está implementada a escala gran planta piloto, como se recoge en la Tabla 1.3 (Zhao et al., 2016), en la que se recogen 4 instalaciones que están en marcha. Cabe destacar que en la planta de Australia observaron que los contactores de membranas de PP sufrieron graves problemas de

mojado. Los módulos de Politetrafluoroetileno (PTFE) por su parte también experimentaron mojado, aunque en menor medida que los de PP, y los módulos no porosos de Polidimetilsiloxano (PDMS) no tuvieron ningún problema con la humedad. Sin embargo, los valores del coeficiente global de transferencia de materia de los contactores de PDMS fueron dos órdenes de magnitud menores que los de PP. Con el fin de evitar los problemas de mojado de las fibras de PP, en el proyecto de Holanda se utiliza una solución aminoácido acuosa. El proyecto de Noruega, por su parte, ha demostrado que la tecnología de absorción no dispersiva es la mejor alternativa a las columnas de absorción convencionales, con una reducción significativa tanto en el tamaño como en el peso y en el coste. Finalmente la planta de EEUU utiliza contactores de poli éter cetona (PEEK), y logra una eficacia superior al 90% con un 95% de pureza del dióxido de carbono.

*Tabla 1.3: Ejemplos de plantas de captura de CO<sub>2</sub> basadas en contactores de membranas a nivel gran piloto, así como su ubicación.*

Material Fibras	Absorbente	Ubicación
PP	Solución aminoácida acuosa	Holanda
PTFE	MDEA	Noruega
PP, PTFE, PDMS	Disolvente comercial a base de aminoácidos	Australia
PEEK	aMDEA <sup>*</sup> /K <sub>2</sub> CO <sub>3</sub>	EEUU

*\*aMDEA: metildietanolamina activada*

El uso de contactores de fibra hueca supone añadir una nueva resistencia al transporte de materia en los sistemas de post-combustión, además de las resistencias de la fase líquida y gaseosa, la de la membrana. La Figura 1.5 muestra las distintas resistencias que aparecen en el proceso (Lu et al., 2007).

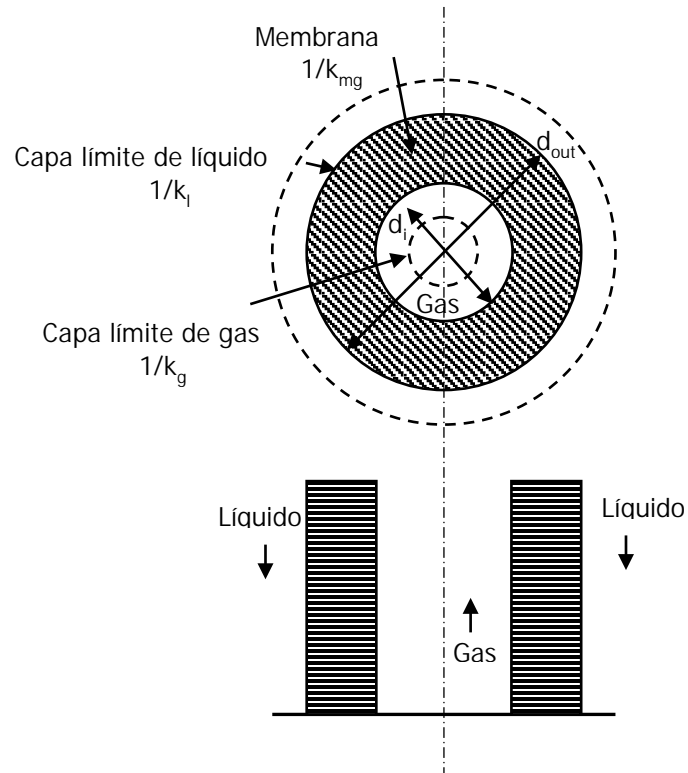


Figura 1.5: Resistencias al transporte de materia en el proceso.

La resistencia de la membrana debe ser tenida en cuenta, en aquellos casos en los que hay mojado de la membrana (Zhao et al., 2016). Cuando esto no ocurre, además de lograrse una eficacia mayor, los poros de la membrana se llenan únicamente con el gas y la resistencia de la membrana puede considerarse despreciable (Luis et al., 2007; Ortiz et al., 2010). Además, en los casos en los que no hay mojado la difusividad efectiva es varios órdenes de magnitud mayor que la resultante cuando los poros están llenos de líquido debido al mojado. La Figura 1.6 muestra de manera esquemática, el no-mojado y mojado de la membrana (adaptado de Zhao et al., 2016).

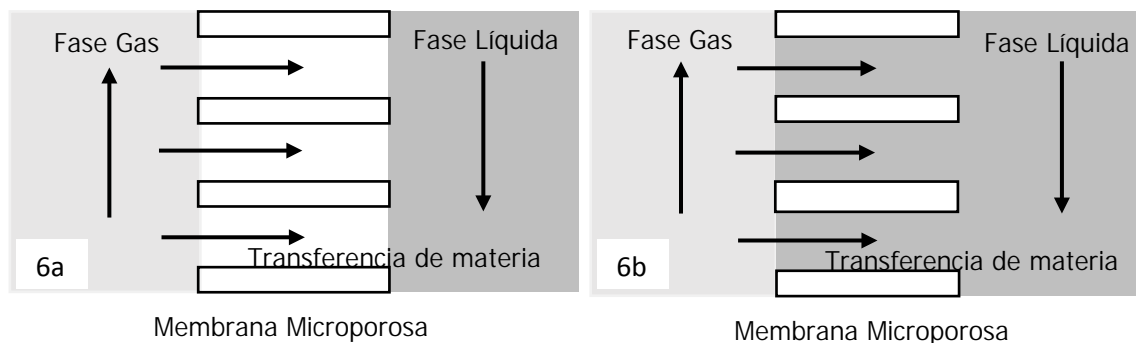


Figura 1.6: No mojado (6a) y mojado (6b) de la membrana.

El modelado y simulación del proceso resultan muy útiles para avanzar en la intensificación del proceso a nivel mayor que la escala laboratorio, ya que permiten predecir el comportamiento del sistema en diferentes condiciones de operación, realizar análisis de sensibilidad de las principales variables y cálculos de escalado, tal como se resume en la Figura 1.7 (adaptada de Zhao et al., 2016):

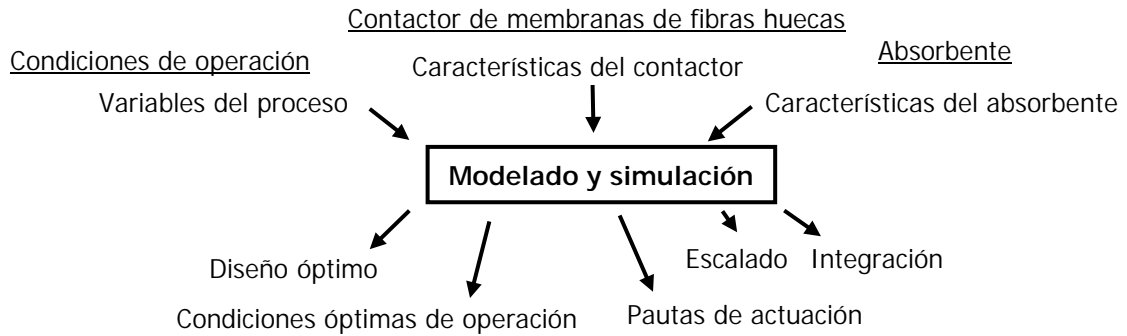


Figura 1.7: Esquema general de modelado y simulación de procesos, aplicado a la captura de CO<sub>2</sub> mediante tecnologías de membranas.

Zhao et al., (2016) recopila en su trabajo las cuatro estrategias de modelado propuestas para la descripción de los contactores de membranas de fibras huecas. La Tabla 1.4, muestra un resumen de estas estrategias con los supuestos que se tienen en cuenta.

Tabla 1.4: Resumen de las estrategias de modelado de los contactores de membranas de fibras huecas.

Estrategia de modelado	Supuestos*
Coefficiente global de transferencia de materia, $K_{overall}$	$T, P, K_{overall}, Q_g$ constantes Líquido de absorción lejos de saturación Flujo pistón en fase gas
Resistencias en serie (1D)	$T, k_g$ y $k_l$ constantes $C_1$ y $P$ variables Flujo pistón en fases gas y líquida Se considera la posibilidad de reacción química
Convección y difusión (2D)	$T$ y $P$ constantes Convección axial y difusión radial en fases gas y líquida Se considera la posibilidad de reacción química
Sistema no isoterma (2D)	$P$ constante Convección axial y difusión radial en fases gas y líquida Se considera la posibilidad de reacción química

Acronimos:  $K_{overall}$ : Coeficiente global de transferencia de materia;  $k_g$ : Coeficiente de transferencia de materia en la fase gas;  $k_l$ : Coeficiente de transferencia de material en la fase líquida.

### 1.3.2. Líquidos iónicos

Los líquidos iónicos son compuestos que están siendo considerados prometedores en los últimos años, en cuanto a disolventes se refiere, para la recuperación de dióxido de carbono

en sustitución de los solventes tradicionales como las alcanolaminas (Albo e Irabien 2012). Los ILs son sales que, por lo general, tienen un catión orgánico y un anión inorgánico lo cual permite ajustar sus propiedades físico-químicas y optimizarlos para una aplicación específica (Seddon, 1997; Freemantle 1998; Stark y Seddon, 2007). Sus ventajas más destacadas son las siguientes (Ramdin et al., 2012):

- Estabilidad térmica y baja presión de vapor: Los ILs tienen una gran estabilidad térmica por lo que no sufren degradación así como una presión de vapor insignificante (Wappel et al., 2009, Luis et al., 2009), reduciendo los posibles riesgos medioambientales asociados a la contaminación del aire. En el caso concreto de los contactores de membranas para la captura de un determinado gas, el uso de solventes fácilmente volátiles puede provocar que su vapor llene los poros e incluso penetrar en la membrana lo que perjudicaría gravemente la captura.
- Modularidad: Esta propiedad es probablemente una de las más importantes ya que permite el diseño de líquidos iónicos específicos de acuerdo a los requerimientos del proceso.
- Tensión superficial: Puesto que las membranas utilizadas generalmente para la captura de CO<sub>2</sub> son hidrófobas es recomendable usar solventes con baja tensión superficial. Lo ideal es escoger un líquido que sea incapaz de mojar la membrana, de modo que los poros se llenen únicamente de gas, incluso a presiones altas.
- Facilidad de regeneración: Gracias a esta característica los líquidos iónicos pueden ser reutilizados en numerosas ocasiones y por tanto se necesita mucha menos cantidad que con otros disolventes como las alcanolaminas.

Respecto a la selección de un líquido iónico para la separación de dióxido de carbono mediante módulos de fibras huecas es importante realizar en primer lugar un estudio de la compatibilidad química entre el IL y el material de la membrana. El mojado de la membrana, en ocasiones, puede ser causada por una reacción entre el disolvente y la membrana lo que conduce a cambios en la superficie y consecuentemente a modificaciones en la morfología de la membrana. La compatibilidad es un factor importante que decide la estabilidad a largo plazo del módulo de fibras huecas.

En la captura de dióxido de carbono, los líquidos iónicos convencionales presentan, por lo general, absorción física y los ILs funcionalizados, en cambio, suelen presentar absorción química (Gurau et al., 2011; Maginn, 2004). La modularidad de los ILs, además, permite realizar multitud de funcionalizaciones distintas, aunque el coste y la estabilidad de estas

combinaciones se convierten en consideraciones importantes. La Tabla 1.5 muestra los distintos tipos de líquidos iónicos (Boot-Handford et al., 2014).

Tabla 1.5: Tipos y ejemplos de líquidos iónicos

Tipo de Líquidos Iónicos	Ejemplos*
Carboxilados	[emim][Ac]; [bmim][Ac]
Fluorados	[bmim][BF <sub>4</sub> ]; [bmim][PF <sub>6</sub> ]
Amino funcionalizados	[aP <sub>4443</sub> ][Gly]; [aP <sub>4443</sub> ][Ala]
Reversibles	(TEtSAC); (TPSAC)
Próticos	[C <sub>1</sub> Im]Cl; [C <sub>2</sub> Im][BF <sub>4</sub> ]
Membranas soportadas	PES-[bmim][BF <sub>4</sub> ]; Ps-[hmim][Tf <sub>2</sub> N]
Poli-líquidos iónicos	(PVBIT); (PBIMT)

\*Acrónimos: [emim][Ac]: 1-etil-3-metilimidazolio acetato; [bmim][Ac]: 1-butil-3-metilimidazolio acetato [bmim][BF<sub>4</sub>]: 1-butil-3-metilimidazolio tetrafluoroborato; [bmim][PF<sub>6</sub>]: 1-butil-3-metilimidazolio hexafluorofosfato; [aP<sub>4443</sub>][Gly]: sal de ácido (3-aminopropil) fosfonio tributilo aminoetanoico; [aP<sub>4443</sub>][Ala]: sal de ácido (3-aminopropil) tributil-fosfonio l-α-aminopropiónico; (TEtSA): (3-aminopropil)-trietilsilano; (TPSAC): (3-aminopropil)-trioisopropilsilano; [C<sub>1</sub>Im]Cl: cloruro de 1-metilimidazolio; [C<sub>2</sub>Im][BF<sub>4</sub>]: tetrafluoroborato de 1-etilimidazolio; PES-[emim][BF<sub>4</sub>]: Polietersulfona-1-butil-3-metilimidazolio tetrafluoroborato; Ps-[hmim][Tf<sub>2</sub>N]: Polisulfona-1-hexil-3-metilimidazolio bis (trifluorometilsulfonil) imida; (PVBIT): poli [1- (bencil 4-vinil) -3-metilimidazolio tetrafluoroborato]; (PBIMT): poli [2- (1-butilimidazolio-3-yl) etil metacrilato tetrafluoroborato].

La Tabla 1.6, por su parte, muestra algunos ejemplos de líquidos iónicos comunes según el tipo de absorción del CO<sub>2</sub>; si es mediante fisisorción o quimisorción. Los ILs [emim][EtSO<sub>4</sub>], [bmim][Tf<sub>2</sub>N], [bmim][BF<sub>4</sub>] y [bmim][PF<sub>6</sub>] son ejemplos de fisisorción (Zarca et al., 2015; Dai et al., 2016). Sin embargo, los líquidos iónicos [N<sub>1114</sub>][Tf<sub>2</sub>N], [emim][Ac], [bmim][Ac], [P<sub>66614</sub>][Pro] son ejemplos de quimisorción ya que son capaces de formar enlaces químicos con el dióxido de carbono (Maginn, 2004; Gurau et al., 2011; Dai et al., 2016).

Tabla 1.6: Ejemplos de líquidos iónicos comunes y tipo de absorción. Valores de capacidad de absorción de CO<sub>2</sub> reportados por Maginn (2004); Gurau et al. (2011); Dai et al. (2016).

Líquido Iónico*	Tipo de absorción	Capacidad absorción CO <sub>2</sub> (mol L <sup>-1</sup> )
[emim][EtSO <sub>4</sub> ]	Fisorción	0.064
[bmim][Tf <sub>2</sub> N]	Fisorción	0.078
[bmim][BF <sub>4</sub> ]	Fisorción	0.064
[bmim][PF <sub>6</sub> ]	Fisorción	0.076
[emim][eFAP]	Fisorción	0.086
[N <sub>1114</sub> ][Tf <sub>2</sub> N]	Quimisorción	0.082
[emim][Ac]	Quimisorción	2.09
[bmim][Ac]	Quimisorción	1.57
[P <sub>66614</sub> ][Pro]	Quimisorción	0.761

\*Acrónimos: [emim][EtSO<sub>4</sub>]: 1-etil-3-metilimidazolio etilsulfato; [bmim][Tf<sub>2</sub>N]: 1-butil-3-metilimidazolio bis (trifluorometilsulfonil) imida; [bmim][BF<sub>4</sub>]: 1-butil-3-metilimidazolio tetrafluoroborato; [bmim][PF<sub>6</sub>]: 1-butil-3-metilimidazolio hexafluorofosfato; [emim][eFAP]: 1-Etil-3-methylimidazolium Tris(pentafluoroetil) trifluorofosfato; [N<sub>1114</sub>][Tf<sub>2</sub>N]: N-trimetil-N-butilamonio bis(trifluorometanosulfonil) imida; [emim][Ac]: 1-etil-3-metilimidazolio acetato; [bmim][Ac]: 1-butil-3-metilimidazolio acetato; [P<sub>66614</sub>][Pro]: trihexil (tetradecil) fosfonio prolinato.

La quimisorción del CO<sub>2</sub> en líquidos iónicos que contienen un anión carboxílico puede ser una alternativa prometedora a los procesos de aminas comunes (Blath et al., 2012, Gurau et al., 2011). El líquido iónico 1-etil-3-metilimidazolio acetato, [emim][Ac] es un ejemplo de IL capaz de formar enlaces químicos (Shiflett and Yokozeki, 2009; Gurau et al., 2011; Ramdin et al., 2012; Blath et al., 2012; Papatryfon et al., 2014). Gurau et al. (2011) propuso el posible mecanismo de reacción de este líquido iónico con el dióxido de carbono, con la formación de carboxilato, tal como se muestra en la Figura 1.8.

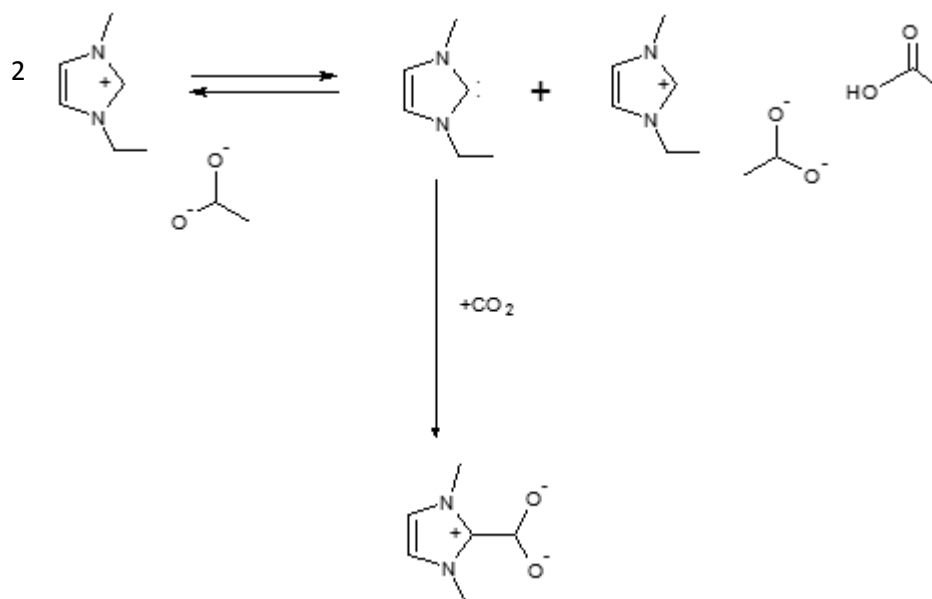


Figura 1.8: Esquema de reacción  $[emim][Ac]-CO_2$  propuesto por Gurau et al. (2011).

Finalmente, es importante seleccionar líquidos iónicos para la captura de dióxido de carbono que no sean tóxicos. Trabajos previos del grupo de investigación, Alvarez-Guerra e Irabien (2011), han abordado los aspectos de la ecotoxicidad de los ILs, que resultan de gran utilidad desde las primeras etapas del proceso de diseño de un proceso de absorción no dispersiva con ILs, para poder seleccionar aquellos que respeten el medioambiente.

#### **1.4. Objetivos y estructura de la Tesis**

La presente Tesis se ha desarrollado principalmente en el marco de dos proyectos, por una lado el denominado ENE2010-14828 "Desarrollo de un proceso de captura y reciclado de  $CO_2$ " y por otro el CTQ2013-48280-C3-1-R "Desarrollo e Integración de Procesos con membranas para la Captura y Valorización de Dióxido de Carbono", liderados por el Prof. A. Irabien y la Dra Garea, en el grupo de investigación DePro, de la Universidad de Cantabria.

El objetivo general de esta Tesis **es el desarrollo de la captura eficiente de dióxido de carbono en corrientes de gases post-combustión mediante absorción no dispersiva en módulos de fibras huecas, empleando líquidos iónicos.**

Los objetivos específicos planteados en esta Tesis se concretan en:

- Preparación y caracterización de módulos de fibras huecas basados en PVDF con distintos aditivos así como con los líquidos iónicos comerciales: 1-etil-3-metilimidazolio

etilsulfato [emim][EtSO<sub>4</sub>] y 1-etil-3-metilimidazolio acetato [emim][Ac], inmovilizados en ellas.

- Estudio de la eficacia del proceso de captura de CO<sub>2</sub> en función de la influencia del caudal de gas y la temperatura, en módulos de membranas de fibras huecas de diferentes materiales; polipropileno (PP), fluoruro de polivinilideno (PVDF) y polisulfona (Ps), en combinación con los dos líquidos iónicos comerciales [emim][EtSO<sub>4</sub>] y [emim][Ac]. Además, trabajando con el [emim][Ac] se ha estudiado la presencia de agua para calcular la cantidad de agua requerida para aprovechar las ventajas del [emim][Ac] y contrarrestar sus inconvenientes (básicamente, su alta viscosidad).
- Evaluación del coeficiente global de transferencia de materia así como de las distintas resistencias que afectan al proceso.
- Modelado del proceso con los distintos contactores, así como cálculo de los distintos parámetros del proceso necesarios para poder conseguir una eficacia competitiva (90%) con el proceso convencional (uso de torres de absorción y aminas), y el factor de intensificación que supone el proceso propuesto respecto al convencional (tomando como referencia la absorción con MEA 30% ac)

De acuerdo con los objetivos específicos, y considerando la normativa para una Tesis basada en un compendio de artículos, el presente trabajo se desarrolla en cuatro capítulos distribuidos de la siguiente forma:

- El Capítulo 1 incluye el planteamiento de la presente Tesis.
- El Capítulo 2 describe de forma detallada los materiales y métodos empleados para la realización de la Tesis, así como un resumen global de los principales resultados y la discusión de los mismos
- El Capítulo 3 resume las conclusiones generales obtenidas así como las claves para seguir desarrollando la absorción no dispersiva.
- El Capítulo 4 supone el núcleo central de la Tesis, incluyendo copia de los artículos que la sustentan.

### **1.5. Referencias del capítulo 1**

Albo J, Irabien A., Non-dispersive absorption of CO<sub>2</sub> in parallel and cross-flow membrane modules using EMISE, *J. Chem. Technol. Biotechnol.* **2012**, 87 1502–1507.

Albo J., Luis P., Irabien A., Carbon dioxide capture from flue gases using a cross-flow membrane contactor and the ionic liquid 1-ethyl-3-methylimidazolium ethylsulfate, *Ind. Eng. Chem. Res.* **2010**, 49, 11045-11051.

Alvarez-Guerra M., Irabien A., Document Design of ionic liquids: An ecotoxicity (*Vibrio fischeri*) discrimination approach, *Green Chem.* **2011**, 13(6), 1507-1516.

Blath J., Deubler N., Hirth T., Schiestel T., Chemisorption of carbon dioxide in imidazolium based ionic liquids with carboxylic anions, *Chem. Eng. J.* **2012**, 181-182, 152–158.

Boot-Handford M.E., Abanades J.C., Anthony E.J., Blunt M.J., Brandani S., Dowell N.M., Fernández J.R., Ferrari M.C., Gross R., Hallett J.P., Haszeldine R.S., Heptonstall P., Lyngfelt A., Makuch Z., Mangano E., Porter R.T.J., Pourkashanian M., Rochelle G.T., Shah N., Yoo J.G., Fennell P.S., Carbon capture and storage update, *Energy Environ. Sci.* **2014**, 7, 130.

Bottino A., Capannelli G., Comite A., Di Felice R., Firpo R., CO<sub>2</sub> removal from a gas stream by membrane contactor. *Sep. Purif. Technol.* **2008**, 59, 85-90.

Dai Z., Noble R.D., Gin D.L., Zhang X., Deng L., Combination of ionic liquids with membrane technology: A new approach for CO<sub>2</sub> separation, *J. Membr. Sci.* **2016**, 497, 1-20.

European Commission: Strategic Energy Technologies Information Systems: SETIS, **2016** (acceso: julio 2016), <https://setis.ec.europa.eu/publications/setis-magazine/carbon-capture-utilisation-and-storage>.

Falk-Pedersen O., Grønvold M.S., Nøkleby P., Bjerve F., Svendsen H.F., CO<sub>2</sub> Capture with Membrane Contactors, *Int. J. Green Energy.* **2005**, 2, 157-165.

Fang M., Ma Q., Wang Z., Xiang Q., Jiang W., Xia Z., A novel method to recover ammonia loss in ammonia-based CO<sub>2</sub> capture system: ammonia regeneration by vacuum membrane distillation, *Greenhouse Gas Sci. Technol.* **2015**, 5, 1-11.

Fashandi H., Ghodsi A., Saghafi R., Zarrebini M., CO<sub>2</sub> absorption using gas-liquid membrane contactors made of highly porous poly(vinyl chloride) hollow fiber membranes *Int. J. Greenh. Gas Control.* **2016**, 52, 13-23.

Favre E., Membrane processes and postcombustion carbon dioxide capture: Challenges and prospects, *Chem. Eng. J.* **2011**, 171, 782-793.

Feron P.H.M., Jansen A.E., Klaassen R., Membrane technology in carbon dioxide removal, *Energy Convers. Manage.* **1992**, 33(5-8), 421-428.

Freemantle M., Designer solvents. *Chem. Eng. News.* **1998**, 76(13), 32-37.

Gurau G., Rodríguez H., Kelley S.P., Janiczek P., Kalb R.S., Rogers R.D., Demonstration of chemisorption of carbon dioxide in 1,3-dialkylimidazolium acetate ionic liquids, *Angew. Chem. Int. Ed.* **2011**, 50, 12024-12026.

Heile S., Rosenberger S., Parker A., Jefferson B., Mc Adam E.J., Establishing the suitability of symmetric ultrathin wall polydimethylsiloxane hollow-fibre membrane contactors for enhanced CO<sub>2</sub> separation during biogas upgrading, *J. Membr. Sci.* **2014**, 452, 37-45.

IEAGHG, Assessment of Emerging CO<sub>2</sub> Capture Technologies and their Potential to Reduce Costs, 2014/TR4, **2014**.

Khaisri S., Montigny D., Tontiwachwuthikul P., Jiraratananona R., CO<sub>2</sub> stripping from monoethanolamine using a membrane contactor, *J. Membr. Sci.* **2011**, 376, 110-118.

Khalilpour R., Mumford K., Zhai H., Abbas A., Stevens G., Rubin E.S., Membrane-based carbon capture from flue gas: a review, *J. Clean. Prod.* **2015**, 103, 286-300.

Korminouri F., Rahbari-Sisakht M., Matsuura T., Ismail A.F., Surface modification of polysulfone hollow fiber membrane spun under different air-gap lengths for carbon dioxide absorption in membrane contactor system, *Chem. Eng. J.* **2015**, 264, 453-461.

Levenspiel O., Flujo de fluidos e intercambio de calor, Oregon State University Corvallis, Oregon. Editorial Reverté S.A. **1993**.

Li J.L., Chen B.H., Review of CO<sub>2</sub> absorption using chemical solvents in hollow fiber membrane contactors, *Sep. Purif. Technol.* **2005**, 41, 109-122.

Li S., Rocha D.J., Zhou S.J., Meyer H.S., Bikson B., Ding Y., Post-combustion CO<sub>2</sub> capture using super-hydrophobic, polyether ether ketone, hollow fiber membrane contactors, *J. Membr. Sci.* **2013**, 430, 79-86.

Lin S.H., Chiang P.C., Hsieh C.F., Li M.H., Tung K.L., Absorption of carbon dioxide by the absorbent composed of piperazine and 2-amino-2-methyl-1-propanol in PVDF membrane contactor, *J. Chin. Inst. Chem. Eng.* **2008**, 39, 13-21.

Lin S.H., Hsieh C.F., Li M.H., Tung K.L., Determination of mass transfer resistance during absorption of carbon dioxide by mixed absorbents in PVDF and PP membrane contactor, *Desalination*. **2009a**, 249, 647-653.

Lin S.H., Tung K.L., Cheng W.J., Chang H.W. Absorption of carbon dioxide by mixed piperazine–alkanolamine absorbent in a plasma-modified polypropylene hollow fiber contactor, *J. Membr. Sci.* **2009b**, 333 (1–2) 30–37.

Liu Y., Li H., Wei G., Zhang H., Li X., Jia Y., Mass transfer performance of CO<sub>2</sub> absorption by alkanolamine aqueous solution for biogas purification, *Sep. Purif. Technol.* **2014**, 133, 476–483.

Liu L., Qiu W., Sanders E.S., Ma C., Koros W., Post-combustion carbon dioxide capture via 6FDA/BPDA-DAM hollow fiber membranes at sub-ambient temperatures, *J. Membr. Sci.* **2016**, 510, 447-454.

Lu J.G., Zheng Y.F., Cheng M.D., Wang L.J., Effects of activators on mass-transfer enhancement in a hollow fiber contactor using activated alkanolamine solutions, *J. Membr. Sci.* **2007**, 289, 138-149.

Lu J., Zheng Y., Cheng M., Membrane contactor for CO<sub>2</sub> absorption applying amino-acid salt solutions, *Desalination*. **2009**, 249, 498-502.

Luis P., Ortiz I., Aldaco R., Garea A., Irabien A. Recovery of sulfur dioxide using non-dispersive absorption. *Int. J. Chem. React. Eng.* **2007**, 5, 1-9.

Luis P., Garea A., Irabien A., Zero solvent emission process for sulfur dioxide recovery using a membrane contactor and ionic liquids, *J. Membr. Sci.* **2009**, 330, 80–89.

Luis P., Van Gerven T., Van Der Bruggen B., Recent developments in membrane-based technologies for CO<sub>2</sub> capture, *Prog. Energy Combust. Sci.* **2012**, 38, 419-448.

Lv Y., Yu X., Jia J., Tu S.T., Yan J., Dahlquist E., Fabrication and characterization of superhydrophobic polypropylene hollow fiber membranes for carbon dioxide absorption, *Appl. Energy*. **2012**, 90:167-174.

Maginn E.J., Design and Evaluation of Ionic Liquids as Novel CO<sub>2</sub> Absorbents, National Energy Technology Laboratory, US, **2004**.

Mansourizadeh, A., Ismail, A.F., Hollow fiber gas liquid membrane contactors for acid gas capture: a review, *J. Hazard. Mater.* **2009**, 171, 38-53.

Mansourizadeh A., Ismail A.F., Effect of additives on the structure and performance of polysulfone hollow fiber membranes for CO<sub>2</sub> absorption, *J. Membr. Sci.* **2010**, 348, 260-267.

Mansourizadeh A., Ismail A.F., A developed asymmetric PVDF hollow fiber membrane structure for CO<sub>2</sub> absorption, *Int. J. Greenh. Gas Control.* **2011**, 5, 374-380.

Mansourizadeh A., Experimental study of CO<sub>2</sub> absorption/stripping via PVDF hollow fiber membrane contactor, *Chem. Eng. Res. Des.* **2012**, 90, 555-562.

Mansourizadeh A., Aslmahdavi Z., Ismail A.F., Matsuura T., Blend polyvinylidene fluoride/surface modifying macromolecule hollow fiber membrane contactors for CO<sub>2</sub> absorption, *Int. J. Greenh. Gas Control.* **2014**, 26, 83-92.

Mavroudi M., Kaldis S.P., Sakellaropoulos G.P., A study of mass transfer resistance in membrane gas-liquid contacting processes, *J. Membr. Sci.* **2006**, 272, 103-115.

Merkel T.C., Lin H., Wei X., Baker R., Power plant post-combustion carbon dioxide capture: An opportunity for membranes. *J. Membr. Sci.* **2010**, 359(1-2), 126-139.

Ortiz A., Gorri D., Irabien A., Ortiz I., Separation of propylene/propane mixtures using Ag<sup>+</sup>-RTIL solutions. Evaluation and comparison of the performance of gas-liquid contactors, *J. Membr. Sci.* **2010**, 360, 130-141.

Papatryfon X.L., Heliopoulos N.S., Molchan I.S., Zubeir L.F., Bezemer N.D., Arfanis M.K., Kontos A.G., Likodimos V., Iliev B., Romanos G.E., Falaras P., Stamatakis K., Beltsios K.G., Kroon M.C., Thompson G.E., Klöckner J., Schubert T.J.S., CO<sub>2</sub> capture efficiency, corrosion properties, and ecotoxicity evaluation of amine solutions involving newly synthesized ionic liquids, *Ind. Eng. Chem. Res.* **2014**, 53(30) (2014) 12083-12102.

Ramdin M., De Loos T.W., Vlught T.J.H., State-of-the-art of CO<sub>2</sub> capture with ionic liquids, *Ind. Eng. Chem. Res.* **2012**, 51, 8149-8177.

Rongwong W., Jiraratananon R., Atchariyawut S., Experimental study on membrane wetting in gas-liquid membrane contacting process for CO<sub>2</sub> absorption by single and mixed absorbents, *Sep. Purif. Technol.* **2009**, 69, 118-125.

Rao A.B., Rubin E.S., A technical, economic and environmental assessment of amine-based CO<sub>2</sub> capture technology for power plant greenhouse gas control. *Environ. Sci. Technol.* **2002**, 36, 4467-4475.

- Roussanaly S., Anantharaman R., Lindqvist K., Zhai H., Rubin E., Membrane properties required for post-combustion CO<sub>2</sub> capture at coal-fired power plants, *J. Membr. Sci.* **2016**, 511, 250-264.
- Rubin E.S., Mantripragada H., Marks A., Versteeg P., Kitchin J., The outlook for improved carbon capture technology, *Prog. Energy Combust. Sci.* **2012** 38(5), 630-671.
- Saeed M., Deng L., CO<sub>2</sub> facilitated transport membrane promoted by mimic enzyme, *J. Membr. Sci.* **2015**, 494, 196–204.
- Sanders D.F., Smith Z.P., Guo R., Robeson L.M., McGrath J.E., Paul D.R., Freeman B.D., Energy-efficient polymeric gas separation membranes for a sustainable future: A review, *Polymer.* **2013**, 54, 4729-4761.
- Seddon K.R., Ionic liquids for clean technology, *J. Chem. Technol. Biot.* **1997**, 68(4), 351-356.
- Shiflett M.B., Yokozeki A., Phase behavior of carbon dioxide in ionic liquids: [emim][acetate], [emim][trifluoroacetate], and [emim][acetate] + [emim][trifluoroacetate] mixtures, *J. Chem. Eng. Data.* **2009**, 54, 108-114.
- Singh B., Strømman A.H., Hertwich E.G., Comparative life cycle environmental assessment of CCS technologies, *Int. J. Greenh. Gas Control.* **2011**, 5, 911–921.
- Stark A., Seddon K.R., Ionic liquids, in: Kirk-Othmer Encyclopedia of Chemical Technology, *John Wiley & Sons, Inc.*, Vol. 26. **2007**, pp. 836-920.
- Wang Z., Fang M.X., Yan S.P., Yu H., Wei C.C., Luo Z.Y., Optimization of blended amines for CO<sub>2</sub> absorption in a hollow-fiber membrane contactor, *Ind. Eng. Chem.* **2013**, 52, 12170-12182.
- Wappel D., Gronald G., Kalb R., Draxler J., Ionic liquids for post-combustion CO<sub>2</sub> absorption, *Int. J. Greenh. Gas Control.* **2010**, 4, 486–494.
- Zarca G., Ortiz I., Urtiaga A., Recovery of carbon monoxide from flue gases by reactive absorption in ionic liquid imidazolium chlorocuprate(I): Mass transfer coefficients, *Chin. J. Chem. Eng.* **2015**, 23, 769-774.
- Zhang H.Y., Wang R., Liang D.T., Tay J.H., Theoretical and experimental studies of membrane wetting in the membrane gas liquid contacting process for CO<sub>2</sub> absorption, *J. Membr. Sci.* **2008**, 308, 162-170.
- Zhang Y., Wang R., Gas-liquid membrane contactors for acid gas removal: recent advances and future challenges, *Curr. Opin. Chem. Eng.* **2013**, 2(2) 255–262.

Zhang L., Ou R., Sha Y., Wang X., Yang L., Membrane gas absorption for CO<sub>2</sub> capture from flue gas containing fine particles and gaseous contaminants, *Int. J. Greenh. Gas Control.* **2015**, 33, 10-17.

Zhao S., Feron P.H.M., Deng L., Favre E., Chabanon E., Yan S., Hou J., Chen V., Qi H., Status and progress of membrane contactors in post-combustion carbon capture: A state-of-the-art review of new developments, *J. Membr. Sci.* **2016**, 511, 180–206.

# Desarrollo

---

---

*“El experimentador que no sabe lo que está buscando  
no comprenderá lo que encuentra”*

*Claude Bernard (1813-1878)*

*Médico y filósofo francés*



## **CAPITULO 2: DESARROLLO**

### **2.1. Método experimental**

#### **2.1.1. Líquidos iónicos**

Se han utilizado dos líquidos iónicos comerciales a lo largo del presente trabajo:

- 1-etil-3-metilimidazolio etilsulfato, [emim][EtSO<sub>4</sub>], Sigma Aldrich, y
- 1-etil-3-metilimidazolio acetato, [emim][Ac], Sigma Aldrich

El [emim][EtSO<sub>4</sub>] (≥95%) fue escogido debido a su bajo coste (285.50 €/kg) así como su baja viscosidad (144 cP a 291K) y baja toxicidad.

El [emim][Ac] (≥90%) se seleccionó, además de por no presentar toxicidad, debido a la alta solubilidad del CO<sub>2</sub> (8.6%) y porque al poseer un anión carboxílico se considera prometedor para la captura de dióxido de carbono, con la formación de carboxilato en el mecanismo de quimisorción (Gurau et al., 2011; Blath et al., 2012). Debido a que el [emim][Ac] comercial era de relativa baja pureza, se midió su solubilidad mediante un método termogravimétrico utilizando una termobalanza TG-DTA 60H Shimadzu (Japón) y así se confirmó que cumplían los ratios de solubilidad de referencia (Santos et al., 2014, Albo et al., 2012a). La figura 2.1 muestra la estructura de ambos líquidos iónicos.

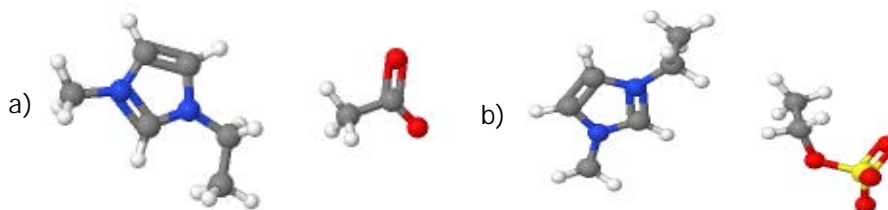


*Figura 2.1: Estructura de a) [emim][Ac] y b) [emim][EtSO<sub>4</sub>].*

#### **2.1.2. Preparación de módulos de PVDF**

##### **2.1.2.1. Materiales y métodos utilizados**

A continuación, se explica la caracterización y construcción de módulos de fluoruro de polivinilideno (PVDF) con los líquidos iónicos [emim][EtSO<sub>4</sub>] y [emim][Ac]. Esta parte del trabajo fue realizado en el Laboratorio de Ingeniería Química en la Universidad de Toulouse III-Paul Sabatier bajo la supervisión de Jean Christophe Remigy.

Se seleccionaron cuatro tipos de fibras huecas distintas a base de PVDF combinadas con distintos aditivos de entre un total de 200 elaboradas en un trabajo previo consistente en una Tesis Doctoral (Savart, 2013). Como criterio se tomaron aquellas que, a priori, poseían

mayor permeabilidad al CO<sub>2</sub> así como un alto punto de burbuja. Los cuatro tipos de fibras seleccionados fueron llamadas A, B, C y D y se fabricaron mediante inversión de fase. El material utilizado para la fabricación de las fibras fue, PVDF HSV900, proporcionado por Arkema (Francia); n-metil-pirrolidona, NMP, suministrado por Sigma Aldrich (Francia) que se utilizó como disolvente y Cloruro de Litio, LiCl, también suministrado por Sigma Aldrich (Francia) con un copolímero de bloque que fueron utilizados como aditivos. El copolímero consistía en dos bloques denominados 1 y 2. El primero, 1, era un bloque hidrófobo compuesto por poli(metacrilato de metilo) (75% en peso) y el segundo, 2, era un bloque hidrófilo compuesto de poli(acrilato de butilo) (20% en peso) y metacrilato de hidroxietilo (5% en peso) (Savart, 2013, Lorain et al., 2014 y Medina-Gonzalez et al., 2012).

Los parámetros de operación utilizados para la preparación de las fibras huecas se muestran en la Tabla 2.1. Las soluciones dopadas para fabricar las fibras A y B estaban compuestas por un 15% de PVDF HSV900 y 3% LiCl. Las fibras C estaban formadas por un 15% PVDF HSV900, 3% de copolímero de bloque y 3% LiCl. Por último, las fibras D estaban compuestas de 15% PVDF HSV900, 3% copolímero de bloque, 3% LiCl y 1% de agua (Savart, 2013, Lorain et al., 2014). La única diferencia entre las fibras A y B fue el flujo de fluido interno, 1.8 y 3.9 ml min<sup>-1</sup>, respectivamente (Tabla 2.1). En el caso de las fibras D, un 1% de agua se inmovilizó en la solución de dopaje.

Tabla 2.1: Condiciones de preparación de las fibras huecas de PVDF.

	Q <sub>c</sub> (mL min <sup>-1</sup> )	Q <sub>i</sub> (mL min <sup>-1</sup> )	Composición (relación masa)	T <sub>c</sub> (K)	T <sub>baño de coagulación</sub> (K)	T <sub>Interna</sub> (K)	Air gap (cm)	Velocidad (m min <sup>-1</sup> )
A	7.2	1.8	Agua/NMP 70/30	350	322	351	10	11
B	7.2	3.9	Agua/NMP 70/30	350	322	351	10	11
C	7.2	1.8	Agua/NMP 85/15	308	333	308	10	11
D	7.2	1.8	Agua/NMP 70/30	323	323	323	32	11

Durante la preparación de las membranas, el LiCl fue eliminado mediante una etapa de lavado con agua (Savart, 2013). El copolímero de bloque fue parcialmente eliminado ya que aunque no se pudo cuantificar el contenido de copolímero final en la fibra sí se observó que tras la etapa de coagulación, que se produce clásicamente con técnicas de inversión de fase, el copolímero de bloque se encontró en el baño de coagulación. Tras un análisis más detallado con la tecnología de espectrometría de masas de iones secundarios (SIMS, por sus siglas en inglés) se mostró que el copolímero no solo estaba presente en la fibra en la superficie del polímero, sino también dentro de la matriz de PVDF (Savart, 2013). Para el secado de las fibras, en los casos en los que se utilizaban en forma seca, éstas se mantuvieron durante, aproximadamente, 72 horas en un horno a una temperatura de 50°C y a presión atmosférica.

Posteriormente, las fibras C y D fueron tratadas para inmovilizar en ellas los líquidos iónicos, el [emim][EtSO<sub>4</sub>] y el [emim][Ac]. Para ello, los líquidos iónicos se incluyeron en los cuatro tipos de fibras vírgenes mediante la adición de 150 mL líquido en agitado permanente durante 48 h. Este tipo de impregnación con líquidos iónicos es sumamente novedoso (Kim et al., 2011; Wickramanayake et al., 2014).

### **2.1.2.2. Caracterización de las fibras de PVDF**

El diámetro externo e interno y el espesor de las fibras fueron medidos a través de la microscopía electrónica de barrido (SEM, en inglés) mediante un equipo suministrado por Hitachi TM1000 (Japón). Para poder realizar los cortes transversales de las fibras y llevar a cabo las medidas mencionadas anteriormente, éstas fueron sumergidas primero en etanol, luego crio-fracturadas en nitrógeno líquido, y posteriormente sometidas a una pulverización catódica con oro. La figura 2.2 muestra el equipo SEM utilizado.



*Figura 2.2: Equipo de microscopía electrónica de barrido.*

### **2.1.2.3. Propiedades mecánicas de las fibras**

Las propiedades mecánicas de las fibras también se evaluaron utilizando un dispositivo de ensayo de tracción (INSTRON, modelo 3342) y el software Bluehill (Bluehill 2 Software, Instron). A partir de los datos, se determinaron la resistencia a la tracción (MC), la deformación por tracción en la rotura (CC), el alargamiento en el límite elástico ( $\epsilon_b$ ) y el Módulo de Young de cada tipo de fibra.

#### **2.1.2.4. Ensayos de permeabilidad**

La permeación de gas de las fibras huecas se midió usando CO<sub>2</sub> puro, y con unos módulos de acero inoxidable fabricados en el propio laboratorio. Para las mediciones, tres fibras de aproximadamente 30 cm de largo fueron ensambladas dentro de cada módulo. Las medidas se repitieron al menos dos veces con cada uno de los tipos de fibras. El gas fue introducido a través de la carcasa, y el flujo de permeación de gas se midió a la salida de las fibras mediante un controlador de flujo másico (MFC Brooks Instrument 5850, Emerson Process Management España). La descripción del sistema experimental se muestra en la Figura 2.3. Se varió la presión entre 0 y 15 bares en intervalos de 0,5 bares. Para asegurar que el sistema estaba estable, se esperó un tiempo de estabilización de 100s para medir la permeabilidad en cada cambio de presión.

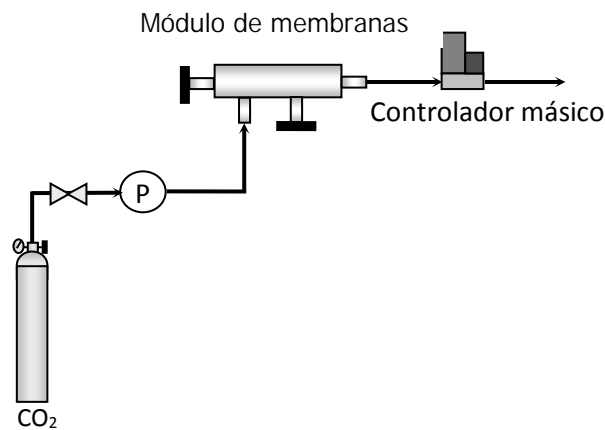


*Figura 2.3: Esquema de la planta de permeación para ensayos de permeabilidad.*

#### **2.1.2.5. Calculo del punto burbuja**

Para terminar de realizar la caracterización de las fibras, se midió el punto burbuja. Para ello, cada tipo de fibra fue sumergida en agua y una corriente de aire comprimido fue inyectada por el interior de la fibra. La presión de la corriente de aire fue variando de 0 a 7.16 bar con un intervalo de 0.1 bar, manteniendo el lado del agua a presión atmosférica. Con la primera burbuja en la superficie del agua, determina la presión del punto burbuja.

### 2.1.3. Captura de CO<sub>2</sub>

Los experimentos se llevaron a cabo en una planta a escala laboratorio, actualmente operativa, situada en el laboratorio 538 del Departamento de Ingenierías Química y Biomolecular de la Universidad de Cantabria, y que ha sido adaptada a partir de los trabajos previos (Gomez-Coma et al., 2014).

La Figura 2.4 muestra un esquema de la planta de absorción no dispersiva de dióxido de carbono en contactores de membrana. La planta está constituida por dos líneas, la de gas y la de líquido. Las líneas operan en contracorriente para permitir una mayor eficacia en el contacto. La línea de gas parte de las tomas de salida del dióxido de carbono y el nitrógeno. Ambos gases han sido suministrados por Air Liquide (España) y tienen una pureza de  $99.7 \pm 0.01$  vol.% y  $99.999 \pm 0.001$  vol.% para el CO<sub>2</sub> y N<sub>2</sub> respectivamente. El caudal de gas se ajusta por medio de controladores de caudal másico de la marca Emerson Process Management (España).

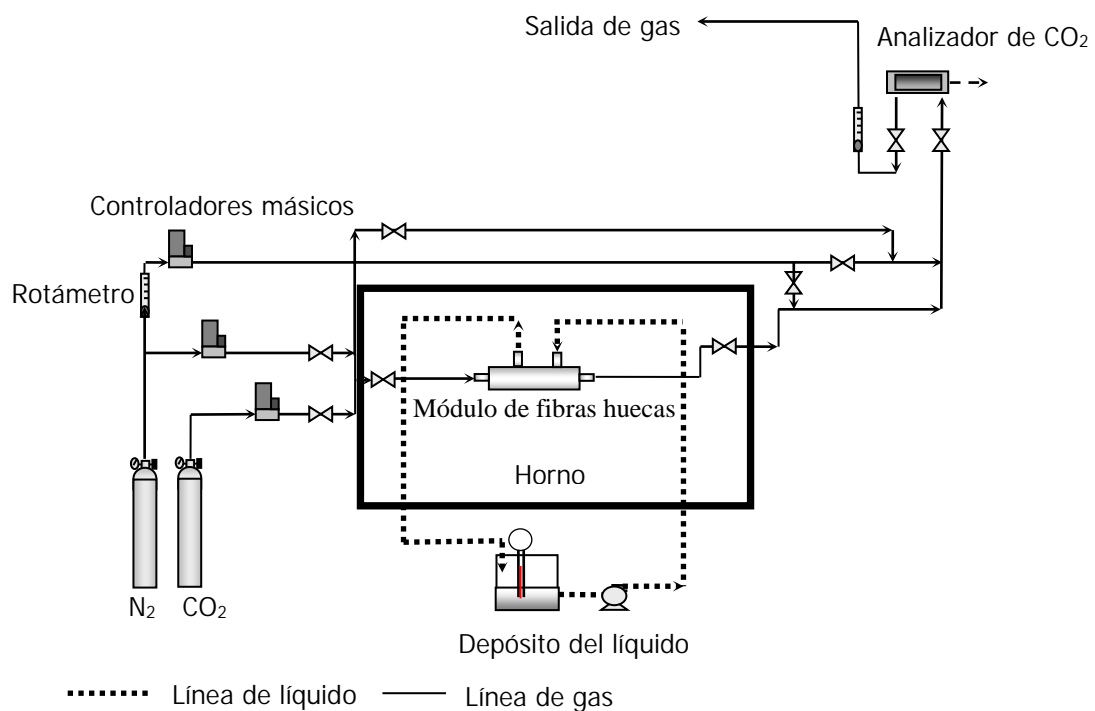


Figura 2.4: Esquema de la planta experimental de captura de CO<sub>2</sub> en módulo de fibras huecas.

La línea de líquido está constituida por un reactor de vidrio para el depósito del líquido, y una bomba de engranajes digital (Cole Parmer Instrument Company, Hucoa-Erloss SA, España) para impulsar el líquido a través del contactor. Al final de cada experimento el líquido es desorbido mediante una corriente de gas constituida únicamente por N<sub>2</sub>.

Para poder operar a distintas temperaturas y en condiciones isoterma se utilizaron dos mecanismos distintos, primero unas cintas calefactoras (Selecta, España) y, posteriormente estas fueron sustituidas por un horno (Mettler UNE 200, España) en el cual se introducía el módulo y gran parte de las líneas de gas y líquido. Cada experimento fue repetido tres veces bajo las mismas condiciones de operación y se calcularon, el valor medio y el error experimental. La Figura 2.5 muestra un módulo de fibras huecas introducido en el horno.



*Figura 2.5: Detalle de un módulo de fibras huecas introducido en el horno.*

En todos los experimentos realizados la composición del gas de entrada fue de un 15% CO<sub>2</sub> y 85% N<sub>2</sub>, condiciones típicas de concentración de CO<sub>2</sub> de post-combustión. La corriente gaseosa fue introducida al módulo a través de las fibras, ya que la parte menos viscosa y fácil de limpiar es la idónea para atravesar las fibras (Levenspiel, 1993). Antes de enviar la corriente de salida al analizador, fue necesario diluir la muestra con N<sub>2</sub> para conseguir el mínimo caudal necesario requerido (al menos 200 ml min<sup>-1</sup>). El analizador, suministrado por Emerson Process Management, está basado en espectroscopia de infrarrojos no dispersiva (NDIR, por sus siglas en inglés). La concentración de dióxido de carbono en la corriente de gas de salida se monitorizó mediante el software NGA Win-Control. El estado estacionario fue indicado mediante una concentración de CO<sub>2</sub> constante en la corriente de gas de salida.

Para poder determinar el material de las fibras idóneo para la captura de dióxido de carbono, en este trabajo se evaluaron distintos módulos de fibras huecas de flujo paralelo (Gomez-Coma et al., 2014; Gomez-Coma et al., 2016a-d):

- Módulo de Polipropileno (PP) suministrado por Liqui-Cel® (EEUU). Este contactor fue escogido debido a su competitividad en el mercado debido a su bajo coste y la gran hidrofobicidad que presenta este material. Como desventaja este material únicamente soporta temperaturas de hasta 318K sin sufrir daños en el módulo. Los experimentos fueron realizados a temperatura ambiente (291), 298, 318 y 333K con cada líquido iónico. Operando a la temperatura de 333 K se observó degradación del módulo tras un número de experimentos, por

lo que no se recomienda el uso del módulo de PP a esta temperatura, al no ofrecer estabilidad térmica. La Figura 2.6 muestra el módulo de PP utilizado.



*Figura 2.6: Módulo de fibras huecas de PP.*

- Módulo de fluoruro de polivinilideno (PVDF) impregnado con [emim][Ac] (Figura 2.7). Este módulo se preparó en el Laboratorio de Ingeniería Química en la Universidad de Toulouse III-Paul Sabartier bajo la supervisión de Jean Christophe Remigy. La fabricación de dicho módulo se preparó de acuerdo a lo explicado en el apartado 2.1.2.1 (las fibras utilizadas fueron las tipo D). Este material, PVDF, se seleccionó debido a que posee valores bajos de energía superficial además de ser un polímero hidrófobo que se puede disolver en disolventes comunes para preparar membranas asimétricas a través de un proceso de inversión de fase. El PVDF permite trabajar a temperaturas superiores al PP sin sufrir ningún tipo de daño. Los experimentos con este material fueron realizados a las temperaturas de 303, 313, 323 y 333K.



*Figura 2.7: Módulo de fibras huecas de PVDF.*

- Módulo de Polisulfona (Ps) suministrado por VWR International Eurolab, S.L. (Spain) (Figura 2.8). Este material se seleccionó porque permite la posibilidad de trabajar a temperaturas aún más elevadas que el PVDF sin sufrir ningún tipo de desperfecto las fibras. La polisulfona, es un polímero poroso y asimétrico que ha sido ampliamente estudiado para la permeación y separación de gases, debido a su baja permeabilidad y comparativamente alta selectividad, que lo acercan al límite superior del gráfico de Robeson, el cual compara materiales en función de su permeabilidad y selectividad (Casado-Coterillo et al., 2012). Este material posee una excelente resistencia mecánica, alta estabilidad térmica y química y no está considerado estrictamente como hidrófobo (Korminouri et al., 2015; Nabian et al., 2015). Utilizando el módulo de Ps los experimentos se llevaron a cabo a las temperaturas de 303, 313, 323 y 343K.



Figura 2.8: Módulo de fibras huecas de Ps.

La Tabla 2.2 muestra un resumen de las principales características de los contactores de membranas utilizados. Como se puede apreciar en ella, el módulo de polipropileno y el de polisulfona tenían el mismo área aunque el de PP poseía muchas más fibras.

Tabla 2.2: Características de los distintos módulos de fibras huecas utilizados.

Material de la membrana	PVDF	PP	Ps
Diámetro exterior, $d_o$ (m)	$7.7 \cdot 10^{-4}$	$3 \cdot 10^{-4}$	$1.3 \cdot 10^{-3}$
Diámetro interior, $d_i$ (m)	$4.51 \cdot 10^{-4}$	$2.2 \cdot 10^{-4}$	$7 \cdot 10^{-4}$
Longitud de la fibra, $L$ (m)	0.295	0.115	0.347
Número de fibras, $n$	11	2300	400
Área efectiva interna de la membrana, $A$ (m <sup>2</sup> )	$4.60 \cdot 10^{-3}$	0.18	0.18
Porosidad (%)	30	40	43
Factor de empaquetamiento	0.04	0.39	0.43
Tortuosidad <sup>a</sup>	3.3	2.5	2.3

<sup>a</sup>Asumiendo  $1/\epsilon$

#### **2.1.4. Cálculo de las resistencias que afectan al proceso**

En los procesos de captura de dióxido de carbono utilizando contactores de membrana, se produce una transferencia de materia sin dispersión ya que la membrana actúa como una barrera entre la zona por la que circula el líquido (la carcasa) y la zona por la que pasa el gas (las fibras).

La Figura 2.9 muestra los tres pasos consecutivos que tienen lugar para la transferencia de materia en el proceso cuando los poros de la membrana están llenos de gas, ya que se asume que en los tres materiales de fibras utilizados no existe mojado de la membrana.

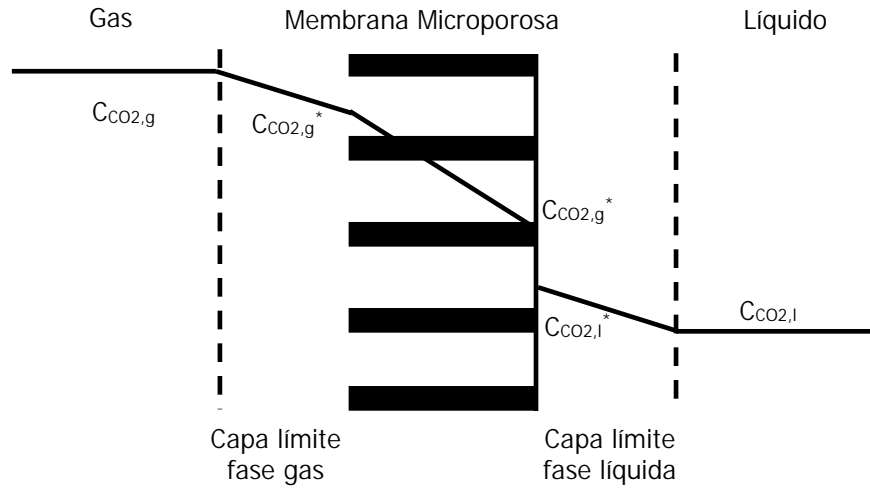


Figura 2.9: Resistencias a la transferencia de materia y concentraciones locales en la membrana.

La resistencia global de transferencia de materia,  $R_{overall}$  se calcula como la suma de las distintas resistencias individuales dispuestas en serie, de acuerdo a la Ecuación 2.1.

$$R_{overall} = R_g + R_m + R_l \quad (2.1)$$

donde  $R_g$ ,  $R_m$  y  $R_l$  representan las resistencias en la fase gas, en la membrana y en la fase líquida respectivamente.

Para una configuración en la que el gas circula por dentro de las fibras huecas y la fase líquida fluye a través de la carcasa, la interfaz de gas-líquido se encuentra en el diámetro exterior de los tubos. Teniendo en cuenta una reacción química en el lado del líquido (expresada mediante el factor de mejora,  $E_A$ ) la Ecuación utilizada para obtener la resistencia global es la siguiente (Ortiz et al., 2010, Luis et al., 2009):

$$\frac{1}{K_{overall}} = \frac{d_o}{k_g d_i} + \frac{d_o}{k_{mg} d_{lm}} + \frac{1}{k_l H_d E_A} \quad (2.2)$$

donde  $d_o$ ,  $d_i$  y  $d_{lm}$  son el diámetro exterior, interior y medio de las fibras, expresados en m,  $H_d$  representa la constante adimensional de Henry y  $k_g$ ,  $k_{mg}$ ,  $k_l$ , son los coeficientes de transferencia de materia individuales de la fase gaseosa, la membrana y la fase líquida respectivamente ( $m \cdot s^{-1}$ ). El coeficiente global de transferencia de materia,  $K_{overall}$ , está expresado en  $ms^{-1}$ .

Si las contribuciones de la fase gaseosa y de la membrana pueden considerarse insignificantes, la Ecuación 2.2 se puede simplificar dando lugar a la Ecuación 2.3 (Ortiz et al., 2010).

$$\frac{1}{K_{overall}} = \frac{1}{k_l H_d E} \quad (2.3)$$

La densidad de flujo de dióxido de carbono se ha calculado de acuerdo a la Ecuación 2.4, asumiendo que en el estado estacionario se igualan los flujos de CO<sub>2</sub> de la fase gas y líquida. De esta forma, el coeficiente global de transferencia de materia,  $K_{overall}$ , puede ser evaluado experimentalmente mediante la densidad de flujo a través de la membrana.

$$N_{CO_2,g} = \frac{Q_g}{A} (C_{CO_2,in} - C_{CO_2,out}) = K_{overall} \frac{\Delta y_{lm} P_T}{RT} \quad (2.4)$$

donde  $Q_g$  representa el flujo de gas ( $m^3 s^{-1}$ ),  $A$  es el área de la membrana ( $m^2$ ),  $P_T$  es la presión total en la fase gaseosa y por último  $\Delta y_{lm}$  es la media logarítmica de la fuerza impulsora sobre las fracciones molares de la fase gas. Teniendo en cuenta la concentración de dióxido de carbono en la entrada es  $y_{CO_2,in}$  y a la salida del módulo de fibras huecas es  $y_{CO_2,out}$  y suponiendo que la concentración de CO<sub>2</sub> en el líquido iónico está muy lejos de la saturación,  $\Delta y_{lm}$  puede ser calculado como:

$$\Delta y_{lm} = \frac{(y_{CO_2,in}) - (y_{CO_2,out})}{\ln((y_{CO_2,in})/(y_{CO_2,out}))} \quad (5)$$

Para el cálculo de la eficacia total del proceso, en función del dióxido de carbono capturado, se ha utilizado la Ecuación 2.6:

$$Eficacia (\%) = \left(1 - \frac{C_{CO_2,out}}{C_{CO_2,in}}\right) 100 \quad (2.6)$$

En cuanto al cálculo de la transferencia de materia en la fase líquida, numerosos autores han propuesto diferentes correlaciones empíricas, cuando el absorbente circula a través del lado de la carcasa. En el presente trabajo, la correlación de Kartohardjono fue la utilizada para calcular  $k_l$  ya que tanto el factor de empaquetamiento como el número de Reynolds estaban dentro del intervalo de aplicación de dicha ecuación para los diferentes módulos utilizados ( $0,029 < \phi < 0,53$ ;  $Re < 400$ ) (Shen et al., 2010):

$$Sh = \left(\frac{k_l d_h}{D_{CO_2,l}}\right) = 0.1789 (\phi^{0.86}) Re^{0.34} Sc^{\frac{1}{3}} \quad (2.7)$$

donde  $D_{CO_2,l}$  es el coeficiente de difusión del dióxido de carbono en el líquido,  $L$  es la longitud de la fibra y  $d_h$  es el diámetro hidráulico, éste último es calculado a través de la Ecuación 2.8:

$$d_h = \frac{d_{cont}^2 - n d_0^2}{n d_0} \quad (2.8)$$

El coeficiente de transferencia de materia en la fase líquida,  $k_l$ , depende de las propiedades físicas del líquido iónico y de las características del contactor de membranas. Por

esta razón, Morgan et al. (2005) propuso una correlación que expresa la dependencia de la difusividad del gas con la viscosidad del líquido utilizada (Ecuación 2.9):

$$D_{CO_2,l} = 2.66 \cdot 10^{-3} \frac{1}{\mu_{lL}^{0.66} V_{CO_2}^{1.04}} \quad (2.9)$$

siendo  $\mu_{lL}$  la viscosidad del líquido iónico (medida en cP),  $V_{CO_2}$  el volumen molar de dióxido de carbono en el punto de ebullición normal ( $33.3 \text{ cm}^3 \text{ mol}^{-1}$ ), se obtiene la difusividad  $D_{CO_2,l}$  en  $\text{cm}^2 \text{ s}^{-1}$ .

### 2.1.5. Modelado de la absorción de dióxido de carbono

Utilizando el software Aspen Custom Modeler (Aspen Technology, Inc.), se ha modelado el proceso de captura de  $CO_2$  usando contactores de membrana. Los principales objetivos de esta parte del trabajo son, por una parte, realizar una descripción del proceso mediante el modelo de difusión convección para comparar los resultados que se hayan obtenido de forma experimental y así poder dar validez al modelado y, por otra, realizar una simulación para calcular los valores de los parámetros necesarios para lograr un 90% de captura de dióxido de carbono en el proceso, ya que alcanzando dicho valor de eficacia se consideraría el presente proceso de intensificación, un proceso competitivo en comparación con los procesos tradicionales que usan torres de absorción y aminas.

En un modo de operación basado en el no-mojado de la membrana, el  $CO_2$  se transfiere a la fase líquida por difusión a través de los poros de la membrana, los cuales están llenos de gas. Sin embargo, en un modo de operación en mojado, los poros están llenos de líquido y el  $CO_2$  tiene que difundirse a través de líquido estancado dentro de los poros.

La Figura 2.10 muestra las coordenadas que se tomaron en la fibra hueca: la posición radial  $r=0$  representa el centro de la fibra y la distancia axial de  $z=0$  indica la posición inicial del gas en la fibra.

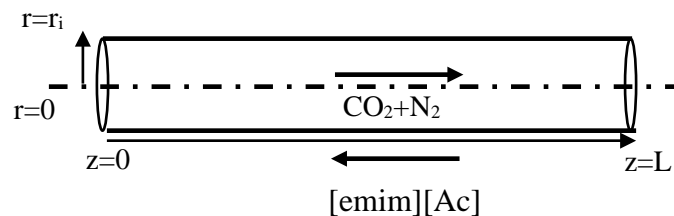


Figura 2.10: Coordenadas de la fibra en el contactor de fibras huecas.

La Ecuación 2.10 describe el balance de materia diferencial al CO<sub>2</sub> asumiendo las siguientes consideraciones: (1) una concentración insignificante del gas soluble en el líquido de absorción, (2) estado estacionario y condiciones isotermas, (3) no hay difusión axial, (4) el comportamiento de los gases es ideal, (5) perfil de velocidad parabólico en el interior de la fibra y (6) presiones constantes tanto en el lado de la carcasa como en el de las fibras (Luis et al., 2007; Luis et al., 2010).

$$u_z \frac{\partial C_{CO_2}}{\partial z} = D \left[ \frac{1}{r} \frac{\partial}{\partial r} \left( r \frac{\partial C_{CO_2}}{\partial r} \right) \right] \quad (2.10)$$

Assumiendo que la velocidad del gas es un modelo de flujo laminar, la Ecuación 2.10 se expresa según la siguiente ecuación (Luis et al., 2007):

$$2u_m \left[ 1 - \left( \frac{r}{R} \right)^2 \right] \frac{\partial C_{CO_2}}{\partial z} = D \left[ \frac{1}{r} \frac{\partial}{\partial r} \left( r \frac{\partial C_{CO_2}}{\partial r} \right) \right] \quad (2.11)$$

Adimensionalizando todos los términos la ecuación queda de la siguiente forma (Ecuación 2.12):

$$\frac{Gz}{2} [1 - \bar{r}^2] \frac{\partial \bar{C}_{CO_2}}{\partial \bar{z}} = \frac{1}{\bar{r}} \frac{\partial}{\partial \bar{r}} \left( \bar{r} \frac{\partial \bar{C}_{CO_2}}{\partial \bar{r}} \right) \quad (2.12)$$

donde las variables adimensionales han sido definidas como:

$$\bar{r} = \frac{r}{R} \quad (2.13.a)$$

$$\bar{z} = \frac{z}{L} \quad (2.13.b)$$

$$\bar{C}_{CO_2} = \frac{C_{CO_2}}{C_{CO_2,inlet}} \quad (2.13.c)$$

Las condiciones frontera utilizadas han sido las siguientes:

$$\bar{r} = 0 \rightarrow \frac{\partial \bar{C}_{CO_2}}{\partial \bar{r}} = 0 \quad (2.14.a)$$

$$\bar{r} = 1 \rightarrow \frac{\partial \bar{C}_{CO_2}}{\partial \bar{r}} = -\frac{Sh}{2} \bar{C}_{CO_2} \quad (2.14.b)$$

$$\bar{z} = 0 \rightarrow \bar{C}_{CO_2} = 1 \quad (2.14.c)$$

Los números adimensionales de Graetz (Gz) y Sherwood (Sh) utilizados se han definido de acuerdo a las siguientes ecuaciones:

$$Gz = \frac{u_m d_i^2}{D L} \quad (2.15.a)$$

$$Sh = \frac{K_{overall} di}{D} \quad (2.15. b)$$

Finalmente, la concentración adimensional de dióxido de carbono a la salida del módulo se ha calculado con la siguiente ecuación:

$$\bar{C}_{CO_2=L} = 4 \int_0^1 \bar{C}_{CO_2} [1 - \bar{r}^2] \bar{r} d\bar{r} \quad (2.16)$$

## **2.2. Resultados**

A continuación se resumen los principales resultados de este trabajo, que se recogen en las publicaciones que componen el núcleo de esta Tesis (páginas 101-178).

### **2.2.1 Caracterización de los módulos de fibras huecas de PVDF fabricados**

#### **2.2.1.1. Caracterización SEM de las fibras huecas**

Los cuatro tipos de fibras huecas a base de PVDF combinadas con distintos aditivos (A, B, C y D) fueron caracterizados mediante la microscopía electrónica de barrido. Además, en las fibras C y D se inmovilizaron los líquidos iónicos [emim][EtSO<sub>4</sub>] y [emim][Ac]. Cada medida se realizó un total de tres veces y se calcularon el valor medio y el error. La Tabla 2.3, muestra los valores del diámetro interior (di), espesor (e) y longitud (L) de cada tipo de fibras en modo mojado y seco.

*Tabla 2.3: Medidas realizadas a partir de microscopía SEM y longitud de las fibras huecas.*

	Mojado			Seco		
	di (10 <sup>4</sup> m)	e (µm)	L (cm)	di (10 <sup>4</sup> m)	e (µm)	L (cm)
A	484	139	82.6	739	90	78,5
B	572	101	82.6	584	109	78.6
C	410	137	82.6	488	157	78.6
D	475	184	82.6	455	174	78.9
<i>Líquido Iónico inmovilizado</i>						
C+[emim][EtSO <sub>4</sub> ]	496	154	82.5	439	143	84.2
C+[emim][Ac]	515	165	82.5	436	151	82.0
D+[emim][EtSO <sub>4</sub> ]	379	146	82.5	443	159	85.3
D+[emim][Ac]	472	172	82.5	451	160	81.7

La mayor desviación fue de un 5.88%.

Como se aprecia en la Tabla 2.3, al secar las fibras se redujo aproximadamente un 5% su longitud. Los tamaños de las fibras, están en concordancia con los valores de la literatura para contactores de escala laboratorio. Rezaei et al. (2014) trabajó con unas fibras de diámetros interior y exterior de  $0,455 \pm 0,025$  y  $0,825 \pm 0,025$  mm, respectivamente. Por su parte, Naim et al. (2013) obtuvo unas fibras con  $d_i = 0,550 \pm 0,020$  mm y  $d_{out} = 0,800 \pm 0,030$  mm. La mayor diferencia entre los diámetros en seco y mojado se produjo con las fibras tipo A. En el caso de las fibras tipo D y cuando se añade el [emim][Ac], tanto el diámetro interior como el espesor disminuyeron en la forma seca, posiblemente debido a la contracción de la fase de polímero. En la forma seca, las fibras C y D en presencia y ausencia de IL presentan los grosores de pared más altos. Las fibras C cuando fueron inmovilizadas con los líquidos iónicos también mostraron un descenso en los diámetros cuando se secaban. Este resultado podría atribuirse principalmente al hecho de que los líquidos iónicos hincharon las fibras vírgenes y disolvieron la matriz polimérica.

La Tabla 2.4 muestra las imágenes de las fibras tipo A y B. La Tabla 2.5, por su parte muestra la comparación estructural realizadas por SEM para observar cómo se modificaba la apariencia de la membrana cuando se inmovilizaban en la misma los ILs. Las fibras vírgenes estaban húmedas. Por lo tanto, las fibras se secaron después de la adición del IL. Como se observa en las tablas, cuando se inmoviliza el IL en la fibra se rellenan los huecos que existían en ausencia de IL, especialmente en la forma mojada. Esto se puede atribuir principalmente a la creación de una nueva capa.

Tabla 2.4: Imágenes SEM de las fibras huecas tipo A y B.

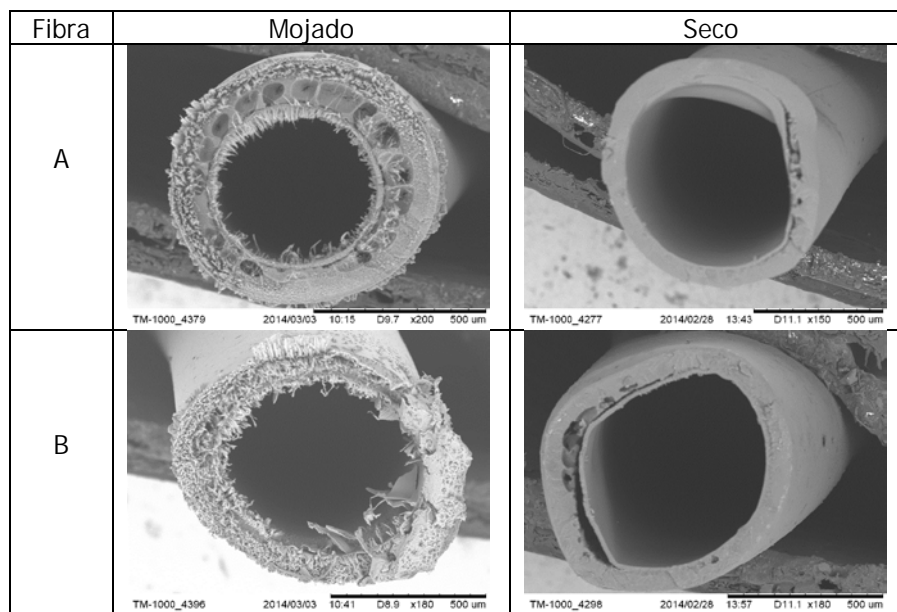
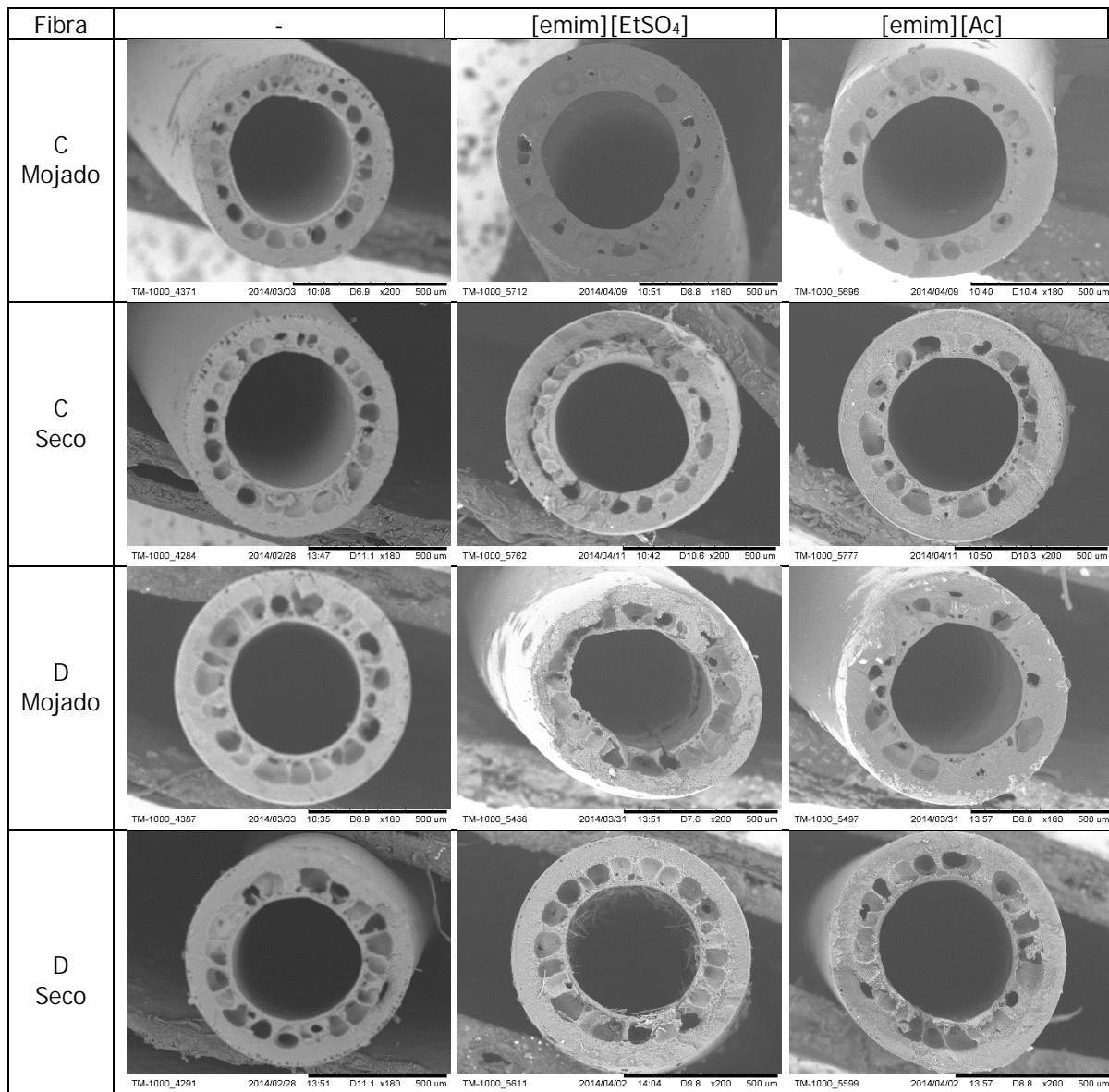


Tabla 2.5: Imágenes SEM de las fibras huecas tipo C y D en presencia y ausencia de IL.



### **2.2.1.2. Propiedades mecánicas de las fibras huecas**

Las propiedades mecánicas de las fibras se recogen en la Tabla 2.6. Al igual que en el apartado de caracterización, cada medida se realizó tres veces, y se calcularon el valor medio y el error. Como se puede apreciar en ella, las fibras de tipo B fueron las que mostraron mayor elasticidad. La tensión de rotura cuando fueron inmovilizados los ILs sufrió cambios significativos. En forma seca, las fibras C y D sufrieron una disminución del 17% y 26% respectivamente; y en forma húmeda, las fibras C+[emim][EtSO<sub>4</sub>] y C+[emim][Ac] se produjo una disminución de hasta un 50%. Por otro lado, la deformación en estas fibras ( $\epsilon_b$ ) fue por lo menos dos veces mayor cuando se inmovilizaron los líquidos iónicos.

Tabla 2.6: Propiedades mecánicas de las fibras huecas.

	Mojado			Seco		
	MC (N)	CC (Mpa)	ε <sub>b</sub> (%)	MC (N)	CC (Mpa)	ε <sub>b</sub> (%)
A	1.60	5.91	158.68	1.62	7.90	150.38
B	1.62	7.58	181.53	1.61	6.23	150.53
C	1.88	8.00	76.67	2.07	6.53	74.89
D	1.78	4.68	63.71	1.95	5.67	50.03
<i>Líquido Iónico Inmovilizado</i>						
C+[emim][EtSO <sub>4</sub> ]	1.35	4.29	145.53	1.37	5.25	142.42
C+[emim][Ac]	1.60	4.40	128,05	1.56	5.61	116.89
D+[emim][EtSO <sub>4</sub> ]	1.28	5.32	168.33	1.26	4.18	142.92
D+[emim][Ac]	1.47	4.20	110.12	1.49	4.87	95.32

La mayor desviación fue de un 6.40%.

A partir de los resultados de la Tabla 2.6, se calculó también el módulo de Young (Tabla 2.7). En función del valor de este parámetro se puede determinar si hay o no interacción entre el IL y la matriz polimérica: si el valor del módulo disminuye cuando se adiciona el líquido iónico quiere decir que hay interacción y por tanto el IL plastifica al polímero y la fibra se hincha. El módulo de Young (N mm<sup>-2</sup>) se calculó usando la Ecuación 2.17.

$$E = \frac{\sigma}{\epsilon} = \frac{\frac{F}{S}}{\frac{\Delta L}{L}} \quad (2.17)$$

donde E es el módulo de Young (módulo de elasticidad), F es la fuerza ejercida sobre un objeto bajo tensión, ΔL es la variación de longitud de fibra, L es la longitud original de la fibra, y S es la sección de la fibra.

Tabla 2.7: Valores del módulo de Young de las fibras huecas.

	Mojado	Seco
	E (N mm <sup>-2</sup> )	E (N mm <sup>-2</sup> )
C	180.74	188.23
D	98.11	183.11
C+[emim][EtSO <sub>4</sub> ]	18.29	12.36
C+[emim][Ac]	40.03	81.86
D+[emim][EtSO <sub>4</sub> ]	65.40	9.28
D+[emim][Ac]	41.94	68.42

A la vista de la Tabla 2.7, se puede concluir que sí hubo interacción con la matriz polimérica, la reducción de los valores una vez inmovilizado el líquido iónico fue superior al 50%.

### 2.2.1.3. Permeabilidad de las fibras huecas

Los resultados de permeabilidad con dióxido de carbono puro se presentan en las Figuras 2.11-2.14. Cuando se compararon las fibras A, B, C y D sin inmovilizar IL en ellas, se pudo observar cómo las afectaba la humedad relativa (Figura 2.11). Las fibras A en forma húmeda sufren una compactación en torno a los dos bares y el flujo de CO<sub>2</sub> es menor que en las fibras B y C. La tendencia en el caso de este último tipo de fibras (B y C) es de tipo lineal alcanzando un flujo de más de  $1.2 \cdot 10^5$  NL m<sup>-2</sup> h<sup>-1</sup> a 6 y 7 bar respectivamente.

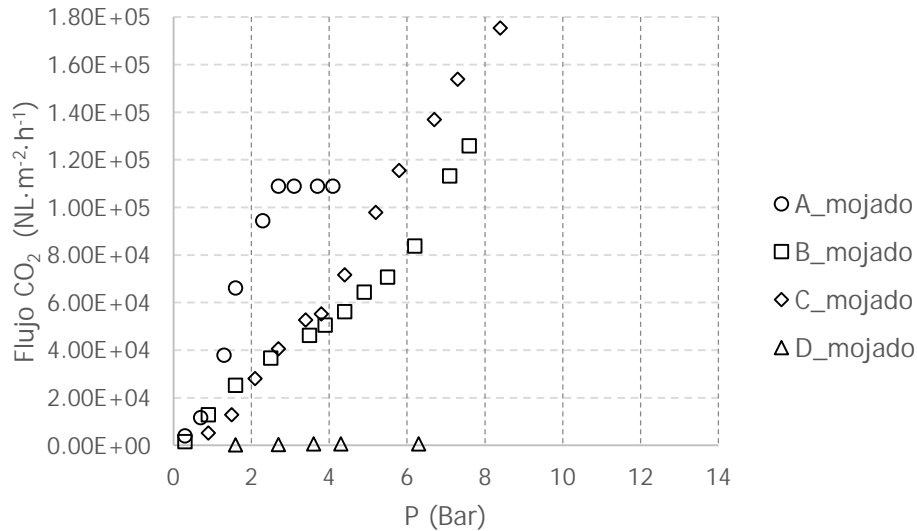


Figura 2.11: Permeabilidad de las fibras huecas en forma mojada.

La Figura 2.12, muestra los resultados de permeabilidad con las fibras secas. En el caso de las fibras C y D se observó una permeabilidad elevada. En cambio, cuando se trabajó con las fibras A y B, los resultados de permeabilidad arrojaron valores menores que cuando se trabajó en forma húmeda, además de una compactación en torno a los 2 bares. Con estos resultados de permeabilidad en forma seca, queda justificada la decisión de inmovilizar en las fibras C y D los ILs ya que potencialmente conducirán a mejores datos de eficacia en la absorción de CO<sub>2</sub>.

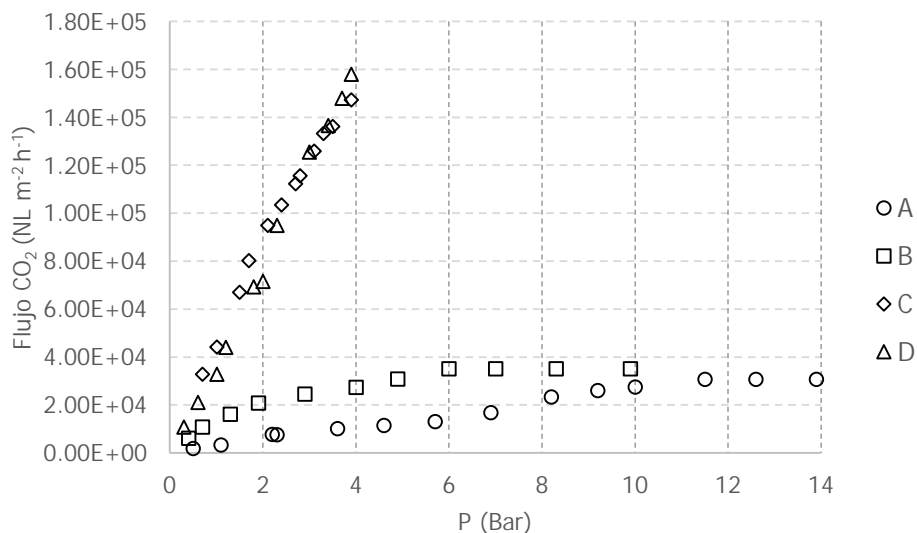


Figura 2.12: Permeabilidad de las fibras huecas en forma seca.

Las Figuras 2.13 y 2.14 muestran los resultados de los ensayos de permeación de CO<sub>2</sub> de las fibras C y D con los líquidos iónicos inmovilizados. Un cambio en las dimensiones de las fibras, diámetros exterior e interior y longitud, cuando los líquidos iónicos se añaden no implica una relación directa en el resultado de los valores de permeabilidad. Las líneas de puntos que acompañan a cada serie en cada gráfico muestran una clara tendencia lineal.

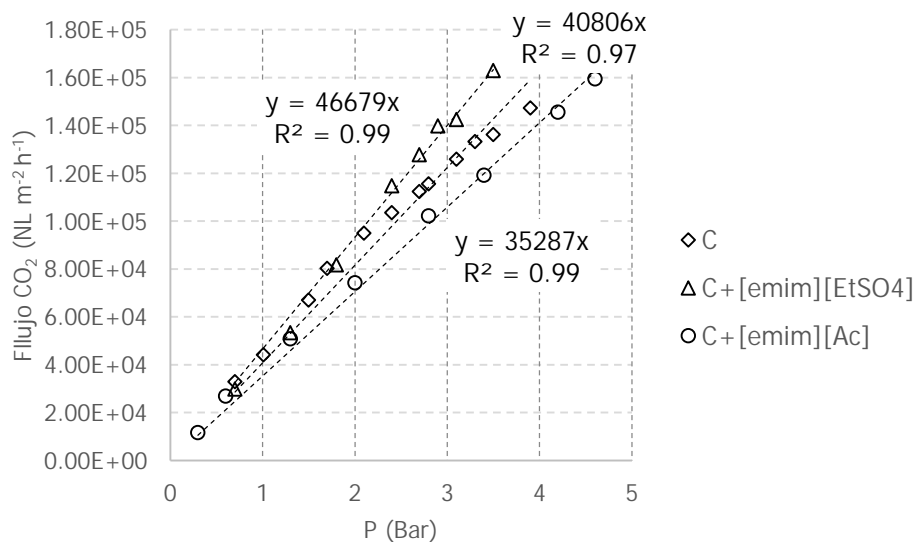


Figura 2.13: Permeabilidad de las fibras huecas tipo C en forma seca y con los ILs.

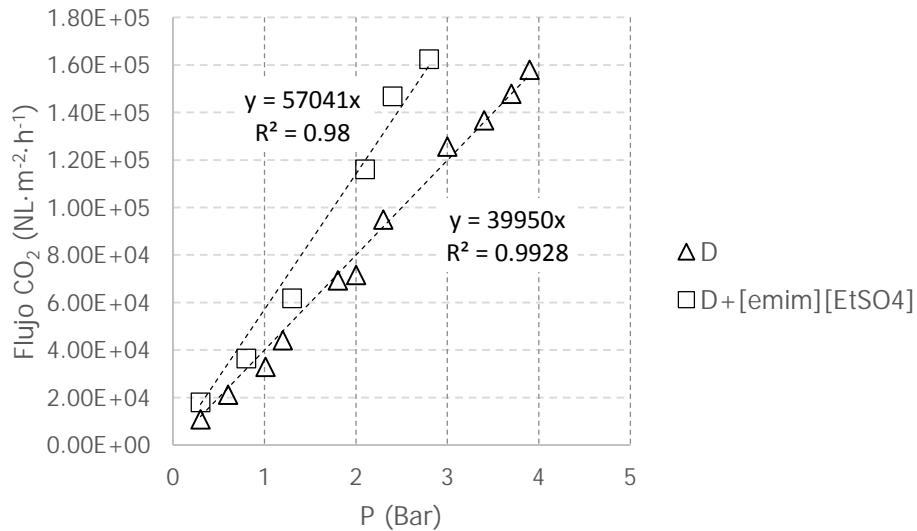


Figura 2.14: Permeabilidad de las fibras huecas tipo D en forma seca y con [emim][EtSO<sub>4</sub>].

Tanto con las fibras C como con las fibras D, la permeabilidad al añadir el líquido iónico [emim][EtSO<sub>4</sub>] aumentó. En el caso de C+[emim][EtSO<sub>4</sub>], la permeabilidad alcanzó un valor de 46679 NL m<sup>-2</sup> h<sup>-1</sup> bar<sup>-1</sup> y en el caso de D+[emim][EtSO<sub>4</sub>] el valor fue de 57041 NL m<sup>-2</sup> h<sup>-1</sup> bar<sup>-1</sup>; éste último valor corresponde a un aumento del 43% en comparación con las fibras cuando no está el IL inmovilizado.

El test de permeabilidad, en un rango de 0 a 14 bar con CO<sub>2</sub>, utilizando las fibras D y el líquido iónico [emim][Ac] no dio lugar a ningún valor, lo que podría atribuirse al hecho de que el líquido iónico llenó los poros, y por lo tanto, el gas fue incapaz de entrar en fibras. Si se pudiesen alcanzar presiones más altas en la planta, llegará un momento en el que el gas pasaría a través de los poros. Este fenómeno significaría que estas fibras son adecuadas para la absorción de CO<sub>2</sub> y que el líquido iónico se integra perfectamente en las fibras. Después de las pruebas de permeación, las fibras conservaban la misma apariencia homogénea.

La Tabla 2.8 compara los valores de permeabilidad con CO<sub>2</sub> de las fibras C y D y con líquido iónico inmovilizado respecto a resultados obtenidos en otros trabajos referenciados en la bibliografía.

Tabla 2.8: Comparación de los valores de permeabilidad con los valores reportados en la bibliografía.

Material de las fibras	CO <sub>2</sub> (NL h <sup>-1</sup> m <sup>-2</sup> bar <sup>-1</sup> )	Referencia
PVDF C (seco)	40806	Gómez-Coma et al., 2016 <sup>a</sup>
PVDF C+[emim][EtSO <sub>4</sub> ] (seco)	46679	Gómez-Coma et al., 2016 <sup>a</sup>
PVDF C+[emim][Ac] (seco)	35287	Gómez-Coma et al., 2016 <sup>a</sup>
PVDF D (seco)	39950	Gómez-Coma et al., 2016 <sup>a</sup>
PVDF D+[emim][EtSO <sub>4</sub> ] (seco)	57041	Gómez-Coma et al., 2016 <sup>a</sup>
PTMSP	5580 - 3070	Nguyen et al., 2011
Teflon AF2400	5900 - 4590	Nguyen et al., 2011
PVDF (Agua/NMP/PVA)	53200 - 365	Medina-Gonzalez et al., 2012
PES_PTMS	8915 - 5588	Lasseguette et al., 2013
PES_Teflon AF2400	9930 - 6000	Lasseguette et al., 2013
Oxyplan_PTMS	3070	Lasseguette et al., 2013
Oxyplan_Teflon AF2400	5120	Lasseguette et al., 2013
TPX	2710 - 1350	Makhloufi et al., 2014
PSF 5% packing density	44200	Skog et al., 2014

En base a los valores presentados en la Tabla 2.8 es importante destacar que el valor de permeabilidad al CO<sub>2</sub> de las fibras tipo D+[emim][EtSO<sub>4</sub>], superó significativamente los valores que aparecen en la bibliografía para contactores de PVDF y Teflón de fibras huecas.

#### **2.2.1.4. Punto burbuja de las fibras huecas**

Los valores del punto burbuja se presentan en la Tabla 2.9. El punto burbuja indica la presión transmembrana necesaria para empujar el IL fuera del poro. Tanto las fibras C como D en presencia y ausencia de IL alcanza una presión bastante alta en comparación con la presión transmembrana en contactores G/L (Vospornik et al., 2003; Alame et al., 2010; Chabanon et al., 2014).

Tabla 2.9: Valores del punto burbuja.

Fibra	Punto burbuja (Bar)
C	4.9
C+[emim][EtSO <sub>4</sub> ]	6.4
C+[emim][Ac]	4.4
D	>7.1
D+[emim][EtSO <sub>4</sub> ]	>7.1
D+[emim][Ac]	>7.1

Los resultados con las fibras C indicaron que en el caso del líquido iónico [emim][EtSO<sub>4</sub>], el punto de burbuja fue mayor que en el caso de fibras sin líquido iónico, ya

que se obtuvieron valores de 6,4 y 4,9 bar respectivamente. Estos valores fueron ligeramente más bajos que los obtenidos con las fibras C+[emim][Ac] (4,4 bar). Los resultados con las fibras D no condujeron a conclusiones definitivas, ya que se superó el valor máximo medido por el equipo (7,1 bar).

A partir de los resultados presentados en este apartado 2.2.1, se puede destacar:

- (i) En el caso de fibras huecas preparadas en laboratorio, como las objeto de este trabajo, de PVDF, es necesario realizar una caracterización exhaustiva de las fibras, que permita conocer sus puntos fuertes y débiles, en función de su tamaño, propiedades mecánicas, permeabilidad al gas CO<sub>2</sub> y punto de burbuja y así disponer de herramientas para la selección de las más adecuadas para el proceso de captura de dióxido de carbono.
- (ii) Se ha conseguido inmovilizar los líquidos iónicos [emim][Ac] y [emim][EtSO<sub>4</sub>] dentro de las fibras, y se ha comprobado que al inmovilizar ILs, se rellenan los poros de las fibras lo que lleva a pensar que se crea una nueva capa.
- (iii) En cuanto a la permeabilidad, las fibras en forma seca presentaron valores más altos que en la forma húmeda, e inmovilizando el [emim][EtSO<sub>4</sub>] la permeabilidad aumentó significativamente, en un 43%. Igualmente se han logrado valores de permeabilidad con ambos líquidos iónicos superiores a 35000 (NL CO<sub>2</sub> h<sup>-1</sup> m<sup>-2</sup> bar<sup>-1</sup>), muy favorables respecto a los encontrados en la bibliografía previa.

## **2.2.2. Captura de CO<sub>2</sub> en diferentes contactores de fibras huecas empleando líquidos iónicos. Estudio de variables de operación**

### **2.2.2.1. Resultados experimentales de Eficacia de captura de CO<sub>2</sub>. Influencia de la temperatura**

Utilizando los distintos contactores de fibra hueca, de polipropileno (PP), polisulfona (Ps) y fluoruro de polivinilideno (PVDF). Se han realizado diferentes experimentos para estudiar la influencia del caudal de gas utilizado así como de la temperatura de trabajo. Los experimentos con PP además se realizaron con los dos líquidos iónicos, el 1-etil-3-metilimidazolio etilsulfato, [emim][EtSO<sub>4</sub>] y el 1-etil-3-metilimidazolio acetato, [emim][Ac]. Además se hicieron experimentos con el líquido iónico [emim][Ac] que permite quimisorción y distintas cantidades de agua (10, 20, 30 y 40% en volumen, que suponen una disminución de la viscosidad del medio líquido). La Tabla 2.10 muestra los resultados obtenidos.

Tabla 2.10: Eficacia de captura de CO<sub>2</sub> experimental a distintas temperaturas, módulos y líquidos iónicos.

No.	Material fibras	Líquido iónico	A (m <sup>2</sup> )	Qg (mL min <sup>-1</sup> )	T (K)	Eficacia (%)
1	PP	[emim][EtSO <sub>4</sub> ]	0.18	70	291	10.5
2	PP	[emim][EtSO <sub>4</sub> ]	0.18	70	298	10.2
3	PP	[emim][EtSO <sub>4</sub> ]	0.18	70	318	9.8
4	PP	[emim][EtSO <sub>4</sub> ]	0.18	20	291	28.7
5	PP	[emim][EtSO <sub>4</sub> ]	0.18	20	298	29.5
6	PP	[emim][EtSO <sub>4</sub> ]	0.18	20	318	28.6
7	PP	[emim][EtSO <sub>4</sub> ]	0.18	20	333	31.6
8	PP	[emim][Ac]	0.18	70	291	16.3
9	PP	[emim][Ac]	0.18	70	298	25.0
10	PP	[emim][Ac]	0.18	70	318	33.9
11	PP	[emim][Ac]	0.18	70	333	40.0
12	PP	[emim][Ac]	0.36	70	291	27.3
13	PP	[emim][Ac]	0.36	70	298	31.5
14	PP	[emim][Ac]	0.36	70	318	52.7
15	Ps	[emim][Ac]	0.18	70	291	29.5
16	Ps	[emim][Ac]	0.18	70	298	33.1
17	Ps	[emim][Ac]	0.18	70	318	37.4
18	Ps	[emim][Ac]	0.18	70	333	38.5
19	Ps	[emim][Ac]	0.18	70	348	44.2
20	PVDF	[emim][Ac]	4.60·10 <sup>-3</sup>	70	303	8.2
21	PVDF	[emim][Ac]	4.60·10 <sup>-3</sup>	70	313	9.6
22	PVDF	[emim][Ac]	4.60·10 <sup>-3</sup>	70	343	11.5
23	PVDF	[emim][Ac]	4.60·10 <sup>-3</sup>	20	303	20.5
24	PVDF	[emim][Ac]	4.60·10 <sup>-3</sup>	20	313	27.1
25	PVDF	[emim][Ac]	4.60·10 <sup>-3</sup>	20	323	28.6
26	PVDF	[emim][Ac]	4.60·10 <sup>-3</sup>	20	333	29.3
27	PVDF	[emim][Ac]-10%agua	4.60·10 <sup>-3</sup>	20	303	53.7
28	PVDF	[emim][Ac]-20%agua	4.60·10 <sup>-3</sup>	20	303	67.1
29	PVDF	[emim][Ac]-30%agua	4.60·10 <sup>-3</sup>	20	303	72.5
30	PVDF	[emim][Ac]-40%agua	4.60·10 <sup>-3</sup>	20	303	60.2

La Figura 2.15, muestra los valores de la Tabla 2.10 operando con un caudal de gas de 70 mL min<sup>-1</sup>. En ella se observa de forma clara, cómo los valores con el módulo de polisulfona alcanzan los mayores valores de eficacia de captura de CO<sub>2</sub>. Sin embargo, hay que recordar que el área del módulo de PVDF es 40 veces más pequeño. El módulo de polipropileno, por su parte, alcanzó la máxima temperatura posible de trabajo (333 K).

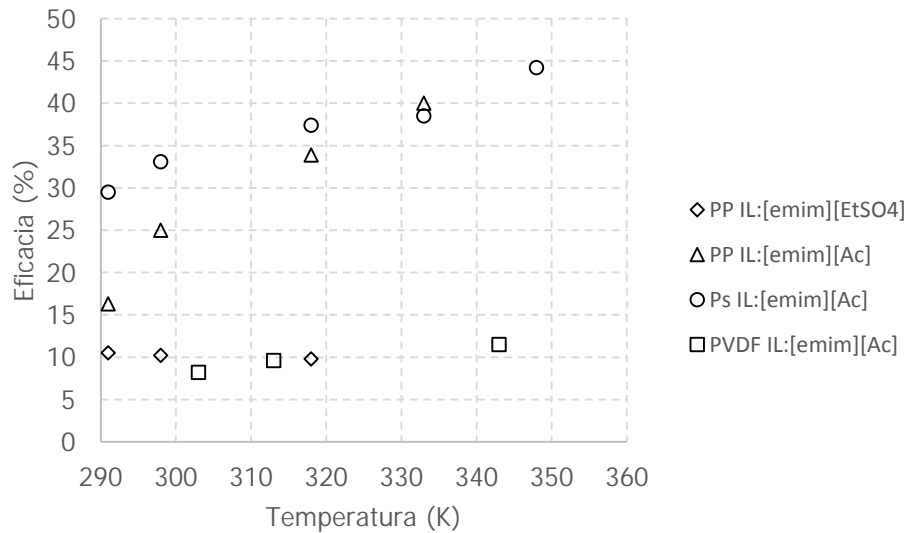


Figura 2.15: Eficacia obtenida con los módulos de PP, PVDF y Ps y los líquidos iónicos [emim][Ac] y [emim][EtSO<sub>4</sub>] utilizando un caudal de gas de 70 mL min<sup>-1</sup>.

La Figura 2.16, representa los valores obtenidos utilizando un caudal de 20 mL min<sup>-1</sup>. En ella, se aprecia como la adición de agua hasta un 30% en volumen al IL [emim][Ac] favorece la absorción significativamente. Además, se puede observar, tanto en la Figura 2.15 como en la 2.16 que utilizando el IL [emim][EtSO<sub>4</sub>] los valores de eficacia no cambian significativamente con la temperatura, a diferencia de lo que sucede cuando se opera con el IL [emim][Ac] que presenta quimisorción.

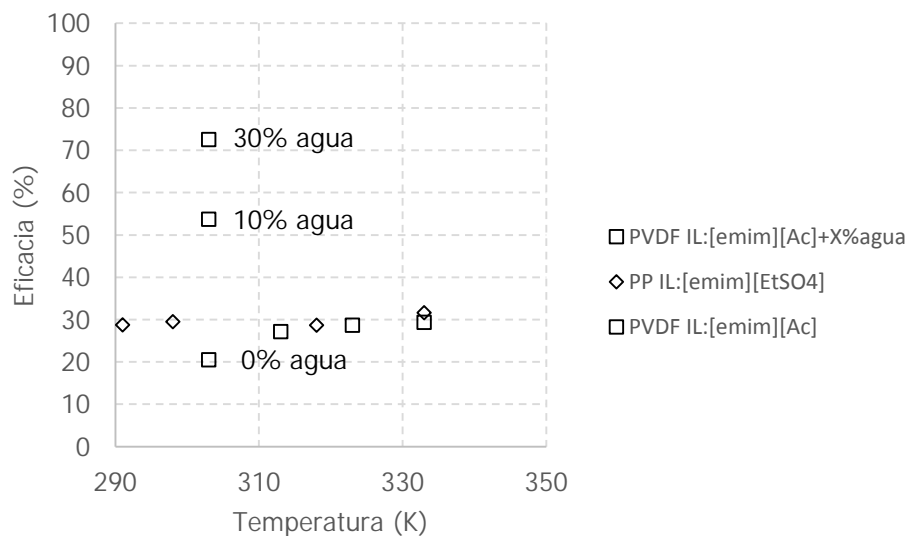


Figura 2.16: Eficacia obtenida con los módulos de PP, PVDF y Ps y los líquidos iónicos [emim][Ac] y [emim][EtSO<sub>4</sub>] utilizando un caudal de gas de 20 mL min<sup>-1</sup>.

En la Figura 2.17, se han representado por un lado, los valores de eficacia obtenida con el módulo de PVDF y por otro los valores de viscosidad cuando se utiliza el [emim][Ac] con distintas cantidades de agua (0, 10, 20, 30 y 40% en volumen) como absorbente. Los valores de viscosidad han sido medidos experimentalmente usando un viscosímetro rotacional (Smart Series, Fungilab España). Estas mediciones se realizaron a 303 K, la misma temperatura de los experimentos de captura de CO<sub>2</sub> cuando se ha trabajado con agua. Se utilizó esta temperatura para asegurar la estabilidad del absorbente híbrido.

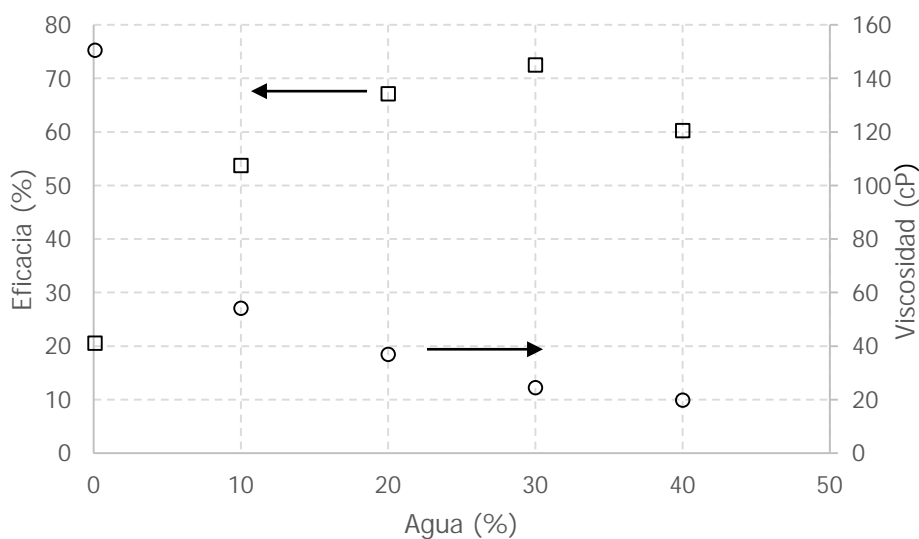


Figura 2.17: Eficacia obtenida con el módulo de PVDF y valores de viscosidad utilizando el [emim][Ac] con distintas cantidades de agua.

---

A partir de los resultados presentados en la Tabla 2.10 y las Figuras 2.15, 2.16 y 2.17, se pueden señalar las siguientes observaciones:

- (i) Ante un aumento de la temperatura, la eficacia sólo mejora en los casos en los que se ha utilizado el líquido iónico [emim][Ac], lo que indica la existencia de absorción tanto física como química, a diferencia del líquido iónico [emim][EtSO<sub>4</sub>] que únicamente presenta absorción física. Un análisis más detallado de la influencia de la temperatura se recoge en el artículo Gómez-Coma et al., (2016b) en el que se cuantifica el efecto de cada uno de los factores que intervienen en el proceso (solubilidad, viscosidad, difusividad y reacción química).
- (ii) A medida que disminuye el caudal de gas, la eficacia aumenta, por lo que habría que llegar a un compromiso entre el número de módulos en paralelo y eficacia de diseño según el caudal de la corriente de gases a tratar.
- (iii) Los mejores resultados se han obtenido con el líquido iónico [emim][Ac] y un 30% de agua en volumen, debido a que la disminución de viscosidad del líquido iónico es más favorable que la disminución en la solubilidad debido a la adición de agua (por ello a 40% ya se pierde eficacia).

#### **2.2.2.2. Aproximación al modelado del proceso: cálculo de resistencias en serie y coeficiente global de transferencia de materia**

Los resultados obtenidos tanto del coeficiente global de transferencia de materia ( $K_{overall}$ ) como de las distintas resistencias a la transferencia de materia; resistencia total  $R_{overall}$ , resistencia en la fase gas ( $R_g$ ), en la membrana ( $R_m$ ) y en la fase líquida ( $R_l$ ) se presentan en la Tabla 2.11. Al igual que en el apartado anterior, los resultados se muestran para comparar la influencia del caudal de gas y la temperatura así como los distintos módulos de fibras huecas PP, Ps y PVDF y los solventes [emim][EtSO<sub>4</sub>], [emim][Ac], y [emim][Ac] con diferentes cantidades de agua (10, 20, 30 y 40% en volumen).

Tabla 2.11: Valores de  $K_{overall}$  y resistencias a la transferencia de materia, a distintas temperaturas, módulos y líquidos iónicos.

No.	Material fibras	Líquidos iónicos	A (m <sup>2</sup> )	Og (mL min <sup>-1</sup> )	T (K)	$K_{overall}$ (10 <sup>6</sup> m s <sup>-1</sup> )	$R_{overall}$ (10 <sup>-5</sup> s m <sup>-1</sup> )	$R_g$ (s m <sup>-1</sup> )	$R_m$ (s m <sup>-1</sup> )	$R_l$ (10 <sup>-5</sup> s m <sup>-1</sup> )
1	PP	[emim][EtSO <sub>4</sub> ]	0.18	70	291	0.71	14	5.3	77	14
2	PP	[emim][EtSO <sub>4</sub> ]	0.18	70	298	0.7	14	5.2	76	14
3	PP	[emim][EtSO <sub>4</sub> ]	0.18	70	318	0.69	15	4.6	72	15
4	PP	[emim][EtSO <sub>4</sub> ]	0.18	20	291	0.68	15	5.4	77	15
5	PP	[emim][EtSO <sub>4</sub> ]	0.18	20	298	0.66	15	5.2	76	15
6	PP	[emim][EtSO <sub>4</sub> ]	0.18	20	318	0.66	15	4.6	72	15
7	PP	[emim][EtSO <sub>4</sub> ]	0.18	20	333	0.67	15	4.3	70	15
8	PP	[emim][Ac]	0.18	70	291	1.1	9.1	5.4	77	9.1
9	PP	[emim][Ac]	0.18	70	298	1.9	5.3	5.2	76	5.3
10	PP	[emim][Ac]	0.18	70	318	2.7	3.7	4.6	72	3.7
11	PP	[emim][Ac]	0.18	70	333	3.2	3.1	4.3	70	3.1
12	PP	[emim][Ac]	0.36	70	291	1	10	5.4	77	10
13	PP	[emim][Ac]	0.36	70	298	1.2	8.3	5.2	76	8.3
14	PP	[emim][Ac]	0.36	70	318	2.5	4	4.6	72	4

Tabla 2.11 (continuación): Valores de  $K_{overall}$  y resistencias a la transferencia de materia, a distintas temperaturas, módulos y líquidos iónicos.

No.	Material fibras	Líquidos iónicos	A (m <sup>2</sup> )	Qg (mL min <sup>-1</sup> )	T (K)	$K_{overall}$ (10 <sup>6</sup> m s <sup>-1</sup> )	$R_{overall}$ (10 <sup>-5</sup> s m <sup>-1</sup> )	$R_g$ (s m <sup>-1</sup> )	$R_m$ (s m <sup>-1</sup> )	$R_i$ (10 <sup>-5</sup> s m <sup>-1</sup> )
15	Ps	[emim][Ac]	0.18	70	291	2.4	0.42	23	77	0.42
16	Ps	[emim][Ac]	0.18	70	298	2.6	0.38	22	76	0.38
17	Ps	[emim][Ac]	0.18	70	318	3.1	0.32	20	72	0.32
18	Ps	[emim][Ac]	0.18	70	333	3.2	0.31	18	69	0.31
19	Ps	[emim][Ac]	0.18	70	348	3.7	0.27	17	67	0.27
20	PVDF	[emim][Ac]	4.60·10 <sup>-3</sup>	70	303	22	0.45	7.4	1.4	0.45
21	PVDF	[emim][Ac]	4.60·10 <sup>-3</sup>	70	313	26	0.38	7	1.3	0.38
22	PVDF	[emim][Ac]	4.60·10 <sup>-3</sup>	70	343	31	0.32	6	1.1	0.32
23	PVDF	[emim][Ac]	4.60·10 <sup>-3</sup>	20	303	17	0.59	7.5	1.4	0.59
24	PVDF	[emim][Ac]	4.60·10 <sup>-3</sup>	20	313	23	0.43	7.1	1.3	0.43
25	PVDF	[emim][Ac]	4.60·10 <sup>-3</sup>	20	323	24	0.42	6.4	1.2	0.42
26	PVDF	[emim][Ac]	4.60·10 <sup>-3</sup>	20	333	25	0.4	6	1.1	0.4
27	PVDF	[emim][Ac]-10%agua	4.60·10 <sup>-3</sup>	20	303	57	0.18	7.5	1.4	0.18
28	PVDF	[emim][Ac]-20%agua	4.60·10 <sup>-3</sup>	20	303	82	0.12	7.5	1.4	0.12
29	PVDF	[emim][Ac]-30%agua	4.60·10 <sup>-3</sup>	20	303	93	0.11	7.5	1.4	0.11
30	PVDF	[emim][Ac]-40%agua	4.60·10 <sup>-3</sup>	20	303	68	0.15	7.5	1.4	0.5

A partir de los datos presentados en la Tabla 2.11, se pueden destacar las siguientes observaciones:

- (i) Las resistencias tanto de la fase gas como de la membrana pueden considerarse despreciables.
- (ii) Los valores del coeficiente global de transferencia de materia,  $K_{overall}$ , cuando se utiliza el líquido iónico [emim][EtSO<sub>4</sub>] son menores que cuando se usa el [emim][Ac] sólo o en presencia de agua.
- (iii) Como ya se observó en el apartado anterior, los valores de  $K_{overall}$  cuando se emplea [emim][EtSO<sub>4</sub>] no dependen significativamente de la temperatura, lo que indica que no hay absorción química.
- (iv) Cuando se utiliza [emim][Ac] si se observa una dependencia en el coeficiente  $K_{overall}$  con la temperatura. Esta dependencia no es acusada, debido probablemente, a la existencia de una absorción química débil y una absorción física fuertemente condicionada por la pérdida de viscosidad y aumento de la difusividad del IL con la temperatura, pero afectada por la pérdida de solubilidad del IL en CO<sub>2</sub> cuando se aumenta la temperatura del proceso.
- (v) Los mayores valores de  $K_{overall}$  se obtienen cuando se trabaja con [emim][Ac] en presencia de agua, pese a que estos experimentos se han realizado únicamente a 303K. Cuando se utiliza [emim][Ac] en ausencia de agua, operando con los módulos de polisulfona y fluoruro de polivinilideno se obtienen los mayores valores de  $K_{overall}$ , en un orden de magnitud superior a los obtenidos empleando el módulo de polipropileno.

En la Tabla 2.12 se han recopilado los valores publicados previamente por otros autores con el fin de comparar los valores obtenidos del coeficiente global de transferencia de materia  $K_{overall}$ , con los módulos de PVDF, al ser con los que se han logrado mejores resultados. En ella, se muestran valores de  $K_{overall}$  en módulos de PVDF, empleando diferentes absorbentes.

Como se puede observar en la última columna de la Tabla 2.12, aparece el término  $K_r$  (s<sup>-1</sup>). Este término resulta de multiplicar el  $K_{overall}$  por el cociente del área correspondiente a las fibras con volumen de la carcasa y puede ser útil para aproximar el comportamiento como un primer orden de reacción química gas-líquido e indica la acumulación de CO<sub>2</sub> en el medio líquido (Albo et al., 2012b).

Tabla 12: Comparación de los valores de  $K_{overall}$  y  $K_r$ , operando con contactores de PDVF y diferentes absorbentes.

Ref.	$d_o$ ( $10^4$ m)	$d_i$ ( $10^4$ m)	L fibra ( $10^1$ m)	L módulo ( $10^1$ m)	Diámetro módulo ( $10^2$ m)	Número de fibras	Area fibra/Volumen carcasa, $m^2 m^{-3}$	Absorbente	$K_{overall}$ ( $10^5 m s^{-1}$ )	$K_r$ ( $10^3 s^{-1}$ )
(Gomez-coma et al., 2016b)	7.7	4.51	2.95	2.95	1.3	11	122	IL [emim][ac]	1.7	2
(Gomez-coma et al., 2016d)	7.7	4.51	2.95	2.95	1.3	11	122	[emim][Ac]-10%agua	5.7	6.97
(Naim e Ismail, 2013)	8	5.5	2.1	2.5	1.5	10	84	[emim][Ac]-20%agua	8.21	10
(Rongwong et al., 2009)	13	8	2.95	2.95	1	35	2742	[emim][Ac]-30%agua	9.34	11.4
(Mansourizadeh et al., 2010)	7.5	4.2	1.5	2.7	1.4	10	48	[emim][Ac]-40%agua	6.81	8.32
(Mansourizadeh e Ismail, 2011)	7.5	4.2	1.5	2.7	1.4	10	48	Agua destilada	1.26	1.06
(Wang et al., 2009)	1.1	8	2.4	2.4	4	150	338	1M MEA	0.08	2.06
(Rahbari-Sisakht et al., 2013)	8.5	4.75	1.5	2.7	1.4	10	55	1M AMP	0.04	1.1
(Boributh et al., 2013)	1.27	7.52	4.5	4.5	0.8	5	265	1M DEA	0.03	0.82
(Korminouri et al., 2014)	8.09	4.54	2.7	1.75	1.4	7	104	Agua	0.01	0.27
								Agua destilada	0.25	0.12
								Agua destilada	0.43	0.21
								1M MEA	0.09	0.32
								Agua destilada	0.49	0.27
								MEA	0.33	0.88
								Agua destilada	0.32	0.33

Como se puede ver, en la Tabla 2.12, el tamaño del módulo de PVDF presentado en este trabajo está en concordancia con los de los otros trabajos realizados a escala laboratorio. Mansourizadeh et al., (2010) y Mansourizadeh e Ismail, (2011) utilizaron fibras con diámetros interior y exterior similares;  $7,50 \cdot 10^{-4}$  y  $4,20 \cdot 10^{-4}$  m, respectivamente. Comparando el número de fibras, varios autores utilizaron entre 5 y 11 (Naim e Ismail, 2013; Mansourizadeh et al., 2010; Mansourizadeh e Ismail, 2011; Rahbari-Sisakht et al., 2013; Boributh et al., 2013; Korminouri et al., 2014). Sin embargo, Rongwong et al., (2009) y Wang et al., (2009) usaron 35 y 150 fibras respectivamente, que unido a que poseían diámetros mayores, es la razón por la que la relación entre el área de la fibra y el volumen de la carcasa fue mayor en estos casos.

En cuanto a los coeficientes  $K_{overall}$  y  $K_r$ , los valores obtenidos para este estudio son prácticamente un orden de magnitud superior respecto a los correspondientes con disolventes convencionales, tales como monoetanolamina (MEA), dietilamina (DEA), monofosfato de adenosina (AMP) y agua. Cabe recordar que tanto el MEA como el DEA y el AMP se han asociado tradicionalmente con problemas de funcionamiento debido a la volatilidad y las pérdidas de disolvente, por lo que en base a estos resultados, los líquidos iónicos se pueden utilizar para eliminar estos inconvenientes ya que poseen presiones de vapor despreciables; alta estabilidad térmica, química y electroquímica además de capacidad de regeneración, y consiguen mejores valores de coeficiente global de transporte de materia (Bara et al., 2009; Ramdin et al., 2012).

### **2.2.3. Simulación y modelado del proceso de captura de CO<sub>2</sub> en contactores de fibras huecas**

Se ha realizado la tarea de modelado del proceso de absorción no dispersiva en contactores de fibras huecas, con los objetivos, por un lado, de aportar la descripción matemática del proceso y evaluar la validez del modelo, en función de las eficacias experimentales y las estimadas; y por otro, de realizar un análisis de sensibilidad para cuantificar la influencia del coeficiente global de transferencia de materia ( $K_{overall}$ ) y de las dimensiones del módulo (variando la longitud, L) sobre la eficacia del proceso de captura de CO<sub>2</sub>, estimando también los valores necesarios para lograr una eficiencia en captura de CO<sub>2</sub> del 90%. Se ha fijado este valor como objetivo de diseño ya que es el valor que se considera para que el proceso con módulos de membranas de fibras huecas y líquidos iónicos sea competitivo con los sistemas convencionales de captura de CO<sub>2</sub> mediante torres de absorción y alcanolaminas. Otros trabajos previos ya marcaron este valor como objetivo (Yeon et al., 2005; Paul et al., 2007; Zhang et al., 2008; Favre, 2011; Wang et al., 2013).

**2.2.3.1. Descripción del proceso mediante el modelo de difusión convección 2D**

Se han resuelto las ecuaciones diferenciales y condiciones frontera correspondientes a la transferencia de CO<sub>2</sub> desde la fase gas a la líquida para la geometría de fibras huecas, con transporte convectivo en la dimensión longitudinal y difusión radial desde el interior de las fibras, por el que circula la corriente gaseosa. Si bien en este trabajo los módulos utilizados presentan no-mojado con los líquidos iónicos, se muestra también a continuación el comportamiento si hubiera mojado de los poros, a modo de comparación. Las Figuras 2.18a y 2.18c muestran la concentración adimensional de CO<sub>2</sub> a lo largo de la longitud adimensional de una fibra hueca. Por otro lado, las Figura 2.18b y 2.18d utilizan la misma abscisa pero en este caso, lo que se representan es la eficiencia de captura de CO<sub>2</sub> (%).

Bajo las condiciones de operación de un contactor de PVDF con [emim][Ac]+30% agua a 303K y un flujo de gas de 20mL min<sup>-1</sup>, que se muestra a modo de ejemplo (Gomez-Coma et al., 2016c) la eficacia del proceso se redujo un 60% cuando los poros de la membrana se mojan (Figura 2.18c-2.18d), respecto a cuando los poros de la membrana se llenan únicamente con gas (Figura 2.18a-2.18b).

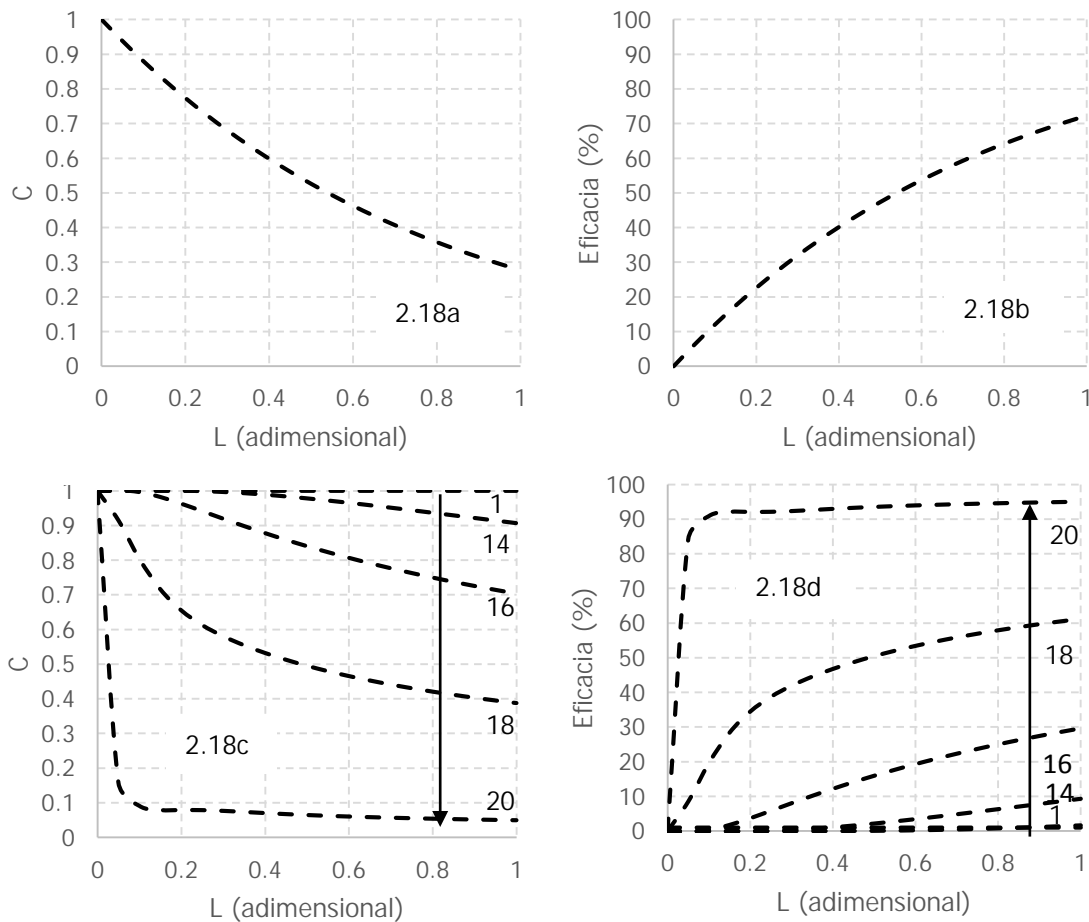


Figura 2.18: Perfiles a lo largo de la longitud de los nodos en función de la concentración adimensional de CO<sub>2</sub> y la eficacia en modo no-mojado (2.18a-2.18b) y mojado (2.18c-2.18d) utilizando el módulo de PVDF. Nodo 1:  $r=0$ , nodo 20:  $r=r_i$ .

Para la validación del modelo propuesto con los diferentes contactores empleados en este trabajo, se han resumido en la Tabla 2.13 los valores de eficacia experimental y simulada por el modelo propuesto con los diferentes contactores y condiciones de operación utilizadas. Únicamente en el caso de las fibras huecas de polisulfona la diferencia en los resultados entre la eficacia simulada y experimental supera el 15% (17.3-18.3%). En el resto de casos (fibras huecas de polipropileno y PVDF) el error es en todos los casos menor al 3%, por lo que se puede concluir que el modelo propuesto es válido para absorción no dispersiva utilizando módulos de membranas de fibras huecas y líquidos iónicos.

Tabla 2.13: Comparación entre los resultados experimentales y simulados con los módulos de fibras huecas de PP, Ps y PVDF.

Material fibras	Absorbente	T (K)	$u_m$ (m s <sup>-1</sup> )	Eficacia Experimental (%)	Eficacia Simulada (%)	/Error absoluto/
PP	[emim][EtSO <sub>4</sub> ]	291	$1.33 \cdot 10^{-2}$	10.5	10.6	0.1
PP	[emim][EtSO <sub>4</sub> ]	298	$1.33 \cdot 10^{-2}$	10.2	10.6	0.4
PP	[emim][EtSO <sub>4</sub> ]	318	$1.33 \cdot 10^{-2}$	9.8	10.5	0.7
PP	[emim][EtSO <sub>4</sub> ]	291	$3.81 \cdot 10^{-3}$	28.7	31.3	2.6
PP	[emim][EtSO <sub>4</sub> ]	298	$3.81 \cdot 10^{-3}$	29.5	31.5	2
PP	[emim][EtSO <sub>4</sub> ]	318	$3.81 \cdot 10^{-3}$	28.6	31.5	2.9
PP	[emim][EtSO <sub>4</sub> ]	333	$3.81 \cdot 10^{-3}$	31.6	31.4	0.2
PP	[emim][Ac]	291	$1.33 \cdot 10^{-2}$	16.3	16.0	0.3
PP	[emim][Ac]	298	$1.33 \cdot 10^{-2}$	25.0	26.0	1
PP	[emim][Ac]	318	$1.33 \cdot 10^{-2}$	33.9	34.7	0.8
PP	[emim][Ac]	333	$1.33 \cdot 10^{-2}$	40.0	39.6	0.4
PP	[emim][Ac]	291	$6.67 \cdot 10^{-3}$	27.3	27.1	0.2
PP	[emim][Ac]	298	$6.67 \cdot 10^{-3}$	31.5	31.5	0.0
PP	[emim][Ac]	318	$6.67 \cdot 10^{-3}$	52.7	54.4	1.7
Ps	[emim][Ac]	291	$7.58 \cdot 10^{-3}$	29.5	46.8	17.3
Ps	[emim][Ac]	298	$7.58 \cdot 10^{-3}$	33.1	49.5	16.4
Ps	[emim][Ac]	318	$7.58 \cdot 10^{-3}$	37.4	55.7	18.3
Ps	[emim][Ac]	333	$7.58 \cdot 10^{-3}$	38.5	56.8	18.3
Ps	[emim][Ac]	348	$7.58 \cdot 10^{-3}$	44.2	62.1	17.9
PVDF	[emim][Ac]	303	$6.61 \cdot 10^{-1}$	8.2	8.7	0.5
PVDF	[emim][Ac]	313	$6.61 \cdot 10^{-1}$	9.6	10.0	0.4
PVDF	[emim][Ac]	343	$6.61 \cdot 10^{-1}$	11.5	11.7	0.2
PVDF	[emim][Ac]	303	$1.90 \cdot 10^{-1}$	20.5	20.9	0.4
PVDF	[emim][Ac]	313	$1.90 \cdot 10^{-1}$	27.1	27.4	0.3
PVDF	[emim][Ac]	323	$1.90 \cdot 10^{-1}$	28.6	28.4	0.2
PVDF	[emim][Ac]	333	$1.90 \cdot 10^{-1}$	29.3	29.4	0.1

Tabla 2.13 (continuación): Comparación entre los resultados experimentales y simulados con los módulos de fibras huecas de PP, Ps y PVDF.

Material fibras	Absorbente	T (K)	$u_m$ ( $m\ s^{-1}$ )	Eficacia Experimental (%)	Eficacia Simulada (%)	/Error absoluto/
PVDF	[emim][Ac]+10%agua	303	$1.90 \cdot 10^{-1}$	53.7	54.5	0.8
PVDF	[emim][Ac]+20%agua	303	$1.90 \cdot 10^{-1}$	67.1	67.8	0.7
PVDF	[emim][Ac]+30%agua	303	$1.90 \cdot 10^{-1}$	72.5	72.6	0.1
PVDF	[emim][Ac]+40%agua	303	$1.90 \cdot 10^{-1}$	60.2	60.9	0.7

### 2.2.3.2. Análisis de sensibilidad

Se ha evaluado la influencia del coeficiente de transferencia de materia y de las dimensiones del contactor en la eficacia de captura de  $CO_2$  en los contactores de fibras huecas, y se han calculado los valores de  $K_{overall}$  y longitud de módulo necesarios para obtener un 90% de eficacia de recuperación de  $CO_2$ . El análisis de sensibilidad realizado en este trabajo resulta útil para escalar el proceso en función del caudal de gas. Una vez conocidos los módulos en serie requeridos para alcanzar una separación mayor al 90% para un flujo de gas concreto, se pueden disponer tantos módulos en paralelo como sean necesarios en base al flujo de gases de combustión requerido (Hoff y Svensen 2013).

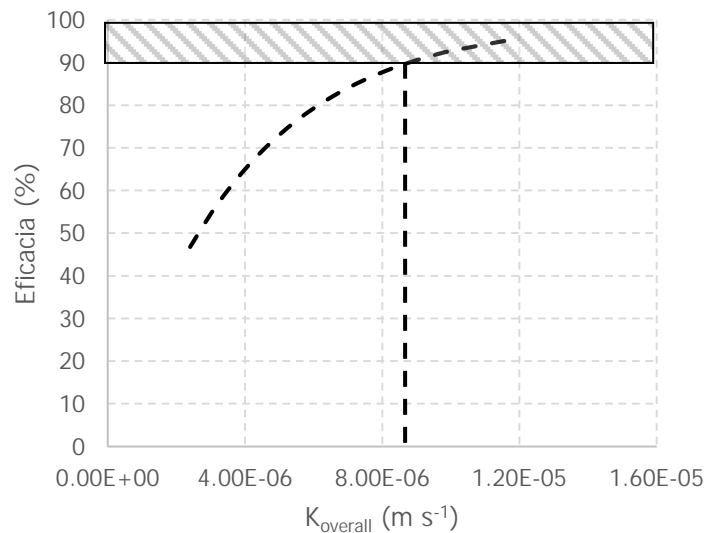


Figura 2.19: Influencia del  $K_{overall}$  en la eficacia de captura de  $CO_2$ , y valor necesario para alcanzar un 90% de eficacia con el módulo de Ps.

La Figura 2.19, muestra los valores de  $K_{overall}$  requeridos cuando se trabaja con el módulo de Ps y con un caudal de gas de 70 mL min<sup>-1</sup>. Un coeficiente global de transporte de materia mayor a  $9.0 \cdot 10^{-6}$  m s<sup>-1</sup> conduciría a eficacia de captura de CO<sub>2</sub> mayor del 90%.

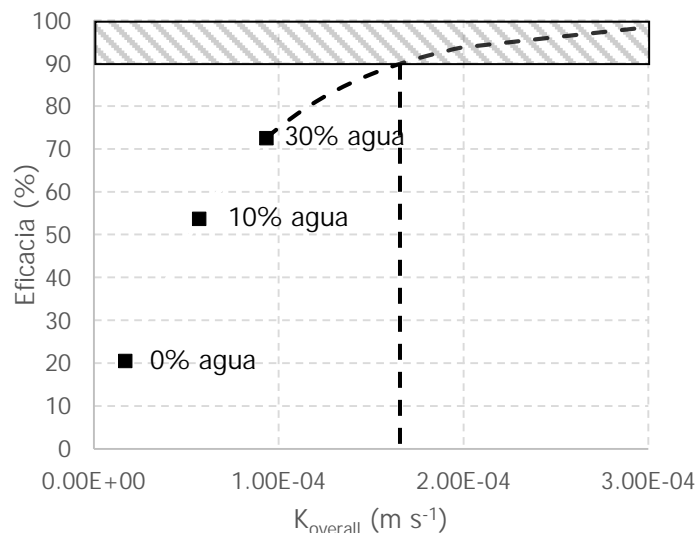


Figura 2.20: Influencia del  $K_{overall}$  en la eficacia de captura de CO<sub>2</sub>, y valor necesario para alcanzar un 90% de eficacia con el módulo de PVDF.

En el caso de los módulos de fluoruro de polivinilideno, como se aprecia en la Figura 2.20, sería necesaria un valor de  $K_{overall}$  de  $1.70 \cdot 10^{-4}$  m s<sup>-1</sup> para alcanzar una eficacia de captura de CO<sub>2</sub> superior al 90%. En la figura, además, se han marcado los puntos obtenidos con las distintas cantidades de agua en el líquido iónico [emim][Ac].

En cuanto al análisis de la longitud de módulo necesaria, se ha estimado, como se muestra en la Figura 2.21, los módulos que son necesarios acoplar en serie para el 90% de eficacia si se trabaja con un caudal de 70 mL min<sup>-1</sup> y a una temperatura de 291K. Para el caso de los módulos de polipropileno, sería necesario disponer de 20 módulos en serie (longitud total de 2.3 m) si se trabaja con el líquido iónico [emim][EtSO<sub>4</sub>] y de 13 (1.5 m) si se trabaja con el líquido iónico [emim][Ac]. Por su parte, el módulo de Ps con [emim][Ac] como absorbente requeriría de únicamente 4 módulos en serie (longitud total 1.4 m).

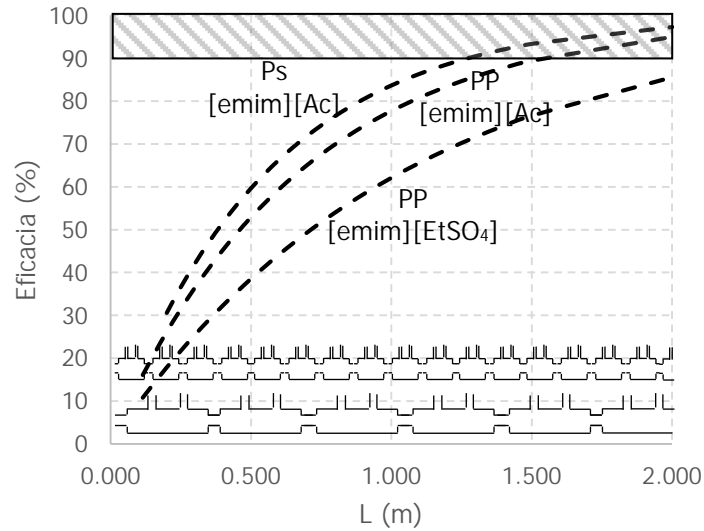


Figura 2.21: Módulos en serie requeridos para alcanzar una eficacia del 90% utilizando un caudal de  $70 \text{ mL min}^{-1}$ .

El análisis con el módulo de PVDF se ha realizado a un caudal de  $20 \text{ mL min}^{-1}$  y 303K. Se han comparado los módulos dispuestos en serie necesarios si se trabaja con el [emim][Ac] en ausencia de agua o con 30% agua-[emim][Ac], expresado en volumen, por ser la combinación que arrojó mejores valores tanto de eficacia como de  $K_{\text{overall}}$ .

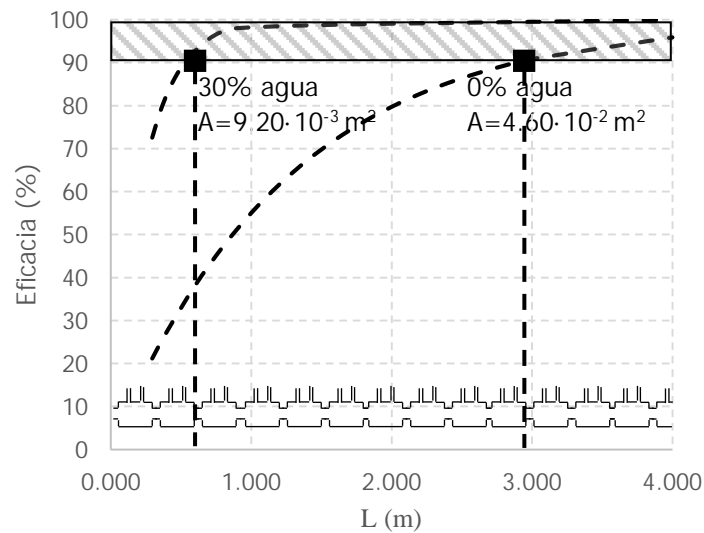


Figura 2.22: Módulos de PVDF en serie requeridos para alcanzar una eficacia del 90% utilizando un caudal de  $20 \text{ mL min}^{-1}$ .

Como se muestra en la Figura 2.22, trabajando en ausencia de agua, 10 módulos de membranas de fibras huecas son necesarios para alcanzar el objetivo de diseño. Sin embargo trabajando con un 30% de agua y [emim][Ac] únicamente son necesarios dos contactores que dispuestos en serie únicamente son 0.59 m.

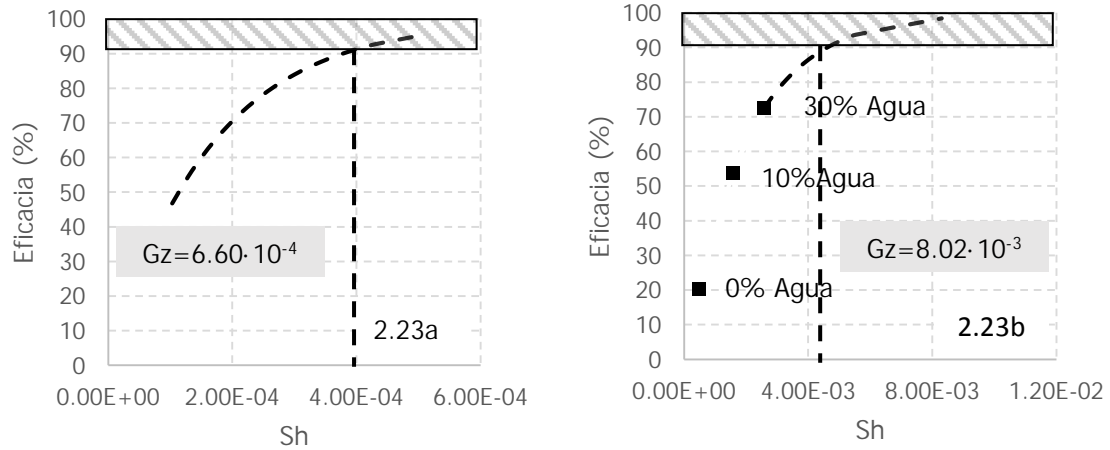


Figura 2.23: Análisis de sensibilidad en función del número de Sherwood.

Finalmente se ha realizado el análisis de sensibilidad en base a los números adimensionales de Sherwood y Graetz. La Figura 2.23, muestra los valores de la eficacia en función del número de Sherwood. La Figura 23a muestra los resultados utilizando el módulo de Polisulfona y en ella se aprecia cómo, utilizando Sh mayores de  $4.00 \cdot 10^{-4}$  se lograrían valores superiores al 90% de eficacia, manteniendo un Graetz fijado de  $6.60 \cdot 10^{-4}$ . Por su parte, la Figura 23b, estudia el número de Sh en el módulo de PVDF y en ella, se consigue la eficacia deseada (>90%) cuando se trabaja con valores de Sh mayores a  $4.70 \cdot 10^{-3}$  usando un valor fijo del Graetz de  $8.02 \cdot 10^{-3}$ .

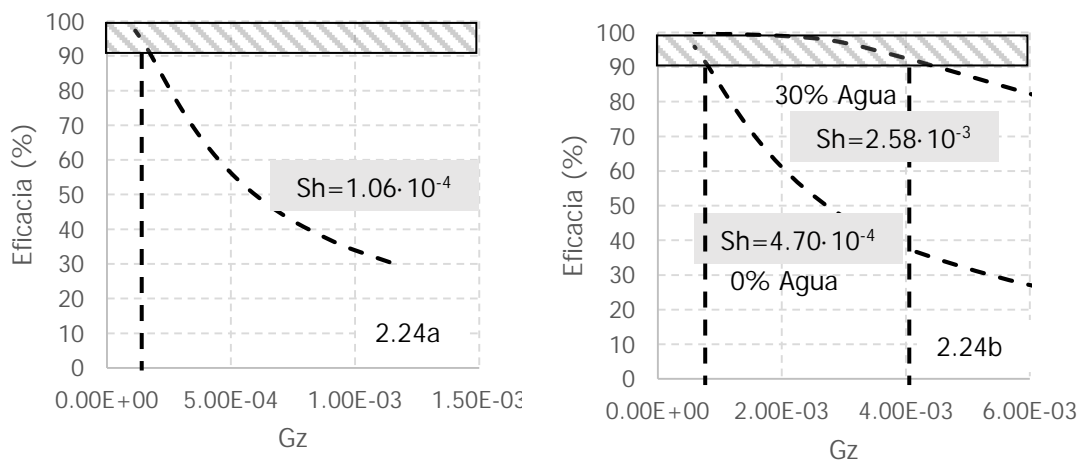


Figura 2.24: Análisis de sensibilidad en función del número de Graetz.

La Figura 2.24, se centra en el análisis de sensibilidad en función del número adimensional de Graetz. Cuando se utiliza el módulo de Ps con un valor fijo de  $Sh=1.06 \cdot 10^{-4}$ , utilizando valores de  $Gz$  menores a  $2.53 \cdot 10^{-4}$ , se consiguen los valores de eficacia requeridos (Figura 2.24a). Por su parte, la Figura 2.24b, muestra los valores del número de Graetz cuando se trabaja con el módulo de PVDF. Utilizando unos números de Sherwood fijos de  $4.70 \cdot 10^{-4}$  y  $2.58 \cdot 10^{-3}$  con valores del número de  $Gz$  menores a  $4.50 \cdot 10^{-3}$  y  $7.89 \cdot 10^{-3}$  para el líquido iónico [emim][Ac] en ausencia de agua y para [emim][Ac]-30%Agua, respectivamente, se logran eficacias mayores al 90% de separación del dióxido de carbono.

A partir de los datos presentados en este apartado de análisis de sensibilidad del proceso se pueden destacar las siguientes observaciones:

- (i) En base a la diferencia entre los resultados experimentales y simulados, el modelo utilizado en el presente trabajo es de total fiabilidad para realizar estimaciones.
- (ii) Los contactores de membrana de fibra hueca han de ser acoplados en paralelo y en serie en función del flujo de gas y la eficacia requerida en cada situación.
- (iii) Trabajando con el módulo de Ps y un caudal de gas  $70 \text{ mL min}^{-1}$ , con un  $K_{\text{overall}}$  de  $9.00 \cdot 10^{-6} \text{ m s}^{-1}$  se alcanzaría una eficacia del 90%. Con el módulo de PVDF sería necesario un  $K_{\text{overall}}$   $1.70 \cdot 10^{-4} \text{ m s}^{-1}$  trabajando con un caudal de  $20 \text{ mL min}^{-1}$ .
- (iv) Utilizando el disolvente híbrido [emim][Ac]-30%Agua, únicamente colocando 2 módulos de PVDF en serie (0.59 m; instalación escala laboratorio) se alcanzaría la eficacia de captura de  $\text{CO}_2$  del 90%. Por su parte, utilizando [emim][Ac] en ausencia de agua, también para el proceso escala laboratorio, serían necesarios 10 (3 m), 4 (1.4 m) y 13 (1.5 m) para los módulos de PVDF, Ps y PP respectivamente. Si se trabaja con el líquido iónico [emim][EtSO<sub>4</sub>] y el módulo de PP se requerirían 20 módulos (2.3 m).

### **2.2.3.3. Factor de intensificación**

Con el objetivo de realizar una comparativa entre los sistemas tradicionales de absorción y el proceso intensificado mediante contactores de membranas de fibras huecas y líquidos iónicos se ha evaluado el factor de intensificación (I). Este factor ha sido descrito en sus trabajos por Bounaceur et al., (2012), y se calcula como el cociente entre la capacidad de absorción volumétrica del contactor de membranas y la capacidad de absorción volumétrica

media de una columna de relleno (en mol CO<sub>2</sub> m<sup>-3</sup> s<sup>-1</sup>). El valor de referencia de una torre de absorción se estima en 1 mol de CO<sub>2</sub> m<sup>-3</sup> s<sup>-1</sup> para una solución acuosa de 30% MEA.

Tabla 2.14: Cálculo del factor de intensificación (I) a partir de los datos experimentales de los módulos de Ps y PVDF.

Material fibras	Líquido iónico	Temperatura (K)	K <sub>overall</sub> (m s <sup>-1</sup> )	Factor de intensificación (I)
Ps	[emim][Ac]	291	2.40 · 10 <sup>-6</sup>	4.1
Ps	[emim][Ac]	298	2.60 · 10 <sup>-6</sup>	4.5
Ps	[emim][Ac]	314	3.10 · 10 <sup>-6</sup>	4.7
Ps	[emim][Ac]	333	3.20 · 10 <sup>-6</sup>	4.8
Ps	[emim][Ac]	348	3.70 · 10 <sup>-6</sup>	5.2
PVDF	[emim][Ac]	303	1.70 · 10 <sup>-5</sup>	1.1
PVDF	[emim][Ac]-10%agua	303	5.70 · 10 <sup>-5</sup>	2.8
PVDF	[emim][Ac]-20%agua	303	8.21 · 10 <sup>-5</sup>	3.4
PVDF	[emim][Ac]-30%agua	303	9.34 · 10 <sup>-5</sup>	3.7
PVDF	[emim][Ac]-40%agua	303	6.81 · 10 <sup>-5</sup>	3.1

La Tabla 2.14 muestra, los resultados del factor de intensificación obtenidos a partir de los resultados experimentales con los módulos de Ps y PVDF. En ella se puede ver cómo se obtienen valores superiores, y por tanto competitivos, a los de referencia para la torre de absorción. En concreto, con el módulo de polisulfona a 348K se consigue un factor superior a 5.

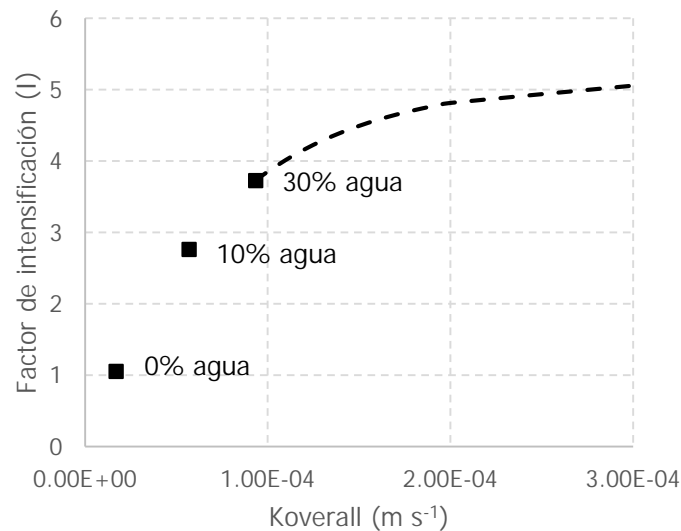


Figura 2.25: Factor de intensificación con el módulo de PVDF.

La Figura 2.25 muestra de forma gráfica los resultados obtenidos del factor de intensificación (I) con el módulo de PVDF. En ella, se aprecia cómo, para un K<sub>overall</sub> de 1.70 · 10<sup>-5</sup>

$m s^{-1}$  obtenido con el [emim][Ac] en ausencia de agua, el valor del factor de intensificación es de 1.05 y cuando se utiliza el [emim][Ac]+30% agua,  $I$  aumenta hasta el valor de 3.73 ( $K_{overall}=9.34 \cdot 10^{-5} m s^{-1}$ ). Además, trabajando con un  $K_{overall}=1.70 \cdot 10^{-4} m s^{-1}$ , correspondiente a una captura de dióxido de carbono del 90%, se alcanza un valor del factor de intensificación de 4.64, lo que demuestra que el módulo de PVDF, con el absorbente híbrido [emim][Ac]-agua, también es competitivo con las torres de absorción convencionales.

### **2.3. Nomenclatura usada en el capítulo 2**

A	[m <sup>2</sup> ]	Área de la membrana efectiva
B	[-]	Factor pre-exponencial
<i>D</i>	[m <sup>2</sup> s <sup>-1</sup> ]	Difusividad
<i>d<sub>h</sub></i>	[m]	Diámetro hidráulico
<i>d<sub>i</sub></i>	[m]	Diámetro interno de la fibra
<i>d<sub>lm</sub></i>	[-]	Media logarítmica de los diámetros de la fibra
<i>d<sub>o</sub></i>	[m]	Diámetro externo de la fibra
E	[-]	Factor de mejora
Gz	[-]	Número de Graetz
<i>H<sub>d</sub></i>	[-]	Número de Henry adimensional
<i>I</i>	[-]	Factor de intensificación
<i>k<sub>g</sub></i>	[m s <sup>-1</sup> ]	Coefficiente de transferencia de materia en la fase gas
<i>k<sub>l</sub></i>	[m s <sup>-1</sup> ]	Coefficiente de transferencia de materia en la fase líquida
<i>k<sub>mg</sub></i>	[m s <sup>-1</sup> ]	Coefficiente de transferencia de materia en la membrana
<i>K<sub>overall</sub></i>	[m s <sup>-1</sup> ]	Coefficiente global de transferencia de materia
L	[m]	Longitud de la fibra
<i>n</i>	[-]	Número de fibras
<i>N<sub>CO2</sub></i>	[mol m <sup>2</sup> s <sup>-1</sup> ]	Flujo de absorción de dióxido de carbono

$P_T$	[bar]	Presión total
$Q$	[m <sup>3</sup> s <sup>-1</sup> ]	Caudal
$R$	[bar L mol <sup>-1</sup> K <sup>-1</sup> ]	Constante de los gases ideales
$Re$	[-]	Número de Reynolds
$R_g$	[s m <sup>-1</sup> ]	Resistencia en la fase gas
$R_l$	[s m <sup>-1</sup> ]	Resistencia en la fase líquida
$R_m$	[s m <sup>-1</sup> ]	Resistencia en la membrana
$R_{overall}$	[s m <sup>-1</sup> ]	Resistencia total
$Sc$	[-]	Número de Schmidt
$Sh$	[-]	Número de Sherwood
$t$	[s]	Tiempo
$T$	[K]	Temperatura
$u_m$	[m s <sup>-1</sup> ]	Velocidad lineal

#### *Subíndices*

g Gas

l Líquido

in Interior del módulo de fibras

out Exterior del módulo de fibras

#### **2.4. Referencias del capítulo 2**

Alame M., Abusaloua A., Pera-Titus M., Guilhaume N., Fiaty K., Giroir-Fendler A., High-performance catalytic wet air oxidation (CWAO) of organic acids and phenol in interfacial catalytic membrane contactors under optimized wetting conditions, *Catal. Today*. **2010**, 157, 327–333.

Albo J., Santos E., Neves L.A., Simeonov S.P., Afonso C.A.M., Crespo J.G., Irabien A., Separation performance of CO<sub>2</sub> through Supported Magnetic Ionic Liquid Membranes (SMILMs), *Sep. Purif. Technol.* **2012a**, 97, 26–33.

Albo J, Irabien A., Non-dispersive absorption of CO<sub>2</sub> in parallel and cross-flow membrane modules using EMISE, *J. Chem. Technol. Biotechnol.* **2012b**, 87 1502–1507.

Bara J.E., Carlisle T.K., Gabriel C.J., Camper D., Finotello A., Gin D.L., Noble R.D., Guide to CO<sub>2</sub> Separations in Imidazolium-Based Room-Temperature Ionic Liquids, *Ind. Eng. Chem. Res.* **2009**, 48, 2739–2751.

Blath J., Deubler N., Hirth T., Schiestel T., Chemisorption of carbon dioxide in imidazolium based ionic liquids with carboxylic anions, *Chem. Eng. J.* **2012**, 181-182, 152–158.

Boributh S., Jiraratananon R., Li K., Analytical solutions for membrane wetting calculations based on log-normal and normal distribution functions for CO<sub>2</sub> absorption by a hollow fiber membrane contactor, *J. Membr. Sci.* **2013**, 429, 459-472.

Bounaceur R., Castel C., Rode S., Roizard D., Favre E., Membrane contactors for intensified post combustion carbon dioxide capture by gas-liquid absorption in MEA: A parametric study, *Chem. Eng. Res. Des.* **2011**, 90, 2325-2337.

Casado-Coterillo C., Soto J., Jimare M.T., Valencia S., Corma S., Tellez C., Coronas J., Preparation and characterization of ITQ-29/polysulfone mixed-matrix membranes for gas separation: Effect of zeolite composition and crystal size, *Chem. Eng. Sci.* **2012**, 73, 116–122.

Chabanon E., Belaisaoui B., Favre E., Gas-liquid separation processes based on physical solvents: opportunities for membranes, *J. of Membr. Sci.* **2014**, 459, 52–61.

Favre E., Membrane processes and postcombustion carbon dioxide capture: Challenges and prospects, *Chem. Eng. J.* **2011**, 171, 782-793.

Gomez-Coma L., Garea A., Irabien A., Non-dispersive absorption of CO<sub>2</sub> in [emim][EtSO<sub>4</sub>] and [emim][Ac]: Temperature influence, *Sep. Purif. Technol.* **2014**, 132, 120–125.

Gomez-Coma L., Garea A., Rouch J.C., Savart T., Lahitte J.F., Remigy J.C., Irabien A., Membrane modules for CO<sub>2</sub> capture based on PVDF hollow fibers with ionic liquids immobilized, *J. Membr. Sci.* **2016a**, 498, 218-226.

Gomez-Coma L., Garea, A., Irabien A. PVDF Membrane contactor for CO<sub>2</sub> capture using the ionic liquid [emim][Ac]: mass transfer analysis, *Chem. Eng. Technol.* **2016b**, under review.

Gomez-Coma L., Garea, A., Irabien A. Carbon dioxide capture by [emim][Ac] ionic liquid in a polysulfone hollow fiber membrane contactor, *Int. J. Greenh. Gas Control.* **2016c**, 52, 1-9.

Gomez-Coma L., Garea, A., Irabien A., Hybrid solvent ([emim][Ac]+water) to improve the CO<sub>2</sub> capture efficiency in a PVDF hollow fiber contactor, *ACS. Sustain. Chem. Eng.* **2016d**, aceptado, octubre 2016.

Gurau G., Rodríguez H., Kelley S.P., Janiczek P., Kalb R.S., Rogers R.D., Demonstration of chemisorption of carbon dioxide in 1,3-dialkylimidazolium acetate ionic liquids, *Angew. Chem. Int. Ed.* **2011**, 50, 12024–12026.

Hoff K.A., Svendsen H.F., CO<sub>2</sub> absorption with membrane contactors vs. packed absorbers- Challenges and opportunities in post combustion capture and natural gas sweetening, *Energy Procedia.* **2013**, 37, 952-960.

Kim D.H., Baek I.H., Hong S.U., Lee H.K., Study on immobilized liquid membrane using ionic liquid and PVDF hollow fiber as a support for CO<sub>2</sub>/N<sub>2</sub> separation, *J. Membr. Sci.* **2011**, 372, 346-354.

Korminouri F., Rahbari-Sisakht M., Rana D., Matsuura T., Ismail A.F., Study on the effect of air-gap length on properties and performance of surface modified PVDF hollow fiber membrane contactor for carbon dioxide absorption, *Sep. Purif. Technol.* **2014**, 132, 601-609.

Korminouri F., Rahbari-Sisakht M., Matsuura T., Ismail A.F., Surface modification of polysulfone hollow fiber membrane spun under different air-gap lengths for carbon dioxide absorption in membrane contactor system, *Chem. Eng. J.* **2015**, 264, 453–461.

Lasseuguette E., Rouch J.C., Remigy J.C., Hollow-fiber coating: Application to preparation of composite hollow-fiber membrane for gas separation, *Ind. Eng. Chem. Res.* **2013**, 52(36), 13146-13158.

Levenspiel O., Flujo de fluidos e intercambio de calor, Oregon State University Corvallis, Oregon. Editorial Reverté S.A. **1993**.

Lorain O., Espenan J.M., Remigy J.C., Lahitte J.F., Rouch J.C., Savart T., Gerard P., Magnet S., Copolymer having amphiphilic blocks, and use thereof for manufacturing polymer filtration membranes, WO2014/139977 (A1) **2014**.

Luis P., Ortiz I., Aldaco R., Garea A., Irabien A., Recovery of sulfur dioxide using non-dispersive absorption. *Int. J. Chem. React. Eng.* **2007**, 5, 1-9.

---

Luis P., Garea A., Irabien A., Zero solvent emission process for sulfur dioxide recovery using a membrane contactor and ionic liquids, *J. Membr. Sci.* **2009**, 330, 80–89.

Luis P., Garea A., Irabien, A., Modelling of a hollow fibre ceramic contactor for SO<sub>2</sub> absorption. *Sep. Purif. Technol.* **2010**, 72, 174–179.

Makhloufi C., Lasseuguette E., Remigy J.C., Belaissaoui B., Roizard D., Favre E., Ammonia based CO<sub>2</sub> capture process using hollow fiber membrane contactors, *J. Membr. Sci.* 455 (2014) 236-246.

Mansourizadeh A., Ismail A.F., Effect of LiCl concentration in the polymer dope on the structure and performance of hydrophobic PVDF hollow fiber membranes for CO<sub>2</sub> absorption, *Chem. Eng. J.* **2010**, 165, 980-988.

Mansourizadeh A., Ismail A.F., A developed asymmetric PVDF hollow fiber membrane structure for CO<sub>2</sub> Absorption, *Int. J. Green. Gas Control.* **2011**, 5, 374-380.

Medina-Gonzalez Y., Lasseuguette E., Rouch J.C., Remigy J.C., Improving PVDF hollow fiber membranes for CO<sub>2</sub> gas capture, *Separ. Sci. Technol.* **2012**, 47(11), 1596-1605.

Morgan D., Ferguson L., Scovazzo P., Diffusivities of gases in room-temperature ionic liquids: data and correlations obtained using a lag-time technique, *Ind. Eng. Chem. Res.* **2005**, 44, 4815–4823.

Nabian N., Ghoreyshi A.A., Rahimpour A., Shakeri M., Performance evaluation and mass transfer study of CO<sub>2</sub> absorption in flat sheet membrane contactor using novel porous polysulfone membrane, *Korean J. Chem. Eng.* **2015**, 32(11), 2204-2211.

Naim R., Ismail A.F., Effect of fiber packing density on physical CO<sub>2</sub> absorption performance in gas–liquid membrane contactor, *Sep. Purif. Technol.* **2013**, 115, 152-157.

Nguyen P.T., Lasseuguette E., Medina-Gonzalez Y., Remigy J.C., Roizard D., Favre E., A dense membrane contactor for intensified CO<sub>2</sub> gas/liquid absorption in post-combustion capture, *J. Membr. Sci.* **2011**, 377(1-2) 261-272.

Ortiz A., Gorri D., Irabien A., Ortiz I., Separation of propylene/propane mixtures using Ag<sup>+</sup>-RTIL solutions. Evaluation and comparison of the performance of gas-liquid contactors, *J. Membr. Sci.* **2010**, 360, 130-141.

Paul S., Ghoshal A.K., Mandal B., Removal of CO<sub>2</sub> by single and blended aqueous alkanolamine solvents in hollow-fiber membrane contactor: modeling and simulation, *Ind. Eng. Chem. Res.* **2007**, 46, 2576-2588.

Rahbari-Sisakht M., Ismail A.F., Rana D., Matsuura T., Emadzadeh D., Effect of SMM concentration on morphology and performance of surface modified PVDF hollow fiber membrane contactor for CO<sub>2</sub> absorption, *Sep. Purif. Technol.* **2013**, 116, 67-72.

Ramdin M., De Loos T.W., Vlucht T.J.H., State-of-the-art of CO<sub>2</sub> capture with ionic liquids, *Ind. Eng. Chem. Res.* **2012**, 51, 8149-8177.

Rezaei M., Ismail A.F., Hashemifard S.A., Bakeri G.H., Matsuura T., Experimental study on the performance and long-term stability of PVDF/montmorillonite hollow fiber mixed matrix membranes for CO<sub>2</sub> separation process, *Int. J. Greenh. Gas Control.* **2014**, 26, 147-157.

Rongwong W., Jiratananon, R., Atchariyawut, S., Experimental study on membrane wetting in gas liquid membrane contacting process for CO<sub>2</sub> absorption by single and mixed absorbents, *Sep. Purif. Technol.* **2009**, 69, 118-125.

Santos E., Albo J., Irabien A., Acetate based Supported Ionic Liquid Membranes (SILMs) for CO<sub>2</sub> separation: Influence of the temperature, *J. Membr. Sci.* **2014**, 452, 277-283.

Savart T., Conception et réalisation de fibres creuses industrielles d'ultrafiltration en poly (fluorure de vinylidène) (PVDF) contenant des copolymères à blocs, PhD thesis. Université Toulouse 3. Paul Sabatier. **2013**.

Shen S., Kentish S.E., Stevens G.W., Shell-side mass-transfer performance in hollow-fiber membrane contactors, *Solvent Extr. Ion Exch.* **2010**, 28, 817-844.

Skog T.G., Johansen S., Hägg M.B., Method to prepare lab-sized hollow fiber modules for gas separation testing, *Ind. Eng. Chem. Res.* **2014**, 53, 9841-9848.

Vospersnik M., Pintar A., Bercic G., Levec J., Mass transfer studies in gas-liquid-solid membrane contactors, *Catal. Today.* **2003**, 79-80, 169-179.

Wang L., Zhang Z., Zhao B., Zhang H., Lu X., Yang, Q. Effect of long-term operation on the performance of polypropylene and polyvinylidene fluoride membrane contactors for CO<sub>2</sub> absorption, *Sep. Purif. Technol.* **2009**, 116, 300-306.

Wang L., Zhang Z., Zhao B., Zhang H., Lu X., Yang Q., Effect of long-term operation on the performance of polypropylene and polyvinylidene fluoride membrane contactors for CO<sub>2</sub> absorption. *Sep. Purif. Technol.* **2013**, 116, 300-306.

Wickramanayake S., Hopkinson D., Myers C., Hong L., Feng J., Seol Y., Plasynski D., Zeh M., Luebke D. Mechanically robust hollow fiber supported ionic liquid membranes for CO<sub>2</sub> separation applications, *J. Membr. Sci.* **2014**, 470, 52-59.

Yeon S.H., Lee K.S., Sea B., Park Y.I., Le K.H., Application of pilot-scale membrane contactor hybrid system for removal of carbon dioxide from flue gas, *J. Membr. Sci.* **2005**, 257, 156–160.

Zhang H.Y., Wang R., Liang D.T., Tay J.H., Theoretical and experimental studies of membrane wetting in the membrane gas–liquid contacting process for CO<sub>2</sub> absorption, *J. Membr. Sci.* **2008**, 308, 162-170.



# Conclusiones

---

## Conclusions

*Uno nunca se da cuenta de lo que se ha hecho,  
sólo puede ver lo que queda por hacer*

Marie Curie (1867-1934)

Científica polaca premio Nobel de física y química (1903 y 1911)



## CAPÍTULO 3: CONCLUSIONES

### 3.1. Conclusiones

Las conclusiones obtenidas a lo largo de la presente Tesis Doctoral han sido difundidas a través de 12 comunicaciones presentadas en congresos internacionales (8 de las mismas recogidas en libros o *Proceedings* con ISBN) y en 5 revistas científicas incluidas en el Journal of Citation Reports-Science Edition (JCR), 4 de ellas publicadas y 1 en proceso de revisión. Las publicaciones en revistas científicas se listan a continuación indicando el índice de impacto en 2015. El listado completo de comunicaciones en congresos se detalla en el anexo.

1. Gomez-Coma L., Garea, A., Irabien A., Carbon dioxide capture by [emim][Ac] ionic liquid in a polysulfone hollow fiber membrane contactor, *Int. J. Greenh. Gas Control.* **2016**, 52, 1-9. Índice de impacto: 4.064. Cuartil: Q1; Ingeniería Medioambiental 10/50.
2. Gomez-Coma L., Garea A., Rouch J.C., Savart T., Lahitte J.F., Remigy J.C., Irabien A., Membrane modules for CO<sub>2</sub> capture based on PVDF hollow fibers with ionic liquids immobilized, *J. Membr. Sci.* **2016**, 498, 218-226. Índice de impacto: 5.557. Cuartil: Q1; Ingeniería Química 7/135.
3. Gomez-Coma L., Garea, A., Irabien A., Non-Dispersive absorption of CO<sub>2</sub> in [emim][EtSO<sub>4</sub>] and [emim][Ac]: Temperature influence, *Sep. Purif. Technol.* **2014**, 132, 120-125. Índice de impacto: 3.299. Cuartil: Q1; Ingeniería Química 21/135.
4. Gomez-Coma L., Garea, A., Irabien A., Hybrid solvent ([emim][Ac]+water) to improve the CO<sub>2</sub> capture efficiency in a PVDF hollow fiber contactor. *ACS. Sustain. Chem. Eng.* **2016**, aceptado, octubre 2016. Índice de impacto: 5.267. Cuartil: Q1; Ingeniería Química 9/135.
5. Gomez-Coma L., Garea, A., Irabien A. PVDF Membrane contactor for CO<sub>2</sub> capture using the ionic liquid [emim][Ac]: mass transfer analysis. *Chem. Eng. Technol.* **2016**, en proceso de revisión. Índice de impacto: 2.385. Cuartil: Q2; Ingeniería Química 39/135.

Las **principales conclusiones** de este trabajo relacionadas con el desarrollo de la captura eficiente de dióxido de carbono en corrientes de post-combustión mediante el uso de una absorción no dispersiva y líquidos iónicos, en el que se ha demostrado experimentalmente su viabilidad a escala de laboratorio son:

(i) **Respecto al estudio de caracterización las fibras de PVDF fabricadas:**

- La **caracterización exhaustiva de las fibras**, mediante la realización de espectroscopias, análisis de propiedades mecánicas, permeabilidad al dióxido de carbono y punto burbuja aporta criterios para la **selección de las más adecuadas en el proceso de captura de CO<sub>2</sub>**.
- **Se ha conseguido inmovilizar los líquidos iónicos** [emim][EtSO<sub>4</sub>] y [emim][Ac] **en fibras de PVDF** fabricadas, lo que supone un **avance en la captura de CO<sub>2</sub>** a partir del cual se podrán diseñar nuevos módulos de membranas con distintos ILs y materiales de fibras.
- Los **valores** logrados **de permeabilidad** al dióxido de carbono con las fibras inmovilizadas con ILs son **superiores a los de la bibliografía**.

(ii) **En cuanto a la eficacia de captura de CO<sub>2</sub> en diferentes contactores de fibras huecas:**

- Ante un aumento de la temperatura del proceso, utilizando el líquido iónico [emim][Ac], mejora la eficacia significativamente, lo que indica la existencia de una **absorción tanto física como química**. Sin embargo, usando el líquido iónico [emim][EtSO<sub>4</sub>], que presenta **absorción física**, no se produce variación en la eficacia al aumentar la temperatura. Por tanto, si se plantea llevar a cabo la captura de CO<sub>2</sub> a altas temperaturas, se propone emplear un líquido iónico que presente quimisorción, como es el [emim][Ac].
- Las variables de proceso: caudal de gas y área del módulo, inciden directamente en la eficacia del proceso y en base a estas se puede proponer una **disposición de módulos en serie/paralelo según la eficacia de captura de CO<sub>2</sub> requerida**.
- Utilizando un **absorbente híbrido** formado por un **30% de agua** y el resto [emim][Ac] se han obtenido los mejores valores de **eficacia de captura de CO<sub>2</sub>: 72.5% en un contactor escala laboratorio (longitud 0,29 m)**, debido al compromiso entre la disminución de la

viscosidad del líquido iónico sin comprometer la solubilidad debido a la adición de agua.

(iii) **En cuanto al coeficiente global de transferencia de materia y las resistencias:**

- Para los materiales de fibras en los que **no hay mojado**, se puede asumir que las **resistencias de la fase gas y de la membrana son despreciables**.
- Utilizando el líquido iónico **[emim][Ac]** como absorbente se observa una dependencia del coeficiente global de transferencia de materia,  $K_{overall}$  con la temperatura, pero no tan acusada como se esperaría si hubiese una quimisorción fuerte. Esto indica, probablemente, la coexistencia de una **absorción química débil** y una **absorción física fuertemente condicionada por la pérdida de viscosidad y aumento de la difusividad del IL con la temperatura, pero afectada por la pérdida de solubilidad del IL en CO<sub>2</sub> cuando se aumenta la temperatura del proceso**.
- Los mayores **valores de  $K_{overall}$**  se han logrado cuando se ha trabajado con **[emim][Ac]** y especialmente con el absorbente híbrido **[emim][Ac]-agua**. Dichos valores son superiores en al menos, **un orden de magnitud a los publicados cuando se utilizan otro tipo de disolventes**, como las alcanolaminas, lo que hace que los líquidos iónicos se presenten prometedores para la captura de CO<sub>2</sub> por todas las ventajas que ofrecen en comparación con los disolventes tradicionales.

(iv) **Respecto al modelado y simulación del proceso**

- Se ha comprobado cómo mediante las asunciones propuestas el modelado permite recrear las condiciones experimentales ya que las **diferencias entre los valores experimentales y simulados son inferiores a 3%, para los contactores de polipropileno y PVDF**
- A través del modelado se pueden conocer los **valores de  $K_{overall}$  y de longitud del módulo, necesarios para alcanzar un 90% de eficacia** con los distintos materiales de los contactores de fibras huecas y de los absorbentes utilizados en el presente trabajo. El valor

de 90% de eficacia de captura de CO<sub>2</sub> se ha tomado como punto de diseño ya **que con este valor se considera que se ha logrado un proceso competitivo con los procesos tradicionales.**

- Utilizando el disolvente híbrido **30%agua-[emim][Ac]** y **fibras de PVDF inmovilizadas con [emim][Ac]**, únicamente **colocando dos módulos en serie (0.59 m)** se consigue, para un caudal de gas de 20 mL min<sup>-1</sup> (instalación escala laboratorio) una **eficacia de captura de CO<sub>2</sub> superior al 90%**. Con el módulo de polipropileno y [emim][Ac] o [emim][EtSO<sub>4</sub>] al mismo caudal se necesitarían 13 (2.3 m) y 20 módulos (1.5 m) respectivamente y con el de polisulfona utilizando [emim][Ac] como absorbente se requerirían 4 contactores (1.4 m) con un caudal de 70mL min<sup>-1</sup>.

### **3.2. Trabajo futuro**

En relación con los resultados de la presente tesis doctoral, se consideran relevantes las siguientes líneas para el progreso científico-técnico futuro:

- 1) Acoplar la etapa de desorción al proceso de captura. Para poder realizar un escalado al proceso de intensificación de captura de dióxido de carbono a nivel industrial propuesto en la presente Tesis Doctoral, es necesario, al igual que se ha hecho con la etapa de absorción, estudiar la desorción usando contactores de membranas de fibras huecas. Para ello, además de añadir la etapa de desorción en la planta escala laboratorio, será necesario realizar un modelado del proceso para conocer los parámetros de operación necesarios para conseguir un proceso competitivo con los procesos tradicionales.
- 2) Fabricación y caracterización de nuevos contactores de membranas. Una vez vista la viabilidad del proceso cuando se disminuye la viscosidad, es conveniente buscar nuevos absorbentes, como los líquidos iónicos reversibles que puedan combinar las ventajas de una alta solubilidad al CO<sub>2</sub> con una baja viscosidad y un bajo coste. Además nuevos materiales de fibras huecas como PEEK, PDMS y PES deben ser estudiados para ver su viabilidad cuando se usan con líquidos iónicos como absorbentes.
- 3) Escalado a planta piloto y estimación de costes. Una vez obtenidos los parámetros requeridos para conseguir un proceso competitivo con los procesos tradicionales que usan torres de absorción y alcanolaminas, en la etapa de absorción, es necesario realizar un análisis económico exhaustivo que valore todos los costes del proceso así como dar un paso más en la captura, implementando la planta a escala planta piloto.

### **3.1 Conclusions**

The conclusions obtained during this PhD thesis have been disseminated by means of 12 communications presented in international conferences and 5 scientific papers in journals included in the *Journal of Citation Reports-Science Edition (JCR)*. The publications in scientific journals are listed below, showing the impact factor in 2015. The complete list of communications in conferences is detailed in the annex.

1. Gomez-Coma L., Garea, A., Irabien A., Carbon dioxide capture by [emim][Ac] ionic liquid in a polysulfone hollow fiber membrane contactor, *Int. J. Greenh. Gas Control.* **2016**, 52, 1-9. Índice de impacto: 4.064. Cuartil: Q1; Ingeniería Medioambiental 10/50.
2. Gomez-Coma L., Garea A., Rouch J.C., Savart T., Lahitte J.F., Remigy J.C., Irabien A., Membrane modules for CO<sub>2</sub> capture based on PVDF hollow fibers with ionic liquids immobilized, *J. Membr. Sci.* **2016**, 498, 218-226. Índice de impacto: 5.557. Cuartil: Q1; Ingeniería Química 7/135.
3. Gomez-Coma L., Garea, A., Irabien A., Non-Dispersive absorption of CO<sub>2</sub> in [emim][EtSO<sub>4</sub>] and [emim][Ac]: Temperature influence, *Sep. Purif. Technol.* **2014**, 132, 120-125. Índice de impacto: 3.299. Cuartil: Q1; Ingeniería Química 21/135.
4. Gomez-Coma L., Garea, A., Irabien A., Hybrid solvent ([emim][Ac]+water) to improve the CO<sub>2</sub> capture efficiency in a PVDF hollow fiber contactor. *ACS. Sustain. Chem. Eng.* **2016**, accepted paper, october 2016. Índice de impacto: 5.267. Cuartil: Q1; Ingeniería Química 9/135.
5. Gomez-Coma L., Garea, A., Irabien A. PVDF Membrane contactor for CO<sub>2</sub> capture using the ionic liquid [emim][Ac]: mass transfer analysis. *Chem. Eng. Technol.* **2016**, under review. Índice de impacto: 2.385. Cuartil: Q2; Ingeniería Química 39/135.

The main conclusions of this work related to the development of an efficient carbon dioxide capture in post-combustion processes by using a non-dispersive absorption and ionic liquids, which has been experimentally proven its viability at laboratory scale are listed below:

(i) **Respect to the intensive study of the manufactured fibers**

- An **exhaustive characterization of the fibers** has been performed by SEM, mechanical properties analysis, pure carbon dioxide permeability and bubble point **in order to select the most suitable fiber material for CO<sub>2</sub> capture process.**
- The **[emim][EtSO<sub>4</sub>]** and **[emim][Ac]** ionic liquids **have been immobilized onto the manufactured PVDF fibers.** This fact constitutes a **new development for CO<sub>2</sub> capture and** based on these new fibers **with different materials and ionic liquids could be developed.**
- The carbon dioxide **permeability values** achieved with ionic liquids immobilized onto the fibers are **higher than reported values in the literature.**

(ii) **In terms of CO<sub>2</sub> capture efficiency with different hollow fiber membrane contactors**

- When the temperature in the process increases using the **[emim][Ac]** ionic liquid, the efficiency improves significantly, because of a **physical and chemical interaction.** However, when the **[emim][EtSO<sub>4</sub>]** is used the efficiency does not vary, there is only a **physical absorption.**
- The variables: gas flow rate and area of the hollow fiber modules, influence directly on the CO<sub>2</sub> capture efficiency. **The configuration of modules in series/parallel is required to achieve a design target of process efficiency.**
- Using a **hybrid solvent** with **[emim][Ac]-30%water** the CO<sub>2</sub> capture **efficiency** value obtained was **72.5% in a module at laboratory scale.** This is due to the compromise between the reduction of the ionic liquid viscosity without compromising the solubility because of the water addition.

(iii) **In terms of overall mass transfer coefficient and the resistances**

- In the **not-wetting** operating mode, it can be assumed that both **gas and membrane resistances are negligible.**

- **Using [emim][Ac] ionic liquid** as absorbent a dependency of overall mass transfer coefficient  $K_{overall}$ , with temperature is observed. However, this dependency is not as strong as expected when a chemisorption is involved. This probably indicates the existence of a **weak-chemisorption and strong-physisorption influenced by the viscosity losses and the increase in diffusivity of the IL but affected by the ionic liquid CO<sub>2</sub> solubility losses when the process is operated at higher temperatures.**
- The highest  $K_{overall}$  values have been achieved when the [emim][Ac] is used as absorbent, especially with the hybrid absorbent [emim][Ac]-water.  **$K_{overall}$  values are at least one order of magnitude higher than the values reported in the literature using other solvents such as alkanolamines. This fact allows the ionic liquid to be presented as a viable alternative for CO<sub>2</sub> capture due to its advantages in comparison with traditional solvents.**

(iv) **Regarding the modeling and simulation process**

- **The modelling task** presented with its assumptions proposed permits to recreate the experimental conditions. **The error between both modelling and experimental results is below 3%, for PP or PVDF hollow fiber contactors.**
- Using the modelling can be known the  **$K_{overall}$  and the length of the module, required to achieve 90% efficiency** with the different materials both for hollow fiber membrane contactors and absorbents used in the present work. This value was chosen as design point because with this value is considered to achieve a competitive with the traditional processes.
- The proposed configuration to accomplish a 90% efficiency is to use two PVDF hollow fiber modules in series and a hybrid solvent based on [emim][Ac]-water, and as many in parallel as the gas flow rate requires in the scaling up process.

### **3.2. On going-research**

Based on the results reported in this PhD thesis, the following relevant lines are considered for the future scientific-technical progress:

- 1) Coupling the desorption stage to the capture process. In order to scale up to the production level the carbon dioxide capture based on an intensification process proposed in this thesis, an intense study on the desorption step using hollow fiber membrane contactors is required. To that end, performing a process modeling to meet the operating parameters required to achieve a competitive process with traditional processes is necessary in addition to couple the desorption step.
- 2) Fabrication and characterization of new hollow fiber membrane contactors. Once observed the process viability when the viscosity decreases, seeking new absorbents such as reversible ionic liquids that may combine the advantages of high CO<sub>2</sub> solubility with low viscosity and low cost is desirable. Moreover, new materials such as PEEK, PDMS and PES should be studied in hollow fiber membrane contactors to determine its viability when the ionic liquids are used as absorbents.
- 3) Scaling to pilot plant and cost estimation. Once the parameters required have been obtained in order to achieve a competitive absorption process in comparison with traditional processes that use absorption towers and alkanolamines, an exhaustive economic analysis is necessary in order to quantify the cost of the process, and the different contributions to the total cost.

# Artículos científicos

---

## Scientific Articles

*“La ciencia no tiene patria”*

Louis Pasteur (1822-1895)

*Químico y bacteriólogo francés*



**4.1. Gómez-Coma L., Garea A., Irabien A., Non-dispersive absorption of CO<sub>2</sub> in [emim][EtSO<sub>4</sub>] and [emim][Ac]: Temperature influence. Sep. Purif. Technol. 2014, 132, 120-125.**

Resumen

El proceso de post-combustión mediante el uso de aminas se ha utilizado convencionalmente para la separación de dióxido de carbono. Sin embargo, en los últimos años, los líquidos iónicos se han convertido en una alternativa atractiva, debido a sus interesantes características, como son las cero emisiones de disolvente en comparación con las aminas. El objetivo del presente trabajo ha sido estudiar la influencia de la temperatura sobre la eficacia con el fin de evaluar tanto la absorción física como química utilizando dos líquidos iónicos distintos, por un lado el 1-etil-3-metilimidazolio etilsulfato, [emim][EtSO<sub>4</sub>] y por otro el 1-etil-3-metilimidazolio acetato, [emim][Ac]. El intervalo de temperatura de estudio ha sido desde temperatura ambiente (291K) hasta 333K. Un módulo de fibras huecas de polipropileno se ha utilizado para llevar a cabo la absorción de CO<sub>2</sub>. La eficacia en la eliminación de CO<sub>2</sub> se obtuvo a partir de datos experimentales. La dependencia de la temperatura sólo se ha observado cuando se ha utilizado el [emim][Ac] donde se ha conseguido duplicar la separación entre 291K y 318K (de 16 a 34% para un módulo y de 27 a 53% cuando se utilizaron dos módulos en serie). El comportamiento del [emim][Ac] se ha correlacionado mediante la transferencia de materia mejorada por una reacción química. Cuando se ha utilizado el [emim][EtSO<sub>4</sub>] se ha comprobado como la eficacia no está influenciada por la temperatura y sólo la solubilidad controla la transferencia de materia en la fase líquida.

Original abstract

Post-combustion capture based on amines is conventionally used for carbon dioxide separation. Ionic liquids have emerged as new attractive alternative solvents because of their zero emission features compared to amines. The aim of the present work is to study the temperature influence on the efficiency in order to evaluate physical and chemical absorption using two ionic liquids, 1-Ethyl-3-methylimidazolium ethylsulfate [emim][EtSO<sub>4</sub>], and 1-Ethyl-3-methylimidazolium acetate [emim][Ac]. The temperature ranges from room temperature to 333 K. A polypropylene hollow fiber module is the membrane device where the CO<sub>2</sub> absorption takes place. The CO<sub>2</sub> removal efficiency was obtained from experimental data, showing a temperature dependence only in the case of using [emim][Ac] which doubles from 291 K to 318 K (16–34% for one contactor and 27–53% when two contactors were operated in series). The behavior of [emim][Ac] was correlated with the mass transfer enhanced by the chemical reaction. When [emim][EtSO<sub>4</sub>] is used, the efficiency is not influenced by the temperature and only the solubility controlled the mass transfer in the liquid phase.





# Non-dispersive absorption of CO<sub>2</sub> in [emim][EtSO<sub>4</sub>] and [emim][Ac]: Temperature influence



L. Gómez-Coma\*, A. Garea, A. Irabien

Departamento de Ingenierías Química y Biomolecular, E.T.S. de Ingenieros Industriales y Telecomunicación, Universidad de Cantabria, 39005 Santander, Spain

## ARTICLE INFO

### Article history:

Received 11 February 2014  
Received in revised form 12 May 2014  
Accepted 13 May 2014  
Available online 21 May 2014

### Keywords:

Carbon dioxide  
Absorption  
Gas-liquid membrane contactors  
Ionic liquids (ILs)  
Temperature

## ABSTRACT

Post-combustion capture based on amines is conventionally used for carbon dioxide separation. Ionic liquids have emerged as new attractive alternative solvents because of their zero emission features compared to amines. The aim of the present work is to study the temperature influence on the efficiency in order to evaluate physical and chemical absorption using two ionic liquids, 1-Ethyl-3-methylimidazolium ethylsulfate [emim][EtSO<sub>4</sub>], and 1-Ethyl-3-methylimidazolium acetate [emim][Ac]. The temperature ranges from room temperature to 333 K. A polypropylene hollow fiber module is the membrane device where the CO<sub>2</sub> absorption takes place. The CO<sub>2</sub> removal efficiency was obtained from experimental data, showing a temperature dependence only in the case of using [emim][Ac] which doubles from 291 K to 318 K (16–34% for one contactor and 27–53% when two contactors were operated in series). The behavior of [emim][Ac] was correlated with the mass transfer enhanced by the chemical reaction. When [emim][EtSO<sub>4</sub>] is used, the efficiency is not influenced by the temperature and only the solubility controlled the mass transfer in the liquid phase.

© 2014 Elsevier B.V. All rights reserved.

## 1. Introduction

Carbon dioxide is one of the major contributors to climate change. The CO<sub>2</sub> capture and sequestration (CCS) is a major concern globally today to reduce the impact on the atmosphere and protect humans against the risks associated with CO<sub>2</sub> pollution. A wide range of technologies exist for CCS based on physical and chemical processes including absorption, adsorption, membranes and cryogenics [1].

Three main methods can be identified on the capture of CO<sub>2</sub>: pre-combustion, post-combustion and oxy-combustion [2]. The present work is focused on post-combustion capture. This process route is ideally suitable for conventional power stations and energy conversion systems. CO<sub>2</sub> at low partial pressure is separated from the gas stream after the fuel has been burned completely [3]. The flue gas from a typical post-combustion process is composed by 10–15% CO<sub>2</sub>, 70–75% N<sub>2</sub> and lower concentrations of other components. The temperature reached in this type of system is between 313 and 348 K [4].

Traditionally, amines have been used for capture due to their high reactivity to CO<sub>2</sub> forming complexes with weak chemical bonds and low cost achieving an outlet stream of very low CO<sub>2</sub>

concentration [5]. The development of more beneficial solvents for the environment is a topic of great current interest.

The CO<sub>2</sub> capture processes on an industrial scale are usually carried out in packed or spray towers. In recent years, an intensification process has been proposed that replaces the equipment for a membrane device [6]. Hollow fiber membrane contactors have many advantages: controlled interfacial area, independent control of gas and liquid flow rates, reduction in solvent losses, much larger contact area per unit volume compared to tray and/or packed columns and no dispersion from one phase into another [7–9]. Different kinds of membrane materials are under research. The most common ones are polypropylene (PP) [5,10–13] and polyvinylidene fluoride (PVDF) [10,14,15]. Generally the membrane equipment operates with gas and liquid flowing on opposite sides of the membrane in parallel configuration [6] but sometimes the cross flow configuration is used [11].

The PP membranes have often been used in membrane contactors due to their low cost, hydrophobicity and commercial availability [16]. This type of asymmetric membranes provides also a great advantage because of their inability to dissolve in common solvents at low temperatures [17].

Ionic liquids (ILs) are compounds that have been considered in the last few years as solvents for CO<sub>2</sub> gas recovery [5]. ILs are salts that have an organic cation and an inorganic anion whose melting point is lower than 373 K and the vapor pressure is negligible

\* Corresponding author. Tel.: +34 942 206777; fax: +34 942 201591.  
E-mail address: [gomezcomal@unican.es](mailto:gomezcomal@unican.es) (L. Gómez-Coma).

## Nomenclature

$A$	effective membrane area ( $\text{m}^2$ )	$R_{\text{overall}}$	overall resistance to mass transfer (experimentally obtained) ( $\text{sm}^{-1}$ )
$D$	diffusivity ( $\text{m}^2 \text{s}^{-1}$ )	$Sc$	Schmidt number
$d_{\text{cont}}$	diameter of the contactor (m)	$Sh$	Sherwood number
$d_h$	hydraulic diameter (m)	$t$	time (s)
$d_i$	inside diameter of the fiber (m)	$T$	temperature (K)
$d_{lm}$	log mean diameter of the fiber	$v$	velocity ( $\text{ms}^{-1}$ )
$d_o$	outside diameter of the fiber (m)	$x$	liquid molar fraction
$E_d$	enhancement factor	$y$	gas molar fraction
$H_d$	Henry's law constant		
$k_g$	mass transfer coefficient in the gas phase ( $\text{ms}^{-1}$ )	<i>Subscripts</i>	
$k_l$	mass transfer coefficient in the liquid phase ( $\text{ms}^{-1}$ )	g	gas
$k_{mg}$	mass transfer coefficient of the membrane ( $\text{ms}^{-1}$ )	l	liquid
$K_{\text{overall}}$	mass transfer coefficient ( $\text{ms}^{-1}$ )	in	inlet of the contactor
$L$	fiber length (m)	out	outlet of the contactor
$n$	number of fibers		
$N_{\text{CO}_2}$	absorption flux of sulfur dioxide ( $\text{mol m}^2 \text{s}^{-1}$ )	<i>Greek letters</i>	
$P_T$	total pressure (bar)	$\delta$	membrane thickness (m)
$Q$	flow rate ( $\text{m}^3 \text{s}^{-1}$ )	$\varepsilon$	porosity of the membrane
$R$	ideal gas constant ( $\text{bar L mol}^{-1} \text{K}^{-1}$ )	$\mu$	viscosity (cP)
$Re$	Reynolds number	$\tau$	tortuosity
$R_g$	resistance in the gas side ( $\text{sm}^{-1}$ )	$\rho$	density ( $\text{kg m}^{-3}$ )
$R_l$	resistance in the liquid side ( $\text{sm}^{-1}$ )	$\varphi$	packing factor
$R_{mg}$	gas filled membrane resistance ( $\text{sm}^{-1}$ )		
$R_{ml}$	liquid filled membrane resistance ( $\text{sm}^{-1}$ )		

[18,19]. An important feature of ILs for potential use in industrial gas treating processes is the knowledge of the solubility and the diffusion coefficients of gases at various temperatures and pressures [20]. Commonly, the  $\text{CO}_2$  absorption in the non-functionalized IL occurs through physisorption [21]. However, some ILs are able of forming chemical complexes with  $\text{CO}_2$  [22]. The chemisorption of  $\text{CO}_2$  in ionic liquids containing a carboxylic anion can be a promising alternative to common amine processes [23]. For this reason the 1-Ethyl-3-methylimidazolium acetate [emim][Ac] is an ideal candidate for  $\text{CO}_2$  capture. An inexpensive and green solvent for petrochemical applications are important features to consider when choosing an ionic liquid for  $\text{CO}_2$  absorption. The 1-Ethyl-3-methylimidazolium ethylsulfate [emim][EtSO<sub>4</sub>] meets these features [24].

The mass transfer behavior for gas absorption into different absorbents liquids appears to be important for the process design. Some studies are reported for different hollow fiber membrane contactor [25], but there is a lack of data for the temperature influence, that is the aim of the present work in order to analyze the relevance of the temperature variable in the removal process efficiency.

The study of the temperature effect in the non-dispersive absorption of  $\text{CO}_2$  was carried out in a polypropylene hollow fiber membrane contactor using two different ionic liquids [emim][Ac] and [emim][EtSO<sub>4</sub>].

## 2. Experimental

### 2.1. Materials

A polypropylene hollow fiber membrane contactor in parallel configuration was supplied by Liquicel-Membrane Contactors (USA). The main characteristics of this system are shown in Table 1. Carbon dioxide 99.7 ± 0.01 vol.% and pure nitrogen 99.999 ± 0.001 vol.% were purchased from Air Liquide (Spain). The ionic liquids were

supplied by Sigma Aldrich. The 1-Ethyl-3-methylimidazolium ethylsulfate [emim][EtSO<sub>4</sub>] (≥95%) was used as absorption liquid due to its low viscosity, low toxicity and low cost [26]. On the other hand, the 1-Ethyl-3-methylimidazolium acetate [emim][Ac] (≥90%) was chosen because of its high  $\text{CO}_2$  solubility. To ensure that the ionic liquid is suitable for our process despite its relatively low purity, solubility rates were measured and, compared with literature data, similar values were obtained [27,28].

### 2.2. Methods

The experimental setup is shown in Fig. 1. The feed gas mixture stream contains 15 vol.%  $\text{CO}_2$  and  $\text{N}_2$  (rest to balance) and it was adjusted by means of a mass flow controller (Brook instrument MFC 5850, Emerson Process Management Spain) that flows through the inside of the hollow fibers. The liquid absorbent flows counter-currently in a closed circuit through the shell side. The ILs were pumped from the storage tank. Control and measurement in the liquid line ( $50 \text{ mL min}^{-1}$ ) was carried out with a digital gear pump (Cole Parmer Instrument Company, Hucoa-Erloss SA, Spain). The liquid storage tank was kept under isothermal conditions

**Table 1**  
Hollow fiber membrane contactor characteristics.

Membrane material	Polypropylene
Fiber o.d. $d_o$ (m)	$3 \times 10^{-4}$
Fiber i.d. $d_i$ (m)	$2.2 \times 10^{-4}$
Fiber length, $L$ (m)	0.115
Number of fibers, $n$	2300
Effective inner membrane area, $A$ ( $\text{m}^2$ )	0.18
Membrane thickness, $\delta$ (m)	$0.4 \times 10^{-4}$
Membrane pore diameter, $d_p$ ( $\mu\text{m}$ )	0.04
Porosity (%)	40
Packing factor	0.39
Tortuosity <sup>a</sup>	2.50

<sup>a</sup> Assumed as  $1/\varepsilon$ .

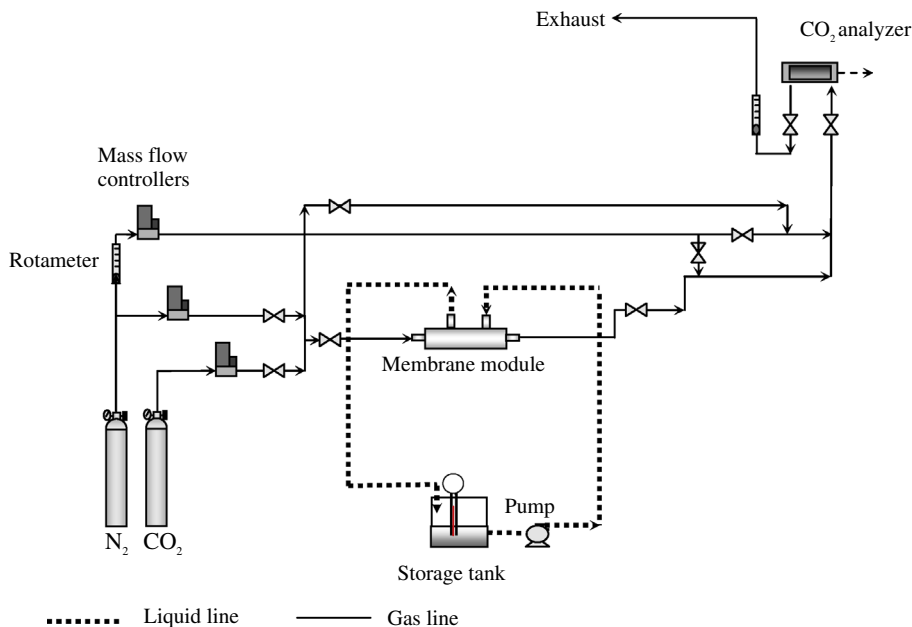


Fig. 1. Experimental setup.

using heating tapes around the pipes. Experiments were carried out at room temperature (291 K), 298, 318 and 333 K with each IL. Each experiment was replicated three times under the same operating conditions and the average value was calculated.

Gas flow rates were varied from 20 to 70 mL min<sup>-1</sup> using [emim][EtSO<sub>4</sub>]. In order to improve the efficiency two hollow fiber membrane contactors were connected in series using [emim][Ac].

Carbon dioxide concentration in the outlet gas stream was continuously monitored by sampling a fraction of the stream through an analyzer (Emerson Process) based on non-dispersive infra-red (NDIR) spectroscopy. Before sending the gas sample to the analyzer, it was necessary to dilute with more N<sub>2</sub> in order to maintain the concentration range for the NDIR analyzer (at least 200 mL min<sup>-1</sup>). The steady state was indicated by a constant CO<sub>2</sub> concentration in the exit gas stream.

3. Results and discussion

3.1. CO<sub>2</sub> absorption

Carbon dioxide absorption experiments with the two ionic liquids were carried out in a polypropylene membrane contactor in order to evaluate the process efficiency at different temperatures. The CO<sub>2</sub> removal efficiency is defined as

$$\text{Efficiency (\%)} = \left( 1 - \frac{C_{\text{CO}_2,\text{out}}}{C_{\text{CO}_2,\text{in}}} \right) 100 \tag{1}$$

Figs. 2 and 3 show the experiments at different temperatures (291, 298, 318 and 333 K) with a gas flowrates of 20 mL min<sup>-1</sup> and 70 mL min<sup>-1</sup>, respectively using the 1-Ethyl-3-methylimidazolium ethylsulfate [emim][EtSO<sub>4</sub>]. The outlet concentration of carbon dioxide calculated as C<sub>CO<sub>2</sub>(g),out</sub>/C<sub>CO<sub>2</sub>(g),in</sub>. Figs. 4 and 5 show

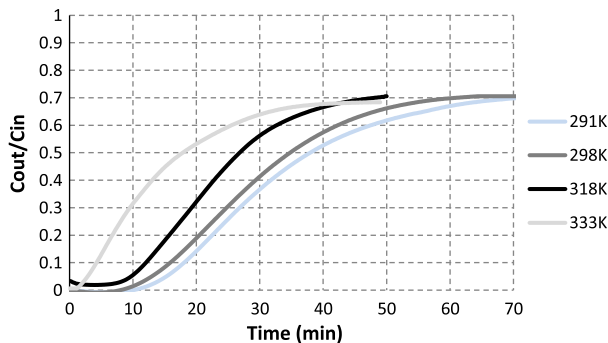


Fig. 3. CO<sub>2</sub> outlet concentration (dimensionless) versus experimental time at different temperatures with [emim][EtSO<sub>4</sub>] and Q<sub>g</sub> = 70 mL min<sup>-1</sup>.

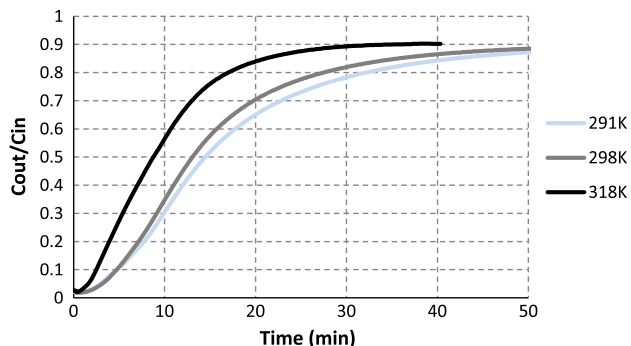


Fig. 2. CO<sub>2</sub> outlet concentration (dimensionless) versus experimental time at different temperatures [emim][EtSO<sub>4</sub>] and Q<sub>g</sub> = 20 mL min<sup>-1</sup>.

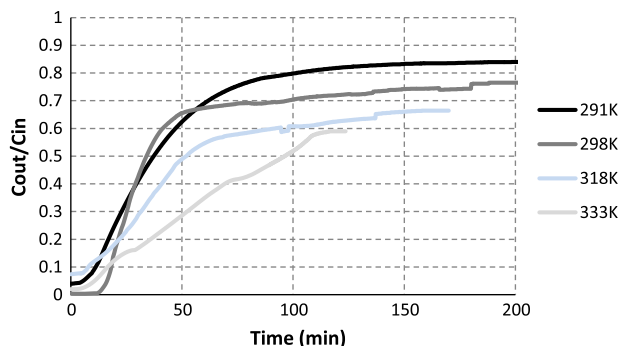


Fig. 4. CO<sub>2</sub> outlet concentration (dimensionless) using [emim][Ac] versus experimental time at different temperatures and Q<sub>g</sub> = 70 mL min<sup>-1</sup>.

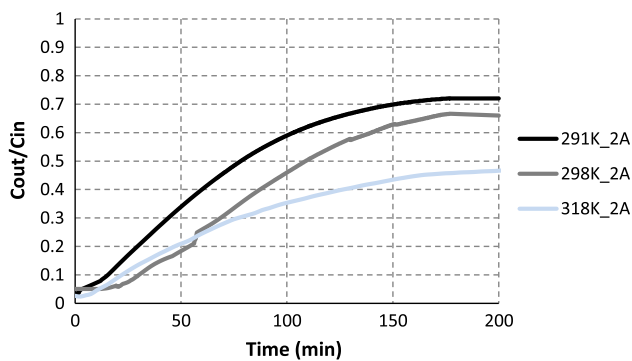


Fig. 5. CO<sub>2</sub> outlet concentration (dimensionless) using [emim][Ac] and two membrane contactors in series at different temperatures and  $Q_g = 70 \text{ mL min}^{-1}$ .

the experiments with the ionic liquid 1-Ethyl-3-methylimidazolium acetate [emim][Ac] operating with a gas flow of  $70 \text{ mL min}^{-1}$  in one contactor (Fig. 4) and two contactors in series (Fig. 5).

The outlet concentration dimensionless of carbon dioxide was calculated for each experiment at pseudo-steady-state, that ranged between 0.7 and 0.9 in the case of the ionic liquid [emim][EtSO<sub>4</sub>] and approximately 0.45–0.85 when [emim][Ac] is used.

The CO<sub>2</sub> removal efficiencies were calculated from inlet and outlet CO<sub>2</sub> concentrations for the absorption experiments (Table 2). From the obtained results some remarks are pointed out: (i) the efficiency increases with decreasing gas flow that provides higher residence time in the contactor, (ii) the efficiency increases with the contacting area (from one to two contactors in series), and more important and (iii) the temperature influence is significant only in the case of using the ionic liquid [emim][Ac], which doubles the efficiency values from 291 K to 318 K: 16–34% for one contactor and 27–53% when two contactors were operated in series.

The behavior of [emim][Ac] was correlated with the mass transfer enhanced by the chemical reaction.

### 3.2. Mass transfer calculations

The resistance in series approach can be used to relate individual mass transfer resistances to the overall mass transfer resistance.

$$R_{\text{overall}} = R_g + R_{mg} + R_l \quad (2)$$

A hollow fiber configuration is selected with the liquid phase flowing in the shell side and the gas phase through the lumen side. The gas–liquid interface is located on the outer diameter of the tubes. Considering chemical reaction in the liquid side (expressed by the enhancement factor,  $E_A$ ) the equation is the following [29].

Table 2  
Experimental efficiency of [emim][EtSO<sub>4</sub>] and [emim][Ac].

No.	IL	A (m <sup>2</sup> )	Q <sub>g</sub> (mL min <sup>-1</sup> )	T (K)	Efficiency (%)
1	[emim][EtSO <sub>4</sub> ]	0.18	20	291	28.7
2	[emim][EtSO <sub>4</sub> ]	0.18	20	298	29.5
3	[emim][EtSO <sub>4</sub> ]	0.18	20	318	28.6
4	[emim][EtSO <sub>4</sub> ]	0.18	20	333	31.6
5	[emim][EtSO <sub>4</sub> ]	0.18	70	291	10.5
6	[emim][EtSO <sub>4</sub> ]	0.18	70	298	10.2
7	[emim][EtSO <sub>4</sub> ]	0.18	70	318	9.8
8	[emim][Ac]	0.18	70	291	16.3
9	[emim][Ac]	0.18	70	298	25.0
10	[emim][Ac]	0.18	70	318	33.9
11	[emim][Ac]	0.18	70	333	40.0
12	[emim][Ac]	0.36	70	291	27.3
13	[emim][Ac]	0.36	70	298	31.5
14	[emim][Ac]	0.36	70	318	52.7

$$\frac{1}{K_{\text{overall}}} = \frac{d_o}{k_g d_i} + \frac{d_o}{k_{mg} d_{lm}} + \frac{1}{k_l H_d E_A} \quad (3)$$

where  $d_o$ ,  $d_i$  and  $d_{lm}$  are the outside, inside and log mean diameters in (m) of the hollow fiber,  $H_d$  represents the dimensionless Henry constant,  $k_g$ ,  $k_{mg}$ ,  $k_l$ , which are the individual mass transfer coefficients of the gas phase, membrane and liquid phase, respectively ( $\text{ms}^{-1}$ ) and  $K_{\text{overall}}$  is the overall mass transfer coefficient ( $\text{ms}^{-1}$ ).

The dimensionless Henry's law constant  $H_d$  is a key parameter in modelling the mass transfer process. The Henry constant has been calculated with the following equation defined in previous works [19]

$$H_d = \frac{C_g^*}{C_l^*} = \frac{y^* P_T}{x_l^* RT} \quad (4)$$

where  $y^*$  and  $x_l^*$  are the molar fractions in the gas and liquid phases respectively,  $\rho_l$  is the molar density of the liquid ( $\text{mol L}^{-1}$ ) and  $P_T$  is the total pressure.

As seen in previous works, the contribution of the gas phase and membrane can be considered negligible [29]. Therefore Eq. (3) is summarized as follows:

$$\frac{1}{K_{\text{overall}}} = \frac{1}{k_l H_d E_A} \quad (5)$$

The mass transfer flux of carbon dioxide has been calculated according to the equation

$$N_{\text{CO}_2, g} = \frac{Q_g}{A} (C_{\text{CO}_2, \text{in}} - C_{\text{CO}_2, \text{out}}) = K_{\text{overall}} \frac{\Delta y_{lm} P_T}{RT} \quad (6)$$

In the steady state CO<sub>2</sub> fluxes are equal in the gas and liquid. The overall mass transfer  $K_{\text{overall}}$  can be experimentally evaluated from the flux through the membrane and concentration gradient.  $Q_g$  is the gas flow rate ( $\text{m}^3 \text{ s}^{-1}$ ),  $A$  is the membrane area ( $\text{m}^2$ ),  $P_T$  is the total pressure in the gas phase and  $\Delta y_{lm}$  is the logarithmic mean of the driving force based on gas phase molar fractions. Taking into account the carbon dioxide concentration in the inlet ( $y_{\text{CO}_2, \text{in}}$ ) and the outlet ( $y_{\text{CO}_2, \text{out}}$ ) of the hollow fiber membrane contactor, assuming that CO<sub>2</sub> concentration in the solvent is very far from the saturation in the experiments,  $\Delta y_{lm}$  can be calculated as:

$$\Delta y_{lm} = \frac{(y_{\text{CO}_2, \text{in}}) - (y_{\text{CO}_2, \text{out}})}{\ln((y_{\text{CO}_2, \text{in}})/(y_{\text{CO}_2, \text{out}}))} \quad (7)$$

Several authors have proposed different empirical correlations for shell-side mass transfer in parallel flow in hollow fiber membrane contactors. In this study Kartohardjono's correlation has been used to estimate  $k_l$  because the packing factor and Reynolds number are within the same range ( $0.029 < \varphi < 0.53$ ;  $Re < 400$ ) [30]:

$$Sh = \left( \frac{k_l d_h}{D_{\text{CO}_2, l}} \right) = 0.1789 (\varphi^{0.86}) Re^{0.34} Sc^{\frac{1}{3}} \quad (8)$$

where  $D_{\text{CO}_2, l}$  is the diffusion coefficient of carbon dioxide in the liquid,  $L$  is the fiber length and  $d_h$  is the hydraulic diameter:

$$d_h = \frac{d_{\text{cont}}^2 - n d_o^2}{n d_o} \quad (9)$$

The mass transfer coefficient in the liquid phase ( $k_l$ ) depends on the physical properties of the ionic liquid and the membrane contactor characteristics. Morgan et al. developed a correlation which expresses the dependency of gas diffusivity with the liquid viscosity as [31]:

$$D_{\text{CO}_2, l} = 2.66 \times 10^{-3} \frac{1}{\mu_{\text{IL}}^{0.66} V_{\text{CO}_2}^{1.04}} \quad (10)$$

where  $\mu_{IL}$  is the viscosity of solvent in cP,  $V_{CO_2}$  is the molar volume of carbon dioxide at the normal boiling point ( $33.3 \text{ cm}^3 \text{ mol}^{-1}$ ) and the diffusivity is obtained in  $\text{cm}^2 \text{ s}^{-1}$ . Assuming an Arrhenius-type dependence of temperature the diffusivity is calculated from room temperature to 318 K [32].

The overall mass transfer coefficient  $K_{\text{Overall}}$  is calculated from the experimental results of  $\text{CO}_2$  fluxes at different temperatures using Eq. (6). As can be seen in Table 3 higher values of the overall mass transfer coefficient were obtained when the ionic liquid [emim][Ac] was used. Fig. 6 shows the different trend in the  $K_{\text{Overall}}$  with the ionic liquids. For the [emim][Ac], the  $K_{\text{Overall}}$  value increases significantly as the temperature rises:  $1.1 \times 10^{-6}$ – $3.2 \times 10^{-6} \text{ ms}^{-1}$  from 291 to 333 K. Nevertheless in the case of [emim][EtSO<sub>4</sub>]  $K_{\text{Overall}}$  remains constant: around  $0.7 \times 10^{-6} \text{ ms}^{-1}$  for the temperature interval 291–333 K.

In Table 4, the results at room temperature are compared with literature values. The mass transfer coefficient using polypropylene membrane contactor with either ionic liquid is lower than with other absorbents. This is attributed to their high viscosity. Therefore, the mass transfer would be favored when the process is operated at higher temperatures, mainly because of the lower viscosity of the ionic liquid and the chemical reaction effect. In this point, the use of ionic liquids is specially indicated as they are stable at high temperatures and it would result in an improved process for  $\text{CO}_2$  capture favored by the chemical reaction with the ionic liquid.

Kartohardjono's equation has been used for the estimation of the individual mass transfer coefficients within the shell-side,  $k_i$ , for the membrane pores filled with gas, non-wetted mode. Tables 5 and 6 show molar fraction, density, viscosity and the estimated liquid side mass transfer coefficient  $k_l$  of [emim][EtSO<sub>4</sub>] and [emim][Ac] at 291, 298, 318 and 333 K respectively.

As expected the overall mass transfer process for the absorption of carbon dioxide into ionic liquids using a hollow fiber membrane contactor is still controlled by the liquid side mass transfer resistance. From the results of  $K_{\text{Overall}}$  and ( $k_l H_d$ ), considering the gas phase and membrane contributions negligible, it is remarkable that only physical absorption takes place in the case of using [emim][EtSO<sub>4</sub>], while the chemical reaction enhances the absorption process when the [emim][Ac] is used.

The enhancement factor,  $E_A$ , determines the absorption rate of the reactant and it leads to quantify how the mass transfer is enhanced by the presence of a chemical reaction [39,40].

The values of  $E_A$  were calculated for both ionic liquids, Eq. (11), from the results of  $K_{\text{Overall}}$  and ( $k_l H_d$ )

$$E_A = \frac{K_{\text{Overall}}}{k_l H_d} \quad (11)$$

**Table 3**  
Experimental  $K_{\text{Overall}}$  and  $E_A$  of [emim][EtSO<sub>4</sub>] and [emim][Ac].

No.	IL	A (m <sup>2</sup> )	Q <sub>g</sub> (mL min <sup>-1</sup> )	T (K)	$K_{\text{Overall}}$ (10 <sup>6</sup> m s <sup>-1</sup> )	$E_A$
1	[emim][EtSO <sub>4</sub> ]	0.18	20	291	0.68	1.1
2	[emim][EtSO <sub>4</sub> ]	0.18	20	298	0.66	1.0
3	[emim][EtSO <sub>4</sub> ]	0.18	20	318	0.66	0.70
4	[emim][EtSO <sub>4</sub> ]	0.18	20	333	0.67	0.99
5	[emim][EtSO <sub>4</sub> ]	0.18	70	291	0.71	1.2
6	[emim][EtSO <sub>4</sub> ]	0.18	70	298	0.70	1.1
7	[emim][EtSO <sub>4</sub> ]	0.18	70	318	0.69	0.70
8	[emim][Ac]	0.18	70	291	1.1	65
9	[emim][Ac]	0.18	70	298	1.9	75
10	[emim][Ac]	0.18	70	318	2.7	57
11	[emim][Ac]	0.18	70	333	3.2	53
12	[emim][Ac]	0.36	70	291	1.0	58
13	[emim][Ac]	0.36	70	298	1.2	49
14	[emim][Ac]	0.36	70	318	2.5	51

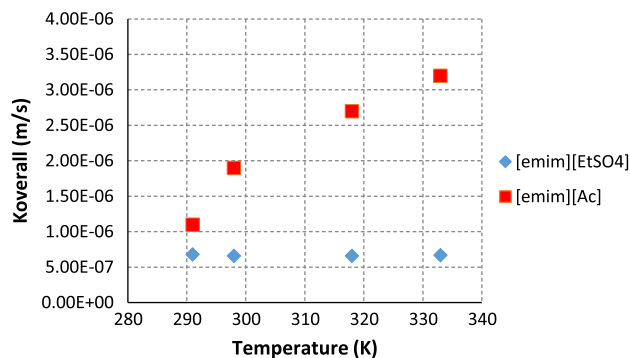


**Fig. 6.**  $K_{\text{Overall}}$  results versus temperature, with both ionic liquids.

**Table 4**  
Comparison with the literature values.

Reference	Absorbent	$K_{\text{Overall}}$ (10 <sup>6</sup> m s <sup>-1</sup> )
This work	[emim][EtSO <sub>4</sub> ]	0.71
This work	[emim][Ac]	1.1
[33]	GLY <sup>a</sup> + Pz <sup>b</sup>	130–230
[33]	GLY <sup>a</sup>	100–170
[34]	MDEA	20–33
[35]	Water	24–40
[35]	Propylene carbonate	10–20

All these references using a PP hollow fiber membranes.

<sup>a</sup> GLY: Glycin salt.

<sup>b</sup> PZ: Piperazine.

**Table 5**  
Molar fraction, density,  $k_l$  and  $k_l H_d$  of [emim][EtSO<sub>4</sub>].

Parameter	291 K	298 K	318 K	333 K
$x^*$ [20]	0.013	0.012	0.010	0.009
$\rho_l$ (mol L <sup>-1</sup> ) [36]	5.3	5.2	5.2	5.1
$\mu$ (cP) [37]	144	110	41	25
$k_l$ (10 <sup>6</sup> m s <sup>-1</sup> )	0.9	1.0	1.4	2.8
$k_l H_d$ (10 <sup>6</sup> m s <sup>-1</sup> )	0.60	0.63	0.98	2.29

**Table 6**  
Molar fraction, density,  $k_l$  and  $k_l H_d$  of [emim][Ac].

Parameter	291 K	298 K	318 K	333 K
$x^*$ [27]	0.29	0.27	0.24	0.22
$\rho_l$ (mol L <sup>-1</sup> ) [38]	6.5	6.5	6.4	6.3
$\mu$ (cP) [38]	203	144	48	26
$k_l$ (10 <sup>6</sup> m s <sup>-1</sup> )	0.9	1.0	1.9	2.3
$k_l H_d$ (10 <sup>6</sup> m s <sup>-1</sup> )	0.021	0.025	0.048	0.060

Also as it is shown in Table 3,  $E_A$  values close to 1 were obtained when the ionic liquid [emim][EtSO<sub>4</sub>] was used, while  $E_A$  higher than 50 were achieved with [emim][Ac]. Hence it can be concluded that the chemical reaction in the liquid phase mainly controls the  $\text{CO}_2$  removal process when [emim][Ac] is used for  $\text{CO}_2$  capture, and therefore the temperature effect is important to be taken into account for the process design.

#### 4. Conclusions

A polypropylene hollow fiber membrane contactor has been used to study the absorption of  $\text{CO}_2$  in ionic liquids at different temperatures. The gas stream has a typical composition of post-combustion processes including  $\text{CO}_2$  (15%) and  $\text{N}_2$  (75%). Two ionic liquids were studied: 1-Ethyl-3-methylimidazolium ethylsulfate

[emim][EtSO<sub>4</sub>], and 1-Ethyl-3-methylimidazolium acetate [emim][Ac]. Higher values of CO<sub>2</sub> flux are achieved when the ionic liquid [emim][Ac] was used instead of [emim][EtSO<sub>4</sub>] at the same gas flow and higher temperature. The overall mass transfer coefficients were obtained showing a higher resistance to mass transfer when the ionic liquid [emim][EtSO<sub>4</sub>] was used. The liquid resistance is the main contribution to be taken into account as expected.

In the case of [emim][EtSO<sub>4</sub>], the overall mass transfer,  $K_{\text{overall}}$ , remains practically constant for the temperature interval 291–333 K. On the other hand, with [emim][Ac], the  $K_{\text{overall}}$  increased significantly, from 1.1 to  $3.2 \times 10^{-6} \text{ ms}^{-1}$ . It can be concluded that a different behavior exists between CO<sub>2</sub> and each of the ionic liquids studied.

The ionic liquid [emim][EtSO<sub>4</sub>] which shows physical absorption, results in an enhancement factor of  $\approx 1$ , and the mass transfer does not depend significantly on the temperature. The ionic liquid [emim][Ac] shows enhancement by chemical absorption, being obtained the value of  $E_A$  higher than 50. Consequently at higher temperatures the [emim][Ac] behaves more efficiently and [emim][EtSO<sub>4</sub>] did not provided any improvement.

The mass transfer coefficient using polypropylene membrane contactor with either ionic liquid is lower than with other absorbents. This is attributed to their high viscosity. For this reason, operation at high temperature is necessary to reduce the viscosity and compete with other absorbents. On the other hand, the temperature appears is a key variable to design the CO<sub>2</sub> capture process by the non-dispersive absorption using ionic liquids, therefore, the study of temperature influence at higher temperatures in the efficiency improvement, especially when the chemical reaction in the liquid phase appears to be the controlling stage.

## Acknowledgement

This research has been funded by the Spanish Ministry Economy and Competitiveness (Project ENE2010-14828).

## References

- [1] A.B. Rao, E.S. Rubin, A technical, economic, and environmental assessment of amine-based CO<sub>2</sub> capture technology for power plant greenhouse gas control, *Environ. Sci. Technol.* (2002) 4467–4475.
- [2] M. Kanniche, R. Gros-Bonnivard, P. Jaud, J. Valle-Marcos, J. Amann, C. Bouallou, Pre-combustion, post-combustion and oxy-combustion in thermal power plant for CO<sub>2</sub> capture, *Appl. Therm. Eng.* 30 (2010) 53–62.
- [3] D.W. Bailey, P.H.M. Feron, Post-combustion decarbonisation processes, *Oil Gas Sci. Technol.* 60 (2005) 461–474.
- [4] M. Ramdin, T.W. De Loos, T.J.H. Vlught, State-of-the-art of CO<sub>2</sub> capture with ionic liquids, *Ind. Eng. Chem. Res.* 51 (2012) 8149–8177.
- [5] J. Albo, A. Irabien, Non-dispersive absorption of CO<sub>2</sub> in parallel and cross-flow membrane modules using EMISE, *J. Chem. Technol. Biotechnol.* 87 (2012) 1502–1507.
- [6] P. Luis, T. Van Gerven, B. Van Der Bruggen, Recent developments in membrane-based technologies for CO<sub>2</sub> capture, *Prog. Energy Combust.* 38 (2012) 419–448.
- [7] Y. Zhang, R. Wang, Gas-liquid membrane contactors for acid gas removal: recent advances and future challenges, *Curr. Opin. Chem. Eng.* 2 (2) (2013) 255–262.
- [8] S.H. Lin, K.L. Tung, H.W. Chang, K.R. Lee, Influence of fluorocarbon flat-membrane hydrophobicity on carbon dioxide recovery, *Chemosphere* 75 (10) (2009) 1410–1416.
- [9] S.H. Lin, K.L. Tung, W.J. Cheng, H.W. Chang, Absorption of carbon dioxide by mixed piperazine-alkanolamine absorbent in a plasma-modified polypropylene hollow fiber contactor, *J. Membr. Sci.* 333 (1–2) (2009) 30–37.
- [10] S.H. Lin, C.F. Hsieh, M.H. Li, K.L. Tung, Determination of mass transfer resistance during absorption of carbon dioxide by mixed absorbents in PVDF and PP membrane contactor, *Desalination* 249 (2009) 647–653.
- [11] J. Albo, P. Luis, A. Irabien, Carbon dioxide capture from flue gases using a cross-flow membrane contactor and the ionic liquid 1-ethyl-3-methylimidazolium ethylsulfate, *Ind. Eng. Chem. Res.* 49 (2010) 11045–11051.
- [12] M. Mavroudi, S.P. Kaldis, G.P. Sakellariopoulos, A study of mass transfer resistance in membrane gas-liquid contacting processes, *J. Membr. Sci.* 272 (2006) 103–115.
- [13] R. Wang, H.Y. Zhang, P.H.M. Feron, D.T. Liang, Influence of membrane wetting on CO<sub>2</sub> capture in microporous hollow fiber membrane contactors, *Sep. Purif. Technol.* 46 (2005) 33–40.
- [14] S.H. Lin, P.C. Chiang, C.F. Hsieh, M.H. Li, K.L. Tung, Absorption of carbon dioxide by the absorbent composed of piperazine and 2-amino-2-methyl-1-propanol in PVDF membrane contactor, *J. Chin. Inst. Chem. Eng.* 39 (2008) 13–21.
- [15] W. Rongwong, R. Jiratananon, S. Atcharyawut, Experimental study on membrane wetting in gas-liquid membrane contacting process for CO<sub>2</sub> absorption by single and mixed absorbents, *Sep. Purif. Technol.* 69 (2009) 118–125.
- [16] S. Rajabzadeh, S. Yoshimoto, M. Teramoto, M. Al-Marzouqi, H. Matsuyama, CO<sub>2</sub> absorption by using PVDF hollow fiber membrane contactors with various membrane structures, *Sep. Purif. Technol.* 69 (2009) 210–220.
- [17] A.F. Ismail, A. Mansourizadeh, A comparative study on the structure and performance of porous polyvinylidene fluoride and polysulfone hollow fiber membranes for CO<sub>2</sub> absorption, *J. Membr. Sci.* 365 (2010) 319–328.
- [18] D. Wappel, G. Gronald, R. Kalb, J. Draxler, Ionic liquids for post-combustion CO<sub>2</sub> absorption, *Int. J. Greenhouse Gas Control* 4 (2010) 486–494.
- [19] P. Luis, A. Garea, A. Irabien, Zero solvent emission process for sulfur dioxide recovery using a membrane contactor and ionic liquids, *J. Membr. Sci.* 330 (2009) 80–89.
- [20] A.H. Jalili, A. Mehdizadeh, M. Shokouhi, A.N. Ahmadi, M. Hosseini-Jenab, F. Fateminassab, Solubility and diffusion of CO<sub>2</sub> and H<sub>2</sub>S in the ionic liquid 1-ethyl-3-methylimidazolium ethylsulfate, *J. Chem. Thermodyn.* 42 (2010) 1298–1303.
- [21] G. Gurau, H. Rodríguez, S.P. Kelley, P. Janiczek, R.S. Kalb, R.D. Rogers, Demonstration of chemisorption of carbon dioxide in 1,3-dialkylimidazolium acetate ionic liquids, *Angew. Chem. Int. Ed.* 50 (2011) 12024–12026.
- [22] E.J. Maginn, Design and Evaluation of Ionic Liquids as Novel CO<sub>2</sub> Absorbents, National Energy Technology Laboratory, US, 2004.
- [23] J. Blath, N. Deubler, T. Hirth, T. Schiestel, Chemisorption of carbon dioxide in imidazolium based ionic liquids with carboxylic anions, *Chem. Eng. J.* 181–182 (2012) 152–158.
- [24] H.J. Liaw, C.C. Chen, Y.C. Chen, J.R. Chen, S.K. Huang, S.N. Liu, Relationship between flash point of ionic liquids and their thermal decomposition, *Green Chem.* 14 (2012) 2001–2008.
- [25] J. Albo, P. Luis, A. Irabien, Absorption of coal combustion flue gases in ionic liquids using different membrane contactors, *Desalination Water Treat.* 27 (2011) 54–59.
- [26] A. Arce, H. Rodríguez, A. Soto, Use of a green and cheap ionic liquid to purify gasoline octane boosters, *Green Chem.* 9 (2007) 247–253.
- [27] E. Santos, J. Albo, A. Irabien, Acetate based supported ionic liquid membranes (SILMs) for CO<sub>2</sub> separation: influence of the temperature, *J. Membr. Sci.* 452 (2014) 277–283.
- [28] A.M. Pinto, H. Rodríguez, A. Arce, A. Soto, Combined physical and chemical absorption of carbon dioxide in a mixture of ionic liquids, *J. Chem. Thermodyn.* (2013), <http://dx.doi.org/10.1016/j.jct.2013.10.023>.
- [29] A. Ortiz, D. Gorri, T. Irabien, I. Ortiz, Separation of propylene/propane mixtures using Ag<sup>+</sup>-RTIL solutions. Evaluation and comparison of the performance of gas-liquid contactors, *J. Membr. Sci.* 360 (2010) 130–141.
- [30] S. Shen, S.E. Kentish, G.W. Stevens, Shell-side mass-transfer performance in hollow-fiber membrane contactors, *Solvent Extr. Ion Exch.* 28 (2010) 817–844.
- [31] D. Morgan, L. Ferguson, P. Scovazzo, Diffusivities of gases in room-temperature ionic liquids: data and correlations obtained using a lag-time technique, *Ind. Eng. Chem. Res.* 44 (2005) 4815–4823.
- [32] M.B. Shiflett, A. Yokozeki, Solubilities and diffusivities of carbon dioxide in ionic liquids: [bmim][PF<sub>6</sub>] and [bmim][BF<sub>4</sub>], *Ind. Eng. Chem. Res.* 44 (2005) 4453–4464.
- [33] J.L. Li, B.H. Chen, Review of CO<sub>2</sub> absorption using chemical solvents in hollow fiber membrane contactors, *Sep. Purif. Technol.* 41 (2005) 109–122.
- [34] L.M. Galán Sánchez, G.W. Meindersma, A.B. De Haan, Kinetics of absorption of CO<sub>2</sub> in amino-functionalized ionic liquids, *Chem. Eng. J.* 166 (2011) 1104–1115.
- [35] J.G. Lu, Y.F. Zheng, M.D. Cheng, Membrane contactor for CO<sub>2</sub> absorption applying amino-acid salt solutions, *Desalination* 249 (2009) 498–502.
- [36] E. Gómez, B. González, N. Calvar, E. Tojo, Á. Domínguez, Physical properties of pure 1-ethyl-3-methylimidazolium ethylsulfate and its binary mixtures with ethanol and water at several temperatures, *J. Chem. Eng. Data* 51 (2006) 2096–2102.
- [37] A.P. Fröba, H. Kremer, A. Leipertz, Density, refractive index, interfacial tension, and viscosity of ionic liquids [EMIM][EtSO<sub>4</sub>], [EMIM][NTf<sub>2</sub>], [EMIM][N(CN)<sub>2</sub>], and [OMA][NTf<sub>2</sub>] in dependence on temperature at atmospheric pressure, *J. Phys. Chem. B* 112 (2008) 12420–12430.
- [38] M.G. Freire, A.R.R. Teles, M.A.A. Rocha, B. Schröder, C.M.S.S. Neves, P.J. Carvalho, D.V. Evtuguin, L.M.N.B.F. Santos, J.A.P. Coutinho, Thermophysical characterization of ionic liquids able to dissolve biomass, *J. Chem. Eng. Data* 56 (2011) 4813–4822.
- [39] J. Lu, L. Wang, X. Sun, J. Li, X. Liu, Absorption of CO<sub>2</sub> into aqueous solutions of methyldiethanolamine and activated methyldiethanolamine from a gas mixture in a hollow fiber contactor, *Ind. Eng. Chem. Res.* 44 (2005) 9230–9238.
- [40] V.Y. Dindore, G.F. Versteeg, Gas-liquid mass transfer in a cross-flow hollow fiber module: analytical model and experimental validation, *Int. J. Heat Mass Transfer* 48 (2005) 3352–3362.

**4.2. Gómez-Coma L., Garea A., Rouch J.C., Savart T., Lahitte J.F., Remigy L.C., Irabien A., Membrane modules for CO<sub>2</sub> capture based on PVDF hollow fibers with ionic liquids immobilized. J. Membr. Sci. 2016, 498, 218-226.**

Resumen

El uso de contactores de membrana de fibra hueca con líquidos iónicos es una alternativa prometedora a las torres de absorción tradicionales que usan aminas para la absorción de dióxido de carbono. Los líquidos iónicos se han erigido como nuevos disolventes debido a sus características de emisión cero de disolvente en comparación con aminas. El objetivo de este trabajo fue comparar fibras a base de PVDF y diferentes aditivos, así como éstas mismas fibras cuando se inmovilizaron en ellas dos líquidos iónicos diferentes. Por un lado, 1-etil-3-metilimidazolio etilsulfato [emim][EtSO<sub>4</sub>] el cual presenta absorción física, y el acetato de 1-etil-3-metilimidazolio [emim][Ac] que presenta absorción química. Para comparar las fibras objeto de estudio, el espesor de la fibra se examinó mediante microscopía electrónica de barrido (SEM). También se evaluaron las propiedades mecánicas de las fibras así como su punto burbuja. La permeación de las fibras al CO<sub>2</sub> puro fue calculada experimentalmente mediante ensayos de permeabilidad, para los cuales se utilizaron módulos de acero inoxidable a medida, preparados en el laboratorio. Todas las pruebas anteriores se realizaron con las fibras en condiciones tanto húmedas como secas. Gracias a estos ensayos se pudo determinar que las fibras con el líquido iónico inmovilizado son prometedoras para la captura de CO<sub>2</sub> ya que la permeación al CO<sub>2</sub> aumentó significativamente. En el caso de las fibras, D+[emim][EtSO<sub>4</sub>], por ejemplo, se logró un aumento del 43% en comparación con las fibras sin la adición del líquido iónico, resultando un valor de permeabilidad al CO<sub>2</sub> de 57040 NL/(h bar m<sup>2</sup>), que es superior a los valores reportados en la literatura para PVDF. Por otra parte, el coeficiente global de transferencia de materia obtenido a partir de los valores de eficacia en la captura de CO<sub>2</sub> utilizando las fibras D+[emim][Ac] también presenta valores muy competitivos.

Original abstract

Hollow fiber membrane contactors with ionic liquids are promising alternatives to traditional spray towers and amines for carbon dioxide absorption. Ionic liquids have emerged as new alternative solvents because of their zero emission features compared with amines. The aim of this work was to compare fibers based on PVDF and different additives, as well as fibers including two different ionic liquids. On the one hand, 1-ethyl-3-methylimidazolium ethylsulfate [emim][EtSO<sub>4</sub>] presents physical absorption, and on the other hand, 1-ethyl-3-methylimidazolium acetate [emim][Ac] presents chemical absorption. To compare the fibers under study, the thickness of the composite fiber was examined using scanning electron microscopy (SEM). The mechanical properties and the bubble point were also evaluated.

Permeability tests were conducted, and the gas permeation of the composite hollow fibers was measured using pure CO<sub>2</sub>. Laboratory-made stainless steel modules were used for the tests. All of the above tests were performed with the fibers in both wet and dry conditions. It was determined that the fibers with the ionic liquid immobilized would be promising for CO<sub>2</sub> capture because the CO<sub>2</sub> permeance significantly increased. Namely, D+[emim][EtSO<sub>4</sub>] achieved a 43% increase compared with the fibers without the addition of the ionic liquid, resulting in a CO<sub>2</sub> permeance value of 57040 NL/(h m<sup>2</sup> bar), which is higher than the values reported in the literature for PVDF. Moreover, the overall mass transfer coefficient for CO<sub>2</sub> capture using the D+[emim][Ac] fibers also presented highly competitive values.



ELSEVIER

Contents lists available at ScienceDirect

## Journal of Membrane Science

journal homepage: [www.elsevier.com/locate/memsci](http://www.elsevier.com/locate/memsci)

# Membrane modules for CO<sub>2</sub> capture based on PVDF hollow fibers with ionic liquids immobilized



L. Gomez-Coma<sup>a,\*</sup>, A. Garea<sup>a</sup>, J.C. Rouch<sup>b,c</sup>, T. Savart<sup>b,c</sup>, J.F. Lahitte<sup>b,c</sup>, J.C. Remigy<sup>b,c</sup>, A. Irbaien<sup>a</sup>

<sup>a</sup> Universidad de Cantabria, Chemical and Biomolecular Engineering Department, E.T.S. de Ingenieros Industriales y Telecomunicación, Avda Los Castros s/n, 39005 Santander, Spain

<sup>b</sup> Université de Toulouse, INPT, UPS, Laboratoire de Genie Chimique, 118 Route de Narbonne, F-31062 Toulouse, France

<sup>c</sup> CNRS, Laboratoire de Genie Chimique, F-31030 Toulouse, France

## ARTICLE INFO

## Article history:

Received 18 May 2015

Received in revised form

6 October 2015

Accepted 7 October 2015

Available online 9 October 2015

## Keywords:

Carbon dioxide capture

Membrane contactors

Fibers

PVDF

Ionic liquids (ILs)

## ABSTRACT

Hollow fiber membrane contactors with ionic liquids are promising alternatives to traditional spray towers and amines for carbon dioxide absorption. Ionic liquids have emerged as new alternative solvents because of their zero emission features compared with amines. The aim of this work was to compare fibers based on PVDF and different additives, as well as fibers including two different ionic liquids. On the one hand, 1-ethyl-3-methylimidazolium ethyl sulfate [emim][EtSO<sub>4</sub>] presents physical absorption, and on the other hand, 1-ethyl-3-methylimidazolium acetate [emim][Ac] presents chemical absorption. To compare the fibers under study, the thickness of the composite fiber was examined using scanning electron microscopy (SEM). The mechanical properties and the bubble point were also evaluated. Permeability tests were conducted, and the gas permeation of the composite hollow fibers was measured using pure CO<sub>2</sub>. Laboratory-made stainless steel modules were used for the tests. All of the above tests were performed with the fibers in both wet and dry conditions. It was determined that the fibers with the ionic liquid immobilized would be promising for CO<sub>2</sub> capture because the CO<sub>2</sub> permeance significantly increased. Namely, D+[emim][EtSO<sub>4</sub>] achieved a 43% increase compared with the fibers without the addition of the ionic liquid, resulting in a CO<sub>2</sub> permeance value of 57040 NL/(h m<sup>2</sup> bar), which is higher than the values reported in the literature for PVDF. Moreover, the overall mass transfer coefficient for CO<sub>2</sub> capture using the D+[emim][Ac] fibers also presented highly competitive values.

© 2015 Elsevier B.V. All rights reserved.

## 1. Introduction

Carbon dioxide capture and sequestration (CCS) is currently a major concern globally to reduce the impact on the atmosphere and protect humans against the associated risks. However, CO<sub>2</sub> capture is the bottleneck step where efforts have to be applied to develop more sustainable processes from technical and economical perspectives [1].

Post-combustion technology constitutes a strategy for reducing the impact of greenhouse gases from fossil fuels in industrial processes. For this reason, the present work is focused on post-combustion capture. This process route is ideally suited for conventional power stations and energy conversion systems. CO<sub>2</sub> at low partial pressure is separated from the gas stream after the fuel has been completely burned [2]. The flue gas from a typical post-

combustion process is composed of 10–15% CO<sub>2</sub>, 70–75% N<sub>2</sub> and lower concentrations of other components. In these systems, the temperature in the absorption step reaches between 313 and 348 K [3].

Traditionally, alkanolamines have been used for carbon dioxide capture due to their high reactivity to CO<sub>2</sub> by forming complexes with weak chemical bonds and low cost, achieving an outlet stream with a very low CO<sub>2</sub> concentration. The development of more beneficial solvents for the environment is currently a topic of great interest. Ionic liquids (ILs) are one of the promising compounds for CO<sub>2</sub> gas recovery [1]. ILs are salts that have an organic cation and an inorganic anion and whose melting point is lower than 373 K, and their vapor pressure is negligible [4,5,6]. Additionally, ILs have good thermal stability, high ionic conductivity and solubility in organic media [7].

The chemisorption of CO<sub>2</sub> in ionic liquids containing a carboxylic anion can be a promising alternative to common amine processes [8]. Recently, the literature has shown that ILs

\* Corresponding author. Fax: +34 942 201591.

E-mail address: [gomezcomal@unican.es](mailto:gomezcomal@unican.es) (L. Gomez-Coma).

containing acetate anions possess a high degree of absorption for CO<sub>2</sub> across a wide range of temperatures [9]. These types of membranes based on ILs have been used in previous works [9–11]. For this reason, 1-ethyl-3-methylimidazolium acetate, [emim][Ac], is an ideal candidate for CO<sub>2</sub> capture. In addition, [emim][Ac] was chosen because of its high CO<sub>2</sub> solubility and chemical absorption [3,4,8,12–14]. On the other hand, an inexpensive and green solvent for industrial applications is an important feature to consider when choosing an ionic liquid for CO<sub>2</sub> absorption. 1-Ethyl-3-methylimidazolium ethyl sulfate, [emim][EtSO<sub>4</sub>], was selected due to its low viscosity, low toxicity and low cost [15]. CO<sub>2</sub> capture processes on an industrial scale require the application of high temperatures to a stripper re-boiler for solvent regeneration and CO<sub>2</sub> desorption, which poses a main drawback to the energy consumption. As an alternative, numerous works based on hollow fiber membrane contactors [16] have been reported in recent years because they offer numerous advantages, such as controlled interfacial area, independent control of the gas and liquid flow rates, reduction in solvent losses, much larger contact area per unit volume compared with tray and/or packed columns and no dispersion from one phase into another [16–19]. Additionally, membranes are a promising option for established industrial technologies for gas and liquid separations because of the lower energy cost and smaller footprint requirements in the process operations [20].

Commercially, the most employed separations using membranes include the separation of O<sub>2</sub> and N<sub>2</sub>; H<sub>2</sub> recovery from mixtures with larger components such as N<sub>2</sub>, CH<sub>4</sub> and CO<sub>2</sub>; and the removal of CO<sub>2</sub> from natural gas mixtures [21]. Traditionally, when dealing with membrane contactors and porous membrane, the main problem is the wetting of pore which probably occurs for long time (even hours sometime) [22]. With a porous membrane, the liquid and gas phases are separated due to the interface which is fixed at the pore entrance due to the Laplace pressure. This one depends on the interfacial tension, the pore diameter and the contact angle. If the transmembrane pressure is higher than the Laplace pressure ( $\sim 1$ – $2$  bars) the liquid will wet the pore [23]. For long term experiment, the contact angle could change due to the adsorption of molecule at the membrane surface or the chemical degradation of the membrane surface properties. Previous works demonstrated that the wetting is avoided when a dense membrane is coated at the membrane surface [24]. In that case, the liquid and gas phase are physically/mechanically separated so the pressure to push the liquid inside a pore is largely increased up to several bars ( $\sim 8$ – $10$  bars) corresponding to the breakage of the membrane. However, in the case of dense composite hollow fiber, the wetting of the fiber could also occur but in a different way. As water in transfer through the membrane by diffusion and in the vapor state, the gas inside the pore is close to be saturated by water so the water vapor could condense inside the pore. In this work the IL is added inside the pore forming a supported liquid membrane. This membrane is used in a membrane contactor so it is a non-porous membrane. To be wetted by water, the water should push the IL. The transmembrane pressure should be higher than the Laplace pressures. The higher viscosity of ionic liquid than water acts as a shock absorber during the transient regime (i.

e variation of transmembrane pressure with too high pressure) [25]. Also to obtain high permeability with a membrane filled with a liquid, a liquid with a high diffusion coefficient of CO<sub>2</sub> and/or with a high CO<sub>2</sub> solubility is necessary, for this reason the [emim][Ac] and [emim][EtSO<sub>4</sub>] were chosen.

A study of different self-made PVDF fibers with different additives in the non-dispersive absorption of CO<sub>2</sub> was performed in a hollow fiber membrane contactor using two different ionic liquids, [emim][Ac] and [emim][EtSO<sub>4</sub>].

## 2. Experimental

### 2.1. Hollow fiber membranes

Four type of hollow fibers were selected among 200 hollow fibers elaborated by Savart [26] based on their high gas permeability and a high bubble point. The most permeable one were selected. The complete description of the fiber manufacturing method is explained in a previous works [26–28]. The hollow fibers based on polyvinylidene fluoride (PVDF) membranes with different additives called A, B, C, D and were homemade by phase inversion. The HSV900 PVDF grade was kindly provided by Arkelma (France), *n*-methyl-pyrrolidone NMP (Aldrich-France) was used as a solvent, and LiCl (Aldrich-France) and a block copolymer were used as additives. The copolymer was a 1–2 diblock copolymer. 1 was a hydrophobic block composed of poly(methyl methacrylate) (75 wt% of the total mass). 2 was a hydrophilic block composed of poly(butyl acrylate) (20 wt%) and hydroxyethylmethacrylate (5 wt%) [26–28]. The dope solutions to make the A and B fibers were composed of 15% PVDF HSV900 and 3% LiCl. The C fibers were composed of 15% PVDF HSV900, 3% block copolymer and 3% LiCl. Finally, the D fibers were composed of 15% PVDF HSV900, 3% block copolymer, 3% LiCl and 1% water [26,27].

The operating parameters used to produce the hollow fibers are shown in Table 1. The letter *Q* indicates the flow rate ( $Q_{\text{collodion}}$ : flow of collodion;  $Q_{\text{internal liquid}}$ : internal fluid flow), and the letter *T* indicates the temperature. The only difference between A and B fibers was the internal fluid flow, 1.8 and 3.9 mL min<sup>-1</sup> respectively. In the case of the D fiber, 1% of water was immobilized in the doping solution. For this reason, the membranes were different due to the presence or absence of water in the doping solution and due to the different operating conditions. During formation of the membranes, the LiCl was eliminated during the water-washing step, so the A and B fibers were only composed of PVDF [26]. The block copolymer was partially eliminated; however, the final copolymer content in the fiber was not measured; after the coagulation step that occurs classically with the phase inversion techniques, the block copolymer was found in the coagulation bath, after extraction from water with IR and NMR analysis. Further analysis with secondary ion mass spectrometry (SIMS) technology showed that the copolymer was present in the fiber at the surface of the polymer but also inside the PVDF matrix [26]. Therefore, different quantities of the copolymer could be found in the two hollow fibers.

For drying, the fibers were maintained for approximately 72 h

**Table 1**  
Operating conditions for manufacturing hollow fibers.

	$Q_{\text{collodion}}$ (mL/min)	$Q_{\text{internal liquid}}$ (mL/min)	Composition Internal liquid (mass ratio)	$T_{\text{collodion}}$ (K)	$T_{\text{bath coagulation}}$ (K)	$T_{\text{Internal liquid}}$ (K)	Air gap (cm)	Speed (m/min)
A	7.2	1.8	Water/NMP 70/30	350	322	351	10	11
B	7.2	3.9	Water/NMP 70/30	350	322	351	10	11
C	7.2	1.8	Water/NMP 85/15	308	333	308	10	11
D	7.2	1.8	Water/NMP 70/30	323	323	323	32	11

in an oven at a temperature of 50 °C and at atmospheric pressure.

Subsequently, new fibers were produced by adding the ILs. The ILs were included into the fibers adding 150 mL of each ionic liquid into virgin fibers and ILs were immobilized into wet virgin fibers for 48 h. 1-Ethyl-3-methylimidazolium ethyl sulfate [emim][EtSO<sub>4</sub>] (≥ 95%) and 1-ethyl-3-methylimidazolium acetate [emim][Ac] (≥ 90%) were supplied by SigmaAldrich. Previous authors reported fibers impregnated with ionic liquids [29,30].

To ensure that the ionic liquid was suitable for our process despite its relatively low purity, the solubility rates were measured, and compared with literature data, similar values were obtained [12,31,32].

The membrane contactors were manufactured by gluing hollow fibers in a PVC shell.

## 2.2. Characterization techniques for the hollow fiber membranes

### 2.2.1. Scanning electron microscopy

The thickness of the composite fiber was examined by scanning electron microscopy (SEM; Hitachi TM1000, Tokyo, Japan). The fibers were first immersed in ethanol, cryofractured in liquid nitrogen, and then sputtered with gold. The thickness was measured from the SEM cross-sectional image.

### 2.2.2. Mechanical properties of the fibers

The mechanical properties of the porous supports were measured using a tensile testing device (INSTRON, Model 3342). The calculations of the deformation due to traction and compression, as well as the elasticity, were performed using the Bluehill program (Bluehill 2 Software, Instron). To obtain information about the mechanical properties of the membranes, the tensile strength (MC), tensile strain at break (CC) and elongation at the elastic limit ( $\epsilon_b$ ) were determined from the results of the tension tests.

### 2.2.3. Permeation tests

The gas permeation of the composite hollow fibers was measured using pure CO<sub>2</sub>. Laboratory-made stainless steel modules were used for these tests. Three fibers approximately 30 cm long were assembled in each module. The gas was fed into the shell side, and the gas permeation flux was measured at the outlet of the lumen side thanks to a mass flow controller (Brooks Instrument MFC 5850, Emerson Process Management Spain). The pressure was increased in steps of 0.5 bar from 0 to 15 bar. Each measurement was recorded after 100 s of flux stabilization and was replicated twice under the same operating conditions. Fig. 1 shows the setup for the gas permeability experiments.

### 2.2.4. Bubble point

To measure the bubble point, fibers were prepared and

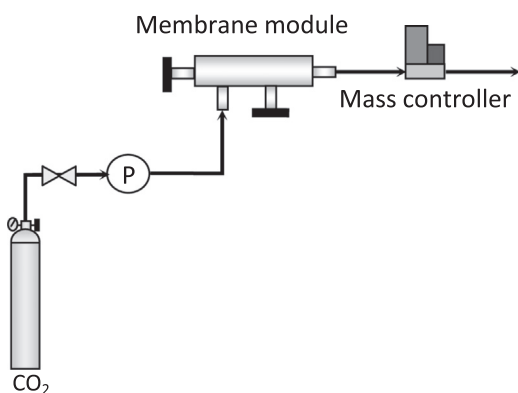


Fig. 1. Experimental setup for gas permeability testing.

submerged in water while compressed air was injected in the fiber lumen. The gas pressure was increased from 0 to 7.16 bar with a step of 0.1 bar while keeping the water side at atmospheric pressure. When the first bubble emerged, the bubble point pressure was determined.

## 2.3. CO<sub>2</sub> capture process

The experimental setup is shown in Fig. 2. The feed gas mixture stream contained 15 vol% CO<sub>2</sub> and N<sub>2</sub> (to balance) and was adjusted using a mass flow controller (Brooks Instrument MFC 5850, Emerson Process Management Spain). Gas stream flowed through the inside of the hollow fibers. The gas flow rate was 20 mL min<sup>-1</sup>. The ionic liquid 1-ethyl-3-methylimidazolium acetate flowed in counter-current through the shell side. The IL was pumped from the storage tank. Control and measurement in the liquid line (50 mL min<sup>-1</sup>) were achieved using a digital gear pump (Cole Parmer Instrument Company, Hucoa-Erloss S.A, Spain).

The experiments were performed over the temperature range of 303–333 K. Each experiment was replicated three times under the same operating conditions, and the average value was calculated. During the operation with these ionic liquids, their properties were stable and no loss was observed with time. Previous works have also reported that [emim][Ac] and [emim][EtSO<sub>4</sub>] can be regenerated without losing their properties [12].

To obtain isothermal conditions, an oven was introduced in the experimental setup, as shown in Fig. 2.

The carbon dioxide concentration in the outlet gas stream was continuously monitored by sampling a fraction of the stream through a gas analyzer (Emerson Process, Rosemount Analytical NGA 2000) based on non-dispersive infrared (NDIR) spectroscopy. Before sending the gas sample to the analyzer, it was necessary to dilute the sample with N<sub>2</sub> to maintain the concentration range for the NDIR analyzer (at least 200 mL min<sup>-1</sup>). Steady state was indicated by a constant CO<sub>2</sub> concentration in the exit gas stream.

## 3. Results and discussion

### 3.1. Results of characterization of the hollow fiber membranes

Table 2 shows the measurements of the inner diameter ( $d_i$ ), wall thickness ( $e$ ), and length ( $L$ ) for fibers in the wet and dry forms. The virgin fibers shrank by approximately 5% of their length as they dried. Note that in the case of the D fibers, both the inner diameter and the wall thickness decreased in the dry form, possibly due to the contraction of the polymer phase. The greatest variation occurred in the A fibers. In the dry form, the C and D fibers presented the highest wall thicknesses.

The mechanical properties results are compiled in Table 3. Note that the B fibers showed the highest elasticity.

Regarding the permeability results with pure CO<sub>2</sub>, the behavior of the wet fibers was affected by the relative humidity (Fig. 3). A fibers in wet form suffer a compaction around 2 bars and the CO<sub>2</sub> flux is smaller than B and C fibers. The trend in the case of this last type of fibers (B and C) is linear reaching fluxes of more than  $1.2 \cdot 10^5$  NL m<sup>-2</sup> h<sup>-1</sup> with 6 and 7 bar respectively.

Fig. 4 shows the permeability results with pure CO<sub>2</sub> and dry fibers. On the one hand, a high permeability and a linear trend were observed in the C and D fibers in dry form, which presented almost identical CO<sub>2</sub> permeabilities. No compaction was observed up to 4 bars in these type of fibers. On the other hand, the results obtained with the A and B fibers indicated that the permeability was very low. The compaction of the fibers occurred at 2 bars for the A fibers as the previous case, mentioned in Fig. 3. The CO<sub>2</sub> flux with wet fibers was considerably higher than with dry fibers in

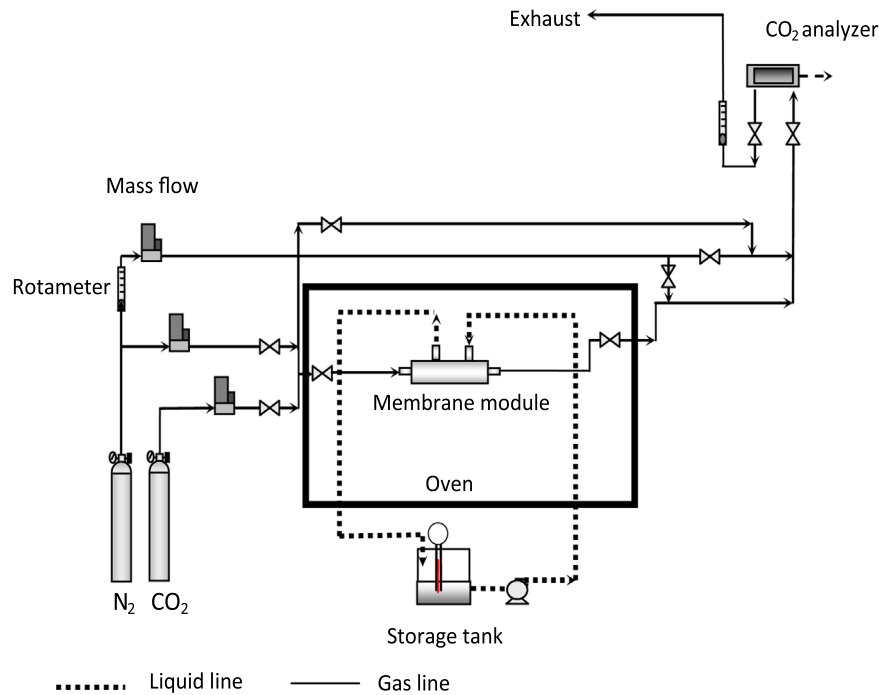


Fig. 2. Experimental setup for CO<sub>2</sub> gas capture.

Table 2

Outer diameter, wall thickness and length of PVDF hollow fibers with different additives and with ionic liquid immobilized.

	Dry			Wet		
	$d_i$ (mm)	$e$ ( $\mu\text{m}$ )	$L$ (cm)	$d_i$ (mm)	$e$ ( $\mu\text{m}$ )	$L$ (cm)
A	0.739	90	78.5	0.484	139	82.6
B	0.584	109	78.6	0.572	101	82.6
C	0.488	157	78.6	0.410	137	82.6
D	0.455	174	78.9	0.475	184	82.6
<i>Ionic liquid embedded</i>						
C+[emim][EtSO <sub>4</sub> ]	0.439	143	84.2	0.496	154	82.5
C+[emim][Ac]	0.436	151	82.0	0.515	165	82.5
D+[emim][EtSO <sub>4</sub> ]	0.443	159	85.3	0.379	146	82.5
D+[emim][Ac]	0.451	160	81.7	0.472	172	82.5

The maximum standard deviation between measurements is 5.88%.

Table 3

Mechanical properties of PVDF hollow fibers with different additives and with ionic liquid immobilized.

	Dry				Wet			
	MC (N)	CC (Mpa)	$\epsilon_b$ (%)	$E$ (N/mm <sup>2</sup> )	MC (N)	CC (Mpa)	$\epsilon_b$ (%)	$E$ (N/mm <sup>2</sup> )
A	1.62	7.90	150.38	161.82	1.60	5.91	158.68	47.50
B	1.61	6.23	150.53	135.33	1.62	7.58	181.53	92.70
C	2.07	6.53	74.89	188.23	1.88	8.00	76.67	180.74
D	1.95	5.67	50.03	183.11	1.78	4.68	63.71	98.11
<i>Ionic liquid embedded</i>								
C+[emim][EtSO <sub>4</sub> ]	1.37	5.25	142.42	12.36	1.35	4.29	145.53	18.29
C+[emim][Ac]	1.56	5.61	116.89	81.86	1.60	4.40	128.05	40.03
D+[emim][EtSO <sub>4</sub> ]	1.26	4.18	142.92	9.28	1.28	5.32	168.33	65.40
D+[emim][Ac]	1.49	4.87	95.32	68.42	1.47	4.20	110.12	41.94

The maximum standard deviation between measurements is 6.4%.

both cases.

Taking into account the high permeability results, the C and D fibers were the most appropriate for the addition of the ionic liquids and consequently for CO<sub>2</sub> absorption.

### 3.2. Results of characterization of selected hollow fibers when Ionic

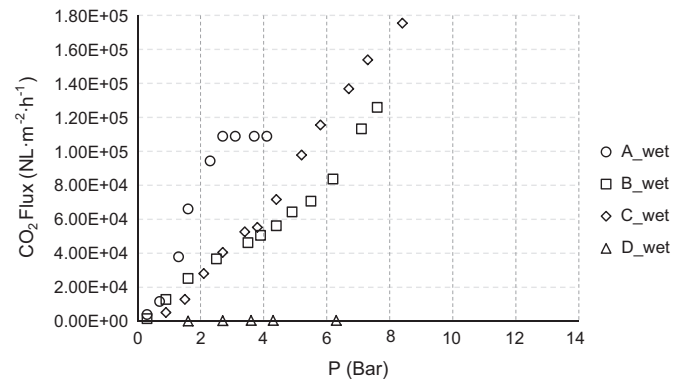


Fig. 3. Permeability results with wet fibers.

liquids were immobilized

Tables 4 and 5 show the structural comparison with or without IL for the two ionic liquids using scanning electron microscopy. The virgin fibers were wet; therefore, the fibers were dried after adding the IL. In the case of D+[emim][EtSO<sub>4</sub>], the results were

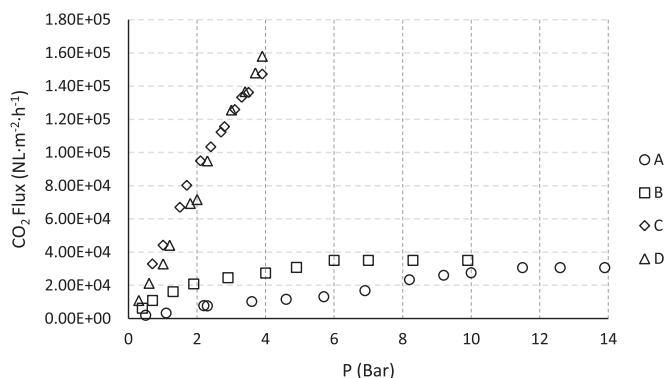


Fig. 4. Permeability results with dry fibers.

highly different in the wet form because the inner and outer diameters decreased (Table 2). The results with D+[emim][Ac] were similar. In the wet form, the fibers when the ionic liquid was added, the pores were filled and possibly creating a new layer, as shown in Table 4. The C fibers immobilized with ionic liquids showed an increment in the diameters in the wet form (Table 2). This result could be primarily attributed to the fact that the ionic liquids swelled the virgin fibers and dissolved the polymeric matrix in the case of the C+[emim][EtSO<sub>4</sub>] and C+[emim][Ac] fibers, as shown in Table 5.

The fiber sizes (Table 2) were in accordance with the literature. Rezaei et al. prepared their own fibers with inner and outer diameters of  $0.455 \pm 0.025$  and  $0.825 \pm 0.025$  mm, respectively [33]. Meanwhile, Naim et al. obtained fibers with  $d_i=0.550 \pm 0.020$  mm and  $d_o=0.800 \pm 0.030$  mm [34].

Table 3 shows the results of the mechanical properties of the fibers with and without ionic liquids. The breaking strain suffered significant changes. C+[emim][EtSO<sub>4</sub>] and C+[emim][Ac] fibers obtained values 50% smaller than without ionic liquids in wet form. Results in dry form with ILs show a decrease around 17% and 26% with C and D fibers respectively. On the other hand, note that the deformation in these modified fibers was at least two-fold greater when the ionic liquids were immobilized. The compression

with the C fibers and the ionic liquids was much lower than without ILs. Young's modulus (N/mm<sup>2</sup>) was calculated using Eq. (1).

$$E = \frac{\sigma}{\epsilon} = \frac{F/S}{\Delta L/L} \quad (1)$$

where  $E$  is Young's modulus (modulus of elasticity),  $F$  is the force exerted on an object under tension (fiber),  $\Delta L$  is the amount by which the length of the fiber changes,  $L$  is the original length of the fiber, and  $S$  is the fiber section.

Young's modulus decreased in the presence of IL, indicating that there was an interaction between the IL and the polymeric matrix. The IL plasticized the polymer, and the fiber swelled.

The bubble point results are presented in Table 6. The results with the D fibers did not lead to any definitive conclusions because they exceeded the maximum measured value of the equipment (7.1 bar). Furthermore, the results with the C fibers indicated that in the case of [emim][EtSO<sub>4</sub>], the bubble point was higher than in the case of fibers without ionic liquid, 6.4 and 4.9 bar respectively. Slightly lower values were obtained with C+[emim][Ac] fibers (4.4 bar). These bubble points show the transmembrane pressure necessary to push the IL outside of the pore. This work achieves pressure quite high compared to the transmembrane pressure in a G/L contactors reported in the literature [35–37].

The results of the CO<sub>2</sub> permeation tests with fibers in dry form are listed in Figs. 5 and 6 for the C and D fibers, respectively, showing the differences produced when the ionic liquids were immobilized. A change in dimensions of the fibers when the ILs were added does not necessarily mean more or less permeability (Figs. 5 and 6). The dotted lines accompanying each graph showed a clear linear trend. On one hand when C fibers were studied the confidence reached  $R^2=0.99$  when the ionic liquids were added and  $R^2=0.97$  without ionic liquids. On the other hand results with D fibers reported a confidence of  $R^2=0.98$  and  $R^2=0.99$  with [emim][EtSO<sub>4</sub>] ionic liquid and without IL respectively.

When fibers C and D were used the permeability with the ionic liquid [emim][EtSO<sub>4</sub>] increased in both cases. In the case of C+[emim][EtSO<sub>4</sub>] the flux achieved a value of  $46679 \text{ NL m}^{-2} \text{ h}^{-1}$  and

Table 4  
Scanning electron microscopy images of the D fibers with ionic liquid immobilized.

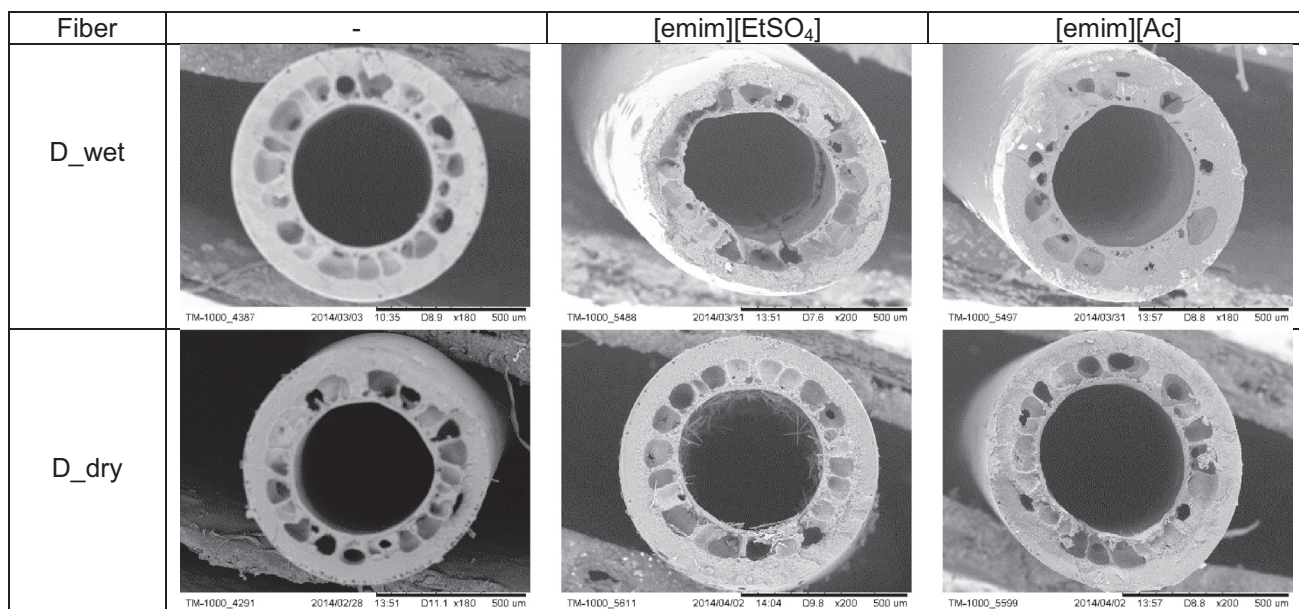


**Table 5**  
Scanning electron microscopy images of the C fibers with ionic liquid immobilized.

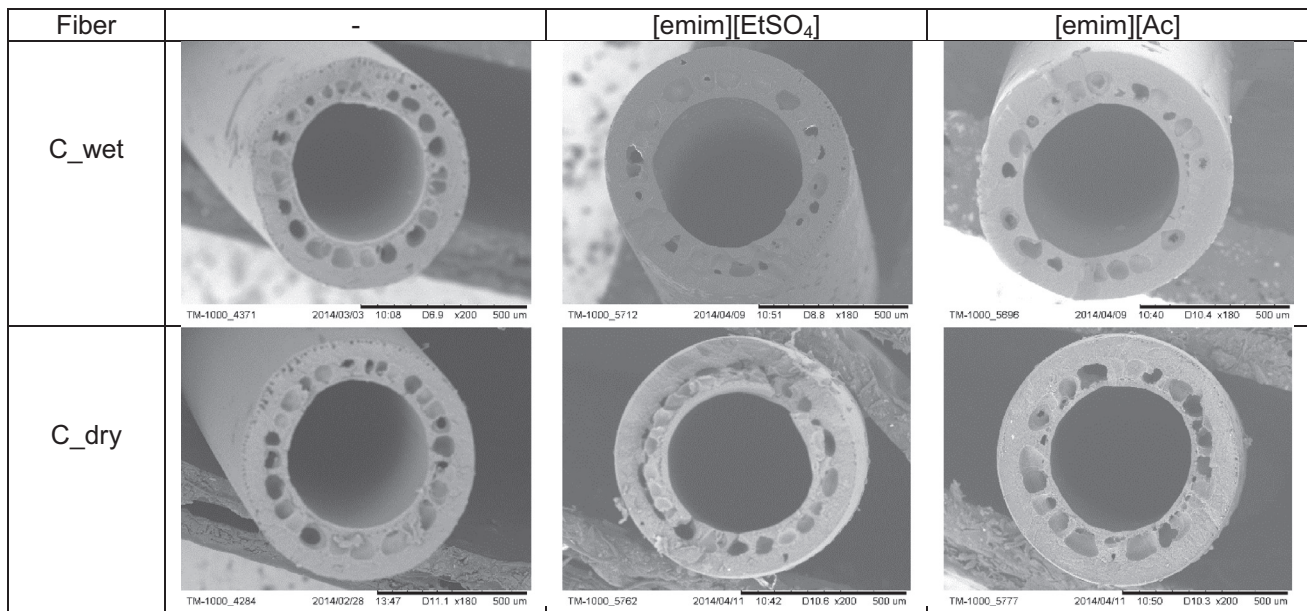


**Table 6**  
Bubble point results of the C and D fibers with ionic liquids immobilized.

Fiber	Bubble point P (Bar)
C	4.9
C+[emim][EtSO <sub>4</sub> ]	6.4
C+[emim][Ac]	4.4
D	> 7.1
D+[emim][EtSO <sub>4</sub> ]	> 7.1
D+[emim][Ac]	> 7.1

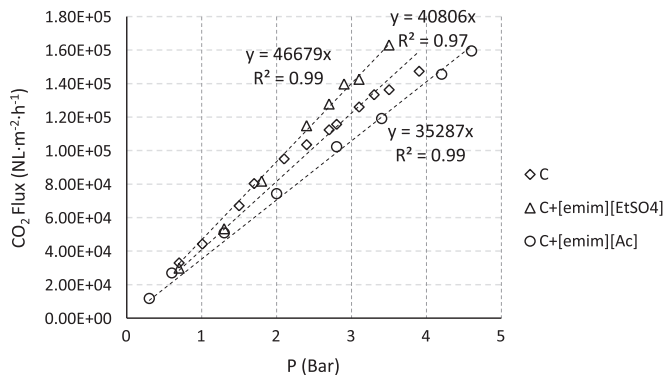


**Fig. 5.** Permeability results with the C fibers and with ionic liquids immobilized.

in the case of D+[emim][EtSO<sub>4</sub>] the value was 57041 NL m<sup>-2</sup> h<sup>-1</sup>. The tests for permeability from 0 to 14 bar with CO<sub>2</sub> using the D fibers with the ionic liquid [emim][Ac] in dry form did not result in any values, which could be attributed to the fact that the ionic liquid filled the pores, and thus, the gas was unable to enter fibers. The explanation may be related to the contraction observed in the pores of the fibers, which may cause that CO<sub>2</sub> cannot enter the fiber. Further work will be planned to confirm this point.

Table 7 shows the calculated CO<sub>2</sub> permeance values, in which the obtained values from previous works are also compiled [22,24,28,38,39]. The important points to note are as follows:

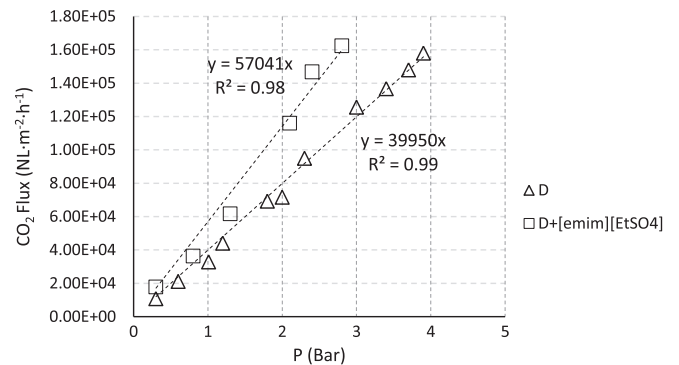


**Fig. 6.** Permeability results with the D fibers, and with ionic liquid immobilized.

**Table 7**  
CO<sub>2</sub> permeance values.

Hollow fibers	CO <sub>2</sub> (NL/(h m <sup>2</sup> bar))	Reference
PVDF C (dry)	40806	This work
PVDF C+[emim][EtSO <sub>4</sub> ] (dry)	46679	This work
PVDF C+[emim][Ac] (dry)	35287	This work
PVDF D (dry)	39950	This work
PVDF D+[emim][EtSO <sub>4</sub> ] (dry)	57041	This work
PTMSP	5580–3070	[24]
Teflon AF2400	5900–4590	[24]
PVDF (Water/NMP/PVA)	53200–365	[28]
PES_PTMS	8915–5588	[22]
PES_Teflon AF2400	9930–6000	[22]
Oxyplan_PTMS	3070	[22]
Oxyplan_Teflon AF2400	5120	[22]
TPX	2710–1350	[38]
PSF 5% packing density	44200	[39]

(i) the hollow fibers immobilized with the ionic liquid [emim][EtSO<sub>4</sub>] presented higher values of CO<sub>2</sub> permeance (43% increase compared with the fibers without the addition of the ionic liquid) for the PVDF fibers denoted D, and (ii) the highest CO<sub>2</sub> permeance value, 57041 NL/(h m<sup>2</sup> bar), exceeded the reported values for PVDF and Teflon self-made hollow fibers.

**Table 8**  
CO<sub>2</sub> capture experiments (15% CO<sub>2</sub> gas phase and membrane module) with the D+[emim][Ac] PVDF fibers.

T (K)	Efficiency (%)	$R_{\text{overall}} \cdot 10^{-4}$ (s m <sup>-1</sup> )	$R_g$ (s m <sup>-1</sup> )	$R_m \cdot 10^{-2}$ (s m <sup>-1</sup> )	$R_l \cdot 10^{-4}$ (s m <sup>-1</sup> )	$K_{\text{overall}}$ (m s <sup>-1</sup> )
303	20.4 ± 2.27	6.02	7.39	1.41	6.01	1.66 · 10 <sup>-5</sup>
313	27.1 ± 3.01	4.37	6.98	1.33	4.35	2.29 · 10 <sup>-5</sup>
323	28.6 ± 2.47	4.10	6.27	1.19	4.09	2.44 · 10 <sup>-5</sup>
333	29.3 ± 1.83	3.98	5.96	1.13	3.97	2.51 · 10 <sup>-5</sup>

### 3.3. Results of CO<sub>2</sub> capture

CO<sub>2</sub> absorption experiments were performed in a PVC membrane contactor to evaluate the process efficiency at different temperatures, working with a gas phase composed of 15% CO<sub>2</sub> and 85% N<sub>2</sub>. Related to the CO<sub>2</sub> interaction, the ionic liquid [emim][EtSO<sub>4</sub>] presents physical absorption, while the ionic liquid [emim][Ac] presents chemical absorption [3,4,8,12–14]. Taking into account this point, the ionic liquid [emim][Ac] was selected for the CO<sub>2</sub> capture study in order to show the mass transfer enhanced by the chemical reaction.

The gas stream was fed through the lumen side, while the liquid (1-ethyl-3-methylimidazolium acetate) flowed in counter-current through the shell-side. A module with 11 D+[emim][Ac] fibers in the dry form was chosen for CO<sub>2</sub> absorption.

The CO<sub>2</sub> removal efficiency was calculated as follows:

$$\text{Efficiency (\%)} = \left(1 - \frac{C_{\text{CO}_2, \text{out}}}{C_{\text{CO}_2, \text{in}}}\right) 100 \quad (2)$$

Table 8 shows the removal efficiencies determined at different temperatures (303–333 K) with a gas flow rate of 20 mL min<sup>-1</sup>.

The resistance in a series approach could be used to relate the individual mass transfer resistances to the overall mass transfer resistance:

$$R_{\text{overall}} = R_l + R_g + R_m \quad (3)$$

Table 8 also reports the values of the calculated resistances in the liquid phase, gas phase and membrane respectively ( $R_g$ ,  $R_l$  and  $R_m$ ), which constitute  $R_{\text{overall}}$ . The contribution of the gas phase and membrane could be considered negligible, in agreement with previous works [12,40,41]. In order to calculate each resistance the Eq. (4) was used.

$$\frac{1}{K_{\text{overall}}} = \frac{d_o}{k_g d_i} + \frac{d_o}{k_{\text{mg}} d_{\text{lm}}} + \frac{1}{k_l H_d E} \quad (4)$$

where  $d_o$ ,  $d_i$  and  $d_{\text{lm}}$  are the outside, inside and log mean diameters in (m) of the hollow fiber,  $H_d$  represents the dimensionless Henry constant,  $k_g$ ,  $k_{\text{mg}}$ ,  $k_l$ , which are the individual mass transfer coefficients of the gas phase, membrane and liquid phase, respectively (m s<sup>-1</sup>) and  $K_{\text{overall}}$  is the overall mass transfer coefficient (m s<sup>-1</sup>).

The overall transfer coefficient,  $K_{\text{overall}}$ , in Table 8 was also calculated using the following equation:

$$N_{\text{CO}_2, \text{g}} = \frac{Q_g}{A} (C_{\text{CO}_2, \text{in}} - C_{\text{CO}_2, \text{out}}) = K_{\text{overall}} \frac{\Delta y_{\text{lm}} \cdot P_T}{RT} \quad (5)$$

where  $Q_g$  is the gas flow rate (m<sup>3</sup> s<sup>-1</sup>),  $A$  is the membrane area (m<sup>2</sup>),  $P_T$  is the total pressure in the gas phase, and  $\Delta y_{\text{lm}}$  is the logarithmic mean of the driving force based on the gas phase molar fractions. The  $K_{\text{overall}}$  values, as expected, rise when the temperature increases (Table 8).

Table 9 compares the  $K_{\text{overall}}$  value obtained at room temperature (298 ± 5 K) with some literature values using other solvents in PVDF membrane contactors for CO<sub>2</sub> capture. Concerning to  $K_{\text{overall}}$ , this work achieved values that were almost one order of

**Table 9**  
 $K_{\text{overall}}$  comparison with literature values.

Reference	Solvent	$K_{\text{overall}}$ (10 <sup>6</sup> m s <sup>-1</sup> )
This work	[emim][Ac]	16.6
[42]	1 M MEA	0.75
[43]	1 M MEA	0.93
[42]	1 M DEA	0.30
[44]	Distilled water	4.85

All these references using a PVDF hollow fiber membranes.

magnitude higher than previous works [42–44] with traditional solvents such as monoethanolamine (MEA) and diethylamine (DEA), which are associated with some operational problems due to volatility and solvent losses; problems that ionic liquids eliminate. Also, It is worth recalling that ILs have some important advantages respect to these absorbents such as negligible vapor pressure, high chemical, electrochemical and thermal stability and can be regenerated.

Related to the temperature dependence, the  $K_{\text{overall}}$  values (m s<sup>-1</sup>) obtained with the PVDF fibers, D+[emim][Ac], show an increase from 1.6 · 10<sup>-5</sup> to 2.5 · 10<sup>-5</sup> m s<sup>-1</sup> in the range of 303–333 K. The overall mass transfer coefficient is favored by temperature increases due to higher chemisorption phenomenon, lower viscosity and higher diffusivity.

The values of  $K_{\text{overall}}$  were also transformed by the term (fiber area/shell volume) in order to compare the results obtained with these PVDF fibers, D+[emim][Ac] and the values obtained when another type of commercial membrane contactor was used (Fig. 7): a polysulfone membrane contactor with different packing densities. This PS module has been used due to excellent mechanical strength, high thermal and chemical stability and perfect solubility in many types of solvents [45,46]. Fig. 7 shows the trend of  $K_r$  (s<sup>-1</sup>) ( $K_{\text{overall}}$  divided by the term fiber area/shell volume), corresponding to the reaction between CO<sub>2</sub> and the ionic liquid [emim][Ac] [3,4,8,12–14].

The temperature dependence was slight because the higher temperature impacted the solubility, viscosity and diffusivity of the ionic liquid, although the mass transfer was favored [12].

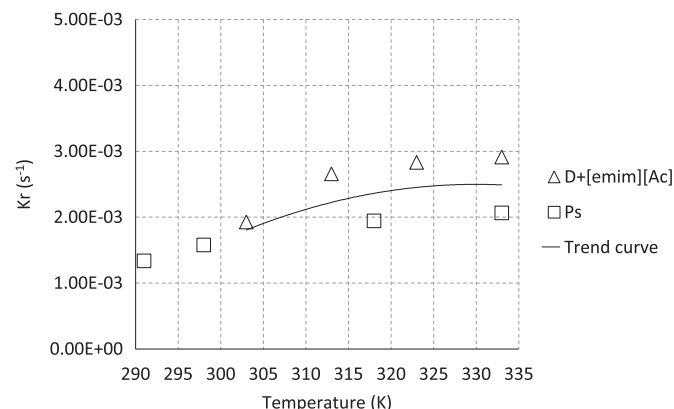


**Fig. 7.**  $K_r$  comparison with commercial Ps and the D+[emim][Ac] hollow fiber membrane contactor. Ps values adapted from [46].

#### 4. Conclusions

Four different types of self-made membranes composed of PVDF hollow fibers (coagulation NMP/water) were studied to obtain the best fibers for CO<sub>2</sub> absorption. The characterization indicated which type of fiber was more adequate due to its good size, good mechanical properties, high CO<sub>2</sub> gas permeability and reasonable bubble point, which were appropriate for a CO<sub>2</sub> absorption process in a gas-liquid membrane contactor system.

C and D fibers are more adequate for CO<sub>2</sub> absorption. For this reason and to improve the absorption rate, two different ionic liquids were immobilized on the two best preforming fibers. On the one hand, the 1-ethyl-3-methylimidazolium ethyl sulfate [emim][EtSO<sub>4</sub>] ionic liquid presented low viscosity, low toxicity, and low cost. On the other hand, the 1-ethyl-3-methylimidazolium acetate [emim][Ac] ionic liquid had high solubility. These ILs were chosen for this work due to its characteristics, reported in the previous literature [3,4,8,12–15].

Concerning the permeability results, two conclusions could be drawn: (i) the fibers in the dry form presented higher values than those in the wet form, and (ii) when the ionic liquid [emim][EtSO<sub>4</sub>] was immobilized, the permeability significantly increased by 43%, resulting in CO<sub>2</sub> permeance data that were higher than the literature values.

The CO<sub>2</sub> capture using PVDF fibers immobilized with the [emim][Ac] ionic liquid achieved a  $K_{overall}$  higher than the values reported in the literature for PVDF hollow fiber membrane contactors using conventional solvents such as MEA and DEA.

Further work is planned for the PVDF fibers immobilized with the [emim][Ac] ionic liquid to evaluate CO<sub>2</sub> capture in a post-combustion environment, as well as to conduct long-term experiments under real operating conditions, including high temperatures. Moreover, the composite fibers designed in this study could also offer interesting potential for other applications, such as gas absorption in physical solvents, liquid degassing by vacuum or gas stripping.

#### Acknowledgments

This research has been funded by the Spanish Ministry Economy and Competitiveness (Projects ENE2010-14828 and CTQ2013-48280-C3-1-R).

#### References

- [1] J. Albo, A. Irabien, Non-dispersive absorption of CO<sub>2</sub> in parallel and cross-flow membrane modules using EMISE, *J. Chem. Technol. Biotechnol.* 87 (2012) 1502–1507.
- [2] D.W. Bailey, P.H.M. Feron, Post-combustion decarbonisation processes, *Oil Gas Sci. Technol.* 60 (2005) 461–474.
- [3] M. Ramdin, T.W. De Loos, T.J.H. Vlucht, State-of-the-art of CO<sub>2</sub> capture with ionic liquids, *Ind. Eng. Chem. Res.* 51 (2012) 8149–8177.
- [4] G. Gurau, H. Rodríguez, S.P. Kelley, P. Janiczek, R.S. Kalb, R.D. Rogers, Demonstration of chemisorption of carbon dioxide in 1,3-dialkylimidazolium acetate ionic liquids, *Angew. Chem. Int. Ed.* 50 (2011) 12024–12026.
- [5] E.J. Maginn, Design and Evaluation of Ionic Liquids as Novel CO<sub>2</sub> Absorbents, National Energy Technology Laboratory, US, 2004.
- [6] Z. Dai, R.D. Noble, D.L. Gin, X. Zhang, L. Deng, Combination of ionic liquids with membrane technology: a new approach for CO<sub>2</sub> separation, *J. Membr. Sci.* 497 (2016) 1–20.
- [7] R. Shindo, M. Kishida, H. Sawa, T. Kidesaki, S. Sato, S. Kanehashi, K. Nagai, Characterization and gas permeation properties of polyimide/ZSM-5 zeolite composite membranes containing ionic liquid, *J. Membr. Sci.* 454 (2014) 330–338.
- [8] J. Blath, N. Deubler, T. Hirth, T. Schiestel, Chemisorption of carbon dioxide in imidazolium based ionic liquids with carboxylic anions, *Chem. Eng. J.* 181–182 (2012) 152–158.
- [9] J. Albo, T. Tsuru, Thin ionic liquid membranes based on inorganic supports with different pore sizes, *Ind. Eng. Chem. Res.* 53 (2014) 8045–8056.
- [10] J. Albo, T. Yoshioka, T. Tsuru, Porous Al<sub>2</sub>O<sub>3</sub>/TiO<sub>2</sub> tubes in combination with 1-ethyl-3-methylimidazolium acetate ionic liquid for CO<sub>2</sub>/N<sub>2</sub> separation, *Sep. Purif. Technol.* 122 (2014) 440–448.
- [11] E. Santos, J. Albo, A. Irabien, Acetate based supported ionic liquid membranes (SILMs) for CO<sub>2</sub> separation: influence of the temperature, *J. Membr. Sci.* 452 (2014) 277–283.
- [12] L. Gomez-Coma, A. Garea, A. Irabien, Non-dispersive absorption of CO<sub>2</sub> in [emim][EtSO<sub>4</sub>] and [emim][Ac]: temperature influence, *Sep. Purif. Technol.* 132 (2014) 120–125.
- [13] M.B. Shiflett, A. Yokozeki, Phase behavior of carbon dioxide in ionic liquids: [emim][acetate], [emim][trifluoroacetate], and [emim][acetate]+[emim][trifluoroacetate] mixtures, *J. Chem. Eng. Data* 54 (2009) 108–114.
- [14] X.L. Papatyfon, N.S. Heliopoulos, I.S. Molchan, L.F. Zubeir, N.D. Bezemer, M. K. Arfanis, A.G. Kontos, V. Likodimos, B. Iliev, G.E. Romanos, P. Falaras, K. Stamatakis, K.G. Beltsios, M.C. Kroon, G.E. Thompson, J. Klöckner, T.J. S. Schubert, CO<sub>2</sub> capture efficiency, corrosion properties, and ecotoxicity evaluation of amine solutions involving newly synthesized ionic liquids, *Ind. Eng. Chem. Res.* 53 (30) (2014) 12083–12102.
- [15] A. Arce, H. Rodríguez, A. Soto, Use of a green and cheap ionic liquid to purify gasoline octane boosters, *Green Chem.* 9 (2007) 247–253.
- [16] P. Luis, T. Van Gerven, B. Van Der Bruggen, Recent developments in membrane-based technologies for CO<sub>2</sub> capture, *Prog. Energy Combust. Sci.* 38 (2012) 419–448.
- [17] S.H. Lin, C.F. Hsieh, M.H. Li, K.L. Tung, Determination of mass transfer resistance during absorption of carbon dioxide by mixed absorbents in PVDF and PP membrane contactor, *Desalination* 249 (2009) 647–653.
- [18] J. Albo, P. Luis, A. Irabien, Carbon dioxide capture from flue gases using a cross-flow membrane contactor and the ionic liquid 1-ethyl-3-methylimidazolium ethylsulfate, *Ind. Eng. Chem. Res.* 49 (2010) 11045–11051.
- [19] M. Mavroudi, S.P. Kaldis, G.P. Sakellariopoulos, A study of mass transfer resistance in membrane gas-liquid contacting processes, *J. Membr. Sci.* 272 (2006) 103–115.
- [20] J.A. Thompson, J.T. Vaughn, N.A. Brunelli, W.J. Koros, C.W. Jones, S. Nair, Mixed-linker zeolitic imidazolate framework mixed-matrix membranes for aggressive CO<sub>2</sub> separation from natural gas, *Microporous Mesoporous Mater.* 192 (2014) 43–51.
- [21] S. Farrukh, F.T. Minhas, A. Hussain, S. Memon, M.I. Bhanjer, M. Mujahid, Preparation, characterization, and applicability of novel calix[4]arene-based cellulose acetate membranes in gas permeation, *J. Appl. Polym. Sci.* 131 (6) (2014), <http://dx.doi.org/10.1002/APP.39985>, 39985 (1–9).
- [22] E. Lasseguette, J.C. Rouch, J.C. Remigy, Hollow-fiber coating: application to preparation of composite hollow-fiber membrane for gas separation, *Ind. Eng. Chem. Res.* 52 (36) (2013) 13146–13158.
- [23] S. Dai, Y. Seol, S. Wickramanayake, D. Hopkinson, Characterization of hollow fiber supported ionic liquid membranes using microfocus X-ray computed tomography, *J. Membr. Sci.* 492 (2015) 497–504.
- [24] P.T. Nguyen, E. Lasseguette, Y. Medina-Gonzalez, J.C. Remigy, D. Roizard, E. Favre, A dense membrane contactor for intensified CO<sub>2</sub> gas/liquid absorption in post-combustion capture, *J. Membr. Sci.* 377 (1–2) (2011) 261–272.
- [25] N. Goyal, S. Suman, S.K. Gupta, Mathematical modeling of CO<sub>2</sub> separation from gaseous-mixture using a hollow-fiber membrane module: physical mechanism and influence of partial-wetting, *J. Membr. Sci.* 474 (2015) 64–82.
- [26] T. Savart, Conception et réalisation de fibres creuses industrielles d'ultrafiltration en poly (fluorure de vinylidène) (PVDF) contenant des copolymères à blocs, Université Toulouse 3, Paul Sabatier, Toulouse, France, 2013.
- [27] O. Lorain, J. M. Espenan, J.C. Remigy, J. F. Lahitte, J. C. Rouch, T. Savart, P. Gerard, S. Magnet, Copolymer having amphiphilic blocks, and use thereof for manufacturing polymer filtration membranes, WO2014/139977 (A1), 2014.
- [28] Y. Medina-Gonzalez, E. Lasseguette, J.C. Rouch, J.C. Remigy, Improving PVDF hollow fiber membranes for CO<sub>2</sub> gas capture, *Sep. Sci. Technol.* 47 (11) (2012) 1596–1605.
- [29] S. Wickramanayake, D. Hopkinson, C. Myers, L. Hong, J. Feng, Y. Seol, D. Plasynski, M. Zeh, D. Luebke, Mechanically robust hollow fiber supported ionic liquid membranes for CO<sub>2</sub> separation applications, *J. Membr. Sci.* 470 (2014) 52–59.
- [30] D.H. Kim, I.H. Baek, S.U. Hong, H.K. Lee, Study on immobilized liquid membrane using ionic liquid and PVDF hollow fiber as a support for CO<sub>2</sub>/N<sub>2</sub> separation, *J. Membr. Sci.* 372 (2011) 346–354.
- [31] M.B. Shiflett, A. Yokozeki, Phase behavior of carbon dioxide in ionic liquids: [emim][Acetate], [emim][Trifluoroacetate], and [emim][Acetate]+[emim][Trifluoroacetate] mixtures, *J. Chem. Eng. Data* 54 (2009) 108–114.
- [32] J. Albo, E. Santos, L.A. Neves, S.P. Simeonov, C.A.M. Afonso, J.G. Crespo, A. Irabien, Separation performance of CO<sub>2</sub> through supported magnetic ionic liquid membranes (SMILMs), *Sep. Purif. Technol.* 97 (2012) 26–33.
- [33] M. Rezaei, A.F. Ismail, S.A. Hashemifard, G.H. Bakeri, T. Matsuura, Experimental study on the performance and long-term stability of PVDF/montmorillonite hollow fiber mixed matrix membranes for CO<sub>2</sub> separation process, *Int. J. Greenh. Gas. Control.* 26 (2014) 147–157.
- [34] R. Naim, A.F. Ismail, Effect of fiber packing density of physical CO<sub>2</sub> absorption performance in gas-liquid membrane contactor, *Sep. Purif. Technol.* 115 (2013) 152–157.
- [35] Matevž. Vospnričnik, Albin Pintar, Gorazd Bercic, Janez Levec, Mass transfer studies in gas-liquid-solid membrane contactors, *Catal. Today* 79–80 (2003) 169–179.
- [36] M. Alame, A. Abusaloua, M. Pera-Titus, N. Guilhaume, K. Fiaty, A. Giroir-Fendler, High-performance catalytic wet air oxidation (CWAO) of organic acids

- and phenol in interfacial catalytic membrane contactors under optimized wetting conditions, *Catal. Today* 157 (2010) 327–333.
- [37] E. Chabanon, B. Belaïssaoui, E. Favre, Gas–liquid separation processes based on physical solvents: opportunities for membranes, *J. Membr. Sci.* 459 (2014) 52–61.
- [38] C. Makhloufi, E. Lasseguette, J.C. Remigy, B. Belaïssaoui, D. Roizard, E. Favre, Ammonia based CO<sub>2</sub> capture process using hollow fiber membrane contactors, *J. Membr. Sci.* 455 (2014) 236–246.
- [39] T.G. Skog, S. Johansen, M.B. Hägg, Method to prepare lab-sized hollow fiber modules for gas separation testing, *Ind. Eng. Chem. Res.* 53 (2014) 9841–9848.
- [40] A. Ortiz, D. Gorri, T. Irabien, I. Ortiz, Separation of propylene/propane mixtures using Ag<sup>+</sup>-RTIL solutions. Evaluation and comparison of the performance of gas–liquid contactors, *J. Membr. Sci.* 360 (2010) 130–141.
- [41] P. Luis, A. Garea, A. Irabien, Zero solvent emission process for sulfur dioxide recovery using a membrane contactor and ionic liquids, *J. Membr. Sci.* 330 (2009) 80–89.
- [42] W. Rongwong, R. Jiraratananon, S. Atcharyawut, Experimental study on membrane wetting in gas–liquid membrane contacting process for CO<sub>2</sub> absorption by single and mixed absorbents, *Sep. Purif. Technol.* 69 (2009) 118–125.
- [43] L. Wang, Z. Zhang, B. Zhao, H. Zhang, X. Lu, Q. Yang, Effect of long-term operation on the performance of polypropylene and polyvinylidene fluoride membrane contactors for CO<sub>2</sub> absorption, *Sep. Purif. Technol.* 116 (2009) 300–306.
- [44] M. Rahbari-Sisakht, A.F. Ismail, D. Rana, T. Matsuura, D. Emadzadeh, Effect of SMM concentration on morphology and performance of surface modified PVDF hollow fiber membrane contactor for CO<sub>2</sub> absorption, *Sep. Purif. Technol.* 116 (2013) 67–72.
- [45] F. Korminouri, M. Rahbari-Sisakht, T. Matsuura, A.F. Ismail, Surface modification of polysulfone hollow fiber membrane spun under different air-gap lengths for carbon dioxide absorption in membrane contactor system, *Chem. Eng. J.* 264 (2015) 453–461.
- [46] L. Gomez-Coma, C. Casado-Coterillo, A. Garea, A. Irabien, Temperature effect in polypropylene and polysulfone hollow fiber membrane contactors using ionic liquids. 21st International Congress of Chemical and Process Engineering, Czech Republic. Prague. pp. 23–27, August 2014.



**4.3. Gómez-Coma L., Garea A., Irabien A., Carbon dioxide capture by [emim][Ac] ionic liquid in a polysulfone hollow fiber membrane contactor. Int. J. Greenh. Gas Control. 2016, 52, 1-9.**

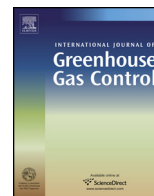
Resumen

Las emisiones de CO<sub>2</sub> tienen que ser controladas y reducidas para poder evitar el efecto invernadero. Este trabajo realiza un análisis de la eficacia en la separación de CO<sub>2</sub> mediante el uso de un contactor de membranas de fibra huecas y un líquido iónico. Esta configuración contribuye a una intensificación de procesos en el campo de la captura y almacenamiento de CO<sub>2</sub>. En este estudio, el líquido iónico 1-etil-3-metilimidazolio acetato [emim][Ac], se utilizó como absorbente debido a su alta solubilidad al CO<sub>2</sub>. El módulo seleccionado fue de polisulfona (Ps), ya que se trata de un polímero bien caracterizado que permite operar a temperaturas moderadas. Los resultados experimentales obtenidos se compararon con resultados anteriores realizados con un módulo de polipropileno. La corriente de gas fluye a través del interior de las fibras huecas. La eficiencia de eliminación de CO<sub>2</sub> obtenida a partir de datos experimentales, muestra una dependencia de la temperatura: de 30 a 45.0%, correspondiente a 291K y 348K, respectivamente, cuando se utilizó el contactor de Ps. Se ha evaluado también el coeficiente global de transferencia de materia  $K_{overall}$ . Además, un análisis de sensibilidad se ha llevado a cabo para estudiar el rendimiento de un contactor de membranas para la captura de CO<sub>2</sub> a fin de estimar las condiciones del proceso necesarias para conseguir un 90% de captura de CO<sub>2</sub>, valor objetivo, para que el sistema se considere competitivo con los procesos de absorción tradicionales.

Original abstract

CO<sub>2</sub> emissions have to be controlled and reduced in order to avoid greenhouse effect. This work reports an analysis of the efficiency of CO<sub>2</sub> separation using a hollow fiber membrane contactor and an ionic liquid. This process configuration contributes to the process intensification approach in the field of CO<sub>2</sub> capture and storage. In this study, the ionic liquid 1-ethyl-3-methylimidazolium acetate, [emim][Ac], was used as absorbent due to its high CO<sub>2</sub> solubility. The module selected was polysulfone (Ps) because it is a well characterized polymer that allows to operate at moderate temperatures. Results were compared to previous studies with a polypropylene module. The gas stream flowed through the inside of the hollow fibers. The CO<sub>2</sub> removal efficiency was obtained from experimental data, showing a temperature dependence: from 30 to 45.0%, corresponding to 291K and 348K respectively, when the Ps contactor was used. The overall mass transfer coefficient  $K_{overall}$  has also been evaluated. In addition, a numerical analysis was carried out to study the performance of the membrane

contactor for the CO<sub>2</sub> capture in order to estimate the process conditions to accomplish 90% CO<sub>2</sub> capture as a target to be competitive with the conventional absorption process.



# Carbon dioxide capture by [emim][Ac] ionic liquid in a polysulfone hollow fiber membrane contactor



L. Gomez-Coma\*, A. Garea, A. Irabien

Universidad de Cantabria, Chemical and Biomolecular Engineering Department, E.T.S. de Ingenieros Industriales y Telecomunicación, Universidad de Cantabria, Avda Los Castros s/n, 39005 Santander, Spain

## ARTICLE INFO

### Article history:

Received 1 April 2016

Received in revised form 23 June 2016

Accepted 11 July 2016

Available online 3 August 2016

### Keywords:

Carbon dioxide capture

Hollow fiber membrane contactor

Polysulfone

[emim][Ac] ionic liquid

## ABSTRACT

CO<sub>2</sub> emissions have to be controlled and reduced in order to avoid greenhouse effect. This work reports an analysis of the efficiency of CO<sub>2</sub> separation using a hollow fiber membrane contactor and an ionic liquid. This process configuration contributes to the process intensification approach in the field of CO<sub>2</sub> capture and storage.

In this study, the ionic liquid 1-ethyl-3-methylimidazolium acetate, [emim][Ac], was used as absorbent due to its high CO<sub>2</sub> solubility. The module selected was polysulfone (Ps) because it is a well characterized polymer that allows to operate at moderate temperatures. Results were compared to previous studies with a polypropylene module. The gas stream flowed through the inside of the hollow fibers. The CO<sub>2</sub> removal efficiency was obtained from experimental data, showing a temperature dependence: from 30 to 45.0%, corresponding to 291 K and 348 K respectively, when the Ps contactor was used. The overall mass transfer coefficient  $K_{overall}$  has also been evaluated.

In addition, a numerical analysis was carried out to study the performance of the membrane contactor for the CO<sub>2</sub> capture in order to estimate the process conditions to accomplish 90% CO<sub>2</sub> capture as a target to be competitive with the conventional absorption process.

© 2016 Elsevier Ltd. All rights reserved.

## 1. Introduction

Climate change resulting from the presence of greenhouse gases is becoming a serious issue of the present century (Ahn et al., 2013). Over 80% of energy needs worldwide are nowadays supplied by fossil fuels (Korminouri et al., 2014) where combustion in power plants is the largest point source contributor to CO<sub>2</sub> emissions (Saeed and Deng, 2015; Mansourizadeh et al., 2014; Mansourizadeh and Ismail, 2011). The CO<sub>2</sub> capture and sequestration (CCS) is a concern globally today to reduce the impact on the atmosphere and protect humans against the risks associated with CO<sub>2</sub> pollution (Boot-Handford et al., 2014). Therefore, it is important to continue developing technologies to mitigate this issue. A wide range of technologies exists for CCS based on physical and chemical processes including absorption, adsorption, membranes and cryogenics (Rao and Rubin, 2002). Considering the dependence on fossil fuels, capture and removal of greenhouse gases is an important subject to study (Korminouri et al., 2014). Three main methods can be identified

on the capture of CO<sub>2</sub>: pre-combustion, post-combustion and oxy-combustion.

For post-combustion capture, CO<sub>2</sub> at low partial pressure must be separated from flue gas after the fuel has been completely burned for energy conversion (Merkel et al., 2010). The typical conditions for post-combustion capture are 10–15% CO<sub>2</sub>, 5–10% H<sub>2</sub>O, 70–75% N<sub>2</sub> and lower concentrations of other components (Ramdin et al., 2012). In the 90% of the total post-combustion treatments the solvent used are alkanolamines (Albo and Irabien, 2012). Previous works showed that process intensification can be performed in two steps to develop a zero solvent emission process (Albo et al., 2010): (i) replace conventional power stations by membrane processes, and (ii) use ionic liquids instead of alkanolamines.

Post-combustion carbon dioxide capture appears to be the most amenable strategy for integration with existing coal-fired power plants (Fernández-Barquín et al., 2015; Low et al., 2013; Dai et al., 2016). Membrane absorption has been identified as an effective approach for CO<sub>2</sub> capture, which combines the advantages of chemical absorption and membrane separation (Zhang et al., 2015). Membrane technology appears to be an attractive option in terms of energy saving, modularity, easy scaling up and control, such as those energy intensive based on wet scrubbing using aqueous amine solutions (Fernández-Barquín et al., 2016).

\* Corresponding author.

E-mail address: [gomezcomal@unican.es](mailto:gomezcomal@unican.es) (L. Gomez-Coma).

The properties of the membrane depend on the material, the structure and thickness, the configuration and the module and system design, which involve the existence of many variables that have to be studied. The common materials for CO<sub>2</sub> separating membranes are organic polymers, such as polysulfone (Ps), polyimide (PA), poly(ethylene oxide) and polycarbonate (PC) (Luis et al., 2012; Wang et al., 2014). In the present work, polysulfone (Ps) was chosen because it is a well characterized polymer (Scholes et al., 2010). Ps is an asymmetric nonporous polymeric material applied for CO<sub>2</sub> capture and has been extensively studied for gas permeation and separation, because of its low permeability and comparatively high selectivity, which bring it close to Robeson's upperbound limit (Casado-Coterillo et al., 2012). This material has also excellent mechanical strength, high thermal and chemical stability and is not necessarily considered as hydrophobic (Korminouri et al., 2015; Nabian et al., 2015). The above properties of this polymer provide a potential application in the membrane gas absorption processes (Mansourizadeh and Ismail, 2010).

The thermal stability of the membrane is an important issue. Under high temperatures, the membrane material may undergo degradation or decomposition. The extent of membrane change depends of the glass transition temperature T<sub>g</sub> for amorphous polymers or the melting point T<sub>m</sub> for crystalline polymers. Over these temperatures, the properties of the polymers change significantly. The glass transition temperatures for the commonly used polymers, in CO<sub>2</sub> membrane contactors, are referenced by Li and Chen (2005). Taking into account the T<sub>g</sub> data, the higher values correspond to PTFE, polyimide, and polysulfone polymers which are the preferred in terms of long-term stability, while PE and PP polymers have very low T<sub>g</sub> values.

Since the 1980s, membrane contactors have been highly regarded due to several advantages over traditional equipment (Mehdipour et al., 2014). In hollow fiber membrane contactors, the two phases (gas and liquid) contact together without dispersion due to the membrane, which provides higher interfacial area, and independent control of the liquid and gas flow rates. Ideally, the membrane is porous and hence CO<sub>2</sub> transfer through the membrane is rapid because the pores are gas filled. This ensures a high overall mass transfer in a small membrane contactor area. For this reason, membrane contactors have high specific surface area and can be made modular. Hence scaling up or down is relatively easy. Finally, the mass transfer occurs by diffusion across the two phases (Albo et al., 2010; Albo and Irabien, 2012; Rahbari-Sisakht et al., 2013a; Scholes et al., 2015).

One of the key factors in the separation of CO<sub>2</sub> for gas mixtures is the type of the absorbent (Reza Razavi et al., 2013). Ionic liquids (ILs) are compounds that have created enormous interest in recent years as solvents for gas recovery (Albo and Irabien, 2012). ILs are salts, which consist exclusively of ions, with a melting point lower than 100 °C (Albo et al., 2011). ILs have several properties that make them useful for carbon dioxide capture such as (nearly) negligible volatility, high thermal stability, nonflammability, tunability, solvation properties, and high CO<sub>2</sub> solubility (Ramdin et al., 2012). The combination of these features can bring new opportunities in the use of IL-based membranes and processes in CO<sub>2</sub> separation applications, which are more energy efficient and environmentally friendly compared with the current commercial separation technologies. The use of ILs in membrane processes has been a research highlight in recent years. A comprehensive review of these research efforts is reported by Dai et al. (2016).

Ionic liquids containing a carboxylic anion are more biodegradable and less toxic than most other ILs (Chen et al., 2014). Moreover, the 1-ethyl-3-methylimidazolium acetate [emim][Ac] possess physical and chemical absorption, that coupled with its high CO<sub>2</sub> solubility make the [emim][Ac] a promising absorbent. Chemical absorption is useful for ILs because of the mechanism

**Table 1**  
Ps and PP membrane contactor characteristics.

Membrane material	Ps	PP
Fiber o.d. $d_o$ (m)	$1.3 \times 10^{-3}$	$3 \times 10^{-4}$
Fiber i.d. $d_i$ (m)	$7.0 \times 10^{-4}$	$2.2 \times 10^{-4}$
Fiber length, $L$ (m)	0.347	0.115
Number of fibers, $n$	400	2300
Effective inner membrane area, $A$ (m <sup>2</sup> )	0.18	0.18
Porosity (%)	43	40
Packing factor	0.43	0.39
Tortuosity <sup>a</sup>	2.33	2.50

<sup>a</sup> Assumed as  $1/\epsilon$ .

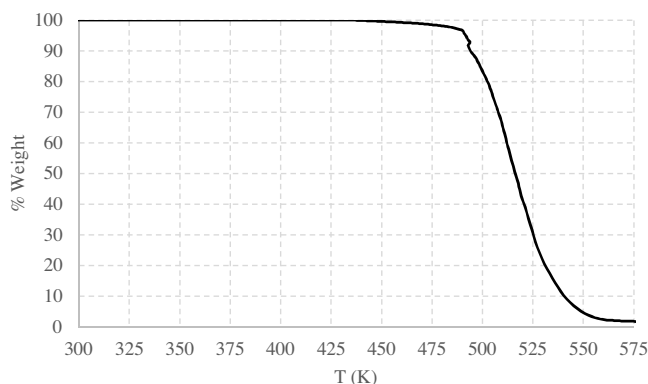


**Fig. 1.** TGA analysis for the [emim][Ac] ionic liquid.

leading to a greater absorption capacity of the gas (Pinto et al., 2014).

In the present work, the study of the CO<sub>2</sub> capture in a polysulfone hollow fiber membrane contactor was carried out at different temperatures using as solvent the ionic liquid [emim][Ac]. The possibility to significantly intensify gas-liquid absorption processes thanks to the membrane contactor has been proposed. In addition, a simulation task was accomplished in order evaluate the set of conditions (i.e. membrane mass transfer coefficient, membrane dimensions, module design) for a significant intensification effect compared to a packed column configuration.

## 2. Materials and methods

Carbon dioxide ( $99.7 \pm 0.01$  vol.%) and pure nitrogen ( $99.999 \pm 0.001$  vol.%) were purchased from Air Liquide (Spain). The gas stream was composed by 15% carbon dioxide and 85% nitrogen. The [emim][Ac] ionic liquid was supplied by Sigma Aldrich (Spain). The 1-Ethyl-3-methylimidazolium acetate [emim][Ac] ( $\geq 90\%$ ) (IL) was chosen because of its high CO<sub>2</sub> solubility. Previous works reported high CO<sub>2</sub> solubility values for [emim][Ac] (Gurau et al., 2011; Ramdin et al., 2012; Papatryfon et al., 2014; Santos et al., 2014). To ensure that the ionic liquid is suitable for our process despite its relatively low purity, solubility rates were measured and, compared with literature data, similar values were obtained. Ps hollow fiber membrane contactor was provided by VWR International Eurolab, S.L. (Spain). The main characteristics of this hollow fiber are shown in Table 1.

To ensure the stability of the ionic liquid for the temperature interval of the CO<sub>2</sub> capture experiments, up to 350K, the thermogravimetric analysis was performed in a TGA-60H Shimadzu Thermobalance. Fig. 1 shows the decomposition temperature. The [emim][Ac] remains without losing its properties until 440K. Table 2 shows the different viscosity values reported by Freire et al. (2011) as a function of temperature.

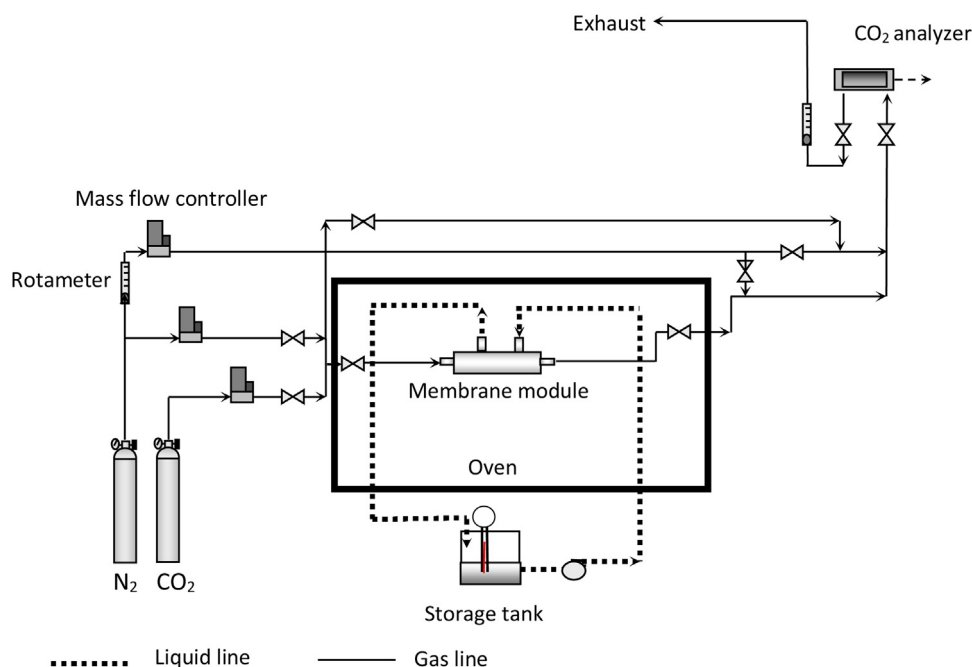


Fig. 2. Experimental set-up of the CO<sub>2</sub> capture system at laboratory scale.

Table 2

Viscosity values as function of temperature (Freire et al., 2011).

T (K)	Viscosity (cP)
291	249
298	144
318	48
333	26
348	16

The experimental setup of the CO<sub>2</sub> capture with [emim][Ac] in the hollow fiber membrane contactor is shown in Fig. 2. The gas flow rate operated at 70 mL min<sup>-1</sup>. The feed gas was adjusted by a mass flow controller (Brook instrument MFC 5850, Emerson Process Management Spain). The gas stream flowed through the inside of the hollow fibers and the [emim][Ac] ionic liquid flowed counter-currently through the shell side. The IL was pumped at 50 mL min<sup>-1</sup>. The temperature was controlled by a Memmert UNE 200 convection oven.

The CO<sub>2</sub> concentration in the outlet gas stream was continuously monitored by sampling a fraction of the stream through an analyzer (Emerson Process, Rosemount Analytical NGA 2000) each 15 s. This analyzer is based on non-dispersive infra-red (NDIR) spectroscopy. The steady state was determined by a constant carbon dioxide concentration in the exit gas stream.

### 3. Results and discussion

#### 3.1. Carbon dioxide capture

Carbon dioxide absorption in 1-ethyl-3-methyl imidazolium acetate was performed in a polysulfone hollow fiber membrane contactor in order to evaluate the process efficiency and compare the results with the previous data reported in the literature.

The outlet concentration of carbon dioxide at pseudo-steady-state in terms of efficiency (%) was calculated according to Eq. (1):

$$\text{Efficiency (\%)} = \left(1 - \frac{C_{\text{CO}_2, \text{out}}}{C_{\text{CO}_2, \text{in}}}\right) \cdot 100 \quad (1)$$

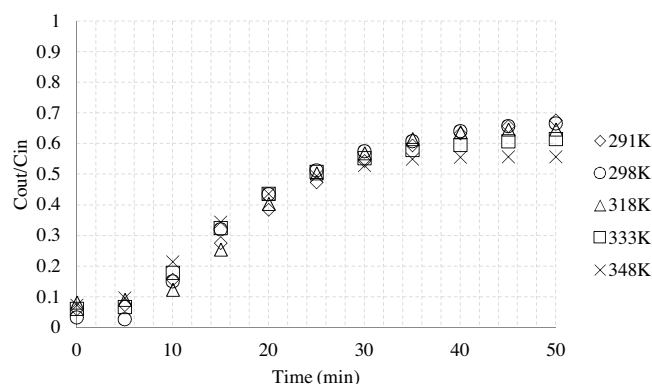


Fig. 3. CO<sub>2</sub> outlet concentration (dimensionless) vs time at different temperatures.

Table 3

Process efficiencies in CO<sub>2</sub> capture experiments at different temperatures.

T (K)	Efficiency (%)
291	29.5 ± 1.7
298	33.1 ± 2.6
318	37.4 ± 1.9
333	38.5 ± 2.2
348	44.2 ± 3.5

where  $C_{\text{CO}_2, \text{out}}$  is the outlet analyzer concentration and  $C_{\text{CO}_2, \text{in}}$  is the inlet concentration (15%). The outlet concentration of carbon dioxide was calculated as  $C_{\text{CO}_2, \text{(g), out}}/C_{\text{CO}_2, \text{(g), in}}$  at pseudo-steady state, ranged between 0.55 and 0.7, which indicates a process efficiency of around 30–45% (291–348 K) according to Eq. (1), for a gas stream containing 15% carbon dioxide and 85% nitrogen.

Fig. 3 represents the experiments continuously monitored at different temperatures; 291, 298, 318, 333 and 348 K with a gas flow rate of 70 mL min<sup>-1</sup>. Pseudo-steady state was obtained after 50 min maximum operating time.

Table 3 indicates the different efficiency values in the temperature interval 291–348 K. Each experiment was replicated three times under the same operating conditions and the average value

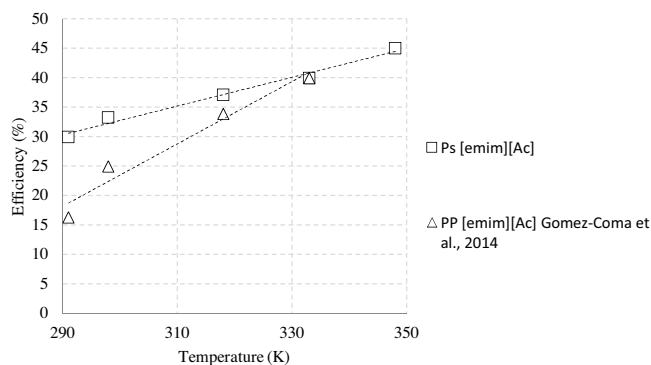


Fig. 4. Comparison between Ps and PP hollow fiber membrane contactors: CO<sub>2</sub> capture efficiencies (%) at different temperatures.

was calculated. As it can be seen, the experimental errors are less than 3.5% in all the cases. The efficiency increases when the temperature rises, being favored the chemical reaction.

The efficiency results showed in Table 3 were also compared with previous data reported in the literature (Gomez-Coma et al., 2014). Fig. 4 presents the polysulfone and the polypropylene (PP) hollow fiber membrane contactors results.

Table 1 shows also the main characteristics of the PP hollow fiber membrane contactor. It should be noted that PP and Ps membrane contactors have the same effective inner membrane area (0.18 m<sup>2</sup>).

The Ps results achieved higher CO<sub>2</sub> capture efficiencies at the same temperatures than PP hollow fiber membrane contactor: using the [emim][Ac] ionic liquid, the efficiencies were 30% and 16% (291 K) with Ps and PP respectively. In addition, the polypropylene hollow fiber membrane contactors are limited by temperature: with polysulfone membranes, the temperature could reach higher values and therefore higher efficiencies (Fig. 4).

Moreover, for the CO<sub>2</sub> absorption from flue gases, membranes with high T<sub>g</sub> may need to be applied because flue gases are often emitted at high temperatures. In this scenario, thermal stability of the membrane material may be the key factor for the membrane performance. This fact supports the selection of the polysulfone membrane contactor for the CO<sub>2</sub> capture.

### 3.2. Mass transfer description

The overall mass transfer coefficient,  $K_{overall}$  was calculated as (Gomez-Coma et al., 2014; Albo and Irbien 2012):

$$N_{CO_2,g} = \frac{Q_g}{A} (C_{CO_2,in} - C_{CO_2,out}) = K_{overall} \frac{\Delta y_{lm} \cdot P_T}{RT} \quad (2)$$

where  $Q_g$  represents the gas flow rate (m<sup>3</sup> s<sup>-1</sup>),  $A$  is the membrane area (m<sup>2</sup>),  $P_T$  is the total pressure in the gas phase, and  $\Delta y_{lm}$  is the logarithmic mean of the driving force based on the gas phase molar fractions.

Fig. 5 shows the overall mass transfer coefficients obtained at different temperatures from 291 K to 348 K when the Ps contactor was used. The  $K_{overall}$  takes values between  $2.4 \times 10^{-6}$  and  $3.7 \times 10^{-6}$  m s<sup>-1</sup> in this range of temperature. The  $K_{overall}$  values increase significantly as the temperature rises: an increment of 60% in 57 K was accomplished. However, the absorption rate did not increase as expected for a process dominated by a chemical reaction. This could be attributed to the fact that temperature favors the CO<sub>2</sub> capture but impacts on other factors such as solubility, viscosity and diffusivity. The values of the overall mass transfer coefficient presented in this work, are higher than other values reported in the previous literature for other fiber materials and traditional solvents such as MEA (Rahbari-Sisakht et al., 2013b; Boributh et al., 2013). This point is crucial due to the advantages of ionic liquids; e.g. negli-

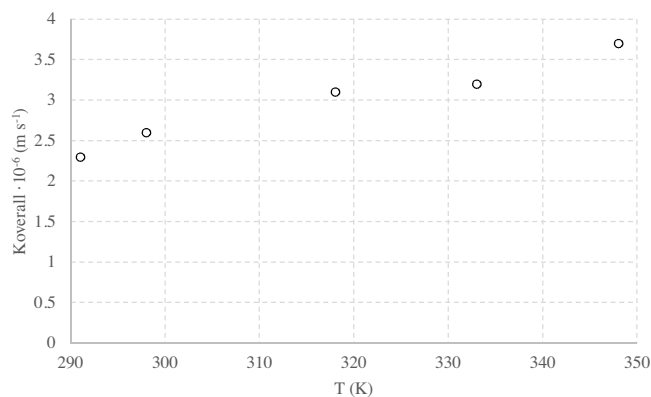


Fig. 5.  $K_{overall}$  values at different temperatures.

Table 4

Contributions to mass transfer. CO<sub>2</sub> absorption with [emim][Ac] in the Ps membrane module.

T (K)	$R_{total} \times 10^{-5}$ (s m <sup>-1</sup> )	$R_g$ (s m <sup>-1</sup> )	$R_m$ (s m <sup>-1</sup> )	$R_l \times 10^{-5}$ (s m <sup>-1</sup> )
291	4.55	23	77	4.5
298	4.03	22	76	4.0
318	3.30	20	72	3.3
333	2.86	18	69	2.9
348	2.34	17	67	2.3

gible vapour pressures, high thermal, electrochemical and chemical stability and loss less regenerative abilities.

The interaction between CO<sub>2</sub> and the ionic liquid may be described by chemisorption as proposed by Gurau et al. (2011) for ILs with anions of remarkable basicity. The crystal structure demonstrated the formation of the imidazolium carboxylate and the role of acetate in complexing acetic acid.

$$R_{total} = R_g + R_m + R_l \quad (3)$$

The resistance in series approach can be used to relate individual mass transfer resistances to the overall mass transfer resistance according to (Eq. (3)). The hollow fiber configuration was selected where the liquid phase flows in the shell side and the gas phase flows through the lumen side. The gas–liquid interface was located on the outer diameter of the tubes. Considering chemical reaction in the liquid side (expressed by the enhancement factor, E) the equation is the following (Eq. (4)) (Ortiz et al., 2010; Luis and Van der Bruggen, 2013).

$$\frac{1}{K_{overall}} = \frac{d_0}{k_g d_i} + \frac{d_0}{k_{mg} d_{lm}} + \frac{1}{k_l H_d E} \quad (4)$$

where  $d_{lm}$  is the log mean diameters (in m) of the hollow fiber,  $H_d$  represents the dimensionless Henry constant and  $k_g$ ,  $k_{mg}$ ,  $k_l$ , are the individual mass transfer coefficients of the gas phase, membrane and liquid phase, respectively (m s<sup>-1</sup>).

The overall mass transfer resistance,  $R_{total}$  is given by the summation of the resistances in the gas ( $R_g$ ), membrane ( $R_m$ ) and liquid ( $R_l$ ) film (Gomez-Coma et al., 2016a,b; Luis et al., 2009; Ortiz et al., 2010). Table 4 shows the calculated resistances, pointing out that the liquid phase produces the main resistance to mass transfer (nearly 100%), in concordance with previous studies (Gomez-Coma et al., 2014; Gomez-Coma et al., 2016b; Ortiz et al., 2010; Luis et al., 2009).

Taking into account that membrane contactors are considered to be the most promising strategy to achieve intensified CO<sub>2</sub> capture by gas–liquid absorption, the intensification effect was also quantified. The intensification factor I is expressed by the volumetric absorption capacity of a membrane contactor divided by the average volumetric absorption capacity of a packed column. This

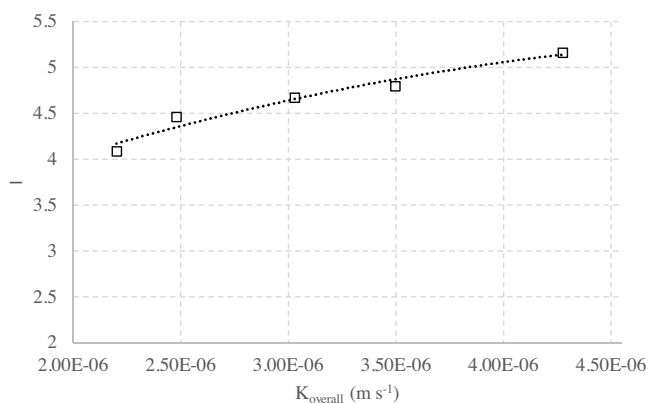


Fig. 6. Intensification factor values at different  $K_{\text{overall}}$  according to Fig. 5.

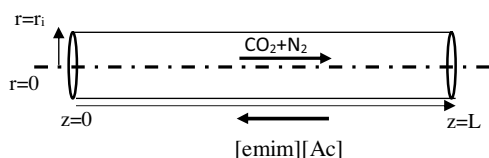


Fig. 7. Coordinates of a fiber in the hollow fiber membrane contactor.

value has a reference value in a classical packed column estimated around  $1 \text{ mol CO}_2 \text{ m}^{-3} \text{ s}^{-1}$ , using MEA 30 wt.% solution as solvent (Bounaceur et al., 2012; Favre, 2011).

Fig. 6 presents the different values of I according to the  $K_{\text{overall}}$  achieved. Values of I upper than 4 were obtained in all the cases. For a value of  $3.73 \times 10^{-6} \text{ m s}^{-1}$  (348 K), an intensification factor of 5.2 was reached. Thus, these values evidence the use of a Ps hollow fiber membrane contactor and the ionic liquid [emim][Ac] as a promising alternative to the conventional  $\text{CO}_2$  capture carried out in packed columns.

### 3.3. Simulation task to estimate mass transfer and operational effects

A numerical analysis was accomplished to study the performance of a polysulfone hollow fiber membrane contactor for the removal of  $\text{CO}_2$  when the [emim][Ac] ionic liquid is used as absorbent. A sensitivity analysis related to the process efficiency was performed to show the influence of the module length and the mass transfer coefficient on the  $\text{CO}_2$  capture efficiency, and to determine the required values for achieving a 90% efficiency as a design target.

The optimal design of a membrane contactor should address the interplay between membrane (mass transfer coefficient), fiber dimensions, and module configuration to achieve target performance in areas, such as maximal process intensification with minimal energy requirements (Zhao et al., 2016).

The modelling of the  $\text{CO}_2$  capture using the Polysulfone hollow fiber membrane module was considered for both wetted and non-wetted operating modes. In a non-wetted operating mode, the carbon dioxide transfers to the liquid phase by diffusion through the pores filled with gas. Otherwise, in a wet operating mode the pores are filled with the liquid (Luis et al., 2007; Luis et al., 2010). The modelling of the  $\text{CO}_2$  transferred from the gas phase to the liquid phase through the membrane barrier was carried out using Aspen Custom Modeler software (Aspen Technology Inc.).

The radial and the axial coordinates of the fiber are presented in Fig. 7. Radial position  $r=0$  is pointed as the center of the fiber and the axial distance of  $z=0$  represents the initial position of the gas in the fiber.

Eq. (5) describes the differential mass balance of  $\text{CO}_2$  in the gas phase in dimensionless form. This equation was based on the following assumptions: a negligible concentration of the soluble gas in the absorption liquid, a steady state and isothermal conditions, no axial diffusion, ideal gas behavior, tube side and shell side constant pressures and the velocity is fully developed in a laminar flow (Luis et al., 2007; Luis et al., 2010; Gomez-Coma et al., 2016b).

$$\frac{Gz}{2} [1 - \bar{r}^2] \frac{\partial \bar{C}_{\text{CO}_2}}{\partial \bar{z}} = \frac{1}{\bar{r}} \frac{\partial}{\partial \bar{r}} \left( \bar{r} \frac{\partial \bar{C}_{\text{CO}_2}}{\partial \bar{r}} \right) \quad (5)$$

The dimensionless variables were defined as:

$$\bar{r} = \frac{r}{R} \quad (6.a)$$

$$\bar{z} = \frac{z}{L} \quad (6.b)$$

$$\bar{C}_{\text{CO}_2} = \frac{C_{\text{CO}_2}}{C_{\text{CO}_2, \text{inlet}}} \quad (6.c)$$

In order to solve the Eq. (5), the boundary conditions used were the following:

$$\bar{r} = 0 \rightarrow \frac{\partial \bar{C}_{\text{CO}_2}}{\partial \bar{r}} = 0 \quad (7.a)$$

$$\bar{r} = 1 \rightarrow \frac{\partial \bar{C}_{\text{CO}_2}}{\partial \bar{r}} = -\frac{Sh}{2} \bar{C}_{\text{CO}_2} \quad (7.b)$$

$$\bar{z} = 0 \rightarrow \bar{C}_{\text{CO}_2} = 1 \quad (7.c)$$

where  $Gz$  and  $Sh$  are the Graetz and Sherwood number respectively (Gomez-Coma et al., 2016b).

Finally the  $\text{CO}_2$  concentration at the outlet of the module is calculated as dimensionless mixing cup (Eq. (8)):

$$\bar{C}_{\text{CO}_2=L} = 4 \int_0^1 \bar{C}_{\text{CO}_2} [1 - \bar{r}^2] \bar{r} d\bar{r} \quad (8)$$

The modelling results using a gas flow rate of  $70 \text{ mL min}^{-1}$  and the different parameters of the Ps hollow fiber membrane contactor (specified in Table 1) were shown in Fig. 8. Different nodes in the radial dimension are shown in these figures, from the center of the fiber ( $r=0$ ) to the membrane layer ( $r=1$ ). In the present study, there is non-wetted model because of the fact that ionic liquid presents hydrophilicity. However, the two different scenarios (non-wetted and wetted) have been shown in order to explain the nodes behavior in both cases and to quantify the possible effect of wetting on the process efficiency.

Fig. 8a and b is focused on a non-wetted operating mode. In this operating model there is not axial diffusion thus all nodes concur. In order to show the differences when wetted mode occurs, Fig. 8c and d was presented. In this last case, there is axial diffusion and therefore the nodes were differentiated. Fig. 8a and c shows the dimensionless carbon dioxide concentration along the dimensionless length. On the other hand, Fig. 8b and d uses the same abscissa but in this case, what is represented is the efficiency (%). Under the operating conditions covered in this study, the process efficiency decreased a 20% if the pores of the membrane get wet, respect to a non-wetted mode. Note that both Fig. 8b and d appears with the  $\text{CO}_2$  efficiency calculated based on the dimensionless mixing cup (Eq. (8)).

An analysis of the set of conditions to be fulfilled in terms of membrane material (i.e. mass transfer coefficient), fiber dimensions and module packing, in order to ensure a significant intensification effect, is an objective that should be considered to offer an evaluation of the interest and limitations of the different membrane materials, fibers and modules which are reported for this application.

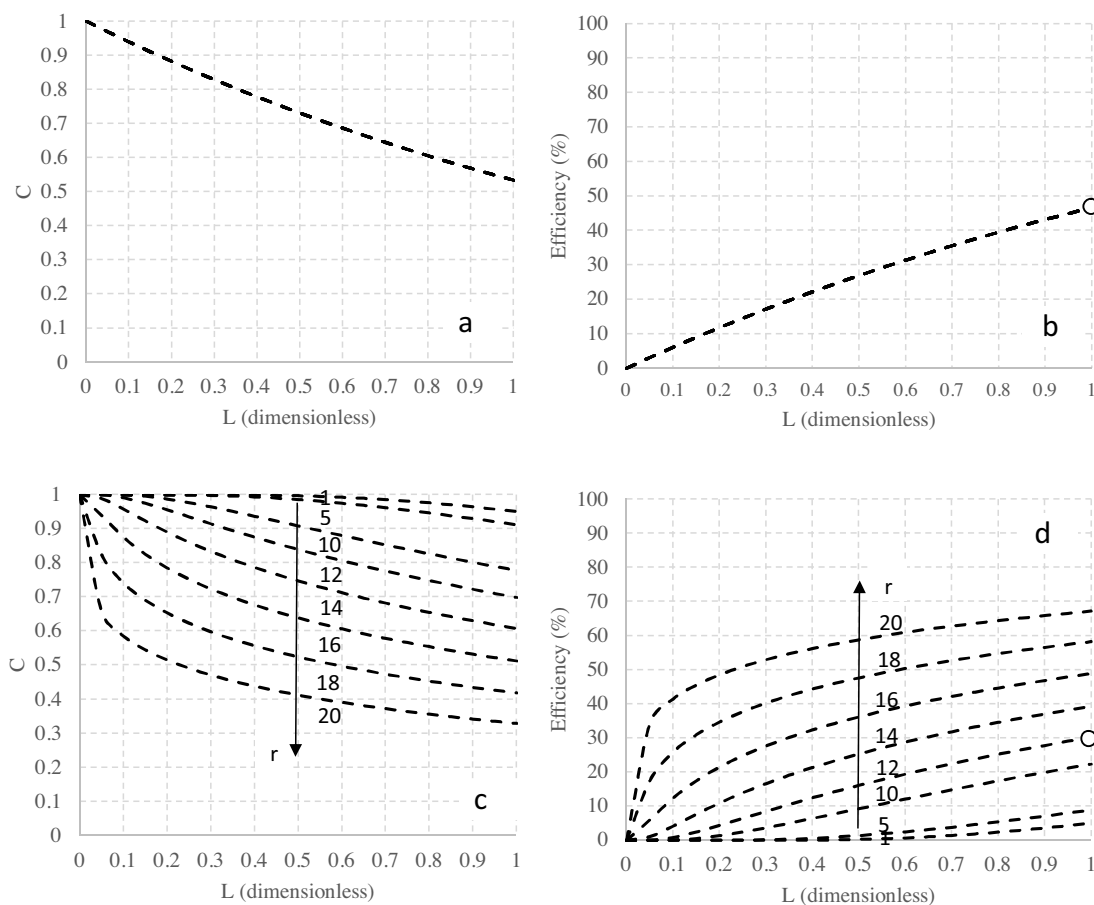


**Fig. 8.** Modelling results: profiles of dimensionless CO<sub>2</sub> outlet concentration (a and c) and process efficiency (%) (b and d) in non-wetted model and wetted model along the fiber length. Node 1:  $r = 0$ ; Node 20:  $r = 1$ .

In order to estimate the mass transfer effect on the CO<sub>2</sub> capture efficiency, a sensitivity analysis was performed. As previous works, a value of 90% efficiency was pointed as design target (Yeon et al., 2005; Paul et al., 2007; Zhang et al., 2008; Favre, 2011; Wang et al., 2013). On this basis, the aim of this simulation is to obtain the parameters required to reach this efficiency, in order to provide a cleaner process without solvent losses, non-toxic and lower equipment. Please note that the ILs are non-volatile, the [emim][Ac] is non-toxic (Alvarez-Guerra and Irabien, 2011) and hollow fiber membrane contactors have high specific surface area per unit volume.

Fig. 9 modifies the overall mass transfer coefficient,  $K_{\text{overall}}$ , from a reference value of  $2.4 \times 10^{-6} \text{ m s}^{-1}$  (291 K), that can be required to obtain high efficiencies. As it can be seen from Fig. 9a, values upper than  $9.0 \times 10^{-6} \text{ m s}^{-1}$  reached efficiency values higher than 90%.

Moreover, a more detailed analysis was carried out in Fig. 9b. The dimensionless Sherwood number was analyzed. Maintaining a fixed dimensionless Graetz number with a value of  $6.6 \times 10^{-4}$  when the Sherwood number takes values higher than  $4 \times 10^{-4}$  the design target is accomplished.

Taking into account the option to implement a multi-stage network of membrane modules for a high efficiency objective, the fiber length was also modified in order to estimate the number of hollow fiber membrane contactors necessary to connect in series to achieve a CO<sub>2</sub> capture efficiencies, upper 90%. Fig. 10a shows the influence of fiber length. Four Ps hollow fiber membrane contactors will be necessary to couple in series to reach a CO<sub>2</sub> free gas flow. In this sense, this work proposes a post-combustion process based

on a set of four Ps membrane modules in series (total length 1.4 m) and a number of these sets in parallel that can be estimated from the basis of flue gas flow rate required (Hoff and Svendsen, 2013). Furthermore, keeping fixed the dimensionless Sherwood number, the Graetz number was varied (Fig. 10b). Graetz values smaller than  $2.53 \times 10^{-4}$  provide efficiencies higher than 90%.

The number of hollow fiber membrane contactors required to connect in series were compared with previous data reported in the literature (Gomez-Coma et al., 2014). Fig. 11 shows the different quantity of membrane contactors needed to achieve the design target (90% efficiency). Ps hollow fiber membrane contactor requires fewer modules in series than using PP modules, which leads to a significant saving in size equipment to achieve high efficiencies.

Further work on membrane contactors should be aimed at optimizing membrane geometry and module design, which is essential for successful scale-up. Operating in more turbulent flow conditions produces greater mass transfer. However, the shorter residence time that results from a greater solvent flow results in lower solvent loadings. At an industrial scale this must be compensated by multiple passes through membrane modules in series, to ensure that a full solvent loading is achieved. The estimation of capture costs should take into account some target values, such as the DOE's goal in 2025 of \$40/t CO<sub>2</sub>.

#### 4. Conclusions

Carbon dioxide capture in a polysulfone (Ps) parallel-flow membrane contactor when the ionic liquid 1-ethyl-3-methylimidazolium acetate [emim][Ac] is used as the absorption

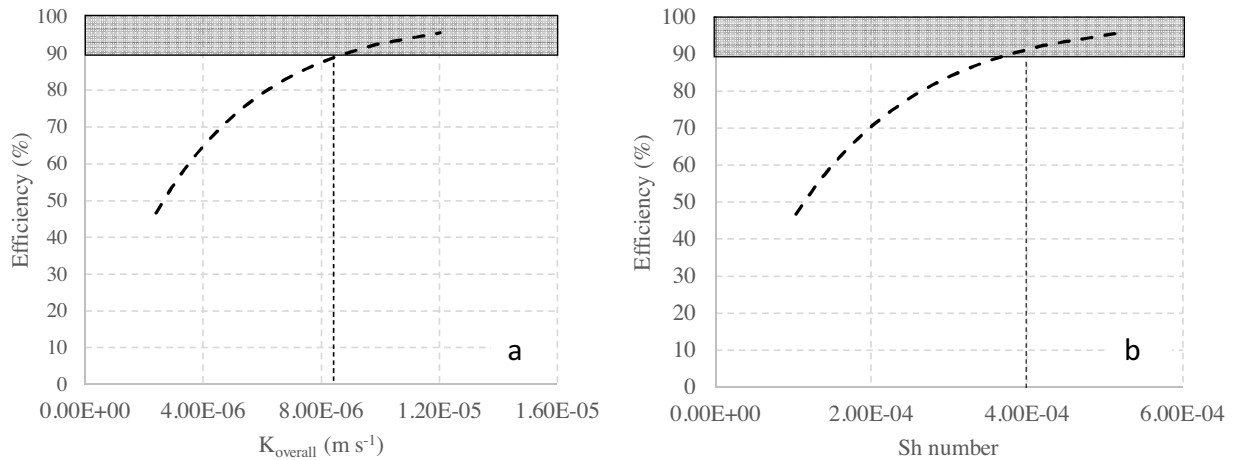


Fig. 9. Sensitivity analysis of overall mass transfer coefficient,  $K_{\text{overall}}$  (a), and the corresponding Sherwood number (b).

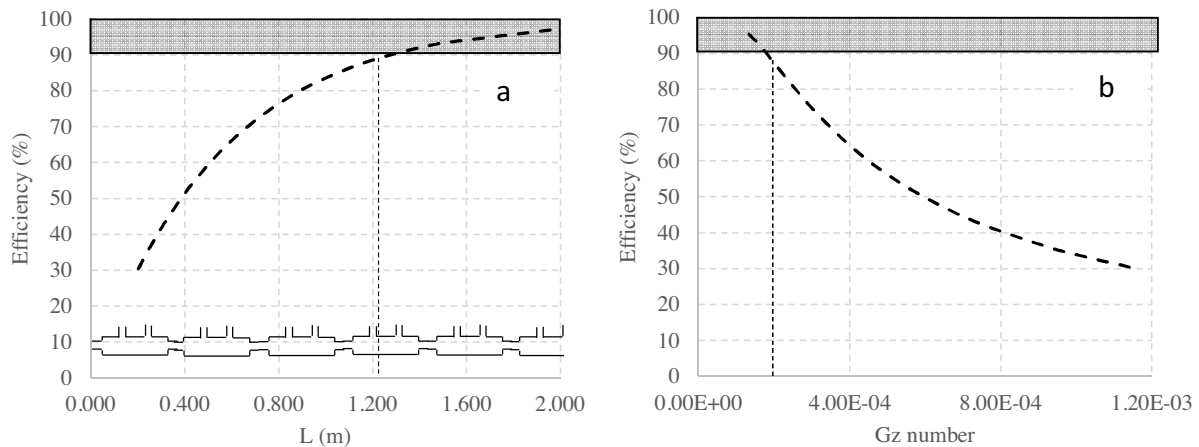


Fig. 10. Sensitivity analysis of length module, L (a), and the corresponding Graetz number (b).

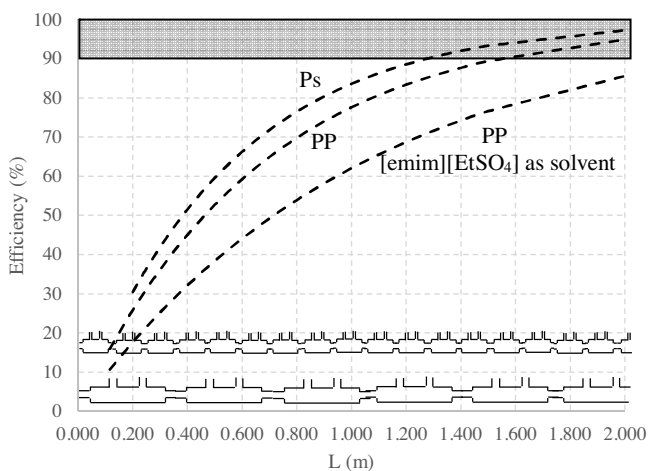


Fig. 11. Quantity of hollow fiber membrane contactors required to achieve 90% efficiency for different materials and solvents.

liquid has been studied by means of efficiency and overall mass transfer coefficient,  $K_{\text{overall}}$ . Taking into account that thermal stability of the Ps polymer, that allows its use for the CO<sub>2</sub> absorption from

flue gases, often emitted at moderate temperatures, the influence of the temperature has been quantified.

An efficiency of 45% has been achieved when the temperature rises to 348 K. On the other hand, working at 318 K the efficiency is higher than with other materials such as polypropylene (PP) comparing the same effective area and the same solvent.

The overall mass transfer coefficient takes values between  $2.4 \times 10^{-6}$  and  $3.7 \times 10^{-6} \text{ m s}^{-1}$  in the range of temperature from 291 to 348 K, which are competitive with other values reported in previous literature. The absorption rate does not increase as expected for a chemical reaction. This is because of the fact that temperature favors the CO<sub>2</sub> capture but impacts on other factors such as solubility, viscosity and diffusivity.

Finally, a theoretical simulation using a base case was carried out. Taking into account a target value of 90% CO<sub>2</sub> capture, (i) the mass transfer coefficient should be higher than  $9.0 \times 10^{-6} \text{ m s}^{-1}$ , or (ii) four Ps hollow fiber membrane modules disposed in series were necessary (corresponding to a total length 1.4 m), being proposed for the scaling-up a network of modules in series and as many in parallel as the flue gas flow rate increases. In addition, a comparative with other materials has been performed. Polysulfone hollow fiber contactor results much more competitive than PP hollow fiber membrane contactor to achieve 90% efficiency. This fact and the thermal stability of the Ps polymer, which is impor-

tant of the long-term use, support the selection of the polysulfone membrane contactor for the CO<sub>2</sub> capture.

Further work on membrane contactors should be aimed at optimizing membrane geometry and module design, which is essential for successful scale-up. The new IL-based absorbents coupled with smart design of the membrane processes and development of more compatible membrane materials offer a competitive alternative to the conventional packed column design.

## Acknowledgement

This research has been funded by the Spanish Ministry Economy and Competitiveness (Project CTQ2013-48280-C3-1-R).

## References

- Ahn, H., Kim, J., Kim, J.H., 2013. Low-temperature vacuum stripping of CO<sub>2</sub> from aqueous amine solutions using thin-film silicalite-filled PDMS composite membranes. *Int. J. Greenh. Gas Control* 18, 165–172.
- Albo, J., Irabien, A., 2012. Non-dispersive absorption of CO<sub>2</sub> in parallel and cross-flow membrane modules using EMISE. *J. Chem. Technol. Biotechnol.* 87, 1502–1507.
- Albo, J., Luis, P., Irabien, A., 2010. Carbon dioxide capture from flue gases using a cross-flow membrane contactor and the ionic liquid 1-ethyl-3-methylimidazolium ethylsulfate. *Ind. Eng. Chem. Res.* 49, 11045–11051.
- Albo, J., Luis, P., Irabien, A., 2011. Absorption of coal combustion flue gases in ionic liquids using different membrane contactors. *Desalin. Water Treat.* 27 (1–3), 54–59.
- Alvarez-Guerra, M., Irabien, A., 2011. Document design of ionic liquids: an ecotoxicity (*Vibrio fischeri*) discrimination approach. *Green Chem.* 13 (6), 1507–1516.
- Boot-Handford, M.E., Abanades, J.C., Anthony, J.E., Blunt, M.J., Brandani, S., Dowell, N.M., Fernández, J.R., Ferrarri, M.C., Gross, R., Hallett, J.P., Haszeldine, R.S., Heptonstall, P., Lyngfelt, A., Makuch, Z., Mangano, E., Porter, R.T.J., Pourkashanian, M., Rochelle, G.T., Shah, N., Yao, J.G., Fennell, P.S., 2014. Carbon capture and storage update. *Energy Environ. Sci.* 7, 130–189.
- Boributh, S., Jiratananon, R., Li, K., 2013. Analytical solutions for membrane wetting calculations based on log-normal and normal distribution functions for CO<sub>2</sub> absorption by a hollow fiber membrane contactor. *J. Membr. Sci.* 429, 459–472.
- Bounaceur, R., Castel, C., Rode, S., Roizard, D., Favre, E., 2012. Membrane contactors for intensified post combustion carbon dioxide capture by gas-liquid absorption in MEA: a parametric study. *Chem. Eng. Res. Des.* 90 (12), 2325–2337.
- Casado-Coterillo, C., Soto, J., Jimare, M.T., Valencia, S., Corma, S., Tellez, C., Coronas, J., 2012. Preparation and characterization of ITQ-29/polysulfone mixed-matrix membranes for gas separation: effect of zeolite composition and crystal size. *Chem. Eng. Sci.* 73, 116–122.
- Chen, Y., Sun, X., Yan, C., Cao, Y., Mu, T., 2014. The dynamic process of atmospheric water sorption in [EMIM][Ac] and mixtures of [EMIM][Ac] with biopolymers and CO<sub>2</sub> capture in these systems. *J. Phys. Chem. B* 118 (39), 11523–11536.
- Dai, Z., Noble, R.D., Gin, D.L., Zhang, X., Deng, L., 2016. Combination of ionic liquids with membrane technology: a new approach for CO<sub>2</sub> separation. *J. Membr. Sci.* 497, 1–20.
- Favre, E., 2011. Membrane processes and postcombustion carbon dioxide capture: challenges and prospects. *Chem. Eng. J.* 171, 782–793.
- Fernández-Barquín, A., Casado-Coterillo, C., Palomino, M., Valencia, S., Irabien, A., 2015. LTA/poly(1-trimethylsilyl-1-propyne) mixed-matrix membranes for high-temperature CO<sub>2</sub>/N<sub>2</sub> separation. *Chem. Eng. Technol.* 38 (4), 658–666.
- Fernández-Barquín, A., Casado-Coterillo, C., Palomino, M., Valencia, S., Irabien, A., 2016. Permselectivity improvement in membranes for CO<sub>2</sub>/N<sub>2</sub> separation. *Sep. Purif. Technol.* 157, 102–111.
- Freire, M.G., Teles, A.R.R., Rocha, M.A.A., Schröder, B., Neves, C.M.S.S., Carvalho, P.J., Evtuguin, D.V., Santos, L.M.N.B.F., Coutinho, J.A.P., 2011. Thermophysical characterization of ionic liquids able to dissolve biomass. *J. Chem. Eng. Data* 56, 4813–4822.
- Gomez-Coma, L., Garea, A., Irabien, A., 2014. Non-dispersive absorption of CO<sub>2</sub> in [emim][EtSO<sub>4</sub>] and [emim][Ac]: temperature influence. *Sep. Purif. Technol.* 132, 120–125.
- Gomez-Coma, L., Garea, A., Rouch, J.C., Savart, T., Lahitte, J.F., Remigy, J.C., Irabien, A., 2016a. Membrane modules for CO<sub>2</sub> capture based on PVDF hollow fibers with ionic liquids immobilized. *J. Membr. Sci.* 498, 218–226.
- Gomez-Coma, L., Garea, A., Irabien, A., 2016b. PVDF membrane contactor for CO<sub>2</sub> capture using the ionic liquid [emim][ac]: mass transfer analysis. *Chem. Eng. Technol.* (submitted for publication).
- Gurau, G., Rodriguez, H., Kelley, S.P., Janiczek, P., Kalb, R.S., Rogers, R.D., 2011. Demonstration of chemisorption of carbon dioxide in 1,3-dialkylimidazolium acetate ionic liquids. *Angew. Chem. Int. Ed.* 50, 12024–12026.
- Hoff, K.A., Svendsen, H.F., 2013. CO<sub>2</sub> absorption with membrane contactors vs. packed absorbers—challenges and opportunities in post combustion capture and natural gas sweetening. *Energy Procedia* 37, 952–960.
- Korminouri, F., Rahbari-Sisakht, M., Rana, D., Matsuura, T., Ismail, A.F., 2014. Study on the effect of air-gap length on properties and performance of surface modified PVDF hollow fiber membrane contactor for carbon dioxide absorption. *Sep. Purif. Technol.* 132, 601–609.
- Korminouri, F., Rahbari-Sisakht, M., Matsuura, T., Ismail, A.F., 2015. Surface modification of polysulfone hollow fiber membrane spun under different air-gap lengths for carbon dioxide absorption in membrane contactor system. *Chem. Eng. J.* 264, 453–461.
- Li, J.L., Chen, B.H., 2005. Review of CO<sub>2</sub> absorption using chemical solvents in hollow fiber membrane contactors. *Sep. Purif. Technol.* 41, 109–122.
- Low, B.T., Zhao, L., Merkel, T.C., Weber, M., Stolten, D., 2013. A parametric study of the impact of membrane materials and process operating conditions on carbon capture from humidified flue gas. *J. Membr. Sci.* 431, 139–155.
- Luis, P., Van der Bruggen, B., 2013. The role of membranes in post-combustion CO<sub>2</sub> capture. *Greenh. Gas. Sci Technol.* 3, 1–20.
- Luis, P., Ortiz, I., Aldaco, R., Garea, A., Irabien, A., 2007. Recovery of sulfur dioxide using non-dispersive absorption. *Int. J. Chem. React. Eng.* 5, 1–9.
- Luis, P., Garea, A., Irabien, A., 2009. Zero solvent emission process for sulfur dioxide recovery using a membrane contactor and ionic liquids. *J. Membr. Sci.* 330, 80–89.
- Luis, P., Garea, A., Irabien, A., 2010. Modelling of a hollow fibre ceramic contactor for SO<sub>2</sub> absorption. *Sep. Purif. Technol.* 72, 174–179.
- Luis, P., Van Gerven, T., Van Der Bruggen, B., 2012. Recent developments in membrane-based technologies for CO<sub>2</sub> capture. *Prog. Energy Combust. Sci.* 38, 419–448.
- Mansourizadeh, A., Ismail, A.F., 2010. Effect of additives on the structure and performance of polysulfone hollow fiber membranes for CO<sub>2</sub> absorption. *J. Membr. Sci.* 348, 260–267.
- Mansourizadeh, A., Ismail, A.F., 2011. A developed asymmetric PVDF hollow fiber membrane structure for CO<sub>2</sub> absorption. *Int. J. Greenh. Gas Control* 5, 374–380.
- Mansourizadeh, A., Aslmahdavi, Z., Ismail, A.F., Matsuura, T., 2014. Blend polyvinylidene fluoride/surface modifying macromolecule hollow fiber membrane contactors for CO<sub>2</sub> absorption. *Int. J. Greenh. Gas Control* 26, 83–92.
- Mehdipour, M., Keshavarz, P., Seraji, A., Masoumi, S., 2014. Performance analysis of ammonia solution for CO<sub>2</sub> capture using microporous membrane contactors. *Int. J. Greenh. Gas Control* 31, 16–24.
- Merkel, T.C., Lin, H., Wei, X., Baker, R., 2010. Power plant post-combustion carbon dioxide capture: an opportunity for membranes. *J. Membr. Sci.* 359, 126–139.
- Nabian, N., Ghoreyshi, A.A., Rahimpour, A., Shakeri, M., 2015. Performance evaluation and mass transfer study of CO<sub>2</sub> absorption in flat sheet membrane contactor using novel porous polysulfone membrane. *Korean J. Chem. Eng.* 32 (11), 2204–2211.
- Ortiz, A., Gorri, D., Irabien, A., Ortiz, I., 2010. Separation of propylene/propane mixtures using Ag<sup>+</sup>-RTIL solutions. Evaluation and comparison of the performance of gas-liquid contactors. *J. Membr. Sci.* 360, 130–141.
- Papatryfon, X.L., Heliopoulos, N.S., Molchan, I.S., Zubeir, L.F., Bezemer, N.D., Arfanis, M.K., Kontos, A.G., Likodimos, V., Iliev, B., Romanos, G.E., Falaras, P., Stamatakis, K., Beltsios, K.G., Kroon, M.C., Thompson, G.E., Klöckner, J., Schubert, T.J.S., 2014. CO<sub>2</sub> capture efficiency, corrosion properties, and ecotoxicity evaluation of amine solutions involving newly synthesized ionic liquids. *Ind. Eng. Chem. Res.* 53 (30), 12083–12102.
- Paul, S., Ghoshal, A.K., Mandal, B., 2007. Removal of CO<sub>2</sub> by single and blended aqueous alkanolamine solvents in hollow-fiber membrane contactor: modeling and simulation. *Ind. Eng. Chem. Res.* 46, 2576–2588.
- Pinto, A.M., Rodriguez, H., Arce, A., Soto, A., 2014. Combined physical and chemical absorption of carbon dioxide in a mixture of ionic liquids. *J. Chem. Thermodyn.* 77, 197–205.
- Rahbari-Sisakht, M., Ismail, A.F., Rana, D., Matsuura, T., Emadzadeh, D., 2013a. Carbon dioxide stripping from water through porous polysulfone hollow fiber membrane contactor. *Sep. Purif. Technol.* 108, 119–123.
- Rahbari-Sisakht, M., Ismail, A.F., Rana, D., Matsuura, T., Emadzadeh, D., 2013b. Effect of SMM concentration on morphology and performance of surface modified PVDF hollow fiber membrane contactor for CO<sub>2</sub> absorption. *Sep. Purif. Technol.* 116, 67–72.
- Ramdin, M., De Loos, T.W., Vlucht, T.J.H., 2012. State-of-the-art of CO<sub>2</sub> capture with ionic liquids. *Ind. Eng. Chem. Res.* 51, 8149–8177.
- Rao, A.B., Rubin, E.S., 2002. A technical, economic, and environmental assessment of amine-based CO<sub>2</sub> capture technology for power plant greenhouse gas control. *Environ. Sci. Technol.* 36, 4467–4475.
- Reza Razavi, M., Javad Razavi, M., Miri, T., Shirazi, S., 2013. CFD simulation of CO<sub>2</sub> capture from gas mixtures in nanoporous membranes by solution of 2-amino-2-methyl-1-propanol and piperazine. *Int. J. Greenh. Gas Control* 15, 142–149.
- Saeed, M., Deng, L., 2015. CO<sub>2</sub> facilitated transport membrane promoted by mimic enzyme. *J. Membr. Sci.* 494, 196–204.
- Santos, E., Albo, J., Irabien, A., 2014. Acetate based supported ionic liquid membranes (SILMs) for CO<sub>2</sub> separation: influence of the temperature. *J. Membr. Sci.* 452, 277–283.
- Scholes, C.A., Chen, G.Q., Stevens, G.W., Kentish, S.E., 2010. Plasticization of ultra-thin polysulfone membranes by carbon dioxide. *J. Membr. Sci.* 346, 208–214.

- Scholes, C.A., Kentish, S.E., Stevens, G.W., deMontigny, D., 2015. Comparison of thin film composite and microporous membrane contactors for CO<sub>2</sub> absorption into monoethanolamine. *Int. J. Greenh. Gas Control* 42, 66–74.
- Wang, L., Zhang, Z., Zhao, B., Zhang, H., Lu, X., Yang, Q., 2013. Effect of long-term operation on the performance of polypropylene and polyvinylidene fluoride membrane contactors for CO<sub>2</sub> absorption. *Sep. Purif. Technol.* 116, 300–306.
- Wang, X., Chen, H., Zhang, L., Yu, R., Qu, R., Yang, L., 2014. Effects of coexistent gaseous components and fine particles in the flue gas on CO<sub>2</sub> separation by flat-sheet polysulfone membranes. *J. Membr. Sci.* 470, 237–245.
- Yeon, S.H., Lee, K.S., Sea, B., Park, Y.I., Le, K.H., 2005. Application of pilot-scale membrane contactor hybrid system for removal of carbon dioxide from flue gas. *J. Membr. Sci.* 257, 156–160.
- Zhang, H.Y., Wang, R., Liang, D.T., Tay, J.H., 2008. Theoretical and experimental studies of membrane wetting in the membrane gas–liquid contacting process for CO<sub>2</sub> absorption. *J. Membr. Sci.* 308, 162–170.
- Zhang, L., Qu, R., Sha, Y., Wang, X., Yang, L., 2015. Membrane gas absorption for CO<sub>2</sub> capture from flue gas containing fine particles and gaseous contaminants. *Int. J. Greenh. Gas Control* 33, 10–17.
- Zhao, S., Feron, P.H.M., Deng, L., Favre, E., Chabanon, E., Yan, S., Hou, J., Chen, V., Qi, H., 2016. Status and progress of membrane contactors in post-combustion carbon capture: a state-of-the-art review of new developments. *J. Membr. Sci.* 511, 180–206.



**4.4. Gómez-Coma L., Garea A., Irabien A., Hybrid solvent ([emim][Ac]+water) to improve the CO<sub>2</sub> capture efficiency in a PVDF hollow fiber contactor. ACS Sustain. Chem. Eng. 2016. Accepted paper.**

Resumen

Los procesos de post-combustión a base de líquidos iónicos y contactores de membrana han surgido como una prometedora alternativa a los sistemas tradicionales en los últimos años. En este trabajo, se ha realizado una absorción no dispersiva a través de un contactor de membrana de fibras huecas de fluoruro de polivinilideno (PVDF) para la captura de CO<sub>2</sub>. El líquido iónico objeto de estudio ha sido el 1-etil-3-metilimidazolio acetato [emim][Ac]. Este IL ha sido elegido debido a su reacción química con el CO<sub>2</sub>.

Diferentes cantidades de agua destilada se han añadido al [emim][Ac] con el fin de resolver los problemas asociados con la viscosidad del líquido iónico. La presencia de agua también puede modificar la interacción con el CO<sub>2</sub>. El propósito de crear el disolvente híbrido formado por agua y el líquido iónico de base acetato y por ello conduce a la formación de carboxilato, reversible en su interacción con el CO<sub>2</sub>, es lograr eficiencias competitivas con los procesos tradicionales y que utilizan alcanolaminas. Cuando se usa un solvente formado por 30% (en volumen) de agua se logra el mejor resultado. Esta mezcla logra un  $K_{overall}$  5 veces mayor que cuando se usa sólo el líquido iónico. Usando un 30% de agua se logra una eficacia de 72.5% y un coeficiente global de transferencia de materia ( $K_{overall}$ ) de  $9.34 \cdot 10^{-5} \text{ m s}^{-1}$ . Los resultados de la simulación y análisis de sensibilidad indicaron que se necesitan sólo dos contactores de membrana de fibra hueca (0.6 m de longitud total; instalación escala laboratorio) o un valor de  $K_{overall}$  de  $1.70 \cdot 10^{-4} \text{ m s}^{-1}$  con el fin de alcanzar una eficacia del 90%. La adición de agua al líquido iónico muestra las ventajas de usar un disolvente híbrido en un proceso de intensificación.

Original abstract

Post-combustion processes based on membrane contactors and ionic liquids have emerged in recent years as an alternative to traditional systems used to capture CO<sub>2</sub>. In this work, non-dispersive absorption in a polyvinylidene fluoride (PVDF) hollow fibre membrane contactor was used as CO<sub>2</sub> capture system. The ionic liquid (IL) 1-ethyl-3-methylimidazolium acetate ([emim][Ac]) was chosen for the study due to its chemical reaction with CO<sub>2</sub>.

Different amounts of distilled water were added to [emim][Ac] to address the issues associated with the viscosity of the ionic liquid. The presence of water may also facilitate the binding of CO<sub>2</sub>. The purpose of this combined sorbent containing water and an ionic liquid comprising a carboxylate moiety such as acetate, which provides reversible chemical interaction

with CO<sub>2</sub>, was to achieve competitive efficiencies with traditional processes based on power stations and alkanolamines. The best combination of water-IL was found to be, 70% [emim][Ac] - 30%(vol) water. This mixture achieved a,  $K_{\text{overall}}$  coefficient 5 times higher than that obtained with only the IL. By using 30% (vol) water, a CO<sub>2</sub> capture efficiency of 72.5% and an overall mass transfer coefficient ( $K_{\text{overall}}$ ) of  $9.34 \cdot 10^{-5} \text{ m s}^{-1}$  were accomplished. The values of  $K_{\text{overall}}$  achieved in the present work lead to the conclusion that the hybrid solvent is clearly competitive with traditional alkanolamine solvents. The simulation results of sensitivity analysis showed that only two hollow fibre membrane contactors (total length 0.6 m) or a  $K_{\text{overall}}$  of  $1.70 \cdot 10^{-4} \text{ m s}^{-1}$  were required to reach an efficiency of 90%. The addition of water to the ionic liquid allows the hybrid solvent to be used in an intensified process.

## **HYBRID SOLVENT ([EMIM][AC]+WATER) TO IMPROVE THE CO<sub>2</sub> CAPTURE EFFICIENCY IN A PVDF HOLLOW FIBRE CONTACTOR**

L. Gomez-Coma\*, A. Garea, A. Irabien

<sup>1</sup> Universidad de Cantabria, Chemical and Biomolecular Engineering Department, E.T.S. de Ingenieros Industriales y Telecomunicación, Universidad de Cantabria, Avda Los Castros s/n 39005 Santander, Spain

\*Corresponding author: Tel: +34 942 206777, Fax: +34 942 201591

email: gomezcomal@unican.es

### **Abstract**

Post-combustion processes based on membrane contactors and ionic liquids have emerged in recent years as an alternative to traditional systems used to capture CO<sub>2</sub>. In this work, non-dispersive absorption in a polyvinylidene fluoride (PVDF) hollow fibre membrane contactor was used as CO<sub>2</sub> capture system. The ionic liquid (IL) 1-ethyl-3-methylimidazolium acetate ([emim][Ac]) was chosen for the study due to its chemical reaction with CO<sub>2</sub>.

Different amounts of distilled water were added to [emim][Ac] to address the issues associated with the viscosity of the ionic liquid. The presence of water may also facilitate the binding of CO<sub>2</sub>. The purpose of this combined sorbent containing water and an ionic liquid comprising a carboxylate moiety such as acetate, which provides reversible chemical interaction with CO<sub>2</sub>, was to achieve competitive efficiencies with traditional processes based on power stations and alkanolamines. The best combination of water-IL was found to be, 70% [emim][Ac] - 30% (vol) water. This mixture achieved a,  $K_{overall}$  coefficient 5 times higher than that obtained with only the IL. By using 30% (vol) water, a CO<sub>2</sub> capture efficiency of 72.5% and an overall mass transfer coefficient ( $K_{overall}$ ) of  $9.34 \cdot 10^{-5} \text{ m s}^{-1}$  were accomplished. The values of  $K_{overall}$  achieved in the present work lead to the conclusion that the hybrid solvent is clearly competitive with traditional alkanolamine solvents. The simulation results of sensitivity analysis showed that only two hollow fibre membrane contactors (total length 0.6 m) or a  $K_{overall}$  of  $1.70 \cdot 10^{-4} \text{ m s}^{-1}$  were required to reach an efficiency of 90%. The addition of water to the ionic liquid allows the hybrid solvent to be used in an intensified process.

**Keywords:** Carbon dioxide capture, ionic liquids (ILs), membrane contactors, PVDF, water, hybrid solvents.

### *1. Introduction*

The removal of acid gases like carbon dioxide is currently an essential part of various industrial processes. The excessive emission of CO<sub>2</sub> results in dramatic increases in global atmospheric temperature, which have drawn increasing attention [1]. Since 2010, the atmospheric CO<sub>2</sub> concentration has maintained a high level, over 390 ppm, which has become an urgent environmental issue [2]. In response the fifth Intergovernmental Panel on Climate Change (IPCC) report said that global CO<sub>2</sub> emissions must be cut by 50–80% by 2050 to avoid the serious damage that climate change could cause [3].

One step towards reducing CO<sub>2</sub> emissions is to capture the CO<sub>2</sub> generated during combustion and to store it in a suitable place. Carbon capture and sequestration (CCS) technology is of particular importance in reducing the anthropogenic CO<sub>2</sub> emissions [4]. CCS has the potential to reduce future world emissions from energy generation by 20%, and carbon dioxide valorization

is under development [5]. CO<sub>2</sub> is the primary greenhouse gas emitted through human activities such as the composition of fossil fuels for energy, transportation and industrial processes [6]. Approximately 30% of CO<sub>2</sub> emissions come from fossil fuel power plants, and coal is the lowest cost fuel used to produce electric power in comparison with oil and gas. Predictions indicate that fossil fuels will be the dominant energy source in the coming decades, and the amount of energy demand will increase further by 53% by 2030 [7-8]. Capture is the most expensive step of the capture storage chain [9]. Despite this, it is gaining attention among researchers and policymakers as a short-midterm solution to contain carbon emissions from existing or future fossil fuelled power plants [10]. Three main methods have received an increasing amount of attention during the past decades: pre-combustion, post-combustion and oxy-combustion [11].

This work is focused on the post-combustion capture method, which can be considered a technical and economic challenge in itself due to the low concentration and pressure of CO<sub>2</sub> in the gas stream and the lack of value of the recovered compound [12]. In a typical post-combustion capture process, treated flue gas is passed through a chemical absorption column where a solvent takes up the carbon dioxide. The CO<sub>2</sub>-rich solvent is regenerated by heating in a stripper unit. The CO<sub>2</sub> is then compressed. The most commonly used industrial solvents are divided into physical and chemical solvents. Physical solvents depend on the physical solubility of the acid gas in the solvent. Chemical solvents involve a chemical reaction between the absorbent and the dissolved acid gas [13].

The main disadvantage in typical capture processes is the low concentration of CO<sub>2</sub> in power-plant flue gas, approximately 15%. This means that a large volume of gas has to be handled, which requires large equipment and results in high capital costs. Traditional solvents such as monoethanolamine (MEA) have been used for CO<sub>2</sub> capture, achieving an outlet stream with a very low CO<sub>2</sub> concentration [14]. However, the cost of absorption/desorption processes based on aqueous alkanolamines is high because of the higher heat duty requirements for the absorbent regeneration [15]. Previous work predicts that an amine system used to capture approximately 90% of the carbon dioxide in flue gas requires approximately 30% of the total power produced by the plant and results in a CO<sub>2</sub> capture cost of \$40–100/tonne of CO<sub>2</sub> [16]. A study of technical performance and cost estimation are required to select optimal operating conditions [16]. Research is underway on some emerging capture technologies such as membranes, ionic liquids and metal organic frameworks (MOFs) with the aim of reducing capture energy consumption and capital investment [17]. The estimation of capture costs should take into account some restrictions, such as the DOE's goal in 2025 of \$40/tonne of CO<sub>2</sub>. Recent works have focused efforts on developing materials and new, techniques and technologies to achieve a carbon capture and sequestration method where in the levelized cost of energy will not be increased by more than 35% [18-19]. To achieve this goal is very difficult because flue gas is hot, dilute in CO<sub>2</sub> content, near atmospheric pressure, high in volume, and often contaminated with other impurities such as O<sub>2</sub>, SO<sub>x</sub>, NO<sub>x</sub>, and ash [19].

Ionic liquids (ILs), have been proposed as alternatives to the conventional volatile, corrosive, and degradation sensitive solvents [20]. ILs are salts that have a melting point lower than 373 K and a negligible vapour pressure, are environmentally benign, have high CO<sub>2</sub> solubility and are recyclable [21, 22].

Previous work has suggested that the CO<sub>2</sub> absorption rate and capacity of ILs are not as high as those of conventional amine solvents. However, this work noted that the practical application of ILs as efficient CO<sub>2</sub> solvents may be feasible by either using high pressure in the scrubbing columns to enhance the absorption capacity or mixing with water to decrease the viscosity and increase the absorption rate [23]. In particular, previous work has noted the mixtures of acetate based ILs with water are promising absorbents for carbon dioxide capture [24]. Moreover, recent developments have shown that ILs can be mixed with water, amines, or other organic compounds to improve the CO<sub>2</sub> separation [25]. Some problems associated with amine based solvents, have to be addressed, such as the volatilization and contamination of the gas phase,

degradation, and regeneration costs. On other hand, water is a cheap solvent that is suitable to reduce the viscosity of the ionic liquid and can be included as a polar co-solvent for improving the CO<sub>2</sub> capture efficiency.

A promising alternative to common amine processes is the chemisorption of carbon dioxide in ILs containing a carboxylic anion [26]. It is of vital importance to choose an ionic liquid with low volatility, low degradability, low corrosivity, high reaction rates with CO<sub>2</sub> and high loading [27]. In spite of the attractive tuneable properties of ionic liquids, their high viscosities and relatively high cost are two significant challenges to their application on the industrial scale. Therefore, to integrate ILs into existing industrial processes, the combination of ILs with one or more non-IL components may be of interest to produce an optimal, IL-based hybrid solution amenable for use within an existing process such as carbon dioxide capture. This approach may be more efficient than to design and synthesize new ILs with the desired properties.

Evidence of a chemical reaction between CO<sub>2</sub> and the liquid (imidazolium acetate ILs) was found by both NMR and molecular simulation [24, 28].

The ionic liquid 1-ethyl-3-methylimidazolium acetate, ([emim][Ac]), has been used in this work due to its high CO<sub>2</sub> solubility, commercial availability, relative low cost and chemical absorption [14, 20, 23, 28-33]. To solve the problems associated with high viscosity in ionic liquids, different quantities of water were added to the ionic liquid [emim][Ac].

This ionic liquid is chemically and thermally stable when it absorbs carbon dioxide as reported in previous studies [28-31]. One of the reasons why [emim][Ac] is stable is because of the absence of a N-heterocyclic carbene [28]. Moreover, Gurau et al. (2011) reported that complex anion formation resulted in the stabilization of the volatile acetic acid that formed, preventing further decomposition reactions and allowing these ILs to act as stable reservoirs of carbenes for direct carbene-based chemistry [28]. Blath et al. (2012) noted that the acetate anion deprotonates the [emim]<sup>+</sup>cation at the C<sub>2</sub> atom of the imidazolium ring. The dissolved carbon dioxide reacts with the negatively charged carbon atom to form a stable carboxylate [29]. On the basis of NMR results, Carvalho et al. (2009) [32] suggested a preferential interaction of the acid carbon of the CO<sub>2</sub> molecule with the carboxylate group of the acetate anion, and this evidence was also supported by molecular simulation carried out by Stevanovic et al. (2012) [24]. When water is incorporated to with imidazolium acetate ILs, the CO<sub>2</sub> absorption may exhibit an absorption behaviour that is typical for a chemical complexation process, as it was proposed by Chinn et al. [33].

Previous work on the CO<sub>2</sub> solubility in the imidazolium acetate ILs [bmim][Ac] and [emim][Ac], supports the point that CO<sub>2</sub> strongly and chemically absorbs in the ionic liquid and that the complex is reversible (verified in separate absorption-desorption experiments conducted at room temperature) [31]. The reversible interaction with CO<sub>2</sub> is a key factor for the regeneration ability of the IL in its industrial application.

Carbon capture with membranes technology is being demonstrated as technically and economically viable due to its compaction and its capacity to be modulated [19]. Merkel et al. (2010) reported that substituting traditional towers with membranes that combined with the power usage could result in a decrease in capture cost to approximately \$23/tonne [16]. Lee et al. (2015) described a post-combustion CO<sub>2</sub> capture plant located at the Boryeong power station (South Korea) that could treat 200 tonnes of CO<sub>2</sub>/day (10 MW equivalent) [34].

Hollow fibre gas-liquid membrane contactors provide the alternative to conventional gas absorption systems for CO<sub>2</sub> capture from gas streams. This type of contactor offers following numerous advantages in comparison with absorption towers: the lack of flooding, channelling or foaming; a stable system that is not sensible to small changes; good mechanical strength; high surface area per unit volume; and independent control of gas and liquid flow rates [26, 35, 36]. In addition, hollow fibre membrane contactors are less sensitive to fouling since there is no convective flow through the membrane pores [37]. Moreover, due to the compact nature of the

membrane device, these type of absorbers have less energy-consumption and less volume and are thus more economical. In addition, the modularity of membrane modules makes their design simple and easy to be scaled up linearly and the interfacial area is known and constant [38, 39]. Using membrane contactors provides operating cost savings of 38-42%, and capital cost savings of 35-40% can be achieved [40].

Currently polymeric membranes appear to be the most advanced option for membrane-based post-combustion carbon capture in terms of CO<sub>2</sub>/N<sub>2</sub> permselectivity [41]. Polyvinylidene fluoride (PVDF), is a hydrophobic polymer that is soluble in common solvents and has been widely used for resistance, which are important parameters for CO<sub>2</sub> absorption and stripping applications. PVDF also possesses a low surface energy [42, 43].

Taking into account the potential of PVDF polymers, the present study of self-custom PVDF fibres was performed in a hollow fibre membrane contactor using different proportions of the ionic liquid [emim][Ac] and distilled water as the absorbent. To improve the properties of the gas absorbent for carbon dioxide capture, the research is focused on the addition of a molecular co-solvent, water, to the ionic liquid. CO<sub>2</sub> capture in terms of efficiency and overall mass transfer coefficient was evaluated. The effect of water on the CO<sub>2</sub> capture efficiency was quantified to determine the best solvent composition when the [emim][Ac] ionic liquid was used. The intensification factor (I) was also evaluated to compare hollow fibre membrane contactors with the traditional processes. Moreover, a simulation task was performed to estimate the mass transfer and as the operational effects required to achieve a 90% CO<sub>2</sub> recovery.

## 2. Experimental set up

For the carbon dioxide capture, a polyvinylidene fluoride (PVDF) hollow fibre membrane contactor improved with the ionic liquid 1-ethyl-3-methylimidazolium acetate [emim][Ac] was produced in the laboratory by phase inversion. The complete description of the fibre manufacturing method is explained in previous studies [14, 44, 45]. The absorption membrane contactor was manufactured by gluing the hollow fibre in a PVC shell [14]. The main characteristics of the membrane contactor are given in Table 1.

**Table 1:** Hollow fibre membrane contactors characteristics.

Membrane material	1AQ2-PVDF
Fibre o.d. $d_o$ , (m)	$7.7 \cdot 10^{-4}$
Fibre i.d. $d_i$ , (m)	$4.51 \cdot 10^{-4}$
Fibre length, $L$ (m)	0.295
Number of fibres, $n$	11
Effective inner membrane area, $A$ (m <sup>2</sup> )	$4.60 \cdot 10^{-3}$
Porosity (%)	30
Packing factor	0.04
Tortuosity <sup>a</sup>	3.33

<sup>a</sup> Assumed  $1/\text{Porosity}$

The [emim][Ac] ( $\geq 90\%$ ) ionic liquid was supplied by Sigma Aldrich (Spain). Despite its relatively low purity, solubility rates were measured and compared with literature data and similar values were obtained [46, 47]. CO<sub>2</sub> solubility was evaluated using a TGA-60H Shimadzu Thermobalance (Izasa, Spain). The sample temperature was measured with an accuracy of  $\pm 0.1$  K, and the TG sensitivity was approximately 1  $\mu\text{g}$ . The experimental

conditions were a CO<sub>2</sub> flow rate of 50 mL min<sup>-1</sup>, a temperature of 303 K and the atmospheric pressure.

The experimental setup is shown in Figure 1. The feed gas mixture stream contains 85 vol.% N<sub>2</sub> and 15 vol.% CO<sub>2</sub>. Carbon dioxide (99.7±0.01 vol.%) and pure nitrogen (99.999±0.001 vol.%) were supplied by Air Liquide (Spain). The flow gas (20 mL min<sup>-1</sup>) was adjusted using a Brook instrument MFC 5850 by Emerson Process Management Spain and flowed through the inside of the hollow fibres. The absorbent flowed counter-currently through the shell side. A digital gear pump (Cole Palmer Instrument Company, Hucoa-Erloss S.A., Spain) was used to control the liquid line (50 mL min<sup>-1</sup>). The experiments were carried out at 303 K. To obtain isothermal conditions, a convection oven was used in the experimental setup (Memmert UNE 200), as shown in Figure 1. Each experiment was replicated three times, and the average value was calculated. It was also ensure that the concentration of gas in the liquid was far from saturation.

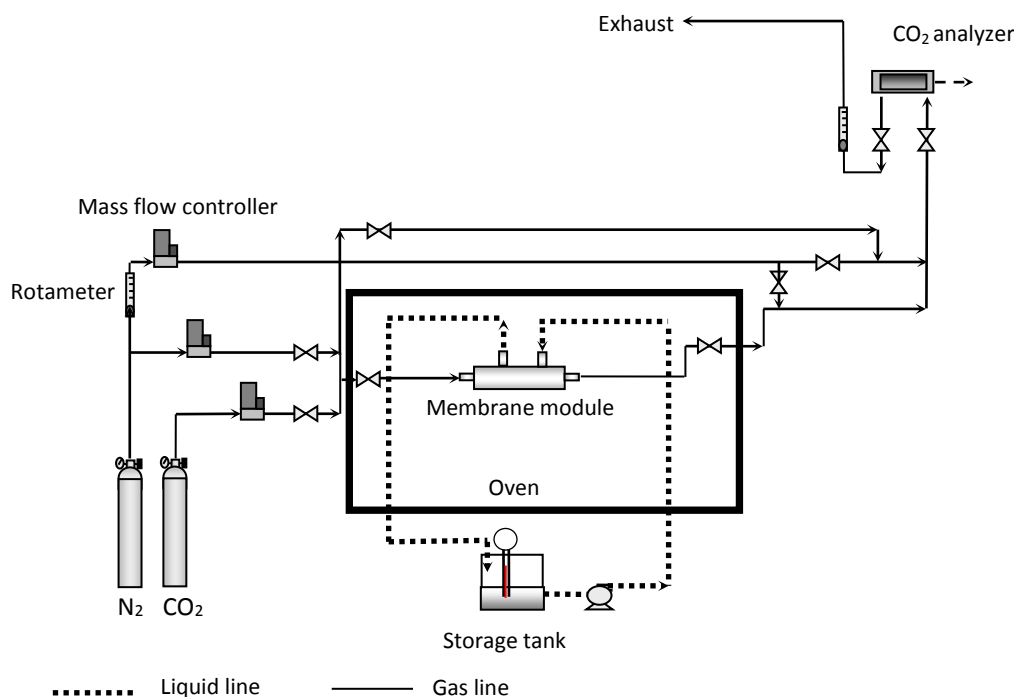


**Figure 1:** Experimental setup.

The outlet CO<sub>2</sub> concentration was continuously monitored using a gas analyser (Emerson Process) based on non-dispersive infrared (NDIR) spectroscopy [30]. Each time the hybrid solvent was used in an experiment, it was desorbed. For this purpose, a sweep stream containing N<sub>2</sub> was passed through the fibres. In addition, the output current was monitored to check when the solvent was desorbed. Evidence of the regeneration ability of [emim][Ac] was also reported by Shiflett et al. (2009) [31] from absorption-desorption experiments conducted at 298 K to show that the complex interaction between the CO<sub>2</sub> and this ionic liquid is reversible.

The base-case was the [emim][Ac] IL as the solvent. To evaluate the influence of water in the efficiency of the process, different amounts of water were added in a range between 10-40% volume added to the absorption liquid. The viscosity of the solvent with different contents of water was measured by a rotational viscometer (Smart Series, Fungilab Spain) and the obtained data are shown in Figure 2. These measurements were performed at 303 K, the same temperature as the CO<sub>2</sub> capture experiments. The shear rate used was 60 rpm because the instrument manual recommended a low spindle (L1) and a high shear rate to increase the accuracy.

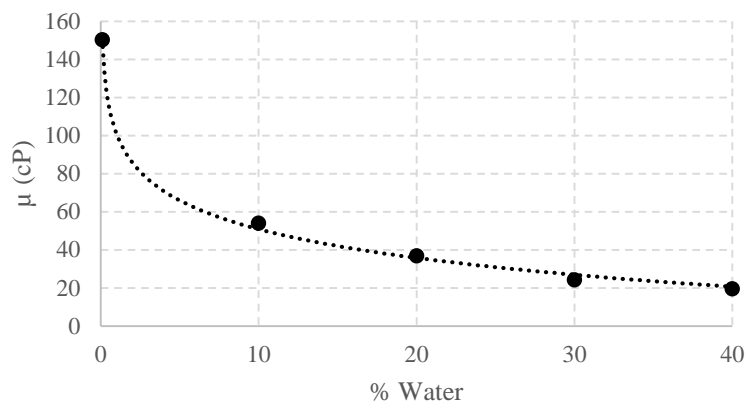


**Figure 2:** Viscosity measurements.

### 3. Results and discussion

#### 3.1 Carbon dioxide capture

The large scale applications of physical ILs for CO<sub>2</sub> capture from flue gas is mainly hindered by the low CO<sub>2</sub> absorption capacity at postcombustion conditions (where the partial pressure of CO<sub>2</sub> is rather low). Functionalized ionic liquids or task-specific ionic liquids have been developed to overcome this limitation. Carboxylate functionalized anions, such as acetate, are included in this category of ILs. The IL selected for this study, [emim][Ac], contains carboxylate functionalized anions and also offers thermal stability and evidence of a reversible chemical interaction with CO<sub>2</sub>.

The experiments were carried out with PVDF hollow fibres to evaluate the process efficiency with different amounts of water in the absorbent liquid. The presence of water in the ionic liquid affects the physico-chemical properties of the liquid mixture, i.e., it lowers the viscosity of the mixture and enhances the mass transfer of the membrane contactor, which are both advantages for industrial applications [24].

The gas phase was composed of 15% CO<sub>2</sub> and 85% N<sub>2</sub>, which are typical in many industrial processes [48]. The liquid stream was fed through the shell side, while the gas flowed in the counter-current direction through the lumen side. The CO<sub>2</sub> capture efficiency in each experiment was calculated as shown in Equation 1:

$$Efficiency (\%) = \left(1 - \frac{C_{CO_2,out}}{C_{CO_2,in}}\right) 100 \quad (Eq. 1)$$

where CO<sub>2,in</sub> is the initial carbon dioxide composition (0.15) and CO<sub>2,out</sub> is the output value from the analyser.

Table 2 shows the results obtained based on the CO<sub>2</sub> capture efficiency ranging between 20.5% in the case of the [emim][Ac] ionic liquid and a maximum value of 72.5% when 30% water was added to [emim][Ac]. All the experiments were performed with a gas flow of 20 mL min<sup>-1</sup> and at 303 K. The results indicate that the water content in the ILs significantly influenced the efficiency of the process. The effect of water in [emim][Ac] on the efficiency acts mainly on the viscosity of the ionic liquid. This behaviour can be explained by the molecular interactions that water promotes in the ionic liquid [49]. It is also suggested that the carboxylate moiety (such as acetate) interacts with water to form a weak reversible bond with CO<sub>2</sub> [33].

**Table 2:** Influence of water content in the absorbent in the process efficiency.

Solvent	Efficiency (%)
[emim][Ac]	20.5*±2.27
[emim][Ac]+10% water	53.7±0.57
[emim][Ac]+20% water	67.1±0.10
[emim][Ac]+30% water	72.5±0.07
[emim][Ac]+40% water	60.2±1.87

\*Ref. [14]

The [emim][Ac] IL absorbed the CO<sub>2</sub> chemically, as Gurau et al. demonstrated using NMR spectroscopy and X-ray diffraction [28]. When water is incorporated to imidazolium acetate ILs, the CO<sub>2</sub> absorption may exhibit an absorption behaviour that is typical for a chemical complexation process, as it was proposed by Chinn et al. (2005) [33].

This work aims to quantify the effect of water for the proper design of the CO<sub>2</sub> capture unit by estimating the membrane area required to achieve a determined target of CO<sub>2</sub> capture efficiency.

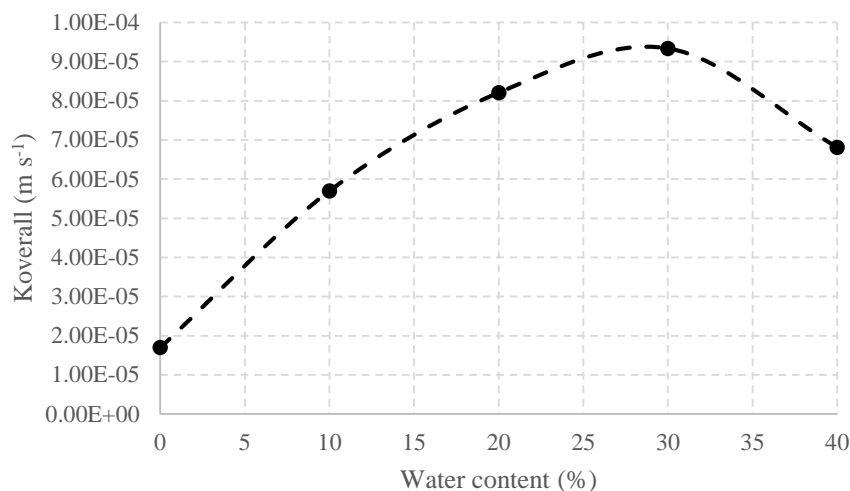
From the obtained results, the following is suggested: (i) the efficiency increases significantly with a higher water content until a maximum of 30% (vol); (ii) the efficiency increases because the solvent viscosity decreases; and (iii) more importantly, the values obtained with a 30% water content (vol) were competitive with traditional alkanolamine solvents such as monoethanolamine (MEA) [50].

In addition, with a water volume approximately 30% in the [emim][Ac], the mass transfer benefited the process. The overall mass transfer coefficient,  $K_{overall}$  expressed in  $m\ s^{-1}$  was calculated according to the equation 2, as in previous studies [14, 30, 52].

$$N_{CO_2,g} = \frac{Q_g}{A} (C_{CO_2,in} - C_{CO_2,out}) = K_{overall} \frac{\Delta y_{lm} P_T}{RT} \quad (Eq. 2)$$

where  $Q_g$  is the gas flow rate ( $m^3\ s^{-1}$ ),  $A$  is the membrane area ( $m^2$ ),  $P_T$  is the total pressure in the gas phase, and  $\Delta y_{lm}$  is the logarithmic mean of the driving force based on gas phase molar fractions [30].

Figure 3 represents the different values of  $K_{overall}$ , with the highest value of  $9.3 \cdot 10^{-5}\ m\ s^{-1}$  corresponding to the 30% water content (vol) in the solvent.


**Figure 3:**  $K_{overall}$  ( $m\ s^{-1}$ ) results.

The overall mass transfer coefficients were also transformed according to equation 3. The resulting constant,  $K_r$  ( $s^{-1}$ ), may be useful for comparisons between different hollow fibre modules [36].

$$K_r (s^{-1}) = K_{overall} (m s^{-1}) \frac{Fiber\ area (m^2)}{Shell\ volume (m^3)} \quad (Eq. 3)$$

Table 3 compares the  $K_r$  values obtained with different amounts of water and previous data reported in the literature. All values were performed in the temperature range of  $300 \pm 3$  K. Different types of hollow fibre membrane contactors were compared. Polypropylene (PP) and polysulfone (Ps) hollow fibre membrane contactors possessed the same effective inner membrane area ( $0.18 \text{ m}^2$ ). Moreover, the results with [emim][Ac] ionic liquid were related with the 1-ethyl-3-methylimidazolium ethylsulfate [emim][EtSO<sub>4</sub>] ionic liquid. [emim][EtSO<sub>4</sub>] exhibits physical absorption and low viscosity [30].

**Table 3:**  $K_r$  ( $s^{-1}$ ) comparison between different  $K_{overall}$  ( $m s^{-1}$ ) and  $K_r$  ( $s^{-1}$ ) values using different hollow fibre membrane contactors.

Fibre Material	Solvent	$K_{overall} 10^{-5} (m s^{-1})$	Fibre Area/Shell volume, $m^2 m^{-3}$	$K_r 10^{-3} (s^{-1})$	Ref
PVDF	[emim][Ac]	1.70	122.20	2.08	[14]
PVDF	[emim][Ac]+10% water	5.70	122.20	6.97	This work
PVDF	[emim][Ac]+20% water	8.21	122.20	10.0	This work
PVDF	[emim][Ac]+30% water	9.34	122.20	11.4	This work
PVDF	[emim][Ac]+40% water	6.81	122.20	8.32	This work
PP	[emim][EtSO <sub>4</sub> ]	0.07	7200	5.04	[30]
PP	[emim][Ac]	0.19	7200	13.7	[30]
Ps	[emim][Ac]	0.26	421.43	1.10	[51]

Results with [emim][Ac] and water were higher than the other values. Only the value of  $K_r$  using a PP membrane contactor and [emim][Ac] ionic liquid ( $13.7 s^{-1}$ ) was slightly higher. This could be attributed to the fact that the relation between the fibre area and the shell volume is increased. While the PP module has an area of  $0.19 \text{ m}^2$ , the area of the PVDF membrane contactor is only  $4.60 \cdot 10^{-3} \text{ m}^2$ . Thus, although the  $K_r$  is seven times lower, the area is 40 times smaller. Therefore, PVDF modules with the hybrid solvent are promising for CO<sub>2</sub> capture.

### 3.2 Simulation task to estimate mass transfer and operational effects

The aim of the numerical analysis was to evaluate the membrane mass transfer coefficient and membrane length, which assure an intensification effect for a membrane contactor compared to a packed column.

A non-wetted operating mode was assumed for modelling the PVDF hollow fibre membrane contactor. According to previous works, CO<sub>2</sub> was transferred to the liquid phase by diffusion through the pores filled with gas [52, 53]. The radial position  $r=0$  shows the centre of the fibre and the axial distance of  $z=0$  refers to the initial position of the gas in the fibre. The dimensionless differential mass balance of CO<sub>2</sub> (eq. 4) was based on the following assumptions according to previous works [51-53]: (1) the absorption liquid has a negligible concentration of the soluble gas; (2) the process is in a steady state and isothermal conditions; (3) there is no axial diffusion; (4) an ideal gas behavior is assumed; (5) there is a constant fibre and shell pressure; and (6) the velocity is fully developed in a laminar flow.

$$\frac{Gz}{2} [1 - \bar{r}^2] \frac{\partial \bar{C}_{CO_2}}{\partial \bar{z}} = \frac{1}{\bar{r}} \frac{\partial}{\partial \bar{r}} \left( \bar{r} \frac{\partial \bar{C}_{CO_2}}{\partial \bar{r}} \right) \quad (Eq. 4)$$

where the dimensionless variables were as follows:

$$\bar{r} = \frac{r}{R} \quad (Eq. 5a)$$

$$\bar{z} = \frac{z}{L} \quad (Eq. 5b)$$

$$\bar{C}_{CO_2} = \frac{C_{CO_2}}{C_{CO_2,inlet}} \quad (Eq. 5c)$$

The following boundary conditions were used:

$$\bar{r} = 0 \rightarrow \frac{\partial \bar{C}_{CO_2}}{\partial \bar{r}} = 0 \quad (Eq. 6a)$$

$$\bar{r} = 1 \rightarrow \frac{\partial \bar{C}_{CO_2}}{\partial \bar{r}} = -\frac{Sh}{2} \bar{C}_{CO_2} \quad (Eq. 6b)$$

$$\bar{z} = 0 \rightarrow \bar{C}_{CO_2} = 1 \quad (Eq. 6c)$$

The following dimensionless numbers were used:

$$Gz = \frac{u_m di^2}{D L} \quad (Eq. 7a)$$

$$Sh = \frac{K_{overall} di}{D} \quad (Eq. 7b)$$

Finally, the CO<sub>2</sub> outlet concentration was calculated as a dimensionless mixing cup:

$$\bar{C}_{CO_2=L} = 4 \int_0^1 \bar{C}_{CO_2} [1 - \bar{r}^2] \bar{r} d\bar{r} \quad (Eq. 8)$$

Aspen Custom Modeler (Aspen Technology Inc.) software was used to solve the set of equations.

Figure 4 shows the modelling profile as a function of the carbon dioxide outlet concentration and the CO<sub>2</sub> capture efficiency along the module length. Each line represents the modelling results along the dimensionless length with different quantities of water. In addition, the final square shows the experimental results obtained. As shown in Figure 4, the experimental and results from the simulation in total concordance. Table 4 states the values of the relative error (simulation with respect to experimental). Moreover, the modelling results have been compared with polysulfone and polypropylene modules.

**Table 4:** Comparison between experimental and simulation results with other hollow fibre membrane contactors.

Fibre Material	Solvent	$\mu\text{m (m}\cdot\text{s}^{-1}\text{)}$	Experimental Efficiency (%)	Simulation Efficiency (%)	/Error/	Ref
	[emim][Ac]	$1.90 \cdot 10^{-1}$	$20.5 \pm 2.27$	20.9	0.4	[14]
	[emim][Ac]+10% water	$1.90 \cdot 10^{-1}$	$53.7 \pm 0.57$	54.5	0.8	This work
PVDF	[emim][Ac]+20% water	$1.90 \cdot 10^{-1}$	$67.1 \pm 0.10$	67.8	0.7	This work
	[emim][Ac]+30% water	$1.90 \cdot 10^{-1}$	$72.5 \pm 0.07$	72.6	0.1	This work
	[emim][Ac]+40% water	$1.90 \cdot 10^{-1}$	$60.2 \pm 1.87$	60.9	0.7	This work
	[emim][Ac]	$1.33 \cdot 10^{-2}$	16.3	16.0	0.3	[30]
PP	[emim][EtSO <sub>4</sub> ]	$1.33 \cdot 10^{-2}$	10.5	10.8	0.3	[30]
	[emim][EtSO <sub>4</sub> ]	$3.81 \cdot 10^{-3}$	28.7	31.3	2.6	[30]
Ps	[emim][Ac]	$7.58 \cdot 10^{-3}$	$29.5 \pm 1.7$	46.76	17.3	[51]

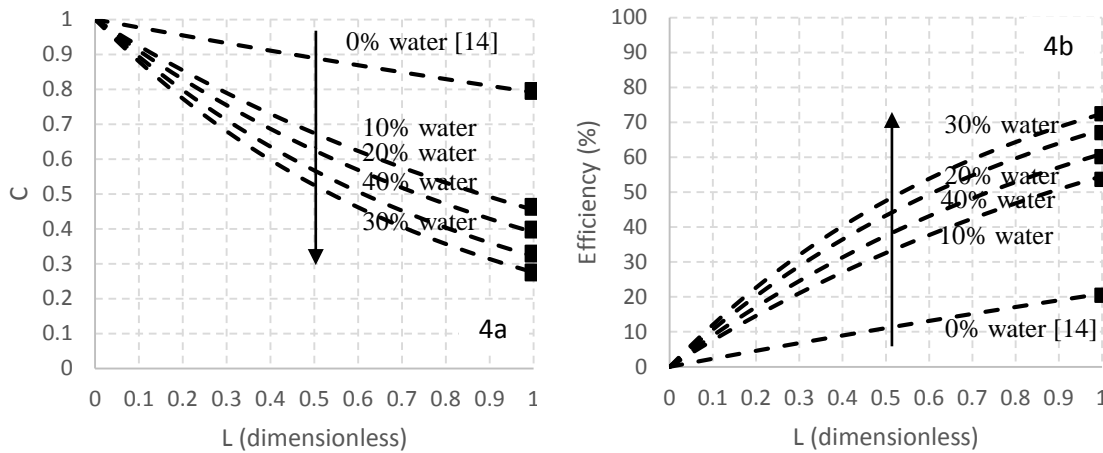


**Figure 4:** Modelling results of the profiles of dimensionless CO<sub>2</sub> concentration and process efficiency (%) along the fibre length, assuming a non-wetted mode. 4a: Profiles of dimensionless CO<sub>2</sub> concentration. 4b: Profiles of process efficiency (%).

Two sensitivity analyses were carried out to estimate the effect of two variables: the mass transfer and the module length, on the CO<sub>2</sub> capture efficiency of the membrane process, with the following findings:

(i) The overall mass transfer coefficient,  $K_{\text{overall}}$ , was varied as shown in Figure 5. Using a  $K_{\text{overall}}$  higher than  $1.70 \cdot 10^{-4} \text{ m s}^{-1}$ , the efficiencies obtained were higher than the target capture efficiency of 90% CO<sub>2</sub> capture (Figure 5a).

(ii) The fibre length was varied (Figure 6) to estimate the number of hollow fibre membrane contactors in a series necessary to achieve at least a 90% efficiency. Figure 6 shows the influence of the fibre length. Using the ionic liquid without water, ten hollow fibres in a series (3 m total length) were necessary to reach the target capture efficiency. When adding 30% (vol) water to the ionic liquid, only two membrane contactors (0.60 m) were required.

Figure 5b also shows the intensification factor (I). This factor was calculated as the volumetric absorption capacity of the membrane contactor divided by the average volumetric absorption capacity of a packed column. The reference value of a classical packed column was estimated as  $1 \text{ mol CO}_2 \text{ m}^{-3} \text{ s}^{-1}$  using a 30 wt.% MEA solution [54]. The intensification factor reached values from 1.05 (0% vol. water) to 3.75 (30% vol. water) for an operating temperature of 303 K.

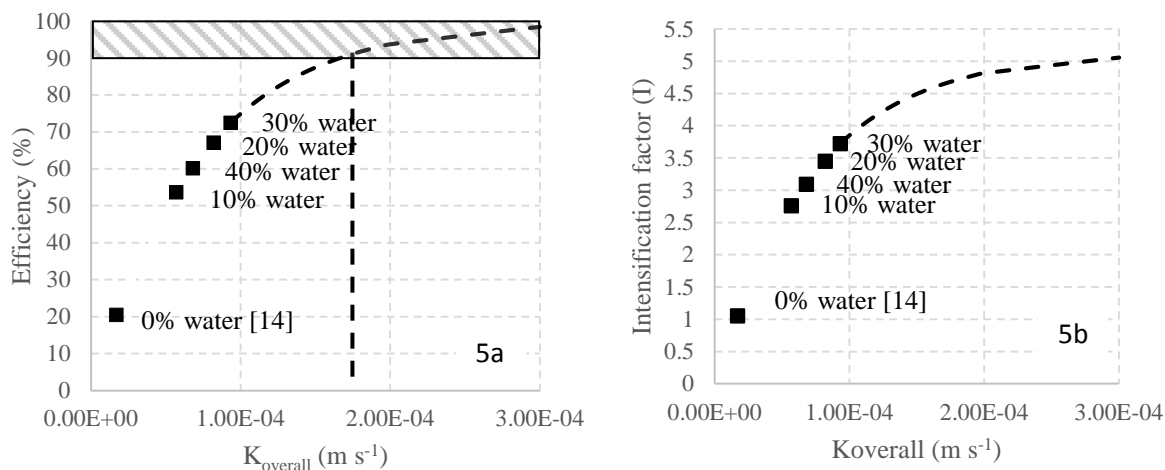


**Figure 5:** Sensitivity analysis of the mass transfer coefficient,  $K_{\text{overall}}$  (5a), and the intensification factor (I) (5b).

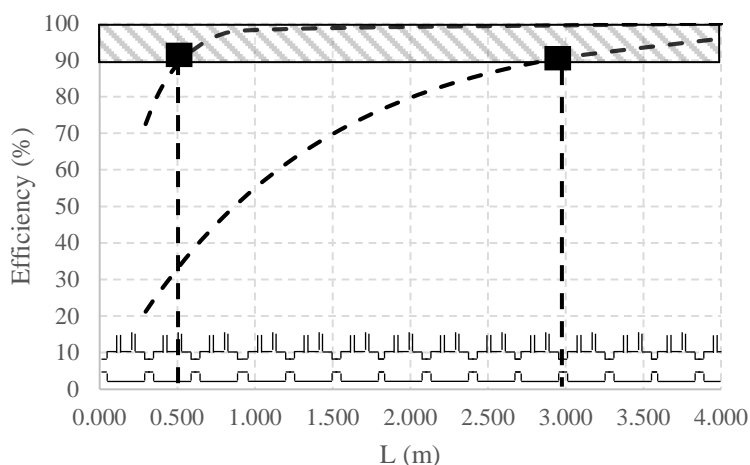


**Figure 6:** Sensitivity analysis of the length module,  $L$

The hollow fibre membrane contactors can be coupled in parallel and in series depending on the gas flow and the efficiency required. This fact allows this membrane technology to compete with traditional systems using amines and absorption towers. The addition of water to the ionic liquid leads to the use of a hybrid solvent in an intensified process. Although the IL price is higher than the MEA price, its use for CO<sub>2</sub> capture is promising taking into account the problems associated to the alkanolamine solvent (volatilization, possible contamination). Further work is focused to estimate the implications of a hybrid solvent in the capture costs. Some previous results working with ILs (without water content) indicated that although the cost of the IL is more than 10 times the cost of the MEA, the equipment cost savings offset some of this difference, providing a significant reduction in the equipment footprint [55]. The reduced cost of the hybrid solvent that incorporates water may lead to a higher cost savings related to the MEA process.

Finally, a study as a function of the dimensionless Sherwood and Graetz numbers was performed. Figure 7a shows an analysis in terms of the Sherwood number using a fixed Graetz number ( $8.02 \cdot 10^{-3}$ ). For Sherwood number values greater than  $4.7 \cdot 10^{-3}$ , efficiencies higher than 90% were achieved. On the other hand, for a constant, dimensionless Sherwood number, the Graetz number was varied (Fig. 7b). Graetz values smaller than  $4.5 \cdot 10^{-3}$  and  $7.89 \cdot 10^{-3}$  allowed for high efficiencies over 90% CO<sub>2</sub> capture, using 30% and 0% water, respectively.

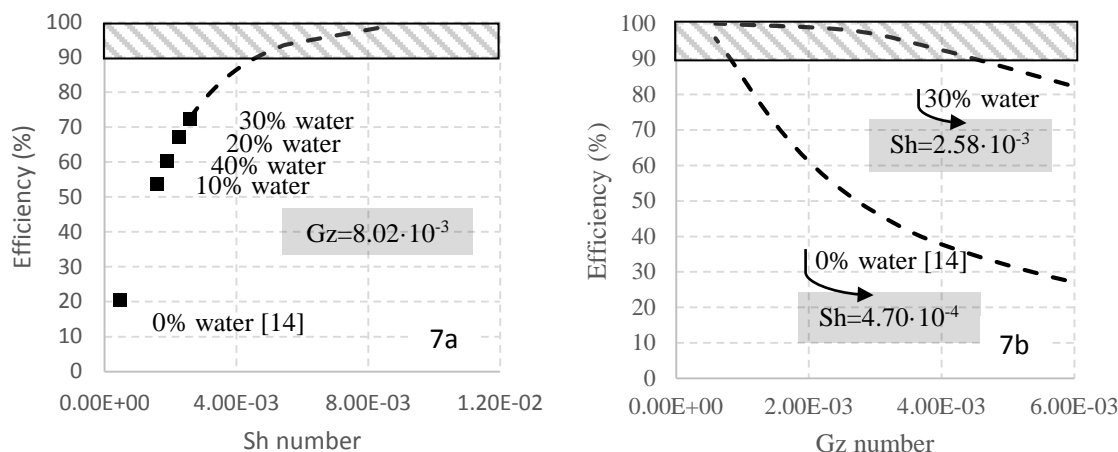


**Figure 7:** Sensitivity analysis as a function of the dimensionless Sherwood (7a) and Graetz numbers (7b).

#### 4. Conclusions

The influence of water on a polyvinylidene fluoride (PVDF) immobilized hollow fibre membrane contactor with [emim][Ac] ionic liquid was investigated in a non-dispersive absorption plant for carbon dioxide capture. The flue gas was composed of 15% CO<sub>2</sub> and 85% N<sub>2</sub>. The ionic liquid 1-ethyl-3-methylimidazolium acetate [emim][Ac] was used as a reference solvent. This ionic liquid was chosen due to its high CO<sub>2</sub> solubility, which exhibits strong chemical absorption for CO<sub>2</sub> that is reversible (an important issue for its regeneration). Different quantities of water were added to study the influence of water in the process. The hybrid solvent based on a combination of 30% water and 70% [emim][Ac] expressed according to the volume of the absorbent, provided a CO<sub>2</sub> capture efficiency of 72.5%, significantly higher than the reference solvent.

The overall mass transfer coefficient was also evaluated. A value of  $9.34 \cdot 10^{-5} \text{ m s}^{-1}$  was reached for the hybrid solvent. The  $K_{\text{overall}}$  was transformed by the ratio of the fibre area to the shell volume and the values were higher than the other values reported in literature for different module contactors. The content of water in the absorbent could significantly affect the mass transfer of the membrane contactor because of the change in viscosity and the molecular interactions that water promotes in the ionic liquid.

The following conclusions were obtained from the sensitivity analysis: (i)  $K_{\text{overall}}$  values higher than  $1.70 \cdot 10^{-4} \text{ m s}^{-1}$  allow CO<sub>2</sub> capture efficiencies higher than 90%; (ii) using only two hollow fibre membrane contactors in a series (0.6 m total length) was required to achieve the target CO<sub>2</sub> capture efficiency that provides competitive results compared with traditional absorption towers, given a significant intensification factor, up to 4, related to the absorption with the MEA solution.

#### Acknowledgements

This research was funded by the Spanish Ministry Economy and Competitiveness (Project CTQ2013-48280-C3-1-R).

## References

- [1] Sheng, Y.; Wang, H.; Liu, J.; Zhang, Y. Enhanced Performance of a Novel Polyvinyl Amine/Chitosan/Graphene Oxide Mixed Matrix Membrane for CO<sub>2</sub> Capture. *ACS Sustainable Chem. Eng.* **2015**, 3, 1819–1829.
- [2] Sun, L.B.; Kang, Y.H.; Shi, Y.Q.; Jiang, Y.; Liu, X.Q. Highly Selective Capture of the Greenhouse Gas CO<sub>2</sub> in Polymers. *ACS Sustainable Chem. Eng.* **2015**, 3, 3077–3085.
- [3] Fang, M.; Ma, Q.; Wang, Z.; Xiang, Q.; Jiang, W.; Xia, Z. A novel method to recover ammonia loss in ammonia-based CO<sub>2</sub> capture system: ammonia regeneration by vacuum membrane distillation. *Greenhouse. Gas. Sci. Technol.* **2015**, 5, 1-11.
- [4] Zulfiqar, S.; Sarwar, M.I. Effect of solvent on the CO<sub>2</sub> capture ability of polyester: A comparative study. *J. Ind. Eng. Chem.* **2015**, 21, 1373–1378.
- [5] Fernández-Barquín, A.; Casado-Coterillo, C.; Palomino, M.; Valencia, S.; Irabien, A. LTA/Poly(1-trimethylsilyl-1-propyne) Mixed-Matrix Membranes for High-Temperature CO<sub>2</sub>/N<sub>2</sub> Separation. *Chem. Eng. Technol.* **2015**, 38(4), 658-666.
- [6] Abdollahi, Y.; Sairi, N.A.; Aroua, M.K.; Masoumi, H.R.F.; Jahangirian, H.; Alias, Y. Fabrication modeling of industrial CO<sub>2</sub> ionic liquids absorber by artificial neural networks. *J. Ind. Eng. Chem.* **2015**, 25, 168–175.
- [7] Luis, P.; Van Gerven, T.; Van Der Bruggen, B. Recent developments in membrane-based technologies for CO<sub>2</sub> capture. *Prog. Energ. Combust.* **2012**, 38, 419-448.
- [8] Wang, J.; Huang, L.; Zheng, Q.; Qiao, Y.; Wang, Q. Layered double hydroxides/oxidized carbon nanotube nanocomposites for CO<sub>2</sub> capture. *J. Ind. Eng. Chem.* **2016**, 36, 255–262.
- [9] Chabanon, E.; Bouallou, C.; Remigy, J.C.; Lasseguette, E.; Medina, Y.; Favre, E.; Nguyen, P.T.; Roizard, D. Study of an innovative gas-liquid contactor for CO<sub>2</sub> absorption. *Energy Procedia.* **2011**, 4, 1769–1776.
- [10] Canepa, R.; Wang, M. Techno-economic analysis of a CO<sub>2</sub> capture plant integrated with a commercial scale combined cycle gas turbine (CCGT) power plant. *Appl. Therm. Eng.* **2015**, 74, 10-19.
- [11] Kanniche, M.; Gros-Bonnivard, R.; Jaud, P.; Valle-Marcos, J.; Amann, J.; Bouallou, C. Pre-combustion, post-combustion and oxy-combustion in thermal power plant for CO<sub>2</sub> capture. *Appl. Therm. Eng.* **2010**, 30, 53-62.
- [12] Luis, P.; Van der Bruggen, B. The role of membranes in post-combustion CO<sub>2</sub> capture. *Greenhouse. Gas. Sci. Technol.* **2013**, 3, 1-20.
- [13] Singh, B.; Strømman, A.H.; Hertwich, E.G. Comparative life cycle environmental assessment of CCS technologies. *Int. J. Greenh. Gas. Control.* **2011**, 5, 911–921.
- [14] Gomez-Coma, L.; Garea, A.; Rouch, J.C.; Savart, T.; Lahitte, J.F.; Remigy, J.C.; Irabien, A. Membrane modules for CO<sub>2</sub> capture based on PVDF hollow fibers with ionic liquids immobilized. *J. Membr. Sci.* **2016**, 498, 218-226.
- [15] Chen, J.; Wang, F. Cost reduction of CO<sub>2</sub> capture processes using reinforcement learning based iterative design: A pilot-scale absorption–stripping system. *Sep. Purif. Technol.* **2014**, 122, 149–158.

- [16] Merkel, C.; Lin, H.; Wei, X.; Baker, T.R. Power plant post-combustion carbon dioxide capture: An opportunity for membranes. *J. Membr. Sci.* **2010**, 359, 126–139.
- [17] Zhang, X.; Singh, B.; He, X.; Gundersen, T.; Deng, L.; Zhang, S. Post-combustion carbon capture technologies: Energetic analysis and life cycle assessment. *Int. J. Greenh. Gas. Control.* **2014**, 27, 289–298.
- [18] Mulukutla, T.; Obuskovic, G.; Sirkar, K.K. Novel scrubbing system for post-combustion CO<sub>2</sub> capture and recovery: Experimental studies. *J. Membr. Sci.* **2014**, 471, 16–26.
- [19] Li, S.; Rocha, D.J.; Zhou, S.J.; Meyer, H.S.; Bikson, B.; Ding, Y. Post-combustion CO<sub>2</sub> capture using super-hydrophobic, polyetherether ketone, hollow fiber membrane contactors. *J. Membr. Sci.* **2013**, 430, 79–86.
- [20] Ramdin, M.; De Loos, T.W.; Vlugt, T.J.H. State-of-the-art of CO<sub>2</sub> capture with ionic liquids. *Ind. Eng. Chem. Res.* **2012**, 51, 8149–8177.
- [21] Farahipour, R.; Karunanithi, T. Life Cycle Environmental Implications of CO<sub>2</sub> Capture and Sequestration with Ionic Liquid 1-Butyl-3-methylimidazolium. *ACS Sustainable Chem. Eng.* **2014**, 2, 2495–2500.
- [22] Ashley, M.; Magiera, C.; Ramidi, P.; Blackburn, G.; Scott, T.G.; Gupta, R.; Wilson, K.; Ghosh, A.; Biswas, A. Nanomaterials and processes for carbon capture and conversion into useful by-products for a sustainable energy future. *Greenhouse. Gas. Sci. Technol.* **2012**, 2, 419–444.
- [23] Papatryfon, X.L.; Heliopoulos, N.S.; Molchan, I.S.; Zubeir, L.F.; Bezemer, N.D.; Arfanis, M.K.; Kontos, A.G.; Likodimos, V.; Iliev, B.; Romanos, G.E.; Falaras, P.; Stamatakis, K.; Beltsios, K.G.; Kroon, M.C.; Thompson, G.E.; Klöckner, J.; Schubert, T.J.S. CO<sub>2</sub> capture efficiency, corrosion properties, and ecotoxicity evaluation of amine solutions involving newly synthesized ionic liquids. *Ind. Eng. Chem. Res.* **2014**, 53(30), 12083–12102.
- [24] Stevanovic, S.; Podgoršek, A.; Pádua, A.A.H.; Costa Gomes M.F. Effect of water on the carbon dioxide absorption by 1-alkyl-3- methylimidazolium acetate ionic liquids. *J. Phys. Chem. B.* **2012**, 116(49), 14416–14425.
- [25] Dai, Z.; Noble, R.D.; Gin, D.L.; Zhang, X.; Deng, L. Combination of ionic liquids with membrane technology: A new approach for CO<sub>2</sub> separation. *J. Membr. Sci.* **2016**, 497, 1–20.
- [26] Hoff, K.A.; Svendsen, H.F. Membrane contactors for CO<sub>2</sub> absorption. *Chem. Eng. Sci.* **2014**, 116, 331–341.
- [27] Pinto, D.D.D.; Knuutila, H.; Fytianos, G.; Haugen, G.; Mejdell, T.; Svendsen, H.F. CO<sub>2</sub> post combustion capture with a phase change solvent. Pilot plant campaign, *Int. J. Greenh. Gas. Control.* **2014**, 31, 153–164.
- [28] Gurau, G.; Rodríguez, H.; Kelley, S.P.; Janiczek, P.; Kalb, R.; Rogers, R.D. Demonstration of chemisorption of carbon dioxide in 1,3-dialkylimidazolium acetate ionic liquids, *Angewa. Chem. Int. Ed.* **2011**, 50, 12024–12026.
- [29] Blath, J.; Deubler, N.; Hirsh, T.; Schiestel, T. Chemisorption of carbon dioxide in imidazolium based ionic liquids with carboxylic anions. *Chem. Eng. J.* **2012**, 181–182, 152–158.

- [30] Gomez-Coma, L.; Garea, A.; Irabien, A. Non-dispersive absorption of CO<sub>2</sub> in [emim][EtSO<sub>4</sub>] and [emim][Ac]: Temperature influence. *Sep. Purif. Technol.* **2014**, 132, 120–125.
- [31] Shiflett, M.B.; Yokozeki, A. Phase behavior of carbon dioxide in ionic liquids: [emim][acetate], [emim][trifluoroacetate], and [emim][acetate] + [emim][trifluoroacetate] mixtures. *J. Chem. Eng. Data.* **2009**, 54, 108-114.
- [32] Carvalho, P.J.; Alvarez, V.H.; Schröder, B.; Gil, A.M.; Marrucho, I.M.; Aznar, M.; Santos, L.; Coutinho, J.A.P. Specific Solvation Interactions of CO<sub>2</sub> on Acetate and Trifluoroacetate Imidazolium Based Ionic Liquids at High Pressures. *J. Phys. Chem. B.* **2009**, 113, 6803-6812.
- [33] Chinn, D.; Vu, Q.; Driver, M.S.; Boudreau, L.C. CO<sub>2</sub> removal from gas using ionic liquid absorbents. **2005**, US7,527,775 B2.
- [34] Lee, J.H.; Kwak, N.S.; Lee, I.Y.; Jang, K.R.; Lee, D.W.; Jang, S.G.; Kim, B.K.; Shim, J.G. Performance and economic analysis of commercial-scale coal-fired power plant with post-combustion CO<sub>2</sub> capture. *Korean. J. Chem. Eng.* **2015**, 32(5), 800-807.
- [35] Hernández, S.; Lei, S.; Rong, W.; Ormsbee, L.; Bhattacharyya D. Functionalization of Flat Sheet and Hollow Fiber Microfiltration Membranes for Water Applications. *ACS Sustainable Chem. Eng.* **2016**, 4, 907–918.
- [36] Albo, J.; Irabien, A. Non-dispersive absorption of CO<sub>2</sub> in parallel and cross-flow membrane modules using EMISE. *J. Chem. Technol. Biot.* **2012**, 87, 1502-1507.
- [37] An, L.; Yu, X.; Yang, J.; Tu, S.T.; Yan, J. CO<sub>2</sub> capture using a superhydrophobic ceramic membrane contactor. *Energy Procedia.* **2015**, 75, 2287–2292.
- [38] Li, J.L.; Chen, B.H. Review of CO<sub>2</sub> absorption using chemical solvents in hollow fiber membrane contactors. *Sep. Purif. Technol.* **2005**, 41, 109–122.
- [39] de Souza-Moraes, L.; Araujo-Kronemberger, F.A.; Conceição-Ferraz, H.; Claudio-Habert, A. Liquid–liquid extraction of succinic acid using a hollow fiber membrane contactor. *J. Ind. Eng. Chem.* **2015**, 21, 206–211.
- [40] Hoff, K.A.; Juliussen, O.; Falk-Pedersen, O.; Svendsen, H.F. Modeling and Experimental Study of Carbon Dioxide Absorption in Aqueous Alkanolamine Solutions Using a Membrane Contactor. *Ind. Eng. Chem. Res.* **2004**, 43, 4908-4921.
- [41] Fernández-Barquín, A.; Casado-Coterillo, C.; Palomino, M.; Valencia, S.; Irabien, A. Permselectivity improvement in membranes for CO<sub>2</sub>/N<sub>2</sub> separation. *Sep. Purif. Technol.* **2016**, 157, 102-111.
- [42] Mansourizadeh, A. Experimental study of CO<sub>2</sub> absorption/stripping via PVDF hollow fiber membrane contactor. *Chem. Eng. Res. Des.* **2012**, 90, 555–562.
- [43] Mansourizadeh, A.; Ismail, A.F. Influence of membrane morphology on characteristics of porous hydrophobic PVDF hollow fiber contactors for CO<sub>2</sub> stripping from water. *Desalination.* **2012**, 287, 220–227.
- [44] Savart, T. Conception et réalisation de fibres creuses industrielles d'ultrafiltration en poly (fluorure de vinylidène) (PVDF) contenant des copolymères à blocs, *PhD thesis*. Université Toulouse 3. Paul Sabatier. **2013**.

- [45] Lorain, O.; Espenan, J.M.; Remigy, J.C.; Lahitte, J.F.; Rouch, J.C.; Savart, T.; Gerard, P.; Magnet, S. Copolymer having amphiphilic blocks, and use thereof for manufacturing polymer filtration membranes. **2014**, WO2014/139977 (A1).
- [46] Santos, E.; Albo, J.; Irabien, A. Acetate based Supported Ionic Liquid Membranes (SILMs) for CO<sub>2</sub> separation: Influence of the temperature. *J. Membr. Sci.* **2014**, 452, 277–283.
- [47] Albo, J.; Santos, E.; Neves, L.A.; Simeonov, S.P.; Afonso, C.A.M.; Crespo, J.G.; Irabien, A. Separation performance of CO<sub>2</sub> through Supported Magnetic Ionic Liquid Membranes (SMILMs). *Sep. Purif. Technol.* **2012**, 97, 26–33.
- [48] Kundu, S.K.; Bhaumik, A. Novel Nitrogen and Sulfur Rich Hyper-Cross-Linked Microporous Poly-Triazine-Thiophene Copolymer for Superior CO<sub>2</sub> Capture. *ACS Sustainable Chem. Eng.* **2016**, 4, 3697–3703.
- [49] Martins, C.F.; Neves, L.A.; Estevão, M.; Rosatella, A.; Alves, V.D.; Afonso, C.A.M.; Crespo, J.G.; Coelho, I.M. Effect of water activity on carbon dioxide transport in cholinium-based ionic liquids with carbonic anhydrase. *Sep. Purif. Technol.* **2016**, 168, 74–82.
- [50] Wang, L.; Zhang, Z.; Zhao, B.; Zhang, H.; Lu, X.; Yang, Q. Effect of long-term operation on the performance of polypropylene and polyvinylidene fluoride membrane contactors for CO<sub>2</sub> absorption. *Sep. Purif. Technol.* **2013**, 116, 300–306.
- [51] Gomez-Coma, L.; Garea, A.; Irabien, A. Carbon dioxide capture by [emim][Ac] ionic liquid in a polysulfone hollow fiber membrane contactor. *Int J Greenh Gas Control.* **2016**, 52, 1–9.
- [52] Luis, P.; Ortiz, I.; Aldaco, R.; Garea, A.; Irabien, A. Recovery of sulfur dioxide using non-dispersive absorption. *Int. J. Chem. React. Eng.* **2007**, 5, 1–9.
- [53] Luis, P.; Garea, A.; Irabien, A. Modelling of a hollow fibre ceramic contactor for SO<sub>2</sub> absorption. *Sep. Purif. Technol.* **2010**, 72, 174–179.
- [54] Bounaceur, R.; Castel, C.; Rode, S.; Roizard, D.; Favre, E. Membrane contactors for intensified post combustion carbon dioxide capture by gas-liquid absorption in MEA: A parametric study. *Chem. Eng. Res. Des.* **2012**, 90, 2325–2337.
- [55] Shiflett, M.B.; Drew, D.W.; Cantini, R.A.; Yokozeki, A. Carbon Dioxide Capture Using Ionic Liquid 1-Butyl-3-methylimidazolium Acetate. *Energy Fuels*, **2010**, 24, 5781–5789.

**4.5. Gómez-Coma L., Garea A., Irabien A., PVDF membrane contactor for CO<sub>2</sub> capture using the ionic liquid [emim][Ac]: mass transfer analysis. Chem. Eng. Technol. 2016. under review.**

Resumen

Los procesos de post-combustión a base de líquidos iónicos y contactores de membrana han surgido como nuevas atractivas alternativas a los sistemas tradicionales. En este trabajo, se ha utilizado una corriente de gas compuesta por un 15% CO<sub>2</sub> y 85% de N<sub>2</sub> y un contactor de membranas de fibras huecas de PVDF con líquido iónico inmovilizado en ellas. El líquido iónico seleccionado fue el 1-etil-3-metilimidazolio [emim][Ac], el cual se utilizó como absorbente debido a su alta absorción química y alta solubilidad al CO<sub>2</sub>. El coeficiente global de transferencia de materia  $K_{overall}$ , la energía de activación ( $E_a$ ), y las resistencias a la transferencia empleando el contactor de fibra hueca se cuantificaron en el intervalo de temperatura 303-343K. El valor de  $K_{overall}$  logrado en el presente trabajo es un orden de magnitud superior a los valores reportados en trabajos anteriores para el uso de disolventes convencionales. Por su parte el valor de la energía de activación asociada a la interacción química IL-CO<sub>2</sub> es más bajo que los valores previamente reportados para otros disolventes.

Una simulación teórica también se recoge en esta publicación, con el objeto de estimar los parámetros de operación requeridos para lograr un 90% de captura al CO<sub>2</sub> operando con módulos de PVDF y para cuantificar los efectos de intensificación respecto a la absorción de CO<sub>2</sub> en una columna de relleno.

*Original abstract*

Post-combustion processes based on ionic liquids and membrane contactors have emerged as new attractive alternatives to traditional systems. In this work, a gas stream composed of 15% CO<sub>2</sub> and 85% N<sub>2</sub> flowed through the lumen side of a hollow fibre membrane contactor containing PVDF-IL fibres. An ionic liquid, 1-ethyl-3-methylimidazolium acetate [emim][Ac], was used as an absorbent due to its high chemical absorption and high CO<sub>2</sub> solubility. The overall mass transfer coefficient, activation energy, and resistances of the hollow fibre membrane were quantified from 303 to 343 K. The  $K_{overall}$  value was one order of magnitude higher than those reported in previous works using conventional solvents, and the  $E_a$  was lower than previously reported values for other solvents.

A theoretical simulation was conducted to estimate the operational parameters required for 90% CO<sub>2</sub> capture and to quantify intensification effects in contrast to CO<sub>2</sub> absorption in a packed column.



**PVDF MEMBRANE CONTACTOR FOR CO<sub>2</sub> CAPTURE  
USING THE IONIC LIQUID [Emim][Ac]: MASS TRANSFER ANALYSIS**

*Lucia Gómez-Coma\*, Aurora Garea, Angel Irabien*

*Universidad de Cantabria, Departamento de Ingenierías Química y Biomolecular, E.T.S. de Ingenieros Industriales y Telecomunicación, Universidad de Cantabria, Avda Los Castros s/n 39005 Santander, Spain*

\*Corresponding author: Tel: +34 942 206777, Fax: +34 942 201591

email: gomezcomal@unican.es

*This article contributes to carbon capture absorption studies strongly in order to advance in the intensified process. A novel technique using a PVDF hollow fibre membrane contactor and [emim][Ac] ionic liquid as absorbent has been performed. Competitive results compared with traditional absorption towers have been accomplished. Moreover, a theoretical simulation has been achieved in order to give the bases for scaling.*

*Abstract*

Post-combustion processes based on ionic liquids and membrane contactors have emerged as new attractive alternatives to traditional systems. In this work, a gas stream composed of 15% CO<sub>2</sub> and 85% N<sub>2</sub> flowed through the lumen side of a hollow fibre membrane contactor containing PVDF-IL fibres. An ionic liquid, 1-ethyl-3-methylimidazolium acetate [emim][Ac], was used as an absorbent due to its high chemical absorption and high CO<sub>2</sub> solubility. The overall mass transfer coefficient, activation energy, and resistances of the hollow fibre membrane were quantified from 303 to 343 K. The K<sub>overall</sub> value was one order of magnitude higher than those reported in previous works using conventional solvents, and the E<sub>a</sub> was lower than previously reported values for other solvents.

A theoretical simulation was conducted to estimate the operational parameters required for 90% CO<sub>2</sub> capture and to quantify intensification effects related to CO<sub>2</sub> absorption in a packed column.

*Keywords*

*CO<sub>2</sub> capture, PVDF membrane contactors, [emim][Ac] ionic liquid, mass transfer coefficient.*

*1. Introduction*

Since the beginning of the industrial revolution, the demand for energy has dramatically increased and has typically been met by burning fossil fuels [1, 2]. The combustion of fossil fuels produces carbon dioxide gas, which should be removed from industrial flue gas streams to mitigate environmental effects [3]. The emissions of carbon dioxide to the atmosphere need therefore to be drastically reduced in order to alleviate the proven effects of global warming [4]. CO<sub>2</sub> concentration in the atmosphere has increased by more than 100 ppm since their pre-industrial levels (280 ppm), reaching 384 ppm in 2007 and nowadays this value is around 400ppm [5]. This value implies that during this period, the CO<sub>2</sub> abundance in the atmosphere increased substantially: the average rate of increase in CO<sub>2</sub> determined by direct instrumental measurements over the period 1960 to 2005 is 1.4 ppm per year [6]. The reduction of greenhouse gas concentrations in the atmosphere, especially CO<sub>2</sub>, has been a significant goal of the 21<sup>st</sup> century. The capture and reuse of CO<sub>2</sub> is typically referred to as carbon capture and utilization (CCU). Current CCU technologies and processes are at different stages of maturity. In general, technical and economical improvements are needed to make CCU competitive. The cost of synthesizing CO<sub>2</sub>-based products is highly dependent on the cost or value associated with a CO<sub>2</sub> unit. Therefore, the processing of CO<sub>2</sub> into other valuable products to mitigate climate change requires the optimization of CO<sub>2</sub> capture systems. Roussanaly et al., (2016)

reported that Carbon Capture and Storage (CCS) is regarded as one of the most promising technologies for reducing man-made carbon atmospheric emissions, and is projected to provide 14% of the reduction in manmade greenhouse gas (GHG) emissions by 2050 [7]. Three primary carbon dioxide capture methods are known: pre-combustion where CO<sub>2</sub> capture from gasified coal synthesis gas; oxy-combustion which separates oxygen from air prior to combustion and produces a nearly sequestration-ready CO<sub>2</sub> effluent and post-combustion, CO<sub>2</sub> capture from power plant flue gas [8, 9]. This work is focused on post-combustion CO<sub>2</sub> capture. Post-combustion carbon capture appears to be the most adequate strategy for integration with existing coal-fired power plants [10]. Flue gases from post-combustion processes typically comprise 10-15% CO<sub>2</sub>, 90-85% N<sub>2</sub> and minor concentrations of other gases [11].

Many methods exist for removing CO<sub>2</sub> capture. One such method utilizes absorption in aqueous solutions of alkanolamines using conventional equipment, such as packed columns, bubble columns, and spray columns [12].

In a typical post-combustion capture process, treated flue gas is passed through a chemical absorption column where solvents absorb carbon dioxide. The CO<sub>2</sub>-rich solvent is then regenerated by heating in a stripper unit. The freed CO<sub>2</sub> is then compressed for storage or use [13].

Most post-combustion processes are compatible with existing coal-fired power plant infrastructures without requiring substantial changes to basic combustion technologies. These processes are leading candidates for retrofitting gas-fired power plants and are promising for the development and commercialisation of integrated coal gasification combined cycle (IGCC) in power generation applications [14].

Hollow fibre gas-liquid membrane contactors are alternatives to conventional gas absorption systems for CO<sub>2</sub> capture. A membrane contactor combines the advantages of membrane technology with those of an absorption liquid [15]. Hollow fibre membrane contactors could potentially overcome the disadvantages of conventional absorption systems and develop more effective CO<sub>2</sub> capture technologies [16]. These membranes are flexible in operation and maintenance, modular, energy efficient, ease of install by skid-mounting, ability to be applied in remote areas (such as offshore) and have high specific surface areas [17]. The absorption process provide very high selectivity and high driving forces for mass transfer even at very low concentrations [18]. The separation of two phases by the membrane leads to the prevention of flooding and foaming of the absorbent liquid [19].

As a means for process intensification, membrane contactors were recently explored by Bounaceur et al. (2012), and Favre (2011) [20, 21]. The application of these contactors include a large number of fields where chemical or physical absorption is the natural separation technology, i.e., natural gas sweetening and dehydration and post and pre-combustion CO<sub>2</sub> capture. A rigorous comparison of the effective intensification potential of membrane contactors with packed columns is necessary to more accurately determine the mass transfer intensification factor, which has been reported over a broad range, i.e., from 0.8 to 10 (with MEA for CO<sub>2</sub> absorption) [20].

A literature review shows that most studies in this area have focused on the absorption of carbon dioxide by hollow fibre microporous membranes comprising hydrophobic polymers, such as poly(propylene) (PP), poly(ethylene) (PE), poly(tetrafluoroethylene) (PTFE) and poly(vinylidene fluoride) (PVDF) [19].

Poly(vinylidene fluoride) (PVDF) membranes have low surface energy values [22]. Many advantages make this polymer a promising candidate to capture carbon dioxide using hollow fibre membrane contactors. PVDF is a hydrophobic polymer and can be dissolved in common solvents to prepare asymmetric membranes via phase-inversion [23]. Hence it can easily be converted to asymmetric membranes via phase inversion method, resulting in easy controlled membrane structure and morphology [24]. PVDF, which has high fluorine content, is relatively

cheap and easily available [25]. Moreover, PVDF fibres have high thermal and chemical resistance along with good mechanical strength [26]. Previous authors, proposed methods to improve the properties of PVDF membranes. One of these methods is the use of a relatively neutral coagulation bath instead of pure water to prevent formation of dense skin layer [24, 27, 28]. The coagulation bath could be formed by water and N,N-dimethylacetamide (DMAc) or N-Methyl-2-pyrrolidone (NMP). DMAc is the most commonly used solvent but NMP satisfies the kinetic criterion coagulation and allows the production of permeable membranes [28]. For this reason, the fabrication parameters during phase-inversion can be controlled to develop appropriate membrane structures for contactor applications [22]. Some previous works supported the use of PVDF membrane contactors in order to capture CO<sub>2</sub> [29-31].

Alkanolamines have been traditionally used for carbon dioxide capture due to their low costs and high reactivity with CO<sub>2</sub>. Alkanolamines are able to form weakly bound complexes with CO<sub>2</sub> to produce effluent streams with very low CO<sub>2</sub> concentration. However, the regeneration temperature for the CO<sub>2</sub>-rich solutions is usually higher than 393 K, which would induce thermal degradation and the volatile loss of solvents [32]. Other problems using these solvents are energy consumption for absorbent regeneration, corrosion of industrial equipment materials and foam production [33].

The combination of ionic liquids (ILs) with membrane technology provides new ways to make membrane-based separations a more competitive CO<sub>2</sub> separation technology [34]. Many studies have improved CO<sub>2</sub> absorption capacities by taking advantage of the tunable properties of ILs [11].

ILs have remarkable properties, such as negligible volatility, high thermal stability, inflammability, tunability, solvation properties, and high CO<sub>2</sub> solubility [35]. ILs could potentially replace traditional industrial solvents, which are often volatile organic compounds (VOCs) [11]. A few ionic liquids have been found to have high solubility capacities for CO<sub>2</sub> and SO<sub>2</sub> and have been studied as potential absorption liquids [36, 37].

ILs with acetate anions possess high degree of absorption for CO<sub>2</sub> across a wide range of temperatures [38]. To achieve a high CO<sub>2</sub> absorption efficiency, a liquid with a high CO<sub>2</sub> diffusion coefficient and/or a high CO<sub>2</sub> solubility is required. For this reason. In this work, 1-ethyl-3-methylimidazolium acetate ([emim][Ac]) ionic liquid was used. This IL is an ideal candidate for CO<sub>2</sub> capture due to its high CO<sub>2</sub> solubility (8.6%) and physical and chemical absorption [39-42]. Additionally, this ionic liquid has been used in other applications, e.g., as a corrosion inhibitor [43]. Carbon dioxide chemisorption by [emim][Ac] has been demonstrated by previous works using NMR spectroscopy and X-ray diffraction [41, 44]. Gurau et al. (2011) proposed a possible reaction of CO<sub>2</sub> with [emim][Ac] [44]. Figure 1 shows the molecular structure of the IL, and a possible reaction mechanism with CO<sub>2</sub>, and the formation of a corresponding imidazolium carboxylate. [emim][Ac] has been well-characterised in other studies [45-47]. Moreover, Carvalho et al.(2009) suggested a preferential interaction of the acid carbon of the CO<sub>2</sub> molecule with the carboxylate group of the acetate anion [48].

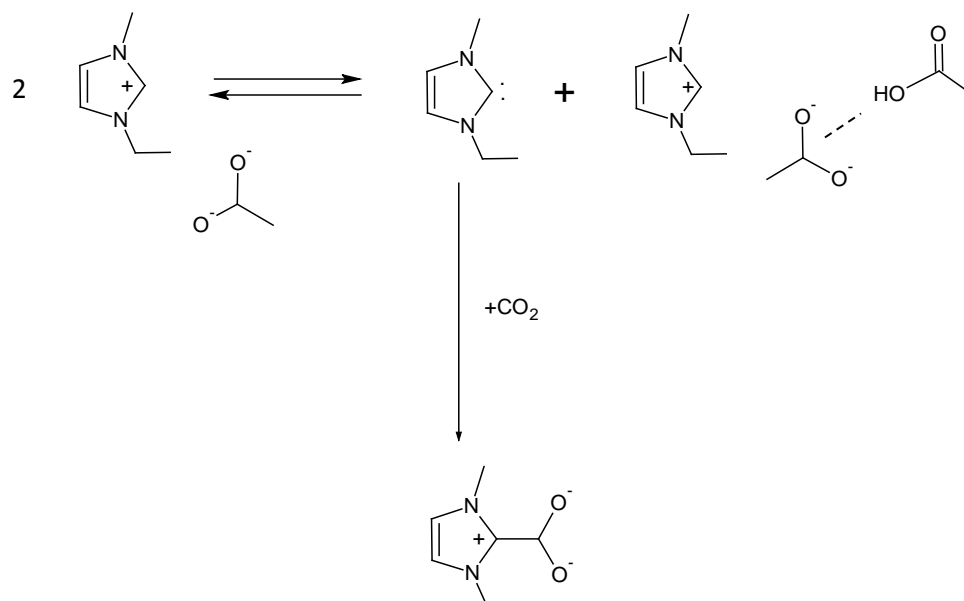


**Figure 1:** Proposed reaction of CO<sub>2</sub>-[emim][Ac] [44].

An intense study of self-made PVDF immobilized with [emim][Ac] hollow fibre membrane contactor using [emim][Ac] were used for the non-dispersive absorption of CO<sub>2</sub>. PVDF membranes due to its high hydrophobicity could be used with ionic liquids and therefore allows working in non-wetted mode. On other hand, it is worth recalling that this ionic liquid possess a carboxylic anion and therefore is promising for CO<sub>2</sub> capture. Moreover, [emim][Ac] has a reversible interaction with CO<sub>2</sub>. This property is a key factor for the regeneration ability of the IL in its industrial application. The CO<sub>2</sub> capture efficiency and mass transfer coefficient  $K_{\text{overall}}$  were also evaluated. Gas, membrane and liquid resistances were also calculated. The obtained values were compared with those reported in the literature. A numerical analysis was carried out to estimate mass transfer effects. The membrane mass transfer coefficient, membrane dimensions, and module design were evaluated to determine whether a significant intensification effect was observed for a membrane contactor when compared with a conventional packed column. The aim of the numerical analysis performed in this work is to contribute to this objective. Additional work on membrane contactors may focus on optimizing membrane geometry and module design. Future work could develop rigorous models essential for the successful scale-up and evaluation of membrane contactors in various applications [49].

## 2. Experimental

### 2.1 Hollow fibre membranes

Poly(vinylidene fluoride) (PVDF) hollow fibre membranes with additives called 1AQ2 fibres were homemade-cast via phase-inversion. The PVDF material was HSV900 grade from Arkema (France). N-methyl-pyrrolidone (NMP) was used as a solvent, and LiCl (Aldrich-France) with a block copolymer were used as additives. The 1AQ2 fibres were composed of 15% PVDF HSV900, 3% block copolymer, 3% LiCl and 1% water [28, 50]. The fibre manufacturing method was explained in detail in a previous works [28, 50-53]. The composition of the fibres were water/NMP:70/30% [28]. Additives first are dissolved in the solvent for 24 hours under mechanical stirring in a water bath at 323K by condensing vapors to prevent solvent evaporation. PVDF is then added raising the temperature to 330K to facilitate dissolution. Removing air bubbles trapped in the collodion by putting the primary vacuum to 353K. Collodions then stored at 323K until use. Besides the dimensions and design of the extrusion die, the operator can play during manufacture of flow rates and temperatures of the internal

liquid collodion and the composition of the internal fluid, the air gap (distance between the die and the coagulation bath), the humidity in the air, the composition and emperature of the coagulation bath and the spinning speed imposed by the cylinders, ten operating parameters, to modify the properties of the manufactured fibre [28]. After phase-inversion, 150mL of IL was added to the developed membrane in continuous stirring during 48h at room temperature. Finally, the virgin fibres were dried after adding the IL. Subsequently, 1-ethyl-3-methylimidazolium acetate [emim][Ac] was immobilized into the fibres.

During drying, the fibres were maintained for approximately 72 hours in an oven at 323 K and atmospheric pressure.

The membrane contactor was manufactured by gluing hollow fibres in a PVC shell. In the 1AQ2 hollow fibre membrane contactor, 11 fibres were assembled. The main characteristics of the membrane contactors are shown in Table 1.

**Table 1:** Hollow fibre membrane contactor characteristics.

Membrane material	1AQ2-PVDF
Fibre o.d. $d_o$ , (m)	$7.7 \cdot 10^{-4}$
Fibre i.d. $d_i$ , (m)	$4.51 \cdot 10^{-4}$
Fibre length, $L$ (m)	0.295
Number of fibres, $n$	11
Effective inner membrane area, $A$ ( $\text{m}^2$ )	$4.60 \cdot 10^{-3}$
Porosity (%)	30
Packing factor	0.04
Tortuosity <sup>a</sup>	3.33

## 2.2 $\text{CO}_2$ capture process

A gas-liquid membrane contactor module was used in order to determine the membrane mass transfer resistance and study the effect of operating parameters on  $\text{CO}_2$  absorption. The membrane has been checked with pure  $\text{CO}_2$  from 0 to 14 bar. At these pressures the fibres were stable and the membrane did not suffer degradation. This could imply that the ionic liquid filled the pores, and thus, the gas was unable to enter fibres. This is a good quality for the fibers because the membrane works in non-wetted mode because the pores are completely filled.

The experimental setup is shown in Figure 2. The feed Gas stream contained 15 vol.%  $\text{CO}_2$  and 85 vol.%  $\text{N}_2$ . The flow gas was adjusted using a mass flow controller (Brooks Instrument MFC 5850, Emerson Process Management, Spain). As can see, there is a rotameter in order to check that the mass flow controllers are calibrated. Feed gas was directed through the inside of the hollow fibres. The gas flow rate varied from 20 to 70  $\text{mL min}^{-1}$ . 1-Ethyl-3-methylimidazolium acetate flowed in a counter-current direction through the shell side. The IL was pumped from a storage tank. The liquid line ( $50 \text{ mL min}^{-1}$ ) was maintained by a digital gear pump (Cole Parmer Instrument Company, Hucoa-Erloss S.A, Spain).

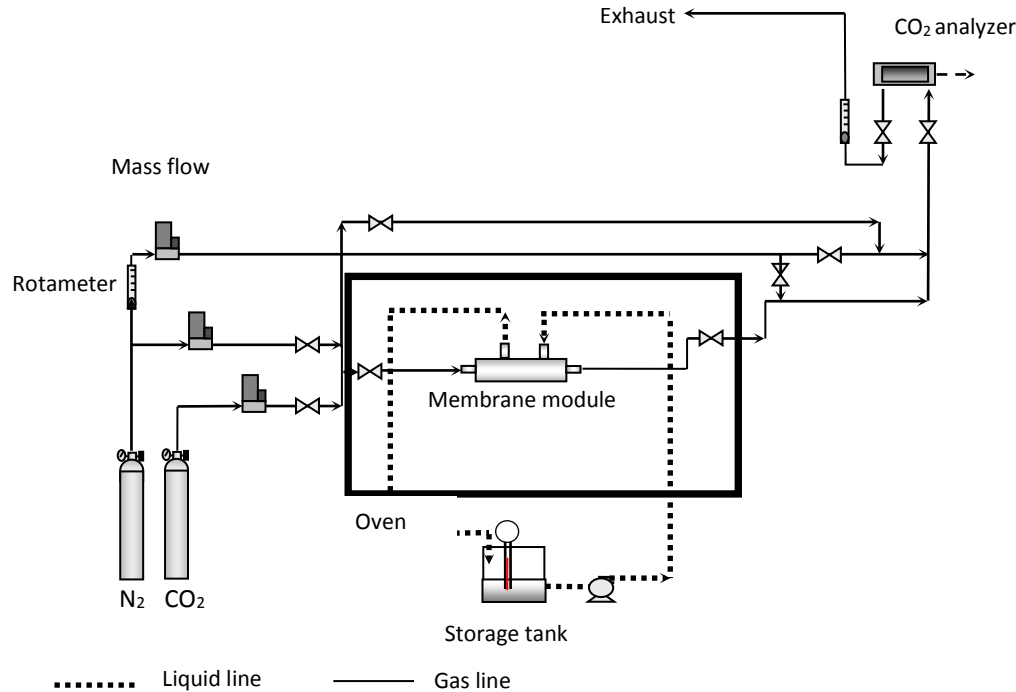


**Figure 2:** Experimental setup for CO<sub>2</sub> gas capture.

The experiments were performed over the temperature range of 303-343 K. Each experiment was replicated three times, and the average value was calculated. To maintain isothermal conditions, the hollow fibre membrane contactor and the liquid line were kept in an oven.

Previous studies have reported that [emim][Ac] can be regenerated without degradation [38, 51]. For this propose, a N<sub>2</sub>-rich gas stream was directed through the lumen side of the hollow fibre membrane until the analyser indicated that the CO<sub>2</sub> concentration was constant and near zero. Previous works have demonstrated that [emim][Ac] exhibited a strong but reversible chemical absorption for CO<sub>2</sub> and that [enim][Ac] is similar to other ionic liquids, such as [bmim][Ac], due to the presence of an imidazolium cation and an acetate anion [40, 53]. It was not necessary change the ionic liquid during the whole experimental planning.

The CO<sub>2</sub> concentration of the outlet gas stream was continuously monitored by sampling a fraction of the stream using a gas analyser (Emerson Process) based on non-dispersive infrared (NDIR) spectroscopy. Before sending the gas sample to the analyser, the sample was diluted with N<sub>2</sub> to maintain a constant concentration range for the NDIR analyser (at least 200 mL min<sup>-1</sup>). A steady state condition was indicated by a constant CO<sub>2</sub> concentration in the exit gas stream.

### 3. Results and discussion

#### 3.1. CO<sub>2</sub> capture efficiencies with [emim][Ac] in a PVDF membrane module.

Carbon dioxide absorption experiments with 1-ethyl-3-methylimidazolium acetate were carried out in a PVDF membrane contactor to evaluate the CO<sub>2</sub> capture efficiency at different temperatures. The outlet concentration of carbon dioxide at pseudo-steady-state was calculated using equation 1:

$$Efficiency (\%) = \left( 1 - \frac{C_{CO_2,out}}{C_{CO_2,in}} \right) \cdot 100 \quad (1)$$

where  $C_{CO_2,out}$  is the outlet concentration of CO<sub>2</sub> and  $C_{CO_2,in}$  is the inlet concentration of CO<sub>2</sub>

(15%).

The CO<sub>2</sub> removal efficiencies were calculated from the inlet and outlet CO<sub>2</sub> concentrations for the absorption experiments (Table 2). The experiments were performed at different temperatures with gas flow rates of 20 mL min<sup>-1</sup> and 70 mL min<sup>-1</sup> using a 1AQ2-PVDF membrane contactor. The efficiency increased when the temperature increased, especially from 303 to 313 K. The experimental error in Table 2 is the deviation of the results of at least three replicated experiments. Within this range, there was a sharp drop in viscosity and low solubility losses.

**Table 2:** Experimental CO<sub>2</sub> absorption efficiency.

Q <sub>g</sub> (mL min <sup>-1</sup> )	T (K)	Efficiency (%)
20	303	20.5±2.27
	313	27.1±3.01
	323	28.6±2.51
	333	29.3±1.83
70	303	8.2±0.18
	313	9.6±0.35
	343	11.5±0.26

Based on the results, the following observations were made: (i) as the gas flow decreased, higher residence times were recorded in the contactor and the efficiency increased; and (ii) the efficiency also increased when the temperature increased. At a gas flow rate of 20 mL min<sup>-1</sup>, the absorption efficiency was 20.5% at 303 K and 29.3% at 333 K. These values allow the non-dispersive absorption using PVDF membranes and [emim][Ac] ionic liquid be considered as a promising technique for carbon dioxide capture. In addition, working at 333K, coupled seven modules in series disposition with a gas a flow rate of 20 mL min<sup>-1</sup> around 90% of CO<sub>2</sub> recovery could be reached. On the other hand it is possible to place as many modules in parallel as be necessary for other gas flow rates.

### 3.2 Overall mass transfer parameter of CO<sub>2</sub> absorption with [emim][Ac] in a PVDF membrane module.

In industrial applications, the mass transfer coefficient is a crucial parameter used to estimate the size of a contactor [54]. This parameter is a diffusion rate constant that relates the mass transfer rate, mass transfer area, and concentration change as driving force.

The overall transfer coefficient,  $K_{overall}$ , can be experimentally determined from the CO<sub>2</sub> flux through the membrane. This parameter is calculated using equation 2 (Table 3):

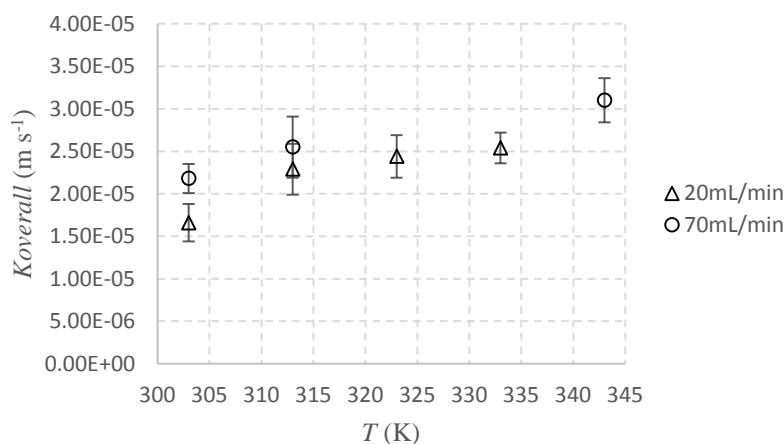
$$N_{CO_2,g} = \frac{Q_g}{A} (C_{CO_2,in} - C_{CO_2,out}) = K_{overall} \frac{\Delta y_{lm} \cdot P_T}{RT} \quad (2)$$

where  $Q_g$  is the gas flow rate (m<sup>3</sup> s<sup>-1</sup>),  $A$  is the membrane area (m<sup>2</sup>),  $P_T$  is the total pressure in the gas phase, and  $\Delta y_{lm}$  is the logarithmic mean of the driving force based on the gas phase molar fractions.

Table 3 shows the values  $K_{overall}$  at different gas flow rates using a hollow fibre membrane contactor with 1AQ2 fibres. The temperature was varied from 303 to 343 K. Figure 3 shows the different values obtained at flow rates of 20 and 70 mL min<sup>-1</sup>. The trend was the same as that in the previous section. The differences were greater from 303 to 313 K due to the influence of viscosity and minimal variation in solubility.

**Table 3:**  $K_{overall}$  values of CO<sub>2</sub> absorption with [emim][ac] in a PVDF hollow fibre membrane modules.

Qg(mL min <sup>-1</sup> )	T(K)	$K_{overall} \cdot 10^5$ (m s <sup>-1</sup> )
20	303	1.7±0.2
	313	2.3±0.3
	323	2.4±0.3
	333	2.5±0.2
70	303	2.2±0.2
	313	2.6±0.4
	343	3.1±0.3


**Figure 3:** Representation of  $K_{overall}$  values versus temperature.

### 3.3. A resistance-in-series approach for CO<sub>2</sub> absorption with [emim][Ac] in the PVDF membrane module.

The resistance-in-series approach can be used to correlate individual mass transfer resistances to the overall mass transfer resistance,  $K_{overall}$ .  $K_{overall}$  is given by the summation of the gas, membrane and liquid film resistances, as indicated in equation 3 [36, 51, 55]:

$$R_{overall} = R_g + R_m + R_l \quad (3)$$

The liquid phase and gas phase were directed through a hollow fibre configuration in the shell side and lumen side, respectively. The mass transfer process consisted of three consecutive steps: diffusion of a gaseous component from the bulk gas phase to the outer surface of the membrane, diffusion through membrane pores to the gas-liquid interface and chemical reaction at the gas-liquid interface [56].

CO<sub>2</sub> absorption essentially takes place at the gas-liquid interface. The role of liquid hydrodynamic distribution (i.e., solvent velocity profile) can be expected to play a minor role [20].

The resistance in series approach (Equation 3) can also be expressed as Equation 4:

$$\frac{1}{K_{overall}} = \frac{d_0}{k_g d_i} + \frac{d_0}{k_{mg} d_{lm}} + \frac{1}{k_l H_d E} \quad (4)$$

where  $d_o$ ,  $d_i$  and  $d_{lm}$  are the outside, inside and log mean diameters (m) of the hollow fibres;  $k_g$ ,  $k_{mg}$ , and  $k_l$  are the individual mass transfer coefficients of the gas phase, membrane and liquid phase, respectively ( $\text{m s}^{-1}$ );  $E$  is the enhancement factor, this factor can be quantified the chemical reaction effect [39, 55, 57];  $K_{overall}$  is the overall mass transfer coefficient ( $\text{m s}^{-1}$ ) and  $H_d$  is the dimensionless Henry constant.  $H_d$  was calculated by Eq. 5 using the Henry's law constant ( $H_c$ ) [55]:

$$H_d = H_c RT \quad (5)$$

Finally,  $k_l$  was estimated using Kartohardjono's correlation (Eq. 6) because the packing factor and Reynolds number were within range ( $0.029 < \phi < 0.53$ ;  $Re < 400$ ) [39]:

$$Sh = \left( \frac{k_l d_h}{D_{CO_2,l}} \right) = 0.1789 (\phi^{0.86}) Re^{0.34} Sc^{\frac{1}{3}} \quad (6)$$

where  $D_{CO_2,l}$  is the diffusion coefficient of carbon dioxide in the liquid,  $L$  is the fibre length and  $d_h$  is the hydraulic diameter.

The gas and membrane phases had resistances of 0.02% and 0.23% of the overall resistance, respectively (Table 4). The liquid phase had the highest resistance to mass transfer at nearly 100% of the overall resistance. This was consistent with the obtained results in previous works [36, 39, 51, 55].

**Table 4:** Contributions to mass transfer. CO<sub>2</sub> absorption with [emim][Ac] in a PVDF membrane module.

Qg (mL min <sup>-1</sup> )	T (K)	Rtotal · 10 <sup>-4</sup> (s m <sup>-1</sup> )	Rg (s m <sup>-1</sup> )	Rm · 10 <sup>-2</sup> (s m <sup>-1</sup> )	RI · 10 <sup>-4</sup> (s m <sup>-1</sup> )
20	303	6.02	7.5	1.4	6.0
	313	4.37	7.1	1.3	4.4
	323	4.10	6.4	1.2	4.1
	333	3.98	6.0	1.1	4.0
70	303	4.59	7.4	1.4	4.6
	313	3.92	7.0	1.3	3.9
	343	3.23	6.0	1.1	3.2

Figure 4 shows the logarithm plot of the different resistances against temperature. As expected, different resistance values of gas, liquid and membrane overlapped for different gas flow rates.

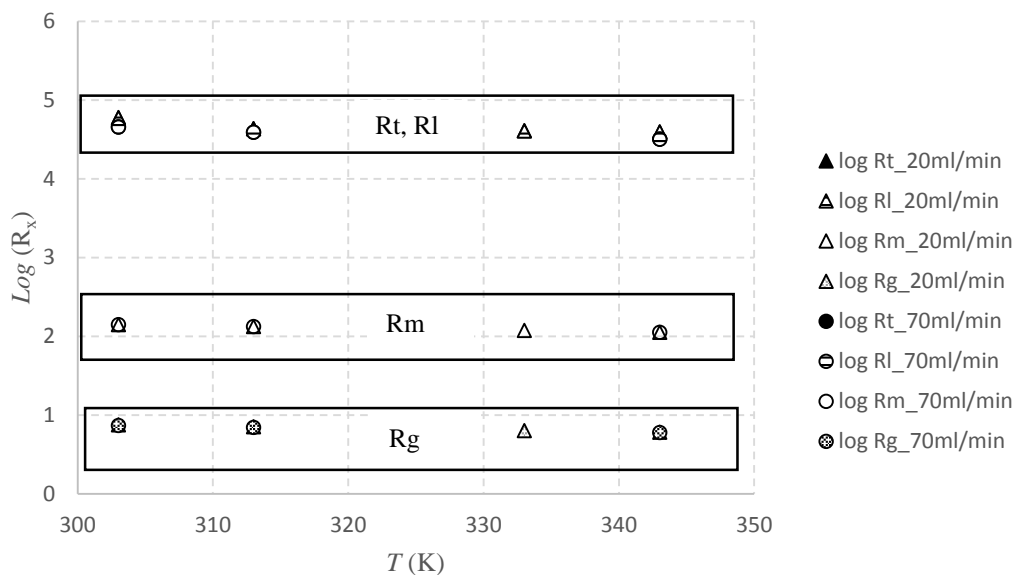


**Figure 4:** Log Rx Vs Temperature.

#### 3.4. Mass transfer enhanced by the chemical reaction for CO<sub>2</sub> absorption with [emim][Ac] in the PVDF membrane module.

Gurau et al. (2011), reported on the single-crystal X-ray structures of solid-state products obtained from the reaction of CO<sub>2</sub> with acetate ILs, which confirm the reaction mechanism: the crystal structure confirmed the formation of imidazolium carboxylate molecules (Figure 1) [44].

In order to contribute to the analysis of the chemical reaction, an approach from the mass transfer results was carried out. The obtained values of  $K_{overall}$  were transformed using equation 7 to compare the results from the 1AQ2 hollow fibre module with previously reported values. The transformed constant,  $K_r$  (s<sup>-1</sup>) may agreed with a first-order, gas-liquid chemical reaction, indicating the accumulation of CO<sub>2</sub> in the liquid media [36].

$$K_r = K_{overall} \frac{\text{fiber area}}{\text{shell volume}} \quad (7)$$

The component diffusivities and the reaction rate steadily increased with the temperature. The solubility decreased as the temperature increased. The temperature increased as a response to competing phenomena and had an opposite effect on the reaction rate and solubility. This could lead to a complex absorption behaviour [56].

Table 5 compares the overall rate constant and transformed rate constant of the PVDF hollow fibre membrane contactor with other reports in the literature for different types of solvent [54, 59-65]. The fibre sizes in the 1AQ2 membrane contactor agreed with those of the literature. Mansourizadeh et al., used fibres with similar inner and outer diameters,  $7.50 \cdot 10^{-4}$  and  $4.20 \cdot 10^{-4}$  m, respectively [60, 61]. Taking into account the number of fibres, several authors used between 5 and 11 [54, 60-64]. However, Rongwong et al. and Wang et al., each used 35 and 150 fibres, respectively [59, 62]. For this reason, the ratios between the fibre area and the shell volume were higher in these cases.

**Table 5:** Fibre size,  $K_{\text{overall}}$  ( $\text{m s}^{-1}$ ) and  $K_r$  ( $\text{s}^{-1}$ ) comparison with literature values in PVDF contactors.

Reference	Fibre o.d., m	Fibre i.d., m	Fibre length, m	Module length, m	Module diameter, m	Number of fibres, n	Fibre Area/Shell volume, $\text{m}^2 \cdot \text{m}^3$	Solvent	$K_{\text{overall}} \cdot 10^5 (\text{m s}^{-1})$	$K_r \cdot 10^3 (\text{s}^{-1})$
This work	$7.70 \cdot 10^{-4}$	$4.51 \cdot 10^{-4}$	$2.95 \cdot 10^{-1}$	$2.95 \cdot 10^{-1}$	$1.30 \cdot 10^{-2}$	11	122	IL [emim][ac]	1.7	2
[54]	$8.00 \cdot 10^{-4}$	$5.50 \cdot 10^{-4}$	$2.10 \cdot 10^{-1}$	$2.50 \cdot 10^{-1}$	$1.50 \cdot 10^{-2}$	10	84	Distilled water	1.26	1.06
[59]	$1.30 \cdot 10^{-3}$	$8.00 \cdot 10^{-4}$	$2.95 \cdot 10^{-1}$	$2.95 \cdot 10^{-1}$	$1.00 \cdot 10^{-2}$	35	2742	1M MEA 1M AMP 1M DEA Pure water	0.08 0.04 0.03 0.01	2.06 1.1 0.82 0.27
[60]	$7.50 \cdot 10^{-4}$	$4.20 \cdot 10^{-4}$	$1.50 \cdot 10^{-1}$	$2.70 \cdot 10^{-1}$	$1.40 \cdot 10^{-2}$	10	48	Distilled water	0.25	0.12
[61]	$7.50 \cdot 10^{-4}$	$4.20 \cdot 10^{-4}$	$1.50 \cdot 10^{-1}$	$2.70 \cdot 10^{-1}$	$1.40 \cdot 10^{-2}$	10	48	Distilled water	0.43	0.21
[62]	$1.10 \cdot 10^{-3}$	$8.00 \cdot 10^{-4}$	$2.40 \cdot 10^{-1}$	$2.40 \cdot 10^{-1}$	$4.00 \cdot 10^{-2}$	150	338	1M MEA	0.09	0.32
[63]	$8.50 \cdot 10^{-4}$	$4.75 \cdot 10^{-4}$	$1.50 \cdot 10^{-1}$	$2.70 \cdot 10^{-1}$	$1.40 \cdot 10^{-2}$	10	55	Distilled water	0.49	0.27
[64]	$1.27 \cdot 10^{-3}$	$7.52 \cdot 10^{-4}$	$4.50 \cdot 10^{-1}$	$4.50 \cdot 10^{-1}$	$8.05 \cdot 10^{-3}$	5	265	MEA	0.33	0.88
[65]	$8.09 \cdot 10^{-4}$	$4.54 \cdot 10^{-4}$	$2.70 \cdot 10^{-1}$	$1.75 \cdot 10^{-1}$	$1.40 \cdot 10^{-2}$	7	104	Distilled water	0.32	0.33

Regarding  $K_{overall}$ , the obtained values for this study were almost one order of magnitude higher than previous works (Table 5) that used traditional solvents, such as monoethanolamine (MEA), diethylamine (DEA), adenosine monophosphate (AMP) and water. As the different parameters such as outer and inner fibre diameter, module length, number of fibres and the fibre area/shell volume are in concordance with the previous articles, the high overall mass transfer coefficient implies that the transfer carbon dioxide-ionic liquid is more facilitated than with traditional solvents. Moreover, these solvents have been traditionally associated with some operational problems due to volatility and solvent losses. Ionic liquids can be used to eliminate these drawbacks. Therefore it is worth recalling that the ILs have a number of advantages over traditional solvents, such as negligible vapour pressures, high thermal, electrochemical and chemical stability and loss less regenerative abilities [11, 35].

As in the previous sections, different values of  $K_r$  were calculated for the different temperatures and flow gas streams (Table 6).

**Table 6:** Interfacial rate constant versus temperature, CO<sub>2</sub>+[emim][ac], PVDF hollow fibre contactor.

Qg(mL min <sup>-1</sup> )	T(K)	$K_r \cdot 10^3$ (s <sup>-1</sup> )
20	303	2.0
	313	2.8
	323	3.0
	333	3.1
70	303	2.7
	313	3.1
	343	3.8

Using the Arrhenius equation and the different values of  $K_r$  at different gas flow rates (Table 6), the activation energy was calculated according to equation 8.

$$K_r = B \cdot e^{\frac{-Ea}{R \cdot T}} \quad (8)$$

where  $B$  is a pre-exponential factor,  $Ea$  is the activation energy (J mol<sup>-1</sup>),  $R$  is the gas constant 8.31 (J K<sup>-1</sup> mol<sup>-1</sup>), and  $T$  is the temperature (K). The activation energy for [emim][Ac] in CO<sub>2</sub> was 9.2 kJ mol<sup>-1</sup> with a confidence of  $R^2=0.92$ .

Table 7 compares the activation energy obtained in the present work with values for different ionic liquids in the literature [66-70]. A few observations can be made: (i) ionic liquids in the presence of other solvents, such as MEA, AMP, aprotic heterocyclic anions (AHA) or water, have higher activation energies than the value obtained herein [65-68]; and (ii) when ILs were not mixed with other solvents, the reported activation energy value agreed with the value calculated in this work. For the same [P<sub>66614</sub>] cation, Burkan et al., reported activation energies of 18 and 11 kJ mol<sup>-1</sup> for the anions [3-CF<sub>3</sub>pyra] and [2-CNpyr], respectively [70].

The reported  $Ea$  values for conventional solvents, such as amines (which react with CO<sub>2</sub>), ranged from 40-55 kJ mol<sup>-1</sup> [70]. These values were significantly higher than the results obtained in this work using the ionic liquid [emim][Ac]. This phenomenon can be explained by a differences in the coupling mechanisms, interfacial reactions and mass transfer in the liquid phase.

**Table 7:** Activation energy comparison with literature values.

Reference	Liquid	Ea kJ mol <sup>-1</sup>
This work	[emim][ac]	9.2
[66]	[n2224][CH <sub>3</sub> COO]-nH <sub>2</sub> O	21.1
[67]	4mol·L <sup>-1</sup> MDEA	43.32
[67]	4mol·L <sup>-1</sup> MDEA+2mol·L <sup>-1</sup> [Bmim][BF <sub>4</sub> ]	8.65
[68]	[N <sub>1111</sub> ][Gly] + AMP	40.7
[69]	30%MEA+65%[Bmim][NO <sub>3</sub> ]+5% H <sub>2</sub> O	77.11
[69]	30%MEA+60%[Bmim][NO <sub>3</sub> ]+10% H <sub>2</sub> O	63.69
[70]	[P <sub>66614</sub> ][3-CF <sub>3</sub> pyra]	18
[70]	[P <sub>66614</sub> ][2-CNpyr]	11
[70]	[P <sub>66614</sub> ][Pro]+(AHA)	43
[70]	[N <sub>1111</sub> ][Gly]	15.4
[70]	2-((2-Aminoethyl)amino)-ethanol	32.5

An approach to describe the overall temperature dependence in reactive absorption processes has been applied to hollow fibre membrane contactors by Boucif et al. (2015) [58], based on the Shah criterion [71]. The use of an effective activation energy was proposed in terms of a parameter  $\gamma_{eff}$  calculated using the Equation 9.

$$\gamma_{eff} = \frac{1}{2}(\gamma_{Da} + \gamma_R) - \gamma_s \quad (9)$$

where  $\gamma$  are dimensionless activation energies, assuming that the solubility, the diffusivity and the reaction rate constant are Arrhenius type dependent on temperature.

$\gamma_{eff}$  explains two different phenomena, on one hand an increase in diffusivity and reaction rate and on the other hand a reduction in solubility for a rise in temperature. Boucif et al., reported the different meanings of  $\gamma_{eff}$  as a function of its positive, negative or zero value [58].

The values of  $\gamma_{eff}$  obtained in this work for the interaction CO<sub>2</sub>-[emim][Ac] are slightly upper than zero (0.4). Thus, the increase in reaction rate coefficient and diffusion coefficient with temperature may play dominant role in the overall temperature dependence.

### 3.5. Simulation task to estimate mass transfer and operational effects.

A set of module conditions have been evaluated (i.e., membrane mass transfer coefficient, membrane dimensions, and module design) to determine whether a significant intensification effect was present for a membrane contactor when compared with a packed column.

A long-term, stable operation of the hollow fibre membrane contactor requires that the pores of the membrane remain completely gas-filled over prolonged operational periods. If the membranes are even partially wetted, the overall mass transfer resistance increases because the absorbed gas has to diffuse through stagnant liquid inside the pores. Because aqueous alkanolamine solutions increase the potential for membrane wetting, other absorption liquids, such as ILs, may offer higher surface tensions and more consistent performance.

The modelling of the transfer of CO<sub>2</sub> from the gas phase to the liquid phase through the membrane barrier was simulated using Aspen Custom Modeler software (Aspen Technology, Inc.). Figure 5 shows the coordinates of the fibre. The radial position  $r=0$  is the centre of the fibre, and the axial distance of  $z=0$  indicates the initial position of the gas in the fibre.

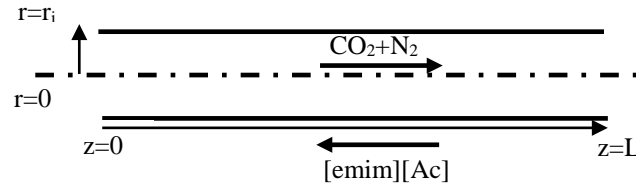


**Figure 5:** Coordinates of the fibre.

The differential mass balance on CO<sub>2</sub> (eq. 10) was based on the following assumptions: a negligible concentration of the soluble gas in the absorption liquid, steady state and isothermal conditions, no axial diffusion, ideal gas behaviour and constant tube side and shell side pressures [72, 73].

$$u_z \frac{\partial C_{CO_2}}{\partial z} = D \left[ \frac{1}{r} \frac{\partial}{\partial r} \left( r \frac{\partial C_{CO_2}}{\partial r} \right) \right] \quad (10)$$

Equation 10 can be transformed assuming the gas velocity is a fully developed laminar flow [72]:

$$2u_m \left[ 1 - \left( \frac{r}{R} \right)^2 \right] \frac{\partial C_{CO_2}}{\partial z} = D \left[ \frac{1}{r} \frac{\partial}{\partial r} \left( r \frac{\partial C_{CO_2}}{\partial r} \right) \right] \quad (11)$$

Equation 11 can be rewritten in the dimensionless form:

$$\frac{Gz}{2} [1 - \bar{r}^2] \frac{\partial \bar{C}_{CO_2}}{\partial \bar{z}} = \frac{1}{\bar{r}} \frac{\partial}{\partial \bar{r}} \left( \bar{r} \frac{\partial \bar{C}_{CO_2}}{\partial \bar{r}} \right) \quad (12)$$

where the dimensionless variables are defined as:

$$\bar{r} = \frac{r}{R} \quad (13.a)$$

$$\bar{z} = \frac{z}{L} \quad (13.b)$$

$$\bar{C}_{CO_2} = \frac{C_{CO_2}}{C_{CO_2, \text{inlet}}} \quad (13.c)$$

The boundary conditions used were the following:

$$\bar{r} = 0 \rightarrow \frac{\partial \bar{C}_{CO_2}}{\partial \bar{r}} = 0 \quad (14.a)$$

$$\bar{r} = 1 \rightarrow \frac{\partial \bar{C}_{CO_2}}{\partial \bar{r}} = -\frac{Sh}{2} \bar{C}_{CO_2} \quad (14.b)$$

$$\bar{z} = 0 \rightarrow \bar{C}_{CO_2} = 1 \quad (14.c)$$

and the dimensionless numbers:

$$Gz = \frac{u_m di^2}{D L} \quad (15.a)$$

$$Sh = \frac{K_{\text{overall}} di}{D} \quad (15.b)$$

The CO<sub>2</sub> concentration at the outlet of the module is calculated as a dimensionless mixing cup:

$$\bar{C}_{CO_2=L} = 4 \int_0^1 \bar{C}_{CO_2} [1 - \bar{r}^2] \bar{r} d\bar{r} \quad (16)$$

The modelling results for a gas flow rate of  $20 \text{ mL min}^{-1}$  and the parameters specified in Table 1 are shown in Figure 6. The  $K_{overall}$  ( $1.7 \cdot 10^{-5} \text{ m s}^{-1}$ ) obtained in paragraph 3.2 was used. Figure 6a shows the dimensionless carbon dioxide concentration and the capture efficiency along the dimensionless length at 303 K (corresponding to  $K_{overall}$  value of  $1.7 \cdot 10^{-5} \text{ m s}^{-1}$ ). Figure 6b shows the simulation results for the temperature interval 303-333 K. These results closely matched the experimental values.

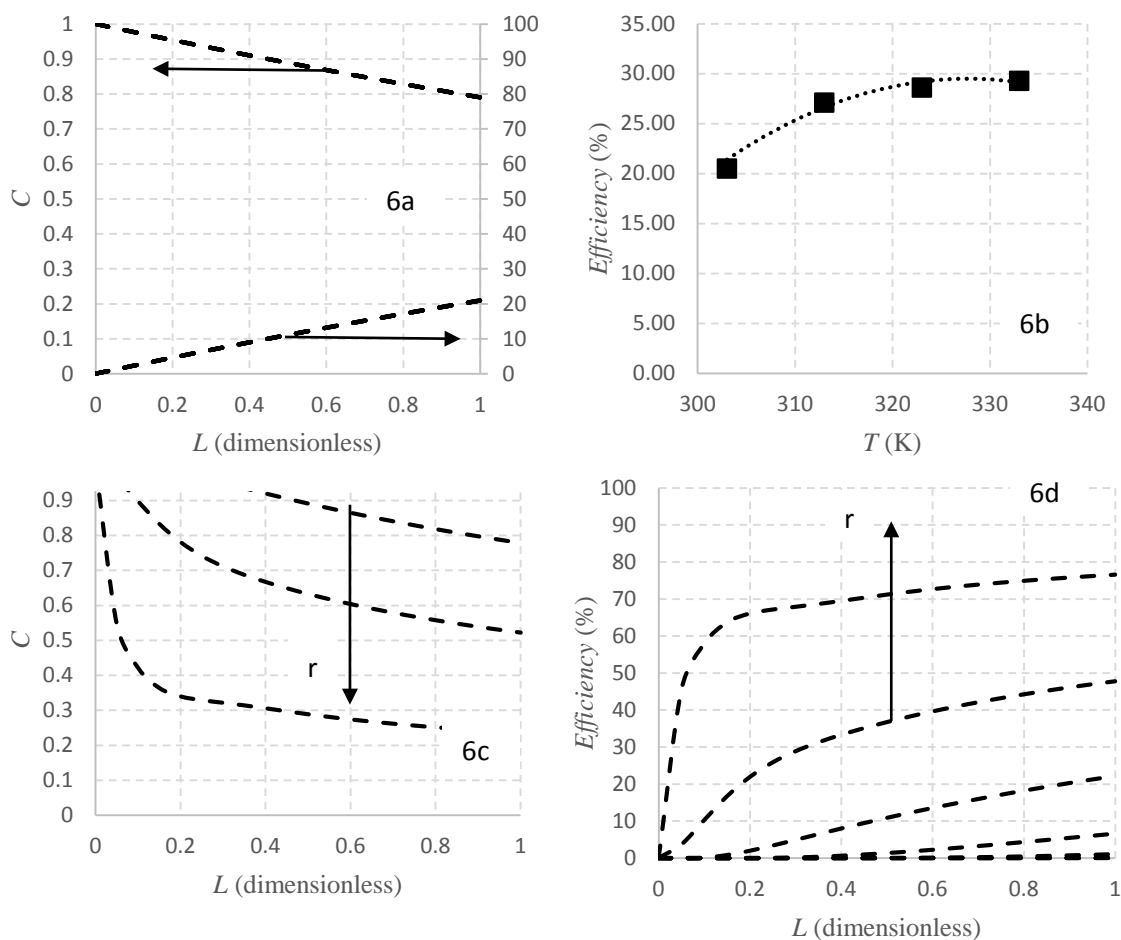


**Figure 6:** Modelling results for non-wetted mode: (6a), profiles of dimensionless CO<sub>2</sub> concentration and process efficiency (%) along the fibre length; (6b) experimental Vs. modelling results at different temperatures. Modelling results for wetted mode: (6c, 6d).

Different radial nodes are shown in these figures from the centre of the fibre ( $r=0$ ) to the membrane surface layer ( $r=1$ ). To show the difference between non-wetted and wetted modes, Figures 6a, 6c and 6d were prepared. Different nodes in the radial dimension are provided from the centre of the fibre ( $r=0$ ) to the membrane surface layer ( $r=1$ ). In the wetted mode, as the Graetz number is large, the concentration profile in the radial dimension builds up, and a significantly lower efficiency (8%) than that of the non-wetted mode was observed.

A sensitivity analysis was performed to estimate the mass transfer effect on the CO<sub>2</sub> capture efficiency operating in non-wetted mode. A 90% efficiency was the design target [21]. Previous works that reported 90% CO<sub>2</sub> capture efficiencies using PVDF membrane contactors used alkanolamines, i.e., primarily MEA [74-77]. The aim of this simulation was to determine the

parameters necessary to reach this efficiency using ionic liquids to provide a cleaner process without solvent loss.

Figure 7 shows different capture efficiencies for varying values of the mass transfer coefficient,  $K_{overall}$  (baseline,  $1.7 \cdot 10^{-5} \text{ m s}^{-1}$ ). Values greater than  $1.7 \cdot 10^{-4} \text{ m s}^{-1}$  yielded efficiencies above 90% (Figure. 7a). A more detailed analysis was carried out in Figure 7b. Values were analysed varying the Sherwood number using a fixed Graetz number. For Sherwood number values greater than  $4.7 \cdot 10^{-3}$  and a fixed Graetz number ( $8.0 \cdot 10^{-3}$ ), at least 90% efficiencies were achieved.

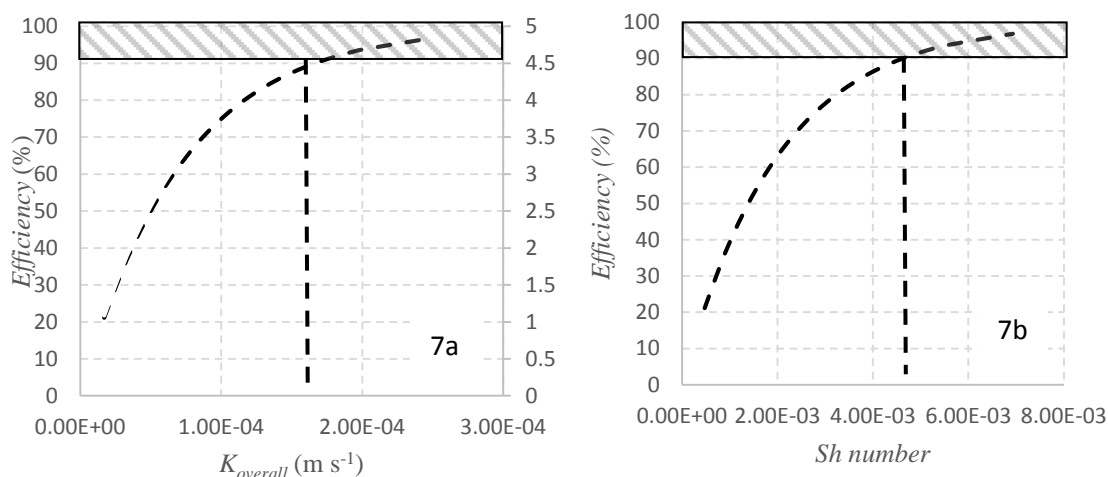


**Figure 7:** Sensitivity analysis of mass transfer coefficient,  $K$  (7a), and the corresponding Sherwood number (7b).

The intensification factor  $I$  was also calculated and shown in Figure 7a. The intensification factor reached the value of 4.5 for the target CO<sub>2</sub> efficiency of 90% and was calculated as the volumetric absorption capacity of the membrane contactor divided by the average volumetric absorption capacity of a packed column. The reference value of a classical packed column was estimated for  $1 \text{ mol CO}_2 \text{ m}^{-3} \text{ s}^{-1}$  using a 30 wt.% MEA solution [20].

Because 1-ethyl-3-methylimidazolium acetate provided higher  $K_{overall}$  values than values reported in the literature, the use of ionic liquids is vital to making membrane contactors competitive at the industrial scale.

In the design of a membrane unit module, membrane elements can be coupled in parallel and in series. In this way, the module can be easily adjusted to achieve a desired removal efficiency. In this simulation, the fibre length was also modified to estimate the number of hollow fibre membrane contactors in series necessary to achieve at least a 90% efficiency. Figure 8a shows the influence of the fibre length. Seven membrane contactors in series (a total length of 2 m) was necessary to reach the target capture efficiency. For a constant, dimensionless Sherwood number, the Graetz number was varied (Fig. 8b). Graetz values smaller than  $9.5 \cdot 10^{-4}$  allowed for high efficiencies over 90%.

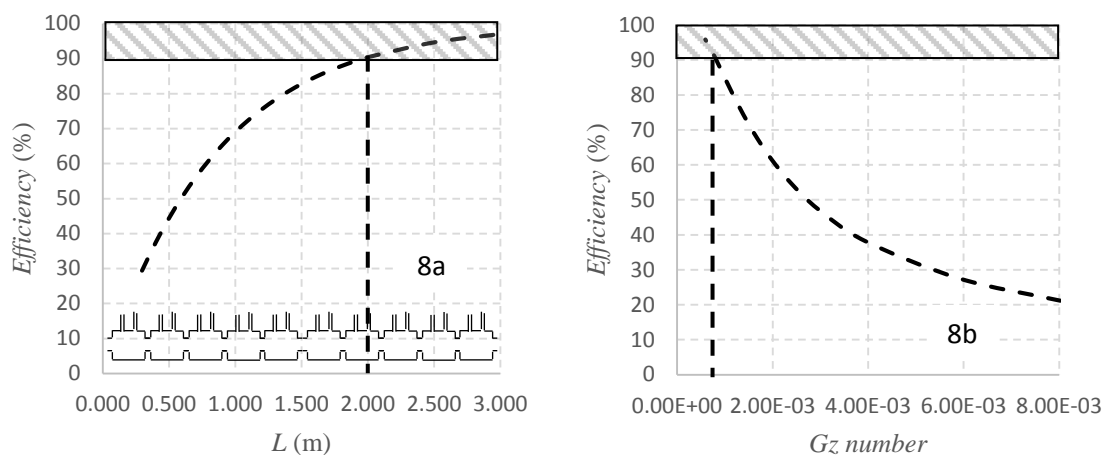


**Figure 8:** Sensitivity analysis of length module,  $L$  (8a), and the corresponding Graetz number (8b).  $K_{overall}$  obtained at 333K ( $2.5 \cdot 10^{-5} \text{ m s}^{-1}$ ) was used as reference value.

Based on these simulation results, the total fibre length of 2 m of the membrane unit should be considered during scale up. The efficiency of  $\text{CO}_2$  capture processes based on sets of membrane modules in series or in parallel that can be estimated based on the desired flue gas flow rate. Furthermore, the footprint size of the contactors could be reduced by more than 65 % if intensification factors are considered [78].

#### 4. Conclusions

The evaluation of carbon dioxide absorption using a poly(vinylidene fluoride) (PVDF)-[emim][Ac] hollow fibre contactor and 1-ethyl-3-methylimidazolium acetate [emim][Ac] absorption ionic liquid was experimentally verified. The results show that approximately 20-30% of carbon dioxide was recovered under a gas flow rate of  $20 \text{ mL min}^{-1}$  from 303 to 333 K. Gas and membrane resistances were negligible compared with the overall mass transfer resistance. Liquid resistance accounted for essentially all mass transfer resistance in the contactor modules.

The mass transfer coefficients of the PVDF membrane contactors were compared with reported values in the literature. Polymeric membranes are of great interest for this application because of their hydrophobic character, their commercial availability and reasonable price.

$\text{CO}_2$  capture using PVDF fibres achieved a  $K_{overall}$  higher than values reported in the literature for other PVDF hollow fibre membrane contactors using conventional solvents. For a gas flow rate of  $20 \text{ mL min}^{-1}$  at 303 K, the mass transfer coefficient was  $1.7 \cdot 10^{-5} \text{ m s}^{-1}$ .

Regarding the activation energy calculations, the hollow fibre membrane contactor with ionic liquid solvent had an activation energy of  $9.2 \text{ kJ mol}^{-1}$ . This energy barrier was much smaller than those obtained with conventional solvents reacting with  $\text{CO}_2$  (such as MDEA at  $43\text{-}44 \text{ kJ mol}^{-1}$ ). This may be explained by a coupling mechanism of the interfacial reaction between  $\text{CO}_2$  and [emim][Ac] and the mass transfer in the liquid phase.

A theoretical simulation was carried out. For a target 90%  $\text{CO}_2$  capture, the simulation revealed that (i) the mass transfer coefficient should be greater than  $1.7 \cdot 10^{-4} \text{ m s}^{-1}$  or (ii) seven hollow fibre membrane modules in series (total length of 2 m) were necessary, being proposed for the scaling-up a network of modules in series and as many in parallel as the flue gas flow rate increases.

The intensification potential of the membrane contactor compared with a packed column performance with 30 wt.% MEA solution was estimated by the intensification factor, which reached a value of 4.5 for 90%  $\text{CO}_2$  capture.

*Acknowledgement*

This research was funded by the Spanish Ministry Economy and Competitive (Project CTQ2013-48280-C3-1-R). The authors thank Dr. J.C. Remigy (Laboratoire de Genie Chimique, UPS, Toulouse, France) for the preparation of 1AQ2-PVDF fibres.

*Symbols used*

$A$	[m <sup>2</sup> ]	effective membrane area
$B$	[-]	pre-exponential factor
$D$	[m <sup>2</sup> s <sup>-1</sup> ]	diffusivity
$d_h$	[m]	hydraulic diameter
$d_i$	[m]	inside diameter of the fibre
$d_{lm}$	[-]	log mean diameter of the fibre
$d_o$	[m]	outside diameter of the fibre
$E$	[-]	enhancement factor
$E_a$	[J mol <sup>-1</sup> ]	activation energy
$Gz$	[-]	Graetz number
$H_d$	[-]	dimensionless Henry's law constant
$H_c$	[mol bar <sup>-1</sup> L <sup>-1</sup> ]	Henry's law constant
$k_g$	[m s <sup>-1</sup> ]	mass transfer coefficient in the gas phase
$k_l$	[m s <sup>-1</sup> ]	mass transfer coefficient in the liquid phase
$k_{mg}$	[m s <sup>-1</sup> ]	mass transfer coefficient of the membrane
$K_{overall}$	[m s <sup>-1</sup> ]	overall mass transfer coefficient
$L$	[m]	fibre length
$n$	[-]	number of fibres
$N_{CO_2}$	[mol m <sup>2</sup> s <sup>-1</sup> ]	absorption flux of carbon dioxide
$P_T$	[bar]	total pressure
$Q$	[m <sup>3</sup> s <sup>-1</sup> ]	flow rate
$R$	[bar L mol <sup>-1</sup> K <sup>-1</sup> ]	ideal gas constant
$Re$	[-]	Reynolds number
$R_g$	[s m <sup>-1</sup> ]	resistance in the gas side
$R_l$	[s m <sup>-1</sup> ]	resistance in the liquid side
$R_m$	[s m <sup>-1</sup> ]	resistance of the membrane
$R_{overall}$	[s m <sup>-1</sup> ]	overall resistance to mass transfer

$Sc$	[-]	Schmidt number
$Sh$	[-]	Sherwood number
$t$	[s]	time
$T$	[K]	temperature
$u_m$	[m s <sup>-1</sup> ]	linear velocity
Subscripts		
g gas		
l liquid		
in inlet of the contactor		
out outlet of the contactor		
Greek letters		
$\varphi$	[-]	packing factor
$\gamma$	[-]	dimensionless activation energy

### References

- [1] K. Wang, X. Wang, P. Zhao, X. Guo, *Chem. Eng. Technol.* **2014**, 37(9), 1552–1558. DOI: 10.1002/ceat.201300584.
- [2] B. Zhu, Q. Liu, Q. Zhou, J. Yang, J. Ding, J. Wen, *Chem. Eng. Technol.* **2014**, 37(4), 635–642. DOI: 10.1002/ceat.201300240.
- [3] S. Khaisri, D. de Montigny, P. Tontiwachwuthikul, R. Jiraratananon, *Energy Procedia* **2011**, 4, 688–692. DOI: 10.1016/j.egypro.2011.01.106.
- [4] I. Merino-García, E. Álvarez-Guerra, J. Albo, A. Irabien, *Chem. Eng. J.* **2016**, 305, 104–120. DOI: 10.1016/j.cej.2016.05.032.
- [5] S. Zhao, P.H.M. Feron, L. Deng, E. Favre, E. Chabanon, S. Yan, J. Hou, V. Chen, H. Qi, *J. Membr. Sci.* **2016**, 511, 180–206. DOI: 10.1016/j.memsci.2016.03.051.
- [6] P. Luis P., T. Van Gerven, B. Van Der Bruggen, *Prog. Energy Combust. Sci.* **2012**, 38, 419–448. DOI: 10.1016/j.peccs.2012.01.004.
- [7] S. Roussanaly, R. Anantharaman, K. Lindqvist, H. Zhai, E. Rubin, *J. Membr. Sci.* **2016**, 511, 250–264. DOI: 10.1016/j.memsci.2016.03.035.
- [8] M. Kanniche, R. Gros-Bonnivard, P. Jaud, J. Valle-Marcos, J. Amann, C. Bouallou, *Appl. Therm. Eng.* **2010**, 30, 53–62. DOI: 10.1016/j.applthermaleng.2009.05.005.
- [9] T.C. Merkel, H. Lin, X. Wei, R. Baker, Power plant post-combustion carbon dioxide capture: An opportunity for membranes. *J. Membr. Sci.* **2010**, 359(1-2), 126–139. DOI: 10.1016/j.memsci.2009.10.041.
- [10] A. Fernandez-Barquin, C. Casado-Coterillo, M. Palomino, S. Valencia, A. Irabien, *Chem. Eng. Technol.* **2015**, 38(4), 658–666. DOI: 10.1002/ceat.201400641.

- [11] M. Ramdin, T.W. Loos, T.J.H. Vlught, *Ind. Eng. Chem. Res.* **2012**, 51, 8149-8177. DOI: 10.1021/ie3003705.
- [12] S. Khaisri, D. de Montigny, P. Tontiwachwuthikul, R. Jiraratananon, *J. Membr. Sci.* **2011**, 376, 110-118. DOI: 10.1016/j.memsci.2011.04.005.
- [13] B. Singh, A.H. Strømman, E.G. Hertwich, *Int. J. Greenh. Gas Control* **2011**, 5, 911-921. DOI: 10.1016/j.ijggc.2011.03.012.
- [14] H. Herzog, J. Meldon, A. Hatton, *Advanced Post-Combustion CO<sub>2</sub> Capture*. Massachusetts Institute of Technology: Cambridge, MA **2009**.
- [15] K. Simons, K. Nijmeijer, M. Wessling, *J. Membr. Sci.* **2009**, 340, 214-220. DOI: 10.1016/j.memsci.2009.05.035.
- [16] S.P. Yan, M.X. Fang, W.F. Zhang, S.Y. Wang, Z.K. Xu, Z.Y. Luo, K.F. Cen, *Fuel Process. Technol.* **2007**, 88, 501-511. DOI: 10.1016/j.fuproc.2006.12.007.
- [17] R. Khalilpour, K. Mumford, H. Zhai, A. Abbas, G. Stevens, E.S. Rubin, *J. Clean. Prod.* **2015**, 103, 286-300. DOI: 10.1016/j.jclepro.2014.10.050.
- [18] A. Mansourizadeh, A.F. Ismail, T. Matsuura, *J. Membr. Sci.* **2010**, 353, 192-200. DOI: 10.1016/j.memsci.2010.02.054.
- [19] A. Trusov, S. Legkov, L. Van den Broeke, E. Goetheer, V. Khotimsky, A. Volkov, *J. Membr. Sci.* **2011**, 383, 241-249. DOI: 10.1016/j.memsci.2011.08.058.
- [20] R. Bounaceur, C. Castel, S. Rode, D. Roizard, E. Favre, *Chem. Eng. Res. Des.* **2012**, 90, 2325-2337. DOI: 10.1016/j.cherd.2012.05.004.
- [21] E. Favre, *Chem. Eng. J.* **2011**, 171, 782-793. DOI: 10.1016/j.cej.2011.01.010.
- [22] A. Mansourizadeh, A.R. Pouranfard, *Chem. Eng. Res. Des.* **2014**, 92, 181-190. DOI: 10.1016/j.cherd.2013.06.028.
- [23] M. Rezaei, A.F. Ismail, S.A. Hashemifard, T. Matsuura, *Chem. Eng. Res. Des.* **2014**, 92, 2449-2460. DOI: 10.1016/j.cherd.2014.02.019.
- [24] M. Rezaei, A.F. Ismail, Gh. Bakeri, S.A. Hashemifard, T. Matsuura, *Chem. Eng. J.* **2015**, 260, 875-8885. DOI: 10.1016/j.cej.2014.09.027.
- [25] Gh. Bakeri, A.F. Ismail, T. Matsuura, M.S. Abdullah, B.C. Ng, M. Mashkour, *Chem. Eng. Res. Des.* **2015**, 104, 367-375. DOI: 10.1016/j.cherd.2015.08.024.
- [26] H. Fashandi, A. Ghodsi, R. Saghafi, M. Zarrebini, *Int. J. Greenh. Gas Control*. **2016**, 52, 13-23. DOI: 10.1016/j.ijggc.2016.06.010.
- [27] M. Peng, H. Li, L. Wu, Q. Zheng, Y. Chen, W. Gu, *J. Appl. Polym. Sci.* **2005**, 98, 1358-1363. DOI: 10.1002/app.22303.
- [28] T. Savart, *PhD thesis*, Université Paul Sabatier, Toulouse France **2013**.
- [29] A. Mansourizadeh, *Chem. Eng. Res. Des.* **2012**, 90, 555-562. DOI:10.1016/j.cherd.2011.08.017.
- [30] H.Y. Zhang, R. Wang, D.T. Liang, J.H. Tay, *J. Membr. Sci.* **2008**, 308, 162-170. DOI: 10.1016/j.memsci.2007.09.050.

- [31] S.H. Lin, P.C. Chiang, C.F. Hsieh, M.H. Li, K.L. Tung, *J. Chin. Inst. Chem. Eng.* **2008**, 39, 13–21. DOI: 10.1016/j.jcice.2007.11.010.
- [32] M. Fang, Z. Wang, S. Yan, Q. Cen, Z. Luo, *Int. J. Greenh. Gas Control* **2012**, 9, 507–521. DOI: 10.1016/j.ijggc.2012.05.013.
- [33] A.B. López, M.D. La Rubia, J.M. Navaza, R. Pacheco, D. Gómez-Díaz, *Chem. Eng. Technol.* **2014**, 37(3), 419–426. DOI:
- [34] Z. Dai, R.D. Noble, D.L. Gin, X. Zhang, L. Deng, *J. Membr. Sci.* **2016**, 497, 1–20. DOI: 10.1016/j.memsci.2015.08.060. [35] J.E. Bara, T.K. Carlisle, C.J. Gabriel, D. Camper, A. Finotello, D.L. Gin, R.D. Noble, *Ind. Eng. Chem. Res.* **2009**, 48, 2739–2751. DOI: 10.1021/ie8016237.
- [36] P. Luis, A. Garea, A. Irabien, *J. Membr. Sci.* **2009**, 330, 80–89. DOI: 10.1016/j.memsci.2008.12.046.
- [37] J. Albo, P. Luis, A. Irabien, *Ind. Eng. Chem. Res.* **2010**, 49, 11045–11051. DOI: 10.1021/ie1014266.
- [38] J. Albo, T. Tsuru, *Ind. Eng. Chem. Res.* **2014**, 53, 8045–8056. DOI: 10.1021/ie500126x.
- [39] L. Gomez-Coma, A. Garea, A. Irabien, *Sep. Purif. Technol.* **2014**, 132, 120–125. DOI: 10.1016/j.seppur.2014.05.012.
- [40] M.B. Shiflett, A. Yokozeki, *J. Chem. Eng. Data* **2009**, 54, 108–114. DOI: 10.1021/je800701j.
- [41] X.L. Papatryfon, N.S. Heliopoulos, I.S., Molchan, L.F. Zubeir, N.D. Bezemer, M.K. Arfanis, A.G. Kontos, V. Likodimos, B. Iliev, G.E. Romanos, P. Falaras, K. Stamatakis, K.G. Beltsios, M.C. Kroon, G.E. Thompson, J. Klöckner, T.J.S. Schubert, *Ind. Eng. Chem. Res.* **2014**, 53(30), 12083–12102. DOI: 10.1021/ie501897d.
- [42] M.S. Shannon, J.E. Bara, *Ind. Eng. Chem. Res.* **2011**, 50(14), 8665–8677. DOI: 10.1021/ie200259h
- [43] M. Hasib-ur-Rahman, F. Larachi, *Ind. Eng. Chem. Res.* **2013**, 52(49), 17682–17685. DOI:
- [44] G. Gurau, H. Rodríguez, S.P. Kelley, P. Janiczek, R.S. Kalb, R.D. Rogers, *Angew. Chem. Int. Edit.* **2011**, 50, 12024–12026. DOI: 10.1002/anie.201105198.
- [45] A. Yokozeki, M.B. Shiflett, C.P. Junk, L.M. Grieco, T. Foo, *J. Phys. Chem. B.* **2008**, 112, 16654–16663. DOI: 10.1021/jp805784u
- [46] M.G. Freire, A.R.R. Teles, M.A.A. Rocha, B. Schroder, C.M.S.S. Neves, P.J. Carvalho, D.V. Evtuguin, L.M.N.B.F. Santos, J.A.P. Coutinho, *J. Chem. Eng. Data* **2011**, 56(12), 4813–4822. DOI: 10.1021/je200790q.
- [47] W. Shi, C.R. Myers, D.R. Luebke, J.A. Steckel, J.A., D.C. Sorescu, *J. Phys. Chem. B.* **2012**, 116, 283–295. DOI: 10.1021/jp205830d.
- [48] P.J. Carvalho, V.H. Alvarez, B. Schröder, A.M. Gil, I.M. Marrucho, M. Aznar, L. Santos, J.A.P. Coutinho, *J. Phys. Chem. B.* **2009**, 113, 6803–6812. DOI: 10.1021/jp901275b.
- [49] K.A. Hoff, H.F. Svendsen, *Chem. Eng. Sci.* **2014**, 116, 331–341. DOI: doi.org/10.1016/j.ces.2014.05.001.

- [50] O. Lorain, J.M. Espenan, J.C. Remigy, J.F. Lahitte, J.C. Rouch, T. Savart, P. Gerard, S. Magnet, *France WO2014/139977 (A1)* **2014**.
- [51] L. Gomez-Coma, A. Garea, J.C. Rouch, T. Savart, J.F. Lahitte, J.C. Remigy, A. Irabien, *J. Membr. Sci.* **2016** 498, 218-226. DOI: 10.1016/j.memsci.2015.10.023.
- [52] Y. Medina-Gonzalez, E. Lasseguette, J.C. Rouch, J.C. Remigy, *Sep. Sci. Technol.* **2012**, 47(11),1596-1605. DOI: 10.1080/01496395.2012.658942.
- [53] M.B. Shiflett, D.J. Kasprzak, C.P. Junk, A. Yokozeki, *J. Chem. Thermodyn.* **2008**, 40, 25–31. DOI: 10.1016/j.jct.2007.06.003.
- [54] R. Naim, A.F. Ismail, *Sep. Purif. Technol.* **2013**, 115, 152-157. DOI: 10.1016/j.seppur.2013.04.045.
- [55] A. Ortiz, D. Gorri, A. Irabien, I. Ortiz, *J. Membr. Sci.* **2010**, 360, 130-141. DOI: 10.1016/j.memsci.2010.05.013.
- [56] J.G. Lu, Y.F. Zheng, M.D. Cheng, L.J. Wang, *J. Membr. Sci.* **2007**, 289, 138-149. DOI: 10.1016/j.memsci.2006.11.042.
- [57] P. Luis, B. Van der Bruggen, *Greenhouse Gas Sci. Technol.* **2013**, 3, 1–20. DOI: 10.1002/ghg.1365.
- [58] N. Boucif, D. Roizard, J.P. Corriou, E. Favre, *Sep. Purif. Technol.* **2015**, 50, 1331-1343. DOI: 10.1080/01496395.2014.969807.
- [59] W. Rongwong, R. Jiraratananon, S. Atchariyawut, *Sep. Purif. Technol.* **2009**, 69, 118-125. DOI: 10.1016/j.seppur.2009.07.009.
- [60] A. Mansourizadeh, A.F. Ismail, *Chem. Eng. J.* **2010**, 165, 980-988. DOI: 10.1016/j.cej.2010.10.034.
- [61] A. Mansourizadeh, A.F. Ismail, *Int. J. Greenh. Gas Control* **2011**, 5, 374-380. DOI: 10.1016/j.ijggc.2010.09.007.
- [62] L. Wang, Z. Zhang, B. Zhao, H. Zhang, X. Lu, Q. Yang, *Sep. Purif. Technol.* **2009**, 116, 300-306. DOI: 10.1016/j.seppur.2013.05.051.
- [63] M. Rahbari-Sisakht, A.F. Ismail, D. Rana, T. Matsuura, D. Emadzadeh, *Sep. Purif. Technol.* **2013**, 116, 67-72. DOI: 10.1016/j.seppur.2013.05.008.
- [64] S. Boributh, R. Jiraratananon, K. Li, *J. Membr. Sci.* **2013**, 429, 459-472. DOI: 10.1016/j.memsci.2012.11.074.
- [65] F. Korminouri, M. Rahbari-Sisakht, D. Rana, T. Matsuura, A.F. Ismail, *Sep. Purif. Technol.* **2014**, 132, 601-609. DOI: 10.1016/j.seppur.2014.06.017.
- [66] G. Wang, W. Hou, F. Xiao, J. Geng, Y. Wu, Z. Zhang, *J. Chem. Eng. Data* **2011**, 56, 1125-1133. DOI: 10.1021/je101014q.
- [67] A. Ahmady, A. Hashim, M.K Aroua, *Chem. Eng. J.* **2012**, 200-202, 317-328. DOI: 10.1016/j.cej.2012.06.037.
- [68] Z. Zhou, G. Jing, L. Zhou, *Chem. Eng. J.* **2012**, 204-206, 235-243. DOI: 10.1016/j.cej.2012.07.108

- [69] X. Zhang, D. Bao, Y. Huang, H. Dong, X. Zhang, S. Zhang, *AIChE J.* **2014**, 60, 2929-2939. DOI: 10.1002/aic.14507.
- [70] B.E. Gurkan, T.R. Gohndrone, M.J. McCready, J.F. Brennecke, *Chem. Chem. Phys.* **2013**, 15, 7796-7811. DOI: 10.1039/c3cp51289d.
- [71] Y.T. Shah, *Chem. Eng. Sci.* **1972**, 27, 1469-1474. DOI: 10.1016/0009-2509(72)85033-4.
- [72] P. Luis, I. Ortiz, R. Aldaco, A. Garea, A. Irabien, *Int. J. Chem. React. Eng.* **2007**, 5, 1-9.
- [73] P. Luis, A. Garea, A. Irabien, *Sep. Purif. Technol.* **2010**, 72, 174-179. DOI: 10.1016/j.seppur.2010.02.003.
- [74] S.H. Yeon, K.S. Lee, B. Sea, Y.I. Park, K.H. Le, *J. Membr. Sci.* **2005**, 257, 156-160. DOI: 10.1016/j.memsci.2004.08.037.
- [75] S. Paul, A.K. Ghoshal, B. Mandal, *Ind. Eng. Chem. Res.* **2007**, 46, 2576-2588. DOI: 10.1021/ie061476f.
- [76] H.Y. Zhang, R. Wang, D.T. Liang, J.H. Tay, *J. Membr. Sci.* **2008**, 308, 162-170. DOI: 10.1016/j.memsci.2007.09.050.
- [77] L. Wang, Z. Zhang, B. Zhao, H. Zhang, X. Lu, Q. Yang, *Sep. Purif. Technol.* **2013**, 116, 300-306. DOI: 10.1016/j.seppur.2013.05.051.
- [78] K.A. Hoff, H.F. Svendsen *Energy Procedia* **2013**, 37, 952-960. DOI: 10.1016/j.egypro.2013.05.190.



# Anexo: Difusión de resultados en congresos

---

---

*“Hay una fuerza motriz más poderosa que el vapor, la electricidad  
y la energía atómica: la voluntad.”*

Albert Einstein (1879-1955)

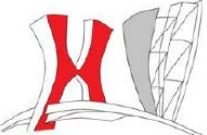
Físico alemán



## Anexo: Difusión de resultados en congresos

A continuación se listan las contribuciones a congresos internacionales del ámbito de la ingeniería química a través de los cuales se ha realizado la difusión de los resultados de la presente Tesis.

### Congresos internacionales:

1. Gomez-Coma L., Garea A., Rouch J.C., Lahitte J.F., Remigy J.C., Irabien A., CO<sub>2</sub> absorption using pvdf self-made membrane contactors and [emim][ac] ionic liquid, 10th European Congress of Chemical Engineering (ECCE10). 27 septiembre - 1 octubre 2015, Niza (Francia) ISBN: 978-2-910239-82-4. Comunicación poster. 
2. Gomez-Coma L., Casado-Coterillo C., Garea A., Irabien A., PVDF membrane contactors for CO<sub>2</sub> absorption, Euromembrane 2015. 6-10 septiembre 2015, Aachen (Alemania). Comunicación poster. 
3. Gomez-Coma L., Garea A., Irabien A., Acoplamiento de la etapa de desorción a una planta de absorción no dispersiva. XXXV Reunión Bienal de la Real Sociedad Española de Química. 19-23 julio 2015, La Coruña (España). ISBN: 978-84-606-9786-2. Comunicación oral. 
4. Gomez-Coma L., Garea A., Irabien A., Efficiency comparison between different membrane contactors and [emim][ac] ionic liquid in CO<sub>2</sub> absorption. XI Simposio de Investigadores Jovenes; Real Sociedad Española de Química-Sigma Aldrich. 4-7 noviembre 2014, Bilbao (España). Comunicación poster. 
5. Gomez-Coma L., Garea A., Irabien A., Rouch J.C., Lahitte J.F., Remigy J.C., Fiber characterization for CO<sub>2</sub> absorption. 13th Mediterranean Congress of Chemical Engineering (13MCCE). 30 septiembre-3 octubre 2014, Barcelona (España). Comunicación oral. 
6. Gomez-Coma L., Albo J., Garea, Irabien A., CO<sub>2</sub> capture using polysulfone membrane contactor and [emim][ac] ionic liquid. XXI International Conference on Chemical Reactors CHEMREACTOR-21. 22-25 septiembre 2014, Delf (Holanda). ISBN: 978-5-906376-06-0 Comunicación poster. 
7. Gomez-Coma L., Casado-Coterillo C., Garea A., Irabien A., Temperature effect in polypropylene and polysulfone hollow fibre membrane contactors using ionic liquids. 21st International Congress of Chemical and Process Engineering CHISA. 23-27 agosto 2014, Praga (República Checa). ISBN: 978-80-02-02555-9. Comunicación póster. 

8. Gomez-Coma L., Santos E., Garea A., Irabien A., Rouch J.C., Lahitte J.F., Remigy J.C., Manufacture of membrane contactors for CO<sub>2</sub> absorption. The ANQUE•ICCE•BIOTEC 2014 Congresses on Chemistry, Chemical Engineering and Biotechnology. 1-4 julio 2014, Madrid (España). ISBN: 978-84-697-0726-5. Comunicación Oral.



9. Gomez-Coma L., Garea A., Irabien A., Rouch J.C., Lahitte J.F., Remigy J.C., Characterization of different type of fibers with PVDF for CO<sub>2</sub> absorption. IX Ibero-american congress on membrane science and technology. 25-28 mayo 2014, Santander (España). ISBN: 978-84-697-0397-7. Comunicación poster y flash.



10. Gomez-Coma L., Garea A., Irabien A., CO<sub>2</sub> capture by non-dispersive absorption in membrane contactors: enhancement factor by chemical reaction with ionic liquids. 4th International Congress on Green Process Engineering (GPE). 7-10 abril 2014, Sevilla (España). ISBN: 978-84-15107-50-7. Comunicación póster.



11. Gomez-Coma L., Garea, A., Irabien A., Captura de CO<sub>2</sub> mediante líquidos iónicos: Influencia de la temperatura. XXXIV Reunión Bienal de la Real Sociedad Española de Química. 15-18 septiembre 2013, Santander (España). ISBN: 978-84-695-8511-5 Comunicación poster.



12. Albo J., Gomez-Coma L., Irabien A., Non-dispersive absorption of CO<sub>2</sub> using membrane contactors and ionic liquids. 22nd International Symposium on Chemical Reaction Engineering (ISCRE 22). 2-5 septiembre 2012, Maastricht (Holanda). Comunicación poster.



Igualmente se ha participado en el curso de verano, "Valorización química sostenible de dióxido de carbono". 27-30 junio 2016, Santander (España). Comunicación poster.

